



N-Glycosylation optimization of recombinant antibodies in CHO cell through process and metabolic engineering

Fan, Yuzhou; Andersen, Mikael Rørdam; Weilguny, Dietmar

Publication date:
2015

Document Version
Publisher's PDF, also known as Version of record

[Link back to DTU Orbit](#)

Citation (APA):

Fan, Y., Andersen, M. R., & Weilguny, D. (2015). N-Glycosylation optimization of recombinant antibodies in CHO cell through process and metabolic engineering. Kgs. Lyngby: Department of Systems Biology, Technical University of Denmark.

DTU Library Technical Information Center of Denmark

General rights

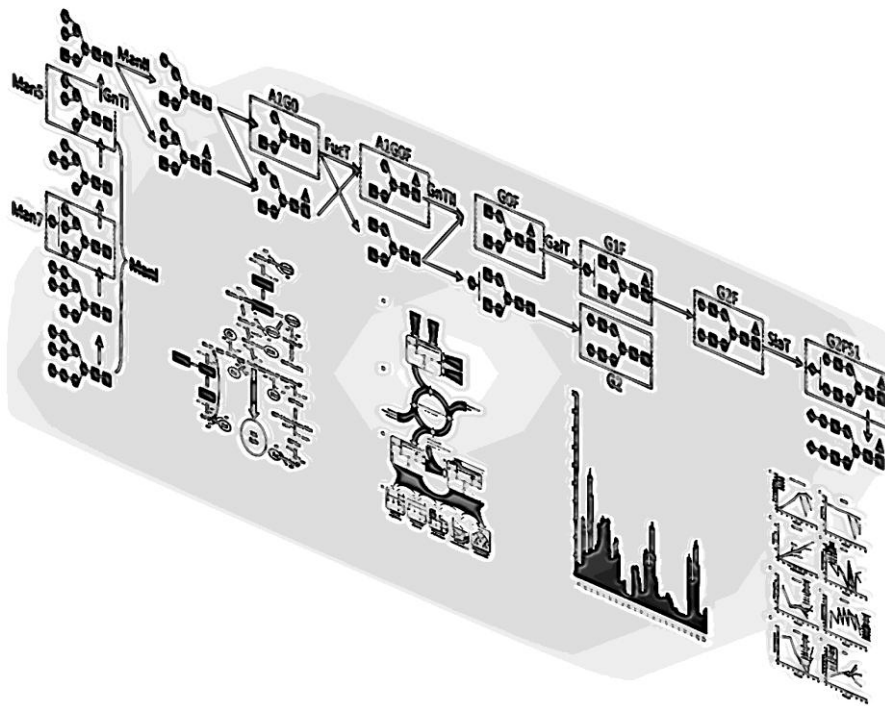
Copyright and moral rights for the publications made accessible in the public portal are retained by the authors and/or other copyright owners and it is a condition of accessing publications that users recognise and abide by the legal requirements associated with these rights.

- Users may download and print one copy of any publication from the public portal for the purpose of private study or research.
- You may not further distribute the material or use it for any profit-making activity or commercial gain
- You may freely distribute the URL identifying the publication in the public portal

If you believe that this document breaches copyright please contact us providing details, and we will remove access to the work immediately and investigate your claim.

N-Glycosylation optimization of recombinant antibodies in CHO cell through process and metabolic engineering

PhD dissertation



Yuzhou Fan

1/31/2015

Preface

During the three years of my PhD study, I have enjoyed an amazing science adventure in the area of glycosylation engineering in Chinese hamster ovary (CHO) cells. It won't be such a great experience without the support from my friends, colleagues and family. Though I can only try my best to express years of gratitude in a few lines here, my affection and appreciation for all of you go far beyond that.

After accomplishing an industrially collaborated Master project at Symphogen A/S, I was encouraged by the Anne B. Tolstrup (former Director at Symphogen), Christian Müller (former Senior Scientist at Symphogen), Torben P. Frandsen (former VP at Symphogen) and Jette W. Sen (Director at Symphogen) and Uffe H. Mortensen (Professor at DTU) to pursue an industrial PhD. With valuable inspirations from them and full support from Mikael R. Andersen (Associated Professor at DTU) and Dietmar Weilguny (Principal Scientist at Symphogen), who later on became my main supervisors of PhD study, a grant application of industrial PhD were submitted to and later on approved by Danish Agency for Science, Technology and Innovation. I would like to address my sincere gratitude to all these people for making the industrial PhD project financially possible.

I would like to express my deepest acknowledgements for the comprehensive guidance and solid help I received from my supervisor team, including Mikael R. Andersen and Dietmar Weilguny as my main supervisors, and Christian Müller, Jette W. Sen, and Uffe H. Mortensen as my co-supervisors. In particular, I would like to thank Mikael and Dietmar who conveyed a great enthusiasm and provided an excellent supervision for me along the whole project. Their optimistic spirit, constructive suggestion, innovative inspiration and endless support make me, a humble student gradually become a confident scientist. I am also especially grateful to Christian, who has shown a genuine interest in me and always has willingness to help me in problem solving.

Through Christian, I was put in touch with two excellent researchers in glycosylation modeling from Imperial College London, UK, Ioscani Jimenez Del Val (former Postdoc at Imperial College) and Cleo Kontoravdi (Lecture at Imperial College), who showed a great hospitality during my visit to their research group. More importantly, they both had great passions and provided tremendous contributions to our collaborative projects. It is such a good luck to find the two personally and scientifically nice collaborators. I sincerely hope that we can continue our collaborations on other projects in the future.

At a later stage of my PhD, I was introduced to Michael J. Betenbaugh (Professor at Johns Hopkins University) by Mikael. Michael was kind enough to invite me for a four month stay in his lab at Johns Hopkins University, US. During that period, Michael supervised me on a number of projects, including proteomics analysis in CHO cells. I also felt a warm welcome from his entire research group both at work and after hours. It was a great pleasure to be one of the members in Michael's research group. I can still remember the scenes of discussing project, watching football game, having dinner and celebrating Halloween together with Michael and his students during my stay. I would like to thank Michael and his group for giving me such a good experience.

Here is the place to express my warmest acknowledgement for all the present and former colleagues at Symphogen and DTU.

I would like to thank Søren K. Rasmussen and our whole cell line generation and upstream process team for their great help in my everyday life at Symphogen. In particular, I also appreciated the following people from other departments of Symphogen for supporting my work from different aspects: Gayle Mills, Ivan D. Horak, Martin Olin, Michael Kragh, Anette Aabo, Martin Ørgaard, Yvonne B. Larsen, Kim Højlyls-Larsen, Magnus Strandh, Martin A. Bendz, Michael V. Grandal, Jan K. Simonsen, Anna Dahlman, Jeff Salka, Linda Egebjerg, and Nina Berg Frølund.

I would like to thank Anne M. Lund, Christian S. Kaas, Jens C. Eriksen and all other members in our reach group of network engineering of eukaryotic cell factories at Systems biology, DTU for your contribution and fruitful discussion to my work.

I would like also thank my friends Chen Zhang, Yifan Zhang, Pengyue Zhang, Nuoya Wang, Xiaoran Liu for their accompany and encouragement during my study.

Last but not least, I would like to express my most sincere gratitude to Xi Fu, Yanmin Fan, and Aiwu Zhang and all my rest family for their love and continuous supports throughout my study and my thesis writing.

Summary

Thanks to the recent advances in Chinese hamster ovary (CHO) “omic” revolution, the development of recombinant therapeutic protein bioprocessing using CHO cell factory started to merge with the new biological mindset called systems biology. In order to produce a CHO-derived recombinant therapeutic protein with ensured safety, efficacy and cost-effectiveness, holistic understanding of titer and N-glycosylation of the protein in relation to cell culture process as well as genomic, proteomic, metabolic and physiological status of the cells becomes a superior approach. Combining the knowledge of CHO cell culture technology, upstream process engineering, metabolic engineering, and glycobiology into a systematic framework allow us to improve the production of recombinant therapeutic protein towards an optimal balance between quantity and quality.

In the presented work, recent know-how on impact, analysis, control and optimization of N-glycosylation were thoroughly reviewed. In particular, how to control and optimize N-glycosylation in CHO cells was exclusively studied. The main focus of this PhD project is to find effective approaches of modulating N-glycosylation of CHO-derived recombinant monoclonal antibody (mAb) towards desired patterns, and at the same time try to understand the underlying mechanisms of that from a systems biology perspective. Two different strategies were used and achieved great success in glyco-optimization: 1) optimize media and culture process; 2) Genetically optimize CHO cell factory.

In the early part of the thesis, the first strategy was displayed by a number of successful case studies, in which process and media engineering approach was successfully used to direct N-glycosylation. Controlling the balance between glucose and amino acid metabolism, using galactose as feed additives, changing process parameters such as seeding density and cultivation duration are all demonstrated to be effective. The causal explanation of their impact on glycosylation can be various, including product, metabolism, proteome and physiology-associated mechanism.

In the middle part of the thesis, both literature reviews and experimental applications were provided to demonstrate how to use omics data and implement systems biology to understand biological activities, especially N-glycosylation in CHO cells.

In the last part of the thesis, the second strategy that apply genetic and metabolic engineering approach to improve N-glycosylation capability of CHO cells was also presented promising results. Overexpression of either N-acetylglucosaminyltransferase I (GnTI) in CHO cells was confirmed to improve the maturation of glycans in mAb.

In conclusion, integrating the concept of systems biology with process and metabolic engineering has been demonstrated through a number of studies to be a superior way of controlling and optimizing N-glycosylation of CHO-derived recombinant therapeutic protein.

Resumé

Takket være nylige fremskridt inden for den "omic" revolution af Chinese hamster ovary (CHO) celler, er udvikling og produktion af rekombinante terapeutiske proteiner i CHO cellefabrikker begyndt at blive præget med afsæt i systembiologi. En holistisk forståelse af titer og N-glykosylering af et produceret rekombinant protein i forhold til den tilknyttede celle kultiverings proces, samt en genomisk, proteomisk, metabolisk og fysiologisk forståelse, vise sig at være yderst effektiv når der samtidig er fokus på sikkerhed, effektivitet og pris, af det enkelte protein. Ved at kombinere og sammensætte viden indenfor CHO celle kultiverings teknologi, upstream proces udvikling, metabolisk optimering, og glyco-biologi, til et systematisk framework med fokus på kvalitet og kvantitet, kan produktionen af rekombinante terapeutiske proteiner blive optimeret.

I det præsenterede arbejde er det seneste know-how indenfor analyse, kontrol og optimering af N-glykosylering, samt indflydelsen af N-glykosylering på terapeutiske proteiner, blevet grundigt revideret og analyseret. Mere specifikt er det blevet undersøgt hvordan man kan kontrollere og optimere N-glykosylering i CHO celler. Hoved fokus i dette PhD projekt har været at udvikle effektive metoder til modelering af N-glycosylering af CHO-producerede rekombinante monoklonale antistoffer (mAb), således at ønskede glycosylerings mønstre kan opnåes, samtidig med at udvide forståelsen for de dybere mekanismer der styrer N-glycosylering set fra et systembiologisk perspektiv. To forskellige strategier blev brugt til at glyko-optimere med stor succes: 1) optimering af medie og kultiverings processer; 2) genetisk forbedring af CHO som cellefabrik.

I den første del af tesen, er den første strategi demonstreret af flere succesfulde case-studies, hvor process- og medieoptimering blev brugt til at styre N-glykosyleringen. Balancen mellem glukose- og aminosyremetabolismen blev kontrolleret ved at bruge galaktose som feed additiv og ved at ændre process parametre såsom udsåningstætheden og længden af kultiveringen. Ved at kontrollere balancen mellem glukose- og aminosyremetabolismen, kunne N-glycosyleringen påvirkes. Der er flere forklaringer på, hvorfor denne balance styrer glykosyleringen, herunder mekanismer associeret med produktion, metabolisme, proteomet, og fysiologi.

I den anden del af tesen bliver både litteraturen og eksperimentelle applikationer undersøgt, for at demonstrere hvorledes omics data og implementering af systembiologi kan udnyttes til at forstå biologiske mekanismer, herunder N-glycosylering i CHO celler.

I den tredje og sidste del af tesen, bliver den anden strategi demonstreret. Lovende resultater viser at det er muligt at optimere N-glykosylering ved at modificere genetikken og metabolismen i CHO celler. Ved at overudtrykke enten N-acetylglucosaminyltransferase I (GnTI) proteiner kunne GlcNAc tilgængeligheden øges, med en medfølgende forbedring af matureringen af glykaner i mAbs.

Resultaterne demonstrerer integrationen af systembiologi koncepter og process- og metabolisme modifikationer, som en effektiv måde hvorved N-glykosylering af CHO-producerede rekombinante terapeutiske proteiner kan kontrolleres og optimeres.

Table of Contents

Preface.....	2
Summary	4
Resumé.....	6
Chapter 1 Introduction	13
1.1. Structure of the thesis	13
Chapter 2 Glycosylation: impact and control in mAb production	15
2.1. N-Glycosylation patterns can affect therapeutic protein properties	17
2.2. Analytical techniques for accessing glycosylation information	19
2.2.1. Glycosylation analysis.....	19
2.2.2. Nucleotide sugar analysis	20
2.2.3. Analysis of CHO glycosylation-related enzymes	20
2.3. N-Glycosylation control and modulation	21
2.3.1. Media, feed and culture process	21
2.3.2. Genetic engineering of glycosylation-related enzymes.....	25
2.4. Executive summary	29
2.5. References	29
Chapter 3 Effect of glucose and amino acid metabolism on N-glycosylation.....	41
Chapter 4 Glycoprofiling the effect of media additives on IgG produced by CHO cells in fed- batch bioreactors	57
Keywords	57
Abstract	58
4.1. Introduction	59
4.2. Materials and Methods	60

4.2.1. Cell culture	60
4.2.2. Fed-batch cultures	60
4.2.3. Cell, metabolite and product analysis.....	61
4.2.4. Purification of IgG.....	61
4.2.5. Cation-exchange chromatography of IgG	62
4.2.6. Intact mass analysis of IgG.....	62
4.2.7. Instant-AB labeled glycoprofiling.....	62
4.2.8. Statistical analysis of glycoform distributions	62
4.3. Results	62
4.3.1. Fed-batch culture	63
4.3.2. Effect of additives on charge heterogeneity and glycosylation of antibody	65
4.4. Discussion.....	67
4.5. Acknowledgements	70
4.6. References	70
Chapter 5 CHO ‘Omics-based bioprocessing	73
Keywords	74
Abstract	74
5.1. Introduction	74
5.2. Potential Applications of Metabolic Models to CHO Cell Cultures	75
5.3. Additional Available Data Sources for Increased Applicability of CHO Models	79
5.3.1. Genomics.....	80
5.3.2. Transcriptomics	81
5.3.3. Proteomics	81
5.3.4. Metabolomics	82

5.4. Overview of Cellular Modelling Efforts in CHO cells and Beyond	83
5.5. Future Perspectives.....	84
5.6. Executive Summary.....	85
5.7. References	87
Chapter 6 Systems biology-based investigation into the effect of glucose starvation and culture duration on fed-batch CHO cell culture.....	97
Keywords	97
Abstract	97
6.1. Introduction	98
6.2. Materials and methods.....	99
6.2.1. Cell culture and fed-batch process	99
6.2.2. Nucleotide sugar analysis.....	100
6.2.3. Semi-high throughput mAb purification	100
6.2.4. Cation-Exchange chromatography	100
6.2.5. mAb Glycoprofiling	101
6.2.6. Statistical analysis of glycoform distributions	101
6.2.7. Sample preparation for proteomics analysis	101
6.2.8. Fractionation of peptides	102
6.2.9. LC-MS/MS analysis	103
6.2.10. MS data analysis	103
6.2.11. Comparative proteomics analysis	103
6.3. Results and Discussion	104
6.3.1. Effect of glucose starvation.....	104
6.3.2. Effect of culture duration	114

6.3.3. Comparative proteomics analysis between growth phase and stationary phase in fed-batch	116
6.4. Conclusion	122
6.5. References	123
Chapter 7 Chinese hamster ovary cell engineering to improve the maturation of recombinant monoclonal antibody N-glycosylation	130
Keywords	130
Abstract	130
7.1. Introduction	131
7.2. Materials and Methods	132
7.2.1. High throughput USER Cloning	132
7.2.2. Transfection and stable cell line generation	133
7.2.3. Confirmation of the overexpression	133
7.2.4. Cell culture and fed-batch process	134
7.2.5. mAb purification and glycoprofiling.....	134
7.2.6. Statistical analysis of glycoform distributions	134
7.2.7. Nucleotide sugar analysis	134
7.3. Results	134
7.3.1. Plasmids and cell line engineering	137
7.3.2. Fed-batch performance and mAb production.....	137
7.3.3. Glycosylation profiles of mAbs produced from engineered and parental cell lines ...	139
7.3.4. Intracellular nucleotide sugar metabolism.....	140
7.4. Discussion.....	140
7.5. Reference	143
Chapter 8 Conclusion and future perspectives.....	147

Appendix I: Supporting information of Chapter 3..... 148

Appendix II: Supporting information of Chapter 4 151

Appendix III: Supporting information of Chapter 6 156

Appendix IV: Supporting information of Chapter 7 157

Chapter 1 Introduction

This PhD thesis presents the work carried from January 2012 to December 2014 under my industrial PhD study. The study has been co-financed by an industrial PhD grant from Danish Agency for Science, Technology and Innovation and Symphogen A/S. The study was performed in collaboration between the research group Network Engineering of Eukaryotic Cell Factories, Department of Systems Biology, Technical University of Denmark and Symphogen A/S. Some of the work also involved international collaboration partners from Center for Process Systems Engineering, Department of Chemical Engineering, Imperial College London and Department of Chemical and Biomolecular Engineering, Johns Hopkins University.

The aim of this thesis is to investigate different possibilities to direct monoclonal antibody (mAb) N-glycosylation in Chinese hamster ovary (CHO) cells towards more desired patterns, and at the same time, to analyze and understand the genetic features, metabolic networks, and physiological properties of the cells that control the process of N-glycosylation. In this thesis, metabolic engineering of CHO cells via both process and genetic manipulations to optimize mAb glycosylation were studied. Many valuable understandings concerning impact, control and improvement of mAb glycosylation were discussed.

The thesis contains a collection of published articles and unpublished manuscripts, which provide both literature reviews with up-to-date knowledge in this field and a number of study cases reflecting industrial applications of the results.

1.1. Structure of the thesis

Chapter 2 provides general background knowledge to this work by presenting a review of the impact of glycosylation on mAb properties and the techniques used for accessing protein glycosylation. Furthermore, to provide status and relevant industrial application in this research field, the chapter also presents a review of process and genetic engineering on N-glycosylation of recombinant proteins. This work has been written as **Fan Y**, Weilguny D, Andersen MR. Glycosylation: impact, analysis and control in biopharmaceuticals (Manuscript in Preparation).

Chapter 3 presents a study case of changing antibody production and glycosylation by controlling amino acid and glucose metabolism in CHO cell fed-batch process. The work provides a comprehensive understanding of glycosylation in CHO cells from metabolic perspectives. The content of this chapter has been published in *Biotechnology and Bioengineering*: **Fan Y**, Jimenez Del Val I, Müller C, Wagtberg Sen J, Rasmussen SK, Kontoravdi C, Weilguny D, Andersen MR.

Amino acid and glucose metabolism in fed-batch CHO cell culture affects antibody production and glycosylation. *Biotechnology and Bioengineering*, 2014 (DOI: <http://dx.doi.org/10.1002/bit.25450>).

Chapter 4 presents another study case of glycosylation manipulation through process engineering, in which impact on N-glycosylation by addition of different feed additives that are expected to be involved in nucleotide sugars (NSs) synthesis pathway were investigated. This work has been drafted as Kildegaard HF, **Fan Y**, Wagtberg Sen J, Larsen B, and Andersen MR. Glycoprofiling the effect of media additives on IgG produced by CHO cells in fed-batch bioreactors (Shared first author; Manuscript in Preparation).

Chapter 5 provides a review of systems biology and genome-scale modeling that has been reported in CHO cells. The application of omics data in generating computational models for predictive and descriptive analysis of CHO cellular metabolism and in providing perspectives for protein production was described. This work has been published as Kaas CS, **Fan Y**, Weilguny D, Kristensen C, Kildegaard HF, Andersen MR. Towards genome-scale-models of the Chinese hamster ovary cells: incentives, status, and perspectives. *Pharmaceutical Bioprocessing*, 2014, 2 (5).

Chapter 6, a study case of applying the concepts from Chapter 5, describes an approach for understanding mAb glycosylation using systems-biology based analysis including metabolic and proteomic data in order to find the suitable operation window of some traditional critical process parameters. This work has been submitted to *Biotechnology and Bioengineering* as **Fan Y**, Jimenez Del Val I, Müller C, Lund AM, Wagtberg Sen J, Rasmussen SK, Kontoravdi C, Betenbaugh MJ, Weilguny D, Andersen MR. Systems-based investigation into the effect of glucose starvation and culture duration on fed-batch CHO cell culture (Submitted).

Chapter 7 describes a case of glyco-optimization via genetic engineering approach in CHO cells. In this study, two key enzymes involved in glycosylation processing were overexpressed in engineered cell lines. The effect of that was studied from glycomic and metabolic points of view. This work has been described in **Fan Y**, Jimenez Del Val I, Müller C, Wagtberg Sen J, Rasmussen SK, Kontoravdi C, Betenbaugh MJ, Weilguny D, Andersen MR. Chinese hamster ovary cell engineering to improve the maturation of recombinant monoclonal antibody N-glycosylation (Manuscript in Preparation).

Finally, **Chapter 8** contains conclusions and perspectives of the obtained results in this thesis.

Chapter 2 Glycosylation: impact and control in mAb production

Yuzhou Fan^{1,2}, Dietmar Weilguny^{2,*}, Mikael R. Andersen^{1,*}

¹Department of Systems Biology, Technical University of Denmark, Denmark

²Symphogen A/S, Ballerup, Denmark

*Corresponding author.

Address correspondence to Mikael Rørdam Andersen, Department of Systems Biology, Technical University of Denmark, Building 223, 2800 Kgs. Lyngby, Denmark; +4545252675; mr@bio.dtu.dk

Address correspondence to Dietmar Weilguny, Cell line and Upstream, Symphogen A/S, Pederstrupvej 93, 2750 Ballerup, Denmark; +4588382683; dw@symphogen.com

Biopharmaceuticals, also known as biologics, is a major source of medical innovation that opens up novel treatment possibilities in the future for many difficult-to-treat diseases. They are normally defined as non-chemically synthesized medicinal products, which manufactured by living organisms using biotechnology other than direct extract from a non-engineered biological source (Rader 2008). They are usually complex macromolecules consisting of proteins, sugars, nucleotides, lipids or their complex combinations, or even living cells and tissues. Until now, the majority of the marketed biopharmaceuticals are within the categories of recombinant vaccines and recombinant therapeutic proteins (Walsh 2014).

In 2013, the market size of biopharmaceuticals increased up to 140 billion USD. Monoclonal antibodies (mAbs), in particular, which could target cancer, infectious disease, inflammatory and autoimmune conditions generate 63 billion USD in sales (Walsh 2014). Mammalian cells will continue to dominant the expression platforms used for producing mAb for the immediate future, mainly because their adaptability in industrial application and capability of making appropriate N-glycosylation of recombinant protein that is suitable for human (Butler 2006; Shi and Goudar 2014). Among mammalian-based expression systems, Chinese hamster ovary (CHO) cells remain as the most commonly used work-horse for mAb production (Walsh 2014).

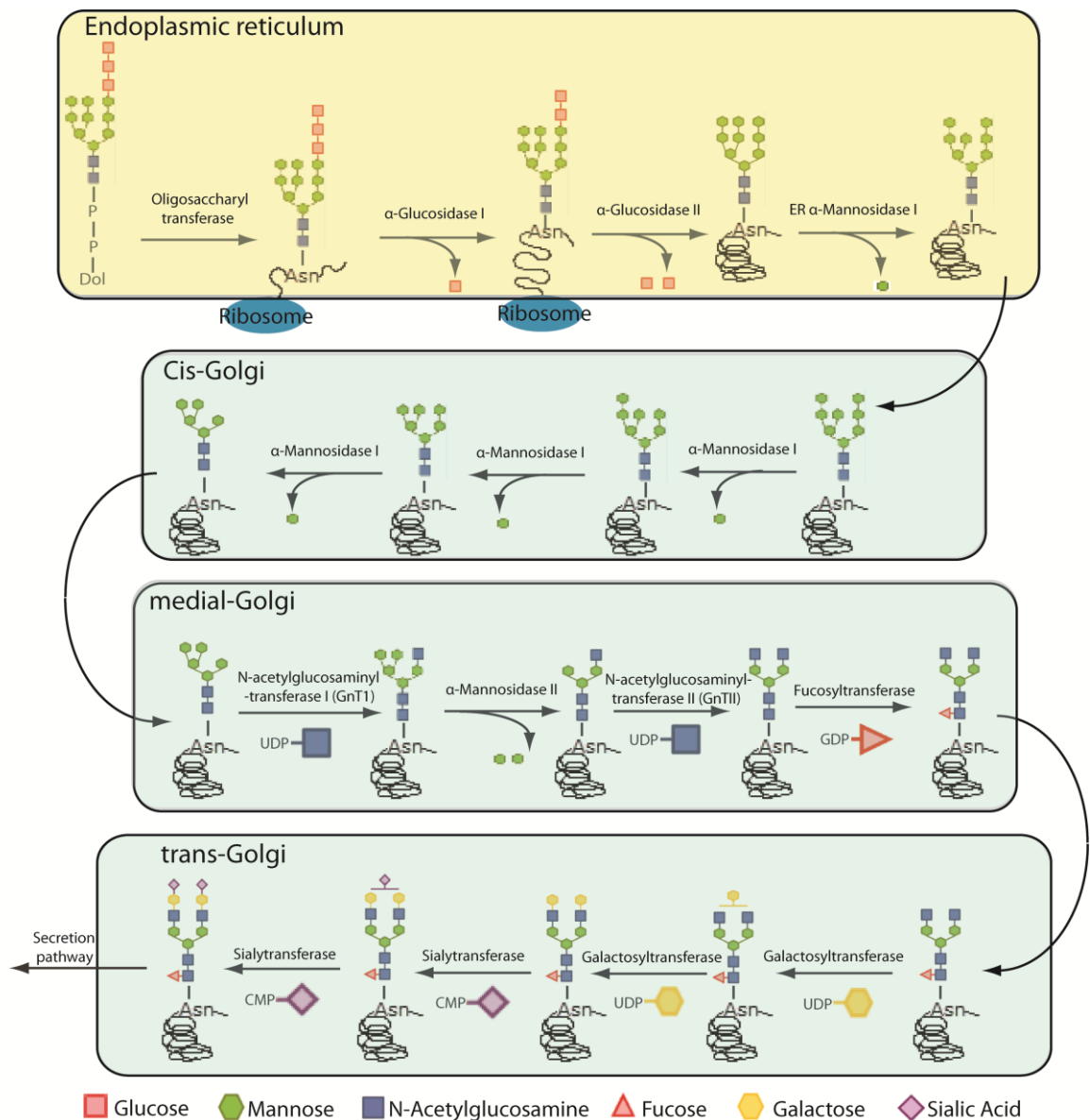


Figure 1. N-glycosylation processing pathway.

N-glycosylation profile is essential to ensure the physicochemical, biological and clinical properties of mAbs, including structure stability, solubility, serum half-life, effector function, efficacy, immunogenicity (Berger et al. 2012; Butler 2006; Costa et al. 2013) Consequently, the ability to monitor and control N-glycosylation becomes crucial in pharmaceutical bioprocessing as well as regulatory approval of mAb.

N-glycosylation is taken place in endoplasmic reticulum (ER) and Golgi apparatus with several steps of catalytic reactions driven by a repertoire of glycotransferases, glycosidases (Figure 1). These reactions consist of attachment of lipid-linked oligosaccharide precursor ($\text{Glc}_3\text{Man}_9\text{GlcNAc}_2\text{-PP-dolichol}$) to N-glycosylation site (an Asn-X-Ser/Thr sequon) of protein in question, a series of

glucose and mannose residues removal reactions and a number of sugar residue addition reactions (e.g. addition of N-acetylglucosamine (GlcNAc), galactose, fucose and sialic acid residues using UDP-GlcNAc, UDP-Galactose, GDP-Fucose, and CMP-Sialic acid as the substrates). Detailed N-glycosylation pathways have been described in the introduction section of Chapter 3.

N-glycosylation patterns are known to be largely dependent on factors such as 3D structure of the recombinant protein (Butler 2006; Hills et al. 2001), residence time in the Golgi, localizations and activities of the glycosylation processing enzymes (Ahn et al. 2008; Gawlitzek et al. 2000; Kodama et al. 1991; Pacis et al. 2011; Rivinoja et al. 2009; Schmelzer and Miller 2002), the availability of intracellular nucleotide sugar substrates (Barnabe and Butler 2000; Chee Fung Wong et al. 2005; Gramer et al. 2011; Hayter et al. 1992; Nyberg et al. 1999; Takuma et al. 2007; Wong et al. 2010b) and physiological condition of the protein processing machinery (Ahn et al. 2008; Senger and Karim 2003). A rapid growing exploration within this context is being conducted, with regard to (1) the impact of different glycoforms on the therapeutic properties of mAb, (2) the analytical techniques for accessing glycosylation information, (3) the influence of diverse process parameters, media and feed during the manufacturing process on mAb glycosylation, and (4) the strategies to engineer and optimize glycosylation to achieve better mAb quality.

2.1. N-Glycosylation patterns can affect therapeutic protein properties

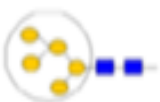
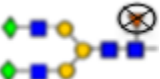




Stability and solubility of biopharmaceuticals is the major concerns for the storage, formulation and clinical application of the product, which has been reported to be largely dependent on appropriate N-glycosylation including site occupancy, length, branch, charge and terminal sugar residues of the glycans attached (Raju and Scallon 2007; Reuter and Gabius 1999; Sola and Griebenow 2009; Wittwer and Howard 1990; Yamane-Ohnuki and Satoh 2009).

Besides its physicochemical effects, glycosylation can also influence the therapeutic efficacy of the product (Table 2.1). First of all, serum half life has been shown to be mediated by structure of the glycans (Erbayraktar et al. 2003; Walsh and Jefferis 2006). In particular, terminal sugar residues of the glycans play a most important role in this property. Terminal mannose (Man) and GlcNAc, galactose (Gal) residues that have high affinity with various types of receptors in human may increase the clearance rate of the therapeutic protein (Jones et al. 2007; Wright et al. 2000). On the other hands, terminal N-acetylneuraminic acid (sialic acids, NANA) will increase the serum half life of the therapeutic protein (Egrie et al. 2003; Zhu 2012).

Secondly, glycosylation of mAb can change the conformational structure of the fragment crystallizable (Fc) region and exert a critical impact on the effector function such as antibody-

dependent cellular cytotoxicity (ADCC) and complement-dependent cytotoxicity (CDC) by modulating the binding specificities and affinities to Fc γ receptors (a protein that can bind to Fc part of a IgG and can be found at the surface of different immune cells, for example B lymphocytes, natural killer cells and macrophages) and complement component C1q (Crispin et al. 2009; Jefferis 2009; Matsumiya et al. 2007; Raju 2008). Thirdly, galactose- α -1,3-galactose and N-glycolylneraminic acid (NGNA) structures in glycans are known to be immunogenic to humans and CHO derived recombinant glycoproteins can bear small amount of this structures (Lammerts van Bueren et al. 2011; Macher and Galili 2008; Padler-Karavani et al. 2008).

Table 2.1. List of reported impact of mAb glycosylation on their therapeutic efficacy

Glycan structures	Impact on mAb therapeutic efficacy	References
High Mannose 	Increased clearance rate; Enhanced ADCC; Reduced CDC; Increased immunogenicity	(Goetze et al. 2011; Jones et al. 2007; Raju 2003; Shi and Goudar 2014; Zhou et al. 2008)
Non-fucosylation 	Enhanced ADCC	(Ferrara et al. 2006; Iida et al. 2006; Shinkawa et al. 2003; Zhou et al. 2008)
Bisecting GlcNAc 	Enhanced ADCC	(Abes et al. 2010; Davies et al. 2001; Umana et al. 1999)
Terminal sialic acid 	Reduced clearance rate; Reduced ADCC	(Anthony et al. 2008; Kaneko et al. 2006; Scallon et al. 2007; Sonderrmann et al. 2001)
Terminal galactose 	Increased clearance rate; Enhanced CDC	(Costa et al. 2013; Hodoniczky et al. 2005; Raju 2003; Shinkawa et al. 2003)
Terminal GlcNAc 	Increased clearance rate; Enhanced CDC	(Jones et al. 2007; Malhotra et al. 1995; Raju 2008)

Galactose- α -1, 3-galactose structure	Highly immunogenic to human	(Lammerts van Bueren et al. 2011; Macher and Galili 2008)
---	-----------------------------	---



N-glycolylneuraminic acid (NGNA) structure	Highly immunogenic to human	(Berger et al. 2012; Padler-Karavani et al. 2008)
--	-----------------------------	---



2.2. Analytical techniques for accessing glycosylation information

Several techniques have been developed for accessing the glycosylation information from different aspects, in order to comprehensively understand and effectively control the process of glycosylation from following three levels: (1) the presence and structure of glycans; (2) the abundance of nucleotide sugars that are used as building blocks for the elongation of glycans; (3) the activity and expression of key enzymes for glycosylation processing such as nucleotide sugar synthetases and transporters, glycosyltransferases and glycosidases.

2.2.1. Glycosylation analysis

Glycosylation analysis can be done at the levels of glycoproteins, glycopeptides as well as glycans in order to measuring the degree of glycosylation.

Analysis of intact glycoproteins and glycopeptides is typically an easy, cheap and fast approach with relatively low resolution. Different degrees of glycosylation such as site occupancy and level of glycan maturation can normally be obtained using this approach. Analytical methods for example SDS-PAGE (Liu et al. 2014; Osborne and Brooks 2006; Roth et al. 2012), cation exchange (CEX)-based HPLC (Gaza-Bulsecu et al. 2008; Yan et al. 2009) (Chapter 6) and LC-MS analysis (Dalpathado and Desaire 2008; Fan et al. 2014) can be used to separate the glycoprotein or glycopeptides based on their molecular weight, surface charge and mass, respectively.

Glycan profiling, on the other hand, is a rather complicated, time-consuming and expensive approach, but is able to provide in-depth structural information of the glycans. This can be normally done by a fluorescent label based chromatographic method (Domann et al. 2007; Fan et al. 2014) or

a matrix-assisted laser desorption ionization (MALDI) or electrospray ionization (ESI) based mass spectrometry method (Marino et al. 2010; Roth et al. 2012).

2.2.2. *Nucleotide sugar analysis*

Nucleotide sugar analysis offers the possibility of accessing glycosylation at the substrate level of glycans. Analytical techniques including ion-pair reversed-phase high-performance liquid chromatography (IPRP HPLC) (Kochanowski et al. 2006; Nakajima et al. 2010; Rabina et al. 2001), high-performance ion-exchange chromatography (HPAEC) (Jimenez Del Val et al. 2013; Pels Rijcken et al. 1990; Tomiya et al. 2001), and capillary electrophoresis (Feng et al. 2008; Soo et al. 2004) were developed. Each method has its advantages and disadvantages in terms of analysis time, resolution and complexity in preparation for the analysis. IPRP HPLC, although is a relatively fast analysis (~30 min per sample), has always limitations in resolving certain species. HPAEC method, on the other hand, providing better resolution with few unresolved peaks, normally requires harsh buffer conditions (high pH) and long analysis time (> 50 min per sample). Additionally, capillary electrophoresis, a fast and high-resolution technique has some downsides of requiring laborious buffer preparation and sophisticated detection methods.

2.2.3. *Analysis of CHO glycosylation-related enzymes*

Since the maturation of glycans are supported and catalyzed by a series of enzymatic reaction, the expression of glycosylation-related enzymes is a key factor for monitoring glycosylation as well. In general, four different types of key enzymes have been considered in recent publications when investigating glycosylation: (1) Glycotransferases are responsible to transfer various sugar residues onto glycan chain using corresponding nucleotide sugars. (2) Glycosidases are the enzymes that can degrade glycans by trimming of specific sugar residues. (3) Nucleotide sugar synthetase drives the biosynthesis of nucleotide sugars, which are as building blocks for glycosylation. (4) Nucleotide sugar transporters that transport nucleotide sugars into ER and Golgi compartments and thus make them available for glycotransferases during the chain elongation reactions of glycan. Different analytical techniques for measuring the expression of CHO glycosylation-related enzymes have been reported. Several traditional approaches including quantitative real-time PCR (qRT-PCR) analysis (Chen and Harcum 2006; Clark et al. 2005; Pacis et al. 2011; Wong et al. 2010a), western blot analysis (Fan et al. 2014), and CHO glyco-gene microarray (Wong et al. 2010b) were successfully carried out and shown to be able to deliver accurate and reproducible results. In the light of the development of CHO genomics (Cao et al. 2012; Lewis et al. 2013; Xu et al. 2011), more advanced approaches became possible for glycosylation-related gene analysis in CHO,

including transcriptome and proteome analysis using RNA-sequencing (RNA-seq) (McGettigan 2013) and the tandem mass spectrometry (Baycin-Hizal et al. 2012), respectively.

In parallel with the maturation of techniques measuring the expressions of glycosylation-related enzymes, functional assays that quantify the activities of these enzymes were also developed. To analyze the activities of glycosyltransferases, conventional radiochemical, immunological, phosphates-coupled and pH-based assays were existed (Palcic and Sujino 2001; Wagner and Pesnot 2010; Wu et al. 2011), but all with limitation in the context of throughput. Recently, novel assays with the ability of high throughput screening of universal glycosyltransferases were developed in the light of the advance in sensor technology, for example fluorescent ATP sensor and 1-Zn(II) NDP sensor (Lee and Thorson 2011; Ryu et al. 2014). Regarding functional analysis of nucleotide sugar transporters, even though some impressive results have been reported (Hadley et al. 2014; Norambuena et al. 2002; Roy et al. 2000; Suda et al. 2004), no high-throughput assay has been developed yet.

2.3. N-Glycosylation control and modulation

N-glycosylation can be controlled and tuned by media and feed, culture process and genetic engineering approaches. In the following section, different strategies to influence protein N-glycosylation will be reviewed.

2.3.1. Media, feed and culture process

Manipulation of process parameters and optimization of media and feed are the traditional approaches to improve cell growth and product titer. These approaches have also been demonstrated to be efficient in controlling protein N-glycosylation (Hossler et al. 2009). Classical media components in animal cell culture, for example glucose, galactose, glutamine, NH_4^+ , and other amino acids and typical feed additives such as manganese, sodium butyrate, and nucleotide and nucleotide sugar precursors have been shown to have a crucial influence on N-glycosylation. Additionally, impact of process parameters including dissolved oxygen, pCO_2 , pH, temperature, agitation rate, and culture duration on N-glycosylation has also been well studied in animal cell culture. In table 2.2, we summarized the updated main findings reported in this field.

Table 2.2. Effect of media, feed and culture process on therapeutic protein N-glycosylation.

IFN- β : Interferon beta; IFN- γ : Interferon gamma; EPO: Erythropoietin; CTLA4Ig: Fusion protein of cytotoxic T-lymphocyte-associated protein 4 and antibodies; TIMP-1: Tissue inhibitor of metalloproteinase 1; TNFR-IgG: Fusion protein of tumor necrosis factor receptor and IgG; tPA: Tissue plasminogen activator.

Variables	Effect on protein N-glycosylation	Reference
Glucose	<ul style="list-style-type: none"> Glucose starvation decreased site occupancy, galactosylation and sialylation of mAb. 	(Liu et al. 2014) (Chee Fung Wong et al. 2005)
	<ul style="list-style-type: none"> Glucose limitation increased high mannose and decreased sialylation of IFN-γ. 	(Nyberg et al. 1999)
	<ul style="list-style-type: none"> Glucose limitation decreased site occupancy of IFN-γ by limiting UTP and consequently UDP-GlcNAc synthesis. 	(Nahrgang et al. 2002) (Fan et al. 2014)
	<ul style="list-style-type: none"> Glucose addition increased galactosylation of mAb. 	(Chapter 6)
	<ul style="list-style-type: none"> High specific glucose consumption rate improved the maturation of glycans of mAb. 	
	<ul style="list-style-type: none"> Glucose starvation at stationary phase of fed-batch culture reduced specific productivity of mAb (q_p) and thus improved the maturation of glycans of mAb. 	
	Galactose	<ul style="list-style-type: none"> Galactose feeding increased fully galactosylated N-glycans.
<ul style="list-style-type: none"> Galactose feeding increased galactosylation of a CTLA4Ig fusion protein. 		(Chapter 4)
<ul style="list-style-type: none"> Galactose addition increased galactosylation of mAb. 		
Glutamine	<ul style="list-style-type: none"> Glutamine limitation decreased site occupancy of IFN-γ by limiting UDP-GlcNAc synthesis. 	(Nyberg et al. 1999) (Fan et al. 2014)
	<ul style="list-style-type: none"> Glutamine limitation increased Man5 glycan in mAb by limiting UDP-GlcNAc synthesis. 	(Gawlitzeck et al. 2000)
	<ul style="list-style-type: none"> Glutamine addition lead to high ammonium accumulation, and thus decreased galactosylation and sialylation of a recombinant TNFR-IgG fusion protein. 	

Amino acids	<ul style="list-style-type: none"> • Supplementing amino acids (cysteine, isoleucine, leucine, tryptophan, valine, asparagine, aspartate, and glutamate) that have been depleted in the cell culture increased sialylation of EPO. • High specific amino acid consumption rate increased NH_4^+ concentration in cell culture and thus increased Man5 glycan of mAb. 	<p>(Crowell et al. 2007)</p> <p>(Fan et al. 2014)</p>
NH_4^+	<ul style="list-style-type: none"> • High NH_4^+ concentration decreased galactosylation and sialylation of a recombinant TNFR-IgG fusion protein. • High NH_4^+ concentration correlated with low GlcNAc occupancy and high Man5 glycan of mAb. 	<p>(Gawlitzeck et al. 2000)</p> <p>(Fan et al. 2014)</p>
Mn_2^+	<ul style="list-style-type: none"> • Addition of Mn_2^+ increased site occupancy of N-glycosylation, galactosylation of EPO. 	<p>(Crowell et al. 2007)</p>
Nucleotide and nucleotide sugar precursors	<ul style="list-style-type: none"> • N-acetylmannosamine (ManNAc) addition increased sialylation of IFN-γ. • Glucosamine addition decreased EPO sialylation. • Glucosamine and uridine supplementation increased N-glycan antennarity, but decreased sialylation of TIMP-1 produced in CHO. • Feeding galactose + uridine + Mn_2^+ increased galactosylation of mAb. • Feeding galactose \pm uridine, glucosamine \pm uridine and ManNAc \pm cytidine increased sialylation of IFN-γ. 	<p>(Gu and Wang 1998)</p> <p>(Yang and Butler 2002)</p> <p>(Baker et al. 2001)</p> <p>(Gramer et al. 2011)</p> <p>(Wong et al. 2010b)</p>
Sodium butyrate	<ul style="list-style-type: none"> • Sodium butyrate addition increased sialylation of IFN-γ. • Sodium butyrate addition decreased mAb galactosylation. • Sodium butyrate addition increased tPA site occupancy of Asn-184. • Sodium butyrate addition decreased N- 	<p>(Lamotte et al. 1999)</p> <p>(Hong et al. 2014)</p> <p>(Andersen et al. 2000)</p> <p>(Borys et al. 2010)</p>

glycolylneuraminic acid (NGNA) content of a recombinant fusion protein.

Glycerol	<ul style="list-style-type: none"> • Glycerol addition increased sialylation of IFN-β 	(Rodriguez et al. 2005)
Monensin	<ul style="list-style-type: none"> • Addition of monensin increased high mannose glycan of mAb. 	(Rothman et al. 1989)
Lipids	<ul style="list-style-type: none"> • Lipids increased site occupancy of IFN-γ. • Lipoprotein addition increased the the proportion of fully-glycosylated IFN-γ. 	<p>(Castro et al. 1995)</p> <p>(Jenkins et al. 1994)</p>
DMSO	<ul style="list-style-type: none"> • DMSO addition decreased sialylation of IFN-β. 	(Rodriguez et al. 2005)
pH	<ul style="list-style-type: none"> • Different culture pH (6.9, 7.2 and 7.4) setpoints affected galactosylation and sialylation of mAb. • Lowering culture pH increased sialylation of EPO. • pH variations (< 6.9 and > 8.2) decreased overall glycosylation of a mouse placental lactogen. • Using sodium hydroxide instead of sodium carbonate as the base to regulate culture pH, decrease NGNA content of a recombinant fusion protein. 	<p>(Muthing et al. 2003)</p> <p>(Yoon et al. 2005)</p> <p>(Borys et al. 1993)</p> <p>(Borys et al. 2010)</p>
pCO ₂	<ul style="list-style-type: none"> • Elevated pCO₂ decreased polysialylation. • Elevated pCO₂ decreased NGNA content of tPA. 	<p>(Zanghi et al. 1998)</p> <p>(Kimura and Miller 1997)</p>
Temperature	<ul style="list-style-type: none"> • Temperature shift from 37°C to 33 or 30°C decreased sialylation of an EPO-Fc fusion protein. • Sialylation profiles of EPO are comparable among culture temperature at 37, 33 or 30°C. • Late temperature shift near the stationary phase compared to early temperature shift at exponential phase decreased NGNA content of a recombinant fusion protein. 	<p>(Trummer et al. 2006)</p> <p>(Yoon et al. 2003)</p> <p>(Borys et al. 2010)</p>

Dissolved oxygen	• Decreased level of DO reduced galactosylation of mAb.	(Kunkel et al. 1998)
	• High DO increased NANA content of a recombinant follicle stimulating hormone.	(Chotigeat et al. 1994) (Lin et al. 1993)
	• Low DO caused almost no change in the glycosylation of tPA.	(Hossler 2012)
	• The effect of DO on glycosylation seems to be cell specific and/or protein specific.	
Agitation rate	• High agitation rate that caused high shear stress decreased N-glycan site occupancy of mAb.	(Senger and Karim 2003)
Culture duration	• Increased culture duration increased high mannose structure of mAb	(Robinson et al. 1994) (Pacis et al. 2011)
	• Increased culture duration increased Man5 glycan of mAb	(Chee Fung Wong et al. 2005) (Chapter 6)
	• Increased culture duration along with reduced viability, decreased sialylation of IFN- γ .	
	• Increased culture duration decreased the GlcNAc occupancy and galactosylation of mAb.	

2.3.2. Genetic engineering of glycosylation-related enzymes

The abilities of processing protein glycosylation inherent in various cell lines are largely related to the activities of a repertoire of glycosylation-related enzymes. These enzymes, such as glycotransferases, glycosidases, and nucleotide sugar transporters are typically located in ER or Golgi and involve in biosynthesis and degradation of glycans. Many successful attempts at modulating protein glycosylation toward desired patterns have been shown by CHO cell line engineering of these enzymes individually or in combinations. These attempts have included strategies such as knock-in of new genes, and overexpression and knock-down/out existed genes in the cells.

As mentioned in earlier section, high NANA content is beneficial for increasing the serum half-life of recombinant therapeutic proteins. Therefore, many effects have been put into the area of maximizing NANA level for recombinant therapeutic proteins. A research group that over-

expressed α -2, 3-sialyltransferase (α -2, 3-SiaT) in CHO cells, significantly increased NANA content and decreased the microheterogeneity in the produced a fusion protein of tumor necrosis factor receptor and IgG (TNFR-IgG) and tissue plasminogen activator (tPA) (Weikert et al. 1999). Another research group targeted this issue from an opposite direction by reducing the removal of NANA residues from glycan. They knock-down sialidase expression using antisense RNA, which increased NANA content of the produced Dnase (Ferrari et al. 1998). Additionally, increasing sialylation has also done by using a strategy of improving the availability of CMP-sialic acid as well. This has been achieved through knock-down the expression of CMP- sialic acid hydroxylase to increase the intracellular level of CMP- sialic acid (Chenu et al. 2003), as well as overexpression of CMP-sialic acid transporter (Wong et al. 2006) to increase CMP-sialic acid abundance in Golgi apparatus.

In order to improve ADCC activity of IgG, many attempts at, for example, adding bisecting GlcNAc structure to glycan and removing fucose residue from glycan were performed. A number of studies showed that knock-in N-acetylglucosaminyltransferase III (GnTIII) in CHO cells can introduce a bisecting GlcNAc structure into the glycan of produced IgG (Davies et al. 2001; Umana et al. 1999). Additionally, many strategies have been proposed to increasing the removal of fucose residue in the glycan. Some of the most pronounced ones are knock-down/out fucosyltransferase VIII (FucTVIII) and/or GDP-mannose 4, 6-dehydratase (GMD) in order to partially or completely block GDP-Fucose biosynthesis and eventually reduce the level of fucosylation (Imai-Nishiya et al. 2007; Kanda et al. 2007; Mori et al. 2004; Yamane-Ohnuki et al. 2004). Alternative approach of reducing fucosylation was also reported by a group of researcher recently. They reduced the availability of GDP-Fucose by knock-in a bacteria enzyme GDP-6-deoxy-D-lyxo-4-hexulose reductase (RMD) found in *Pseudomonas aeruginosa* into a CHO cell line producing IgG (von Horsten et al. 2010). This enzyme can redirect a precursor in the GDP-Fucose biosynthesis pathway towards generating a new compound rather than GDP-Fucose.

Recent CHO genome sequencing presents us great potential and more targets for implementing genetic engineering of glycosylation (Xu et al. 2011). In comparison with human genome, a number of non-expressed genes in CHO-K1 cell line were founded, including GnTIII, α (1,2), α (1,3) and α (1,4)-linked fucosyltransferases and α -2,6-sialyltransferase. Therefore, knock-in of these genes may establish CHO cell lines with gain-of-function phenotypes. On the other hand, there are also glycosylation genes found in CHO genome but not to be expressed in humans, for example cytidine monophosphate-N-acetylneuraminic acid hydroxylase (CMAH) which can hydroxylate NANA to NGNA and α (1,3) galactosyltransferase which can produce galactose- α -1,3-galactose glycan

structure. The expression of these genes has to be well-controlled because they have the potential to produce foreign glycan structure, which may trigger immunogenic responses in human. More successful cases regarding genetic engineering of glycosylation can be reviewed in Table 2.3.

Table 2.3. A list of reported genetic engineering of glycosylation in CHO cells. Abbreviations: GnT: N-acetylglucosaminyltransferase. FucT: fucosyltransferase. SiaT: sialyltransferase. GalT: galactosyltransferase. GMD: GDP-mannose 4,6-dehydratase. RMD: GDP-6-deoxy-D-lyxo-4-hexulose reductase.

Target enzymes	Method	Effect	Reference
α -1,6-FucT (FucTVIII)	Knock-out	Complete removal of fucose in glycans of mAb	(Yamane-Ohnuki et al. 2004)
α -1,6-FucT (FucTVIII)	Knock-down	Increase afucosylation of mAb	(Mori et al. 2004)
α -2,3-SiaT	Overexpression	Increase sialylation of a TNFR-IgG fusion protein	(Weikert et al. 1999)
α -2,6-SiaT	Knock-in	Increase sialylation of EPO	(Zhang et al. 1998)
α -2,6-SiaT	Knock-in	Increase sialylation of mAb	(Jassal et al. 2001)
β -1,4-GalT	Overexpression	Increase galactosylation of a TNFR-IgG fusion protein	(Weikert et al. 1999)
Sialidase	Knock-down	Increase sialylation of DNase	(Ferrari et al. 1998)
CMP-sialic acid transporter	Overexpression	Increase sialylation of IFN- γ	(Wong et al. 2006)
CMP-N-acetylneuraminic acid hydroxylase	Knock-down	Reduce NGNA content of the cells' own glycoconjugates	(Chenu et al. 2003)
UDP-GlcNAc transporter	Overexpression	Partially restored galactosylation of glycoprotein in a mutant CHO cell line defective in UDP-Gal transporter	(Maszczak-Seneczko et al. 2011)

UDP-GlcNAc transporter	Overexpression	Cannot increase GlcNAc and Gal occupancy of mAb	(Chapter 7)
GnTI	Knock-out	Produce mAb with 100% high mannose glycans	(Sealover et al. 2013)
GnTI	Overexpression	Increase GlcNAc occupancy of mAb	(Chapter 7)
GMD	Knock-out	Complete removal of fucose in glycans of mAb	(Kanda et al. 2007)
GMD and α -1,6-FucT (FucTVIII)	Knock-down	Generating fully non-fucosylated mAb	(Imai-Nishiya et al. 2007)
GnT III	Knock-in	Addition of bisecting GlcNAc of mAb	(Davies et al. 2001; Umana et al. 1999)
GnTV	Knock-out	Eliminate all tetra-antennary structures by complete removal of GlcNAc β (1,6)Man α (1,6)-branched N-glycans	(North et al. 2010)
α -1,3-FucT (FucTVI)	Knock-in	Addition of single or multiple fucosylation structures including Lewis ^x , sialyl Lewis ^x structures and their combinations.	(North et al. 2010)
α -1,3-FucT (FucTIV and FucTIX)	Knock-in	Addition of extremely high amount of single or multiple Lewis ^x fucosylation structures.	(North et al. 2010)
α -1,3-FucT (FucTIX)	Knock-in	Addition of single or multiple Lewis ^x fucosylation structures.	(North et al. 2010)
<i>Arthrobacter ureafaciens</i> sialidase A catalytic domain	Knock-in	Decreased sialylation of mAb	(Naso et al. 2010)

2.4. Executive summary

- Understanding and in-depth knowledge on the function of N-glycosylation in therapeutic protein is important in development of biopharmaceuticals as it can provide the target glycopatterns for glycosylation modulation and optimization.
- The future trend of development in analytical techniques accessing N-glycosylation is towards faster, simpler, higher resolution and throughput methods that can analyze factors that involves in glycosylation process from multiple aspects (e.g. structure of glycans, abundance of precursors for glycosylation, activity of glyco-related enzymes) during different stages of process development.
- Controlling and modulating N-glycosylation for better therapeutic proteins can be achieved through process and media optimization, genetic engineering of cell lines and the combinations of these strategies.

2.5. References

- Abes R, Gelize E, Fridman WH, Teillaud JL. 2010. Long-lasting antitumor protection by anti-CD20 antibody through cellular immune response. *Blood* 116(6):926-34.
- Ahn WS, Jeon JJ, Jeong YR, Lee SJ, Yoon SK. 2008. Effect of culture temperature on erythropoietin production and glycosylation in a perfusion culture of recombinant CHO cells. *Biotechnol Bioeng* 101(6):1234-44.
- Andersen D. 2004. Cell culture effects on the glycosylation of therapeutic proteins. *Bioprocess International IBC LifeSciences*.
- Andersen DC, Bridges T, Gawlitzek M, Hoy C. 2000. Multiple cell culture factors can affect the glycosylation of Asn-184 in CHO-produced tissue-type plasminogen activator. *Biotechnol Bioeng* 70(1):25-31.
- Anthony RM, Nimmerjahn F, Ashline DJ, Reinhold VN, Paulson JC, Ravetch JV. 2008. Recapitulation of IVIG anti-inflammatory activity with a recombinant IgG Fc. *Science* 320(5874):373-6.
- Baker KN, Rendall MH, Hills AE, Hoare M, Freedman RB, James DC. 2001. Metabolic control of recombinant protein N-glycan processing in NS0 and CHO cells. *Biotechnol Bioeng* 73(3):188-202.

- Barnabe N, Butler M. 2000. The effect of glucose and glutamine on the intracellular nucleotide pool and oxygen uptake rate of a murine hybridoma. *Cytotechnology* 34(1-2):47-57.
- Baycin-Hizal D, Tabb DL, Chaerkady R, Chen L, Lewis NE, Nagarajan H, Sarkaria V, Kumar A, Wolozny D, Colao J and others. 2012. Proteomic analysis of Chinese hamster ovary cells. *J Proteome Res* 11(11):5265-76.
- Berger M, Kaup M, Blanchard V. 2012. Protein glycosylation and its impact on biotechnology. *Adv Biochem Eng Biotechnol* 127:165-85.
- Borys MC, Dalal NG, Abu-Absi NR, Khattak SF, Jing Y, Xing Z, Li ZJ. 2010. Effects of culture conditions on N-glycolylneuraminic acid (Neu5Gc) content of a recombinant fusion protein produced in CHO cells. *Biotechnol Bioeng* 105(6):1048-57.
- Borys MC, Linzer DI, Papoutsakis ET. 1993. Culture pH affects expression rates and glycosylation of recombinant mouse placental lactogen proteins by Chinese hamster ovary (CHO) cells. *Biotechnology (N Y)* 11(6):720-4.
- Butler M. 2006. Optimisation of the cellular metabolism of glycosylation for recombinant proteins produced by Mammalian cell systems. *Cytotechnology* 50(1-3):57-76.
- Cao Y, Kimura S, Itoi T, Honda K, Ohtake H, Omasa T. 2012. Construction of BAC-based physical map and analysis of chromosome rearrangement in Chinese hamster ovary cell lines. *Biotechnol Bioeng* 109(6):1357-67.
- Castro PM, Ison AP, Hayter PM, Bull AT. 1995. The macroheterogeneity of recombinant human interferon-gamma produced by Chinese-hamster ovary cells is affected by the protein and lipid content of the culture medium. *Biotechnol Appl Biochem* 21 (Pt 1):87-100.
- Chee Fung Wong D, Tin Kam Wong K, Tang Goh L, Kiat Heng C, Gek Sim Yap M. 2005. Impact of dynamic online fed-batch strategies on metabolism, productivity and N-glycosylation quality in CHO cell cultures. *Biotechnol Bioeng* 89(2):164-77.
- Chen P, Harcum SW. 2006. Effects of elevated ammonium on glycosylation gene expression in CHO cells. *Metab Eng* 8(2):123-32.
- Chenu S, Gregoire A, Malykh Y, Visvikis A, Monaco L, Shaw L, Schauer R, Marc A, Goergen JL. 2003. Reduction of CMP-N-acetylneuraminic acid hydroxylase activity in engineered Chinese hamster ovary cells using an antisense-RNA strategy. *Biochim Biophys Acta* 1622(2):133-44.
- Chotigeat W, Watanapokasin Y, Mahler S, Gray PP. 1994. Role of environmental conditions on the expression levels, glycoform pattern and levels of sialyltransferase for hFSH produced by recombinant CHO cells. *Cytotechnology* 15(1-3):217-21.

- Clark KJ, Griffiths J, Bailey KM, Harcum SW. 2005. Gene-expression profiles for five key glycosylation genes for galactose-fed CHO cells expressing recombinant IL-4/13 cytokine trap. *Biotechnol Bioeng* 90(5):568-77.
- Costa AR, Rodrigues ME, Henriques M, Oliveira R, Azeredo J. 2013. Glycosylation: impact, control and improvement during therapeutic protein production. *Crit Rev Biotechnol*.
- Crispin M, Bowden TA, Coles CH, Harlos K, Aricescu AR, Harvey DJ, Stuart DI, Jones EY. 2009. Carbohydrate and domain architecture of an immature antibody glycoform exhibiting enhanced effector functions. *J Mol Biol* 387(5):1061-6.
- Crowell CK, Grampp GE, Rogers GN, Miller J, Scheinman RI. 2007. Amino acid and manganese supplementation modulates the glycosylation state of erythropoietin in a CHO culture system. *Biotechnol Bioeng* 96(3):538-49.
- Dalpathado DS, Desaire H. 2008. Glycopeptide analysis by mass spectrometry. *Analyst* 133(6):731-8.
- Davies J, Jiang L, Pan LZ, LaBarre MJ, Anderson D, Reff M. 2001. Expression of GnTIII in a recombinant anti-CD20 CHO production cell line: Expression of antibodies with altered glycoforms leads to an increase in ADCC through higher affinity for FC gamma RIII. *Biotechnol Bioeng* 74(4):288-94.
- Domann PJ, Pardos-Pardos AC, Fernandes DL, Spencer DI, Radcliffe CM, Royle L, Dwek RA, Rudd PM. 2007. Separation-based glycoprofiling approaches using fluorescent labels. *Proteomics* 7 Suppl 1:70-6.
- Egrie JC, Dwyer E, Browne JK, Hitz A, Lykos MA. 2003. Darbepoetin alfa has a longer circulating half-life and greater in vivo potency than recombinant human erythropoietin. *Exp Hematol* 31(4):290-9.
- Erbayraktar S, Grasso G, Sfacteria A, Xie QW, Coleman T, Kreilgaard M, Torup L, Sager T, Erbayraktar Z, Gokmen N and others. 2003. Asialoerythropoietin is a nonerythropoietic cytokine with broad neuroprotective activity in vivo. *Proc Natl Acad Sci U S A* 100(11):6741-6.
- Fan Y, Jimenez Del Val I, Müller C, Wagtberg Sen J, Rasmussen SK, Kontoravdi C, Weilguny D, Andersen MR. 2014. Amino acid and glucose metabolism in fed-batch CHO cell culture affects antibody production and glycosylation. *Biotechnology and Bioengineering*:n/a-n/a.
- Feng HT, Wong N, Wee S, Lee MM. 2008. Simultaneous determination of 19 intracellular nucleotides and nucleotide sugars in Chinese Hamster ovary cells by capillary electrophoresis. *J Chromatogr B Analyt Technol Biomed Life Sci* 870(1):131-4.

- Ferrara C, Stuart F, Sondermann P, Brunker P, Umana P. 2006. The carbohydrate at FcγRIIIa Asn-162. An element required for high affinity binding to non-fucosylated IgG glycoforms. *J Biol Chem* 281(8):5032-6.
- Ferrari J, Gunson J, Lofgren J, Krummen L, Warner TG. 1998. Chinese hamster ovary cells with constitutively expressed sialidase antisense RNA produce recombinant DNase in batch culture with increased sialic acid. *Biotechnol Bioeng* 60(5):589-95.
- Gawlitzeck M, Ryll T, Lofgren J, Sliwkowski MB. 2000. Ammonium alters N-glycan structures of recombinant TNFR-IgG: degradative versus biosynthetic mechanisms. *Biotechnol Bioeng* 68(6):637-46.
- Gaza-Bulsecu G, Bulsecu A, Chumsae C, Liu H. 2008. Characterization of the glycosylation state of a recombinant monoclonal antibody using weak cation exchange chromatography and mass spectrometry. *J Chromatogr B Analyt Technol Biomed Life Sci* 862(1-2):155-60.
- Goetze AM, Liu YD, Zhang Z, Shah B, Lee E, Bondarenko PV, Flynn GC. 2011. High-mannose glycans on the Fc region of therapeutic IgG antibodies increase serum clearance in humans. *Glycobiology* 21(7):949-59.
- Gramer MJ, Eckblad JJ, Donahue R, Brown J, Shultz C, Vickerman K, Priem P, van den Bremer ET, Gerritsen J, van Berkel PH. 2011. Modulation of antibody galactosylation through feeding of uridine, manganese chloride, and galactose. *Biotechnol Bioeng* 108(7):1591-602.
- Gu X, Wang DI. 1998. Improvement of interferon-gamma sialylation in Chinese hamster ovary cell culture by feeding of N-acetylmannosamine. *Biotechnol Bioeng* 58(6):642-8.
- Hadley B, Maggioni A, Ashikov A, Day CJ, Haselhorst T, Tiralongo J. 2014. Structure and function of nucleotide sugar transporters: Current progress. *Comput Struct Biotechnol J* 10(16):23-32.
- Hayter PM, Curling EM, Baines AJ, Jenkins N, Salmon I, Strange PG, Tong JM, Bull AT. 1992. Glucose-limited chemostat culture of Chinese hamster ovary cells producing recombinant human interferon-gamma. *Biotechnol Bioeng* 39(3):327-35.
- Hills AE, Patel A, Boyd P, James DC. 2001. Metabolic control of recombinant monoclonal antibody N-glycosylation in GS-NS0 cells. *Biotechnol Bioeng* 75(2):239-51.
- Hodoniczky J, Zheng YZ, James DC. 2005. Control of recombinant monoclonal antibody effector functions by Fc N-glycan remodeling in vitro. *Biotechnol Prog* 21(6):1644-52.
- Hong JK, Lee SM, Kim KY, Lee GM. 2014. Effect of sodium butyrate on the assembly, charge variants, and galactosylation of antibody produced in recombinant Chinese hamster ovary cells. *Appl Microbiol Biotechnol* 98(12):5417-25.

- Hossler P. 2012. Protein glycosylation control in Mammalian cell culture: past precedents and contemporary prospects. *Adv Biochem Eng Biotechnol* 127:187-219.
- Hossler P, Khattak SF, Li ZJ. 2009. Optimal and consistent protein glycosylation in mammalian cell culture. *Glycobiology* 19(9):936-49.
- Iida S, Misaka H, Inoue M, Shibata M, Nakano R, Yamane-Ohnuki N, Wakitani M, Yano K, Shitara K, Satoh M. 2006. Nonfucosylated therapeutic IgG1 antibody can evade the inhibitory effect of serum immunoglobulin G on antibody-dependent cellular cytotoxicity through its high binding to FcγRIIIa. *Clin Cancer Res* 12(9):2879-87.
- Imai-Nishiya H, Mori K, Inoue M, Wakitani M, Iida S, Shitara K, Satoh M. 2007. Double knockdown of alpha1,6-fucosyltransferase (FUT8) and GDP-mannose 4,6-dehydratase (GMD) in antibody-producing cells: a new strategy for generating fully non-fucosylated therapeutic antibodies with enhanced ADCC. *BMC Biotechnol* 7:84.
- Jassal R, Jenkins N, Charlwood J, Camilleri P, Jefferis R, Lund J. 2001. Sialylation of human IgG-Fc carbohydrate by transfected rat alpha2,6-sialyltransferase. *Biochem Biophys Res Commun* 286(2):243-9.
- Jefferis R. 2009. Glycosylation as a strategy to improve antibody-based therapeutics. *Nat Rev Drug Discov* 8(3):226-34.
- Jenkins N, Castro P, Menon S, Ison A, Bull A. 1994. Effect of lipid supplements on the production and glycosylation of recombinant interferon-gamma expressed in CHO cells. *Cytotechnology* 15(1-3):209-15.
- Jimenez Del Val I, Kyriakopoulos S, Polizzi KM, Kontoravdi C. 2013. An optimized method for extraction and quantification of nucleotides and nucleotide sugars from mammalian cells. *Anal Biochem* 443(2):172-80.
- Jones AJ, Papac DI, Chin EH, Keck R, Baughman SA, Lin YS, Kneer J, Battersby JE. 2007. Selective clearance of glycoforms of a complex glycoprotein pharmaceutical caused by terminal N-acetylglucosamine is similar in humans and cynomolgus monkeys. *Glycobiology* 17(5):529-40.
- Kanda Y, Imai-Nishiya H, Kuni-Kamochi R, Mori K, Inoue M, Kitajima-Miyama K, Okazaki A, Iida S, Shitara K, Satoh M. 2007. Establishment of a GDP-mannose 4,6-dehydratase (GMD) knockout host cell line: a new strategy for generating completely non-fucosylated recombinant therapeutics. *J Biotechnol* 130(3):300-10.
- Kaneko Y, Nimmerjahn F, Ravetch JV. 2006. Anti-inflammatory activity of immunoglobulin G resulting from Fc sialylation. *Science* 313(5787):670-3.

- Kimura R, Miller WM. 1997. Glycosylation of CHO-derived recombinant tPA produced under elevated pCO₂. *Biotechnol Prog* 13(3):311-7.
- Kochanowski N, Blanchard F, Cacan R, Chirat F, Guedon E, Marc A, Goergen JL. 2006. Intracellular nucleotide and nucleotide sugar contents of cultured CHO cells determined by a fast, sensitive, and high-resolution ion-pair RP-HPLC. *Anal Biochem* 348(2):243-51.
- Kodama S, Endo T, Tsuruoka N, Tsujimoto M, Kobata A. 1991. Carbohydrate structures of human interleukin 5 expressed in Chinese hamster ovary cells. *J Biochem* 110(5):693-701.
- Kunkel JP, Jan DC, Jamieson JC, Butler M. 1998. Dissolved oxygen concentration in serum-free continuous culture affects N-linked glycosylation of a monoclonal antibody. *J Biotechnol* 62(1):55-71.
- Lammerts van Bueren JJ, Rispens T, Verploegen S, van der Palen-Merkus T, Stapel S, Workman LJ, James H, van Berkel PH, van de Winkel JG, Platts-Mills TA and others. 2011. Anti-galactose- α -1,3-galactose IgE from allergic patients does not bind α -galactosylated glycans on intact therapeutic antibody Fc domains. *Nat Biotechnol* 29(7):574-6.
- Lamotte D, Buckberry L, Monaco L, Soria M, Jenkins N, Engasser JM, Marc A. 1999. Na-butyrate increases the production and α 2,6-sialylation of recombinant interferon- γ expressed by α 2,6-sialyltransferase engineered CHO cells. *Cytotechnology* 29(1):55-64.
- Lee HS, Thorson JS. 2011. Development of a universal glycosyltransferase assay amenable to high-throughput formats. *Anal Biochem* 418(1):85-8.
- Lewis NE, Liu X, Li Y, Nagarajan H, Yerganian G, O'Brien E, Bordbar A, Roth AM, Rosenbloom J, Bian C and others. 2013. Genomic landscapes of Chinese hamster ovary cell lines as revealed by the *Cricetulus griseus* draft genome. *Nat Biotechnol* 31(8):759-65.
- Lin AA, Kimura R, Miller WM. 1993. Production of tPA in recombinant CHO cells under oxygen-limited conditions. *Biotechnol Bioeng* 42(3):339-50.
- Liu B, Spearman M, Doering J, Lattova E, Perreault H, Butler M. 2014. The availability of glucose to CHO cells affects the intracellular lipid-linked oligosaccharide distribution, site occupancy and the N-glycosylation profile of a monoclonal antibody. *J Biotechnol* 170:17-27.
- Macher BA, Galili U. 2008. The Gal α 1,3Gal β 1,4GlcNAc-R (α -Gal) epitope: a carbohydrate of unique evolution and clinical relevance. *Biochim Biophys Acta* 1780(2):75-88.
- Malhotra R, Wormald MR, Rudd PM, Fischer PB, Dwek RA, Sim RB. 1995. Glycosylation changes of IgG associated with rheumatoid arthritis can activate complement via the mannose-binding protein. *Nat Med* 1(3):237-43.

- Marino K, Bones J, Kattla JJ, Rudd PM. 2010. A systematic approach to protein glycosylation analysis: a path through the maze. *Nat Chem Biol* 6(10):713-23.
- Maszczyk-Seneczko D, Olczak T, Jakimowicz P, Olczak M. 2011. Overexpression of UDP-GlcNAc transporter partially corrects galactosylation defect caused by UDP-Gal transporter mutation. *FEBS Lett* 585(19):3090-4.
- Matsumiya S, Yamaguchi Y, Saito J, Nagano M, Sasakawa H, Otaki S, Satoh M, Shitara K, Kato K. 2007. Structural comparison of fucosylated and nonfucosylated Fc fragments of human immunoglobulin G1. *J Mol Biol* 368(3):767-79.
- McGettigan PA. 2013. Transcriptomics in the RNA-seq era. *Curr Opin Chem Biol* 17(1):4-11.
- Mori K, Kuni-Kamochi R, Yamane-Ohnuki N, Wakitani M, Yamano K, Imai H, Kanda Y, Niwa R, Iida S, Uchida K and others. 2004. Engineering Chinese hamster ovary cells to maximize effector function of produced antibodies using FUT8 siRNA. *Biotechnol Bioeng* 88(7):901-8.
- Muthing J, Kemminer SE, Conradt HS, Sagi D, Nimtz M, Karst U, Peter-Katalinic J. 2003. Effects of buffering conditions and culture pH on production rates and glycosylation of clinical phase I anti-melanoma mouse IgG3 monoclonal antibody R24. *Biotechnol Bioeng* 83(3):321-34.
- Nahrgang S, Kkagten E, De Jesus M, Bourgeois M, Déjardin S, Von Stockar U, Marison IW. 2002. The Effect of Cell Line, Transfection Procedure and Reactor Conditions on the Glycosylation of Recombinant Human Anti-Rhesus D IgG1. In: Bernard A, Griffiths B, Noé W, Wurm F, editors. *Animal Cell Technology: Products from Cells, Cells as Products*: Springer Netherlands. p 259-261.
- Nakajima K, Kitazume S, Angata T, Fujinawa R, Ohtsubo K, Miyoshi E, Taniguchi N. 2010. Simultaneous determination of nucleotide sugars with ion-pair reversed-phase HPLC. *Glycobiology* 20(7):865-71.
- Naso MF, Tam SH, Scallan BJ, Raju TS. 2010. Engineering host cell lines to reduce terminal sialylation of secreted antibodies. *MAbs* 2(5):519-27.
- Norambuena L, Marchant L, Berninsone P, Hirschberg CB, Silva H, Orellana A. 2002. Transport of UDP-galactose in plants. Identification and functional characterization of AtUTr1, an *Arabidopsis thaliana* UDP-galactose/UDP-glucose transporter. *J Biol Chem* 277(36):32923-9.
- North SJ, Huang HH, Sundaram S, Jang-Lee J, Etienne AT, Trollope A, Chalabi S, Dell A, Stanley P, Haslam SM. 2010. Glycomics profiling of Chinese hamster ovary cell glycosylation mutants reveals N-glycans of a novel size and complexity. *J Biol Chem* 285(8):5759-75.

- Nyberg GB, Balcarcel RR, Follstad BD, Stephanopoulos G, Wang DI. 1999. Metabolic effects on recombinant interferon-gamma glycosylation in continuous culture of Chinese hamster ovary cells. *Biotechnol Bioeng* 62(3):336-47.
- Osborne C, Brooks SA. 2006. SDS-PAGE and Western blotting to detect proteins and glycoproteins of interest in breast cancer research. *Methods Mol Med* 120:217-29.
- Pacis E, Yu M, Autsen J, Bayer R, Li F. 2011. Effects of cell culture conditions on antibody N-linked glycosylation—what affects high mannose 5 glycoform. *Biotechnology and Bioengineering* 108(10):2348-2358.
- Padler-Karavani V, Yu H, Cao H, Chokhawala H, Karp F, Varki N, Chen X, Varki A. 2008. Diversity in specificity, abundance, and composition of anti-Neu5Gc antibodies in normal humans: potential implications for disease. *Glycobiology* 18(10):818-30.
- Palcic MM, Sujino K. 2001. Assays for glycosyltransferases. *Trends Glycosci. Glycotechnol.* 13(72):361–370.
- Pels Rijcken WR, Hooghwinkel GJ, Ferwerda W. 1990. Pyrimidine metabolism and sugar nucleotide synthesis in rat liver. *Biochem J* 266(3):777-83.
- Rabina J, Maki M, Savilahti EM, Jarvinen N, Penttila L, Renkonen R. 2001. Analysis of nucleotide sugars from cell lysates by ion-pair solid-phase extraction and reversed-phase high-performance liquid chromatography. *Glycoconj J* 18(10):799-805.
- Rader RA. 2008. (Re)defining biopharmaceutical. *Nat Biotech* 26(7):743-751.
- Raju TS. 2003. Glycosylation variations with expression systems and their impact on biological activity of therapeutic immunoglobulins. *Bioprocess Int* 1:44-54.
- Raju TS. 2008. Terminal sugars of Fc glycans influence antibody effector functions of IgGs. *Curr Opin Immunol* 20(4):471-8.
- Raju TS, Scallon B. 2007. Fc glycans terminated with N-acetylglucosamine residues increase antibody resistance to papain. *Biotechnol Prog* 23(4):964-71.
- Reuter G, Gabius HJ. 1999. Eukaryotic glycosylation: whim of nature or multipurpose tool? *Cell Mol Life Sci* 55(3):368-422.
- Rivinoja A, Hassinen A, Kokkonen N, Kauppila A, Kellokumpu S. 2009. Elevated Golgi pH impairs terminal N-glycosylation by inducing mislocalization of Golgi glycosyltransferases. *J Cell Physiol* 220(1):144-54.
- Robinson DK, Chan CP, Yu Lp C, Tsai PK, Tung J, Seamans TC, Lenny AB, Lee DK, Irwin J, Silberklang M. 1994. Characterization of a recombinant antibody produced in the course of a high yield fed-batch process. *Biotechnology and Bioengineering* 44(6):727-735.

- Rodriguez J, Spearman M, Huzel N, Butler M. 2005. Enhanced production of monomeric interferon-beta by CHO cells through the control of culture conditions. *Biotechnol Prog* 21(1):22-30.
- Roth Z, Yehezkel G, Khalaila I. 2012. Identification and Quantification of Protein Glycosylation. *International Journal of Carbohydrate Chemistry* 2012:10.
- Rothman RJ, Perussia B, Herlyn D, Warren L. 1989. Antibody-dependent cytotoxicity mediated by natural killer cells is enhanced by castanospermine-induced alterations of IgG glycosylation. *Mol Immunol* 26(12):1113-23.
- Roy SK, Chiba Y, Takeuchi M, Jigami Y. 2000. Characterization of Yeast Yea4p, a uridine diphosphate-N-acetylglucosamine transporter localized in the endoplasmic reticulum and required for chitin synthesis. *J Biol Chem* 275(18):13580-7.
- Ryu J, Eom MS, Ko W, Han MS, Lee HS. 2014. A fluorescence-based glycosyltransferase assay for high-throughput screening. *Bioorg Med Chem* 22(8):2571-5.
- Scallon BJ, Tam SH, McCarthy SG, Cai AN, Raju TS. 2007. Higher levels of sialylated Fc glycans in immunoglobulin G molecules can adversely impact functionality. *Mol Immunol* 44(7):1524-34.
- Schilling BM, Gangloff S, Kothari D, Leister K, Matlock L, Zegarelli SG, Joosten CE, Basch JD, Sakhamuri S, Lee SS. 2008. Production quality enhancements in mammalian cell culture process for protein production. US Patent 7,332,303.
- Schmelzer AE, Miller WM. 2002. Hyperosmotic stress and elevated pCO₂ alter monoclonal antibody charge distribution and monosaccharide content. *Biotechnol Prog* 18(2):346-53.
- Sealover NR, Davis AM, Brooks JK, George HJ, Kayser KJ, Lin N. 2013. Engineering Chinese hamster ovary (CHO) cells for producing recombinant proteins with simple glycoforms by zinc-finger nuclease (ZFN)-mediated gene knockout of mannosyl (alpha-1,3-)-glycoprotein beta-1,2-N-acetylglucosaminyltransferase (Mgat1). *J Biotechnol* 167(1):24-32.
- Senger RS, Karim MN. 2003. Effect of shear stress on intrinsic CHO culture state and glycosylation of recombinant tissue-type plasminogen activator protein. *Biotechnol Prog* 19(4):1199-209.
- Shi HH, Goudar CT. 2014. Recent advances in the understanding of biological implications and modulation methodologies of monoclonal antibody N-linked high mannose glycans. *Biotechnology and Bioengineering* 111(10):1907-1919.
- Shinkawa T, Nakamura K, Yamane N, Shoji-Hosaka E, Kanda Y, Sakurada M, Uchida K, Anazawa H, Satoh M, Yamasaki M and others. 2003. The absence of fucose but not the presence of galactose or bisecting N-acetylglucosamine of human IgG1 complex-type oligosaccharides

- shows the critical role of enhancing antibody-dependent cellular cytotoxicity. *J Biol Chem* 278(5):3466-73.
- Sola RJ, Griebenow K. 2009. Effects of glycosylation on the stability of protein pharmaceuticals. *J Pharm Sci* 98(4):1223-45.
- Sondermann P, Kaiser J, Jacob U. 2001. Molecular basis for immune complex recognition: a comparison of Fc-receptor structures. *J Mol Biol* 309(3):737-49.
- Soo EC, Aubry AJ, Logan SM, Guerry P, Kelly JF, Young NM, Thibault P. 2004. Selective detection and identification of sugar nucleotides by CE-electrospray-MS and its application to bacterial metabolomics. *Anal Chem* 76(3):619-26.
- Suda T, Kamiyama S, Suzuki M, Kikuchi N, Nakayama K, Narimatsu H, Jigami Y, Aoki T, Nishihara S. 2004. Molecular cloning and characterization of a human multisubstrate specific nucleotide-sugar transporter homologous to *Drosophila* fringe connection. *J Biol Chem* 279(25):26469-74.
- Takuma S, Hirashima C, Piret JM. 2007. Dependence on glucose limitation of the pCO₂ influences on CHO cell growth, metabolism and IgG production. *Biotechnol Bioeng* 97(6):1479-88.
- Tomiya N, Ailor E, Lawrence SM, Betenbaugh MJ, Lee YC. 2001. Determination of nucleotides and sugar nucleotides involved in protein glycosylation by high-performance anion-exchange chromatography: sugar nucleotide contents in cultured insect cells and mammalian cells. *Anal Biochem* 293(1):129-37.
- Trummer E, Fauland K, Seidinger S, Schriebl K, Lattenmayer C, Kunert R, Vorauer-Uhl K, Weik R, Borth N, Katinger H and others. 2006. Process parameter shifting: Part I. Effect of DOT, pH, and temperature on the performance of Epo-Fc expressing CHO cells cultivated in controlled batch bioreactors. *Biotechnol Bioeng* 94(6):1033-44.
- Umana P, Jean-Mairet J, Moudry R, Amstutz H, Bailey JE. 1999. Engineered glycoforms of an antineuroblastoma IgG1 with optimized antibody-dependent cellular cytotoxic activity. *Nat Biotechnol* 17(2):176-80.
- von Horsten HH, Ogorek C, Blanchard V, Demmler C, Giese C, Winkler K, Kaup M, Berger M, Jordan I, Sandig V. 2010. Production of non-fucosylated antibodies by co-expression of heterologous GDP-6-deoxy-D-lyxo-4-hexulose reductase. *Glycobiology* 20(12):1607-18.
- Wagner GK, Pesnot T. 2010. Glycosyltransferases and their assays. *ChemBiochem* 11(14):1939-49.
- Walsh G. 2014. Biopharmaceutical benchmarks 2014. *Nat Biotechnol* 32(10):992-1000.
- Walsh G, Jefferis R. 2006. Post-translational modifications in the context of therapeutic proteins. *Nat Biotechnol* 24(10):1241-52.

- Weikert S, Papac D, Briggs J, Cowfer D, Tom S, Gawlitzek M, Lofgren J, Mehta S, Chisholm V, Modi N and others. 1999. Engineering Chinese hamster ovary cells to maximize sialic acid content of recombinant glycoproteins. *Nat Biotechnol* 17(11):1116-21.
- Wittwer AJ, Howard SC. 1990. Glycosylation at Asn-184 inhibits the conversion of single-chain to two-chain tissue-type plasminogen activator by plasmin. *Biochemistry* 29(17):4175-80.
- Wong DC, Wong NS, Goh JS, May LM, Yap MG. 2010a. Profiling of N-glycosylation gene expression in CHO cell fed-batch cultures. *Biotechnol Bioeng* 107(3):516-28.
- Wong NS, Wati L, Nissom PM, Feng HT, Lee MM, Yap MG. 2010b. An investigation of intracellular glycosylation activities in CHO cells: effects of nucleotide sugar precursor feeding. *Biotechnol Bioeng* 107(2):321-36.
- Wong NS, Yap MG, Wang DI. 2006. Enhancing recombinant glycoprotein sialylation through CMP-sialic acid transporter over expression in Chinese hamster ovary cells. *Biotechnol Bioeng* 93(5):1005-16.
- Wright A, Sato Y, Okada T, Chang K, Endo T, Morrison S. 2000. In vivo trafficking and catabolism of IgG1 antibodies with Fc associated carbohydrates of differing structure. *Glycobiology* 10(12):1347-55.
- Wu ZL, Ethen CM, Prather B, Machacek M, Jiang W. 2011. Universal phosphatase-coupled glycosyltransferase assay. *Glycobiology* 21(6):727-33.
- Xu X, Nagarajan H, Lewis NE, Pan S, Cai Z, Liu X, Chen W, Xie M, Wang W, Hammond S and others. 2011. The genomic sequence of the Chinese hamster ovary (CHO)-K1 cell line. *Nat Biotechnol* 29(8):735-41.
- Yamane-Ohnuki N, Kinoshita S, Inoue-Urakubo M, Kusunoki M, Iida S, Nakano R, Wakitani M, Niwa R, Sakurada M, Uchida K and others. 2004. Establishment of FUT8 knockout Chinese hamster ovary cells: an ideal host cell line for producing completely defucosylated antibodies with enhanced antibody-dependent cellular cytotoxicity. *Biotechnol Bioeng* 87(5):614-22.
- Yamane-Ohnuki N, Satoh M. 2009. Production of therapeutic antibodies with controlled fucosylation. *MAbs* 1(3):230-6.
- Yan B, Steen S, Hambly D, Valliere-Douglass J, Vanden Bos T, Smallwood S, Yates Z, Arroll T, Han Y, Gadgil H and others. 2009. Succinimide formation at Asn 55 in the complementarity determining region of a recombinant monoclonal antibody IgG1 heavy chain. *J Pharm Sci* 98(10):3509-21.
- Yang M, Butler M. 2002. Effects of ammonia and glucosamine on the heterogeneity of erythropoietin glycoforms. *Biotechnol Prog* 18(1):129-38.

- Yoon SK, Choi SL, Song JY, Lee GM. 2005. Effect of culture pH on erythropoietin production by Chinese hamster ovary cells grown in suspension at 32.5 and 37.0 degrees C. *Biotechnol Bioeng* 89(3):345-56.
- Yoon SK, Song JY, Lee GM. 2003. Effect of low culture temperature on specific productivity, transcription level, and heterogeneity of erythropoietin in Chinese hamster ovary cells. *Biotechnol Bioeng* 82(3):289-98.
- Zanghi JA, Mendoza TP, Schmelzer AE, Knop RH, Miller WM. 1998. Role of nucleotide sugar pools in the inhibition of NCAM polysialylation by ammonia. *Biotechnol Prog* 14(6):834-44.
- Zhang X, Lok SH, Kon OL. 1998. Stable expression of human alpha-2,6-sialyltransferase in Chinese hamster ovary cells: functional consequences for human erythropoietin expression and bioactivity. *Biochim Biophys Acta* 1425(3):441-52.
- Zhou Q, Shankara S, Roy A, Qiu H, Estes S, McVie-Wylie A, Culm-Merdek K, Park A, Pan C, Edmunds T. 2008. Development of a simple and rapid method for producing non-fucosylated oligomannose containing antibodies with increased effector function. *Biotechnol Bioeng* 99(3):652-65.
- Zhu J. 2012. Mammalian cell protein expression for biopharmaceutical production. *Biotechnol Adv* 30(5):1158-70.

Chapter 3 Effect of glucose and amino acid metabolism on N-glycosylation

In this chapter, we will present our work on manipulating N-glycosylation by changing the amino acid and glucose consumption rates in the CHO fed-batch cultures. This work has been published in *Biotechnology and Bioengineering*, 2014. We demonstrated that during process and media optimization, the balance of glucose and amino acid concentration in the culture was essential for cell growth, IgG titer and N-glycosylation. It was possible to direct glycosylation quality of monoclonal antibody by well controlling the glucose and amino acid metabolism.

Amino Acid and Glucose Metabolism in Fed-Batch CHO Cell Culture Affects Antibody Production and Glycosylation

Yuzhou Fan,^{1,2} Ioscani Jimenez Del Val,³ Christian Müller,² Jette Wagtberg Sen,² Søren Kofoed Rasmussen,² Cleo Kontoravdi,³ Dietmar Weilguny,² Mikael Rørdam Andersen¹

¹Network Engineering of Eukaryotic Cell Factories, Department of Systems Biology, Technical University of Denmark, Building 223, 2800 Kgs, Lyngby, Denmark; telephone: +45-45252675; fax: +45-45884148; e-mail: mr@bio.dtu.dk

²Symphogen A/S, Pederstrupvej 93, 2750, Ballerup, Denmark; telephone: +45-88382683; fax: +45-45265060; e-mail: dw@symphogen.com

³Center for Process Systems Engineering, Department of Chemical Engineering, Imperial College London, London, UK

ABSTRACT: Fed-batch Chinese hamster ovary (CHO) cell culture is the most commonly used process for IgG production in the biopharmaceutical industry. Amino acid and glucose consumption, cell growth, metabolism, antibody titer, and *N*-glycosylation patterns are always the major concerns during upstream process optimization, especially media optimization. Gaining knowledge on their interrelations could provide insight for obtaining higher immunoglobulin G (IgG) titer and better controlling glycosylation-related product quality. In this work, different fed-batch processes with two chemically defined proprietary media and feeds were studied using two IgG-producing cell lines. Our results indicate that the balance of glucose and amino acid concentration in the culture is important for cell growth, IgG titer and *N*-glycosylation. Accordingly, the ideal fate of glucose and amino acids in the culture could be mainly towards energy and recombinant product, respectively. Accumulation of by-products such as NH_4^+ and lactate as a consequence of unbalanced nutrient supply to cell activities inhibits cell growth. The levels of Leu and Arg in the culture, which relate to cell growth and IgG productivity, need to be well controlled. Amino acids with the highest consumption rates correlate with the most abundant amino acids present in the produced IgG, and thus require sufficient availability during culture. Case-by-case analysis is necessary for understanding the effect of media and process optimization on glycosylation. We found that in certain cases the presence of Man5 glycan can be linked to limitation of UDP-GlcNAc biosynthesis as a result of insufficient extracellular Gln. However, under different culture conditions, high Man5 levels can also result from low α -1,3-mannosyl-glycoprotein 2- β -*N*-acetylglucosaminyltransferase (GnTI) and UDP-

GlcNAc transporter activities, which may be attributed to high level of NH_4^+ in the cell culture. Furthermore, galactosylation of the mAb Fc glycans was found to be limited by UDP-Gal biosynthesis, which was observed to be both cell line and cultivation condition-dependent. Extracellular glucose and glutamine concentrations and uptake rates were positively correlated with intracellular UDP-Gal availability. All these findings are important for optimization of fed-batch culture for improving IgG production and directing glycosylation quality.

Biotechnol. Bioeng. 2014;9999: 1–15.

© 2014 Wiley Periodicals, Inc.

KEYWORDS: Chinese hamster ovary cells; amino acids; glucose; metabolism; fed-batch; IgG; upstream process optimization; glycosylation

Introduction

In recent decades, the annual global market of recombinant therapeutic proteins has grown significantly from ca. \$12 billion in the year 2000 to \$33 in 2004 and \$99 billion in 2009 (Walsh, 2003, 2006, 2010). Monoclonal antibodies (mAbs), in particular, which offer novel therapy avenues for cancer, inflammatory diseases, infectious diseases, and autoimmune diseases, have had remarkable success in both regulatory approval and global sales (Jimenez Del Val et al., 2010; O'Callaghan and James, 2008). Chinese hamster ovary (CHO) cells are extensively used for the production of recombinant antibodies as a result of their robust growth and the potential to produce non-immunogenic antibodies with glycosylation patterns similar to humans (Jefferis, 2007; Raju, 2003). *N*-linked glycosylation plays a critical role in the biological properties of therapeutic IgG, for example, effectors function,

Correspondence to: M. R. Andersen and D. Weilguny

Received 5 June 2014; Revision received 12 August 2014; Accepted 5 September 2014

Accepted manuscript online xx Month 2014;

Article first published online in Wiley Online Library

(wileyonlinelibrary.com).

DOI 10.1002/bit.25450

immunogenicity, stability, and clearance rate (Burton and Dwek, 2006; Gooch et al., 1991; Jefferis, 2009a,b; Raju, 2008). Therefore, control of glycosylation is of prime importance to meet regulatory requirements and for quality compliance. Naturally occurring IgG have two conserved *N*-glycosylation sites at Asn²⁹⁷ with the consensus sequence Asn-X-Ser/Thr on the heavy chains, where X is any amino acid except Pro. The heterogeneity of the glycan structures on each glycosylation site can vary according to their biosynthetic stage from less mature forms (e.g., non-glycosylated and high mannose forms) to more mature forms (e.g., galactosylated and sialylated forms).

The process of *N*-glycosylation, although complicated, has been well characterized (Kornfeld and Kornfeld, 1985). Initially in the endoplasmic reticulum (ER), a lipid-linked oligosaccharide precursor (Glc3Man9GlcNAc2-PP-dolichol) is synthesized by transferring *N*-acetylglucosamine, mannose, and glucose residues from UDP-GlcNAc, GDP-mannose, and UDP-glucose (the nucleotide sugars synthesized in cytosol and transported into ER), respectively, to a lipid carrier, dolichol phosphate. These precursors are subsequently transferred to the available *N*-glycosylation sequons present on the nascent polypeptide chain. The three glucose residues present on the now protein-bound oligosaccharide contribute to protein folding via the calnexin–calreticulin cycle. After the cycle has ensured adequate protein folding, all three glucose residues are cleaved from the oligosaccharide (Ellgaard and Helenius, 2003). Then, one mannose residue is trimmed in the ER prior to the IgG being translocated to the Golgi apparatus by means of vesicles (Hossler et al., 2009). In the Golgi, the *N*-linked glycans mature in a step-wise fashion through a number of enzyme-catalyzed reactions where monosaccharide residues are trimmed off or added to the carbohydrate structure. The maturation of glycans is largely dependent on factors such as expression, activity, and localization of the glycosidase and glycosyltransferase enzymes (Jassal et al., 2001; Kanda et al., 2006; Mori et al., 2004; Paulson and Colley, 1989; Weikert et al., 1999), the intracellular levels and availability of nucleotides and nucleotide sugars, for example, GDP-Man, UDP-GlcNAc, UDP-Glc, and UDP-Gal (Baker et al., 2001; Hills et al., 2001; Nyberg et al., 1999), and the accessibility of glycosylation sites on the glycoprotein (Holst et al., 1996). For example, the Man5 glycans can remain unprocessed due to insufficient α -mannosidase II (ManII) activity or when the GlcNAc addition reaction is limited by insufficient availability of intracellular UDP-GlcNAc or low α -1,3-mannosyl-glycoprotein 2- β -*N*-acetylglucosaminyltransferase (GnTI) activity (Pacis et al., 2011).

Glycolysis and glutaminolysis are the key metabolic pathways of CHO cells (Quek et al., 2010). Through glycolysis, CHO cells consume glucose as the main carbon source for energy production and generate lactate as the most common metabolic by-product. Glutaminolysis is the prevalent pathway through which CHO cells assimilate organic nitrogen for biomass synthesis while releasing ammonium as the main by-product (Altamirano et al., 2006; Lu et al., 2005). Fed-batch culture is widely used for the production of recombinant antibodies in industry (Huang et al., 2010). In fed-batch culture, periodic

delivery of appropriate feeds provides sufficient nutrients to support cell growth and metabolism and induce a prolonged and productive culture life (Chee Fung Wong et al., 2005). However, accumulation of cellular by-products may inhibit cell growth, threaten culture longevity, reduce antibody production, and compromise antibody glycosylation (Chen and Harcum, 2005; Dorai et al., 2009; Gawlitzek et al., 2000; Hossler et al., 2009; Li et al., 2012). Understanding the interplay between cell growth, cell metabolism, IgG synthesis and glycosylation and how these factors vary among different cell lines and media composition at the metabolic level will benefit bioprocess optimization, media development and will be useful in identifying screening and engineering targets (Dean and Reddy, 2013).

Aiming at high titer production and adequate glycosylation-related quality of IgG, different strategies have been proposed to improve CHO cell culture performance. Limiting the feed of glucose (Cruz et al., 1999; Gagnon et al., 2011; Gambhir et al., 1999) and glutamine (Chee Fung Wong et al., 2005), substituting glucose (Altamirano et al., 2004, 2006) and glutamine (Altamirano et al., 2000, 2001) with alternative nutrients, addition of feed supplements (Gramer et al., 2011), optimization of process parameters such temperature, pH, agitation rate and osmolality (Ahn et al., 2008; Fox et al., 2004; Pacis et al., 2011; Senger and Karim, 2003; Trummer et al., 2006) and engineering of metabolic (Fogolin et al., 2004; Kim and Lee, 2007; Zhou et al., 2011) and anti-apoptotic (Druz et al., 2013; Mstrangelo et al., 2000) targets have all been attempted. In addition, many efforts have been made on metabolic profiling (Jimenez Del Val et al., 2011; Kochanowski et al., 2008; Sellick et al., 2011), and ¹³C metabolic flux analysis (Ahn and Antoniewicz, 2011; Dean and Reddy, 2013; Quek et al., 2010) of CHO cell culture at different growth stages to further understand the interplay between energy, cell growth, protein production and glycosylation in CHO cells.

Herein, we present the differences in cell growth, IgG production, nutrient consumption, intracellular nucleotide sugar availability, and IgG glycosylation for two IgG-producing cell lines grown in fed-batch cultures with two different chemically-defined proprietary media and feeds. Our results provide an integrative approach to understand the relationship of glucose and amino acid metabolism, nucleotide sugar metabolism, cell growth, IgG production, and glycosylation in fed-batch CHO cell culture and give guidance for future process optimization and media development from a metabolic point of view.

Material and Methods

Cell Lines and Media

Two Symphogen in-house IgG1-producing CHO cell lines (1030 and 4384) were used in this study. Both of them were generated from a dihydrofolate reductase-deficient (DHFR-) CHO DG44 cell line (Urlaub et al., 1983) through methotrexate (MTX) mediated stable transfection with a

vector containing DHFR and the genes for antibody heavy and light chains, followed by fluorescence activated cell sorting (FACS) and adaptation to serum-free medium. All basal media and feeds used in this study are proprietary, chemically defined and serum-free. Cells were maintained and expanded in basal media B in shake flask at 200 rpm in a 37°C humidified culture incubator supplied with 5% CO₂.

Fed-Batch Culture

Cells were seeded at a density of 5×10^5 viable cells/mL for a 2-day passage or 3×10^5 viable cells/mL for a 3-day passage prior to the inoculation of fed-batch cultures. Cells in fed-batch culture were grown in 500 mL shake flasks with an initial culture volume of 70 mL at 37°C, 5% CO₂, 200 rpm. The temperature was shifted from 37 to 33.5°C on day 5. All sampling was carried out before feeding. The culture was harvested when the viability became lower than 60% or on day 14. Viability and viable cell density (VCD) was measured by Vi-CELL XR (Beckman Coulter, Brea, CA). Glucose, glutamine, lactate, ammonium, glutamate, pH, and osmolality were measured by Bioprofile 100plus (Nova BioMedical, Waltham, WA). IgG titer was determined by biolayer interferometry using Octet QK384 equipped with Protein A biosensors (ForteBio, Menlo Park, CA) according to the manufacturer's instructions.

Duplicates of different fed-batch cultures for the 1,030 and 4,384 cell lines were carried out in two different basal media A and B with the corresponding feed media FA and FB.

In the A + FA8 culture (basal media A, feed FA, seeding density at 8×10^5 viable cells/mL), the 1,030 or 4,384 cells were initially seeded at 8×10^5 viable cells/mL in basal media A. Feed FA (3.3% of the initial culture volume) was added to the culture once a day from day 2 onwards. Glucose was adjusted to 8 g/L on days 5 and 7, 10 g/L on days 9 and 11. Cell culture was sampled on days 2, 5, 7, 9, 11, and 13 for measuring cell growth, metabolism, and IgG expression. Additional sampling for nucleotide sugar measurement was performed on days 2, 5, 9, and 11 and for Western blot analysis on days 2 and 11. Samples for amino acid analysis were taken from the 4,384 cell culture on days 5, 7, 11, and 13. The culture was harvested on day 13 according to viability criteria.

Only the 1,030 cells were tested in the A + FA4 cultivation condition. The A + FA4 culture use same basal media and feed as the A + FA8 culture, but with a different seeding density of 4×10^5 viable cells/mL. The feeding strategy is also same as the A + FA8 process. However, no glucose addition was required in the process. Cell culture was sampled on days 2, 5, 7, 9, and 12 for cell growth, metabolism and IgG expression measurement and was harvested on day 12 according to viability criteria.

The B + FB4 culture (basal media B, feed FB, seeding density at 4×10^5 viable cells/mL) started with an initial culture (cells in basal media B with 13% initial culture volume of feed FB) at a seeding density of 4×10^5 viable cells/mL. Feed FB (10% of the initial culture volume) was added to the culture on days 2, 5, 7, 9, and 11. For the 1,030 cell line, glucose was adjusted to 6 g/L

on day 5 and 9 g/L on days 9 and 11. For the 4,384 cell line, glucose was added as described above for the 1,030 cell line, although it was adjusted to 10 g/L on day 9. Cell culture was sampled on days 2, 5, 7, 9, 11, 13, and 14 for measuring cell growth, metabolism, and IgG expression. Additional sampling for intracellular nucleotide sugar quantification was carried out on days 2, 5, 9, and 11 and for Western blot analysis on days 2 and 11. For the 4,384 cell line, cell culture was also sampled for amino acid analysis on days 5, 7, 11, and 13. Fed-batch culture was harvested on day 14.

Free Amino Acid Analysis

Samples from cell culture were clarified by centrifugation at 4,500 rpm for 3 min. To precipitate and remove remaining proteins, 30 µL 4% sulphosalic acid (Sigma-Aldrich, St. Louis, MO) were added into 30 µL clarified sample of the supernatant. After centrifugation (12,000g, 5 min), 20 µL of the resulting suspension was collected and dried using a SpeedVac (Thermo Scientific, Waltham, MA). The dried samples were resuspended in 160 µL of start buffer, containing 0.2 M Trisodium citrate dihydrate (Sigma-Aldrich) and 0.65% v/v HNO₃ (Sigma-Aldrich) with pH = 3.1 prior to injection into the amino acid analyzer system. The system controlled by Millennium32 software (Waters, Milford, MA) is composed of two M510 pumps (Waters), two reagent manager pump (Waters), a M717 refrigerated autosampler (Waters), a M474 fluorescence detector (Ex = 338 nm, Em = 455 nm) (Waters), a column oven (Waters), and a MCI-Gel CK10U column (Mitsubishi Chemical industries, Japan). All chemicals used to prepare the relevant solvents and reagents are purchased from Sigma-Aldrich. Amino acid analysis was performed using cation-exchange chromatography followed by postcolumn derivatization and fluorescence detection. Eluents used were solvent A (0.2 M Trisodium citrate dihydrate, 0.05% v/v phenol, and 5% v/v isopropanol, pH adjusted to 3.1 with nitric acid) and solvent B (0.21 M sodium borate, 5% v/v isopropanol, pH adjusted to 10.2 with NaOH). Eluents were prepared freshly and filtered by 0.2 µm filter units (Nalgene, Thermo Scientific). Chromatography was carried out using a flow rate at 0.32 mL/min and a column temperature at 62°C with the following gradient: $T_{0 \text{ min}} = 0\% \text{ B}$, $T_{150 \text{ min}} = 10\% \text{ B}$, $T_{28 \text{ min}} = 40\% \text{ B}$, $T_{36 \text{ min}} = 50\% \text{ B}$, $T_{40 \text{ min}} = 100\% \text{ B}$, $T_{52 \text{ min}} = 100\% \text{ B}$, $T_{53 \text{ min}} = 0\% \text{ B}$. Post column oxidation and derivatization sequentially took place at 62°C in a 50 cm 0.22 mm i.d. coil with flow of hypochlorite reagent (flow rate = 0.3 mL/min) and a 150 cm 0.5 mm coil with a flow of OPA reagents (flow rate = 0.3 mL/min). Hypochlorite and OPA reagents can be prepared as described in (Barkholt and Jensen, 1989). Peak assignment and integration was done automatically with a user-defined data processing method.

Specific Metabolic Rate

The concentration of a certain nutrient or metabolite in the cell culture before feeding ($C_{x \text{ before}}$) was measured as

described above. Moreover, the concentration after feeding ($C_{x \text{ after}}$) was calculated based on the culture volume and known addition of the proprietary feed at that time point. Additionally, the specific consumption or production rate of certain nutrient or metabolite (q_x) from time point t_1 to time point t_2 was calculated from the following equation:

$$q_x = \frac{C_x^{t_2} - C_x^{t_1}}{IVC^{t_2} - IVC^{t_1}},$$

in which IVC is the integral of viable cell density.

Nucleotide Sugar Analysis

Cell pellets from 2 mL cell culture samples were collected and washed with 2 mL ice-cold 0.9% w/v aqueous NaCl (Sigma–Aldrich) by centrifugation (0°C, 1,000g, 1 min). They were flash-frozen in liquid nitrogen and stored at –80°C until acetonitrile extraction. Under acetonitrile extraction, they were then resuspended and incubated in ice-cold 50% v/v aqueous acetonitrile (Sigma–Aldrich) on ice for 10 min prior to centrifugation (0°C, 18,000g, 5 min). Collected supernatant was dried in a SpeedVac (Savant, Thermo Scientific), resuspended in 240 µL water and store at –80°C until applying on HPLC for high-performance anion-exchange (HPAEC) analysis as describe in (Jimenez Del Val et al., 2013).

IgG Purification

Harvested cell culture was centrifuged at 4,500g for 20 min using Multifuge 3SR (Hereaus, Thermo Scientific). The supernatant was filtered through a 0.22 µm filter (Millipore, Billerica, MA) prior to application onto the self-packed MabSelect SuRe ProteinA column, which contains 200 µL of MabSelect SuRe protein A resin slurry (GE Healthcare, Fairfield, CA) equilibrated with PBS. IgG was captured by the column and eluted by 500 µL of 0.1 M citrate with pH 3.5. The elution was immediately subjected to a buffer exchange procedure by passing through a NAP-5 column (GE Healthcare) equilibrated by a formulation buffer containing 10 mM Citrate (Sigma–Aldrich) and 150 mM NaCl (Sigma–Aldrich) with pH 6.0. IgG concentration was measured using NanoDrop ND-1000 (Thermo Scientific). Purified IgG was stored at –20°C until further analysis.

Intact Mass Analysis of IgG

Intact mass analysis of the purified IgG was performed on a LC–MS system using Dionex Ultimate 3000 RSLC System equipped with Ultimate 3000 RS variable wavelength detector (Dionex, Sunnyvale, CA) and Mass Prep micro desalting 2.1 × 5 mm column (Waters) in conjunction with micrOTOF-Q II (Bruker, Billerica, MA). The flow rate was 0.2 mL/min. The gradient with solvent A (water with 0.1% formic acid; Sigma–Aldrich) and solvent B (acetonitrile with 0.1% formic acid; Sigma–Aldrich) was as follow: $T_{0 \text{ min}} = 5\%$ B, $T_{2 \text{ min}} = 5\%$ B, $T_{2.1 \text{ min}} = 90\%$ B $T_{5 \text{ min}} = 90\%$ B, $T_{5.1 \text{ min}} = 30\%$ B, $T_{6 \text{ min}} = 30\%$ B, $T_{7 \text{ min}} = 90\%$

B, $T_{7.1 \text{ min}} = 5\%$, $T_{11 \text{ min}} = 5\%$. The UV detection was performed at 215 nm. The different combinations of glycans on the IgG was analyzed and quantified according to the peak intensity of each isoform in the intact mass spectrum of IgG using Bruker Compass Data Analysis 4.2 software (Bruker).

Glycoprofiling of IgG

IgG glycoprofiling was carried out using GlykoPrep[®] InstantAB[™] kit (Prozyme, Hayward, CA) for quantifying the total of each N-glycans. Digestion, labeling and cleanup of N-glycans from IgG was performed according to the manufacturer’s instructions. Labeled glycans were buffered in 50% v/v aqueous acetonitrile prior to the HPLC analysis using Dionex Ultimate 3000 RSLC System equipped with Ultimate 3000 RS fluorescence detector (Dionex) and ACQUITY UPLC BEH Glycan 1.7 µm, 2.1 × 150 mm column (Waters). The mobile phase used was solvent A (100% acetonitrile; Sigma–Aldrich) and solvent B (100 mM ammonium formate with pH = 4.5; BDH–Merck, Poole, UK). Elution of the sample was performed using the following flow rate and gradient: $T_{0 \text{ min}} = 25\%$ B with flow rate = 0.5 min/mL, $T_{5 \text{ min}} = 25\%$ B with flow rate = 0.5 min/mL, $T_{51.5 \text{ min}} = 40\%$ B with flow rate = 0.5 min/mL, $T_{53 \text{ min}} = 100\%$ B with flow rate = 0.25 min/mL, $T_{58 \text{ min}} = 100\%$ B with flow rate = 0.25 min/mL, $T_{60 \text{ min}} = 25\%$ B with flow rate = 0.5 min/mL, $T_{70 \text{ min}} = 25\%$ B with flow rate = 0.5 min/mL, $T_{75 \text{ min}} = 25\%$ B with flow rate = 0.5 min/mL. Fluorescence detection were performed at $Ex = 278 \text{ nm}$ and $Em = 344 \text{ nm}$. Analysis of the chromatogram was performed with Chromeleon software (Dionex). Relative quantification was performed using peak area and peak assignment based on retention time of known standards.

Western Blot Analysis

Cell pellets from culture samples were washed with PBS (Invitrogen, Life Technologies, Carlsbad, CA) and lysed in RIPA buffer (Thermo scientific) in the presence of protease inhibitor cocktail (Thermo scientific) on ice. The lysates were sonicated and centrifuged for 2 min at 14,000 G. Total protein concentration in the collected supernatant was quantified by pierce BCA protein assay kit (Thermo scientific). NuPAGE sample loading buffer and reducing buffer (Invitrogen, Life Technologies) were added as required for each supernatant sample containing same amount of total protein. Samples were heated at 90°C for 10 min prior to loading onto NuPAGE 4–12% Bis–Tris gel (Invitrogen, Life Technologies). Electrophoresis was run at 150 V for 1 h using MES buffer (Invitrogen, Life Technologies). Proteins were transferred to nitrocellulose membrane using iBlot system (Invitrogen, Life Technologies). Membrane was blocked in Odyssey blocking buffer (LI–COR) for 1 h (room temperature, 50 rpm), probed with goat anti-MGAT1 antibody (1:1,000; Abcam, Cambridge, UK) and rabbit anti-SLC35A3 antibody (1:1,000; Abcam) and rabbit anti β-actin antibody (1:1,000; Cell Signaling, Danvers, MA) over night (4°C, 50 rpm) and

washed with TBS (BioRad, Hercules, CA) with 0.1% Tween 20 (Millipore, Billerica, MA). After 1 h incubation (room temperature, 50 rpm) with IR Dye 800 CW-conjugated donkey anti-goat and anti-rabbit antibody (1:5,000; LI-COR, Lincoln, NE), the membrane was washed again and subjected to fluorescence detection at 800 nm using Odyssey Scanner (LI-COR). Bands in Western blot were analyzed using image studio lite software (LI-COR).

Results

The B + FB4 culture (basal media B, feed FB, seeding density at 4×10^5 viable cells/mL) is the proprietary first-generation upstream process developed by Symphogen with optimal process parameter fitting with media B and feed FB for most of the IgG-producing cell lines generated by Symphogen. During in-house upstream optimization, we found media A with feed FA has potentially better media capacity for cell growth and antibody production in some cell lines if the cell culture starts at a suitable seeding density (data not shown). Here, we test the A + FA4 (basal media A, feed FA, seeding density at 4×10^5 viable cells/mL), A + FA8 (basal media A, feed FA, seeding density at 8×10^5 viable cells/mL) and B + FB4 cultures in order to demonstrate how the nutrients

(glucose and amino acids) were used differently during the fed-batch culture and what the IgG titer and glycosylation quality were in relation to that.

Culture Behavior and IgG Production

Culture behavior and IgG production constitute essential information for assessing media, feeds and overall upstream process performance. Figure 1 shows the effect of different upstream processes on growth, metabolism and IgG production for two model cell lines 1,030 and 4,384. In general, the durations of A + FA4 and A + FA8 cultures were slightly shorter than the B + FB4 culture. Notably, the A + FA8 culture resulted in faster cell growth and increased the integral of viable cells (IVC) for either cell line compared to the B + FB4 culture. More specifically, in Figure 1A, when using the B + FB4 cultivation condition for the 1,030 and 4,384 cell lines, the peak viable cell concentrations were about 5 and 15×10^6 cells/mL on day 11, respectively. In contrast, the peak viable cell densities were about 15 and 20×10^6 cells/mL already on day 9 in the A + FA8 culture for the 1,030 and 4,384 cell line, respectively. Interestingly, the A + FA4 culture did not exhibit any significant improvement on cell growth compared to the B + FB4 culture. Decline in viability

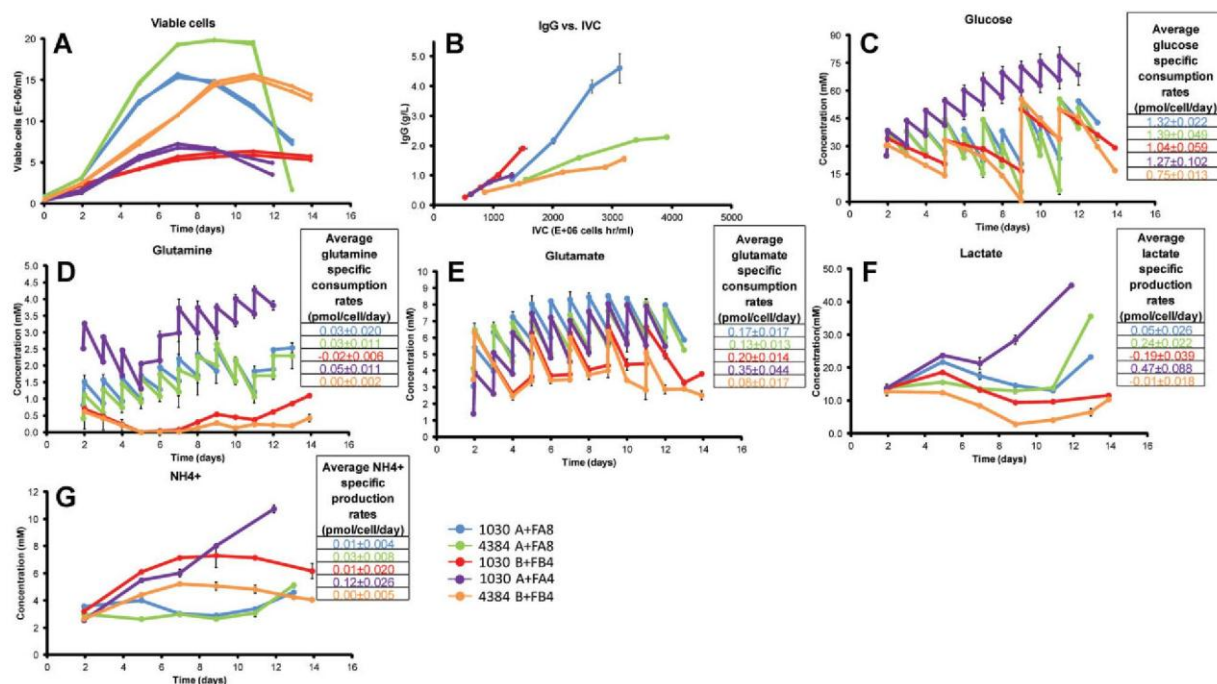


Figure 1. Comparison of five fed-batch cultures with different cell lines and cultivation conditions. Viable cell density and integral of viable cells (IVC) versus IgG titer are presented in (A) and (B), respectively. Time courses of Glucose (C), Glutamine (D), Glutamate (E), Lactate (F), and Ammonia (G) concentrations are also shown. The error bars correspond to one standard deviation calculated from duplicate experiments. In (C), (D), and (E) the data points from B + BA4 culture and A + FA8 culture on days 3, 4, 6, 8, 10, and 12 and from A + FA4 culture on days 3, 4, 6, 8, 10, 11 are unmeasured pseudo points calculated by assuming the consumption rate is constant between the measured points. Average of specific consumption/production rate of certain metabolite was also calculated based on specific consumption/production rate of certain metabolite on each measured time point from day 7 to the harvest (same color codes are used for indicating the cultivation conditions).

occurred earlier and faster in the A + FA4 and A + FA8 cultures than in the B + FB4 culture (Fig. S1A). For either the 1,030 or 4,384 cell line, the A + FA8 culture lead to considerably higher IgG production than the other cultures, as a result of both high cell growth and high specific productivity of IgG (Fig. 1B).

Although the different cultivation conditions are observed to influence specific IgG productivity (q_p), the average q_p of each cell line is relatively constant and calculated to be 40.7 pg/cell/day for 1,030 and 14.2 pg/cell/day for 4,384, as seen in Figure S3.

As a consequence of consumption and feeding, glucose concentration fluctuated at slightly higher level in the A + FA8 culture compared to the B + FB4 culture. Also, quite noticeably, glucose largely accumulated during the A + FA4 culture (Fig. 1C). The accumulation of glutamine after the temperature shift in the A + FA4 culture reached 3.5 mM at harvest. Additionally, the concentration of glutamine was around 1–2 mM before feeding in the A + FA8 culture for both cell lines compared to around 0–1 mM in the B + FB4 culture (Fig. 1C). Glutamate was generally maintained at a higher concentration before feeding in the A + FA8 culture (around 3–6 mM) than in the B + FB4 culture (around 2–4 mM) throughout the fed-batch process (Fig. 1E). The average specific glucose and glutamine consumption rates from day 7 to harvest were found to be generally higher in the A + FA8 culture than in the B + FB4 culture for both cell lines (Fig. 1D and E).

In terms of by-product formation, the accumulation of lactate in the A + FA8 culture was higher than that in the B + FB4 culture for both cell lines (Fig. 1F). In the A + FA4 culture, both lactate accumulation and its average specific production rate were particularly high, which may due to the high glucose concentration in this culture (Fig. 1F). Accumulation of NH_4^+ in the A + FA8 culture was lower than that in the B + FB4 culture for both cell lines from day 5 to 11 (Fig. 1G). However, in the A + FA4 culture, the accumulation of NH_4^+ increased dramatically from 2 up to 10 mM during the culture, which also demonstrated a particularly high average NH_4^+ specific production rate (Fig. 1G).

Amino Acid and Glucose Metabolism

To further understand the culture differences among the cultivation conditions and cell lines tested, the concentrations and specific consumption rates of amino acids and glucose have been assessed. In general, amino acid concentrations for 4,384 cells were more stable in the A + FA8 culture than in the B + FB4 culture between day 5 and 13 (Fig. 2A). Specifically, amino acids such as Asp, Ser, Gly, Val, Met, Ile, Leu, Lys, Arg, and all the aromatic amino acids (Tyr, Phe, His, and Trp) have a clear decline from day 11 onwards in the B + FB4 culture. However, Ala accumulated in both A + FA8 and B + FB4 cultures from day 5 to 13. The majority of amino acids have higher concentration on days 5, 9, 11, and 13 in the B + FB4 culture, apart from Glu and Gln on days 5, 9, 11, and 13 and Cys, Val, and aromatic amino acids (Tyr, Phe, Trp) on days 11 and 13. Interestingly, the specific amino acid consumption rates

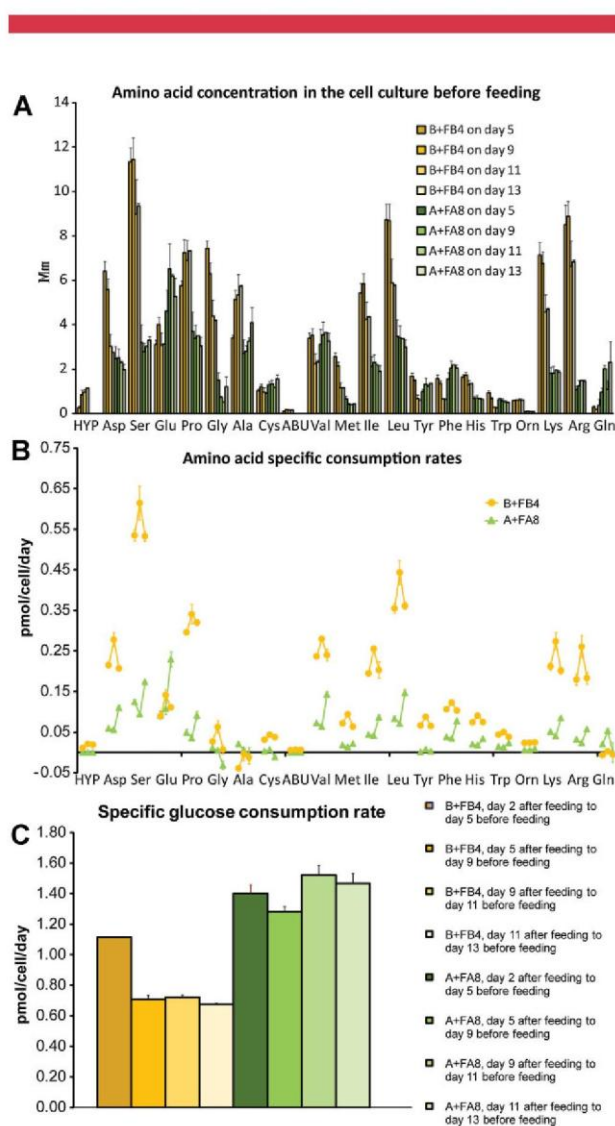


Figure 2. Glucose and amino acids metabolisms of 4,384 cell line in A + FA8 and B + FB4 cultures. (A) Amino acid concentrations on day 5, 9, 11, 13 in the cell culture before feeding. All amino acids were measured by free amino acid analysis, except glutamine, which was measured by Bioprofile 100 plus. Glutamine, threonine, and asparagine eluted as one peak and their concentration cannot be resolved in the chromatogram of the free amino acid analysis. (B) Specific consumption rates of amino acids: from day 5 after feeding to day 9 before feeding (left point), from day 9 after feeding to day 11 before feeding (middle point), from day 11 after feeding to day 13 before feeding (right point). (C) Specific consumption rate of glucose.

are very much dependent on the concentration of corresponding amino acids in the culture. It was indicated by the fact that the specific amino acid consumption rates (except Glu, Gln, and Ala) were higher from day 5 to 13 in the B + FB4 culture. Conversely, the specific glucose consumption rate was always higher in the A + FA8 culture from day 5 to 13 (Fig. 2B and C). We also found that the specific consumption rates of amino acids in the B + FB4 culture in early stationary phase (day 9–11) were higher than in growth phase (day 5–9) and late stationary phase (day 11–13). Conversely, the specific consumption rates

of amino acids (except Glu, Gln, Ala, Cys, Tyr, HYP, and ABU) in the A + FA8 culture are lower in early stationary phase (day 9–11) than in growth phase (day 5–9) and late stationary phase (day 11–13). Furthermore, the specific glucose consumption during the cell culture declined after the temperature shift (day 5) in the B + FB4 culture but was stable in the A + FA8 culture.

Nucleotide Sugar Metabolism

Nucleotide sugars are the donors of sugar chain elongation reactions in glycosylation; they are therefore thought to be one of the major factors that affect the final glycopatterns of the IgG. As shown in Figure 3, nucleotide sugars measured in this study were synthesized from glucose through two pathways: the UDP-Glc/UDP-Gal/UDP-GlcA pathway and the UDP-GalNac/UDP-GlcNac pathway. In general, there was considerable accumulation of UDP-GlcNac and UDP-GalNac during the culture. In addition, their concentration was cell

line-dependent (higher in 1,030 cell line than in 4,384 cell line under both cultivation conditions), and both species in 1,030 cell lines were more sensitive to cultivation condition changes.

Interestingly, the accumulation of UDP-GalNac, UDP-GlcNac and UDP-GlcA has a rather similar trend. Conversely, UDP-Gal and UDP-Glc accumulate to rather lower concentrations compared to UDP-GlcNac and UDP-GalNac, exhibiting similar profiles. Furthermore, their concentration was both cell line-dependent (higher in 1,030 cell line than in 4,384 cell line in either cultivation condition) and cultivation condition-dependent (higher in A + FA8 culture than B + FB4 culture for either cell line).

Abbreviated Reaction Network of Glycosylation Pathway

An abbreviated reaction network is shown in Figure 4 illustrating the sequence of reactions that occur to produce the IgG-bound glycans that were identified in this work.

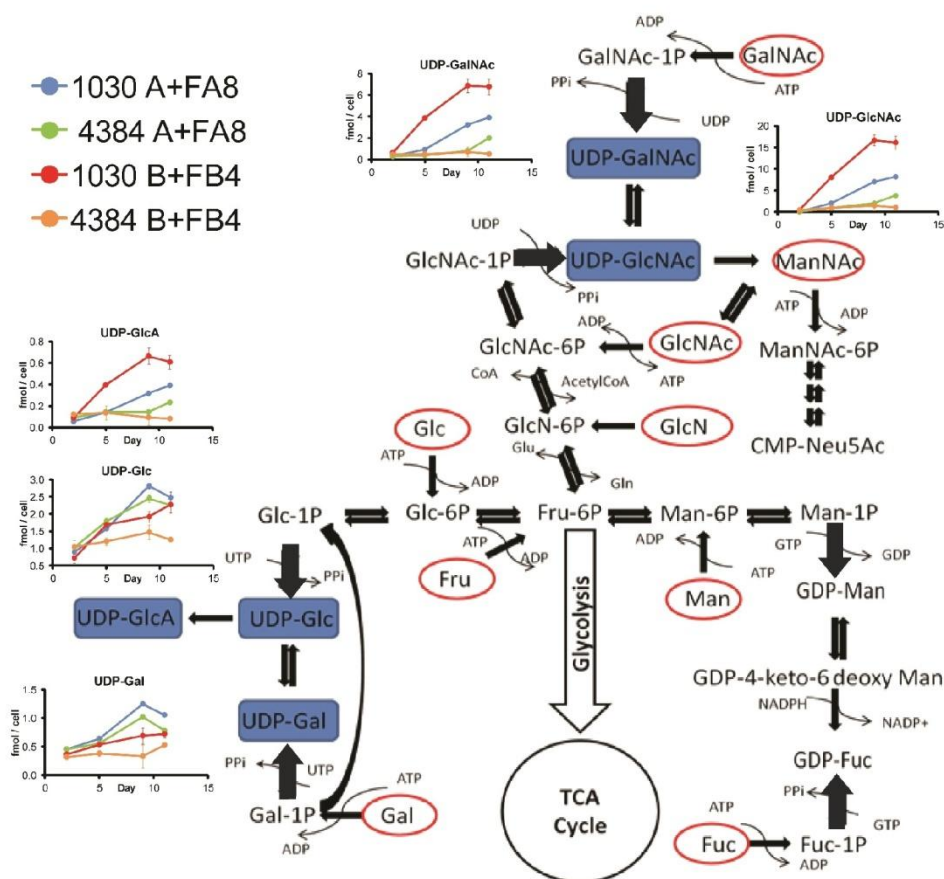


Figure 3. Intracellular nucleotide sugar analysis of cell lysates from fed-batch. Nucleotide sugar synthesis typically starts from degradation of glucose through glycolysis, in which glucose converts into glucose-6-phosphate and fructose-6 phosphate. Glucose-6-phosphate becomes UDP-glucose (UDP-Glc), UDP-galactose (UDP-Gal), and UDP-glucuronic acid (UDP-GlcA) through a series of enzymatic reactions. On the other hand, fructose-6 phosphate supplying further glycolysis and TCA cycle for energy gain can also be directed into two major nucleotide sugar synthesis pathways. One can generate UDP-glucosamine (UDP-GlcNac) and UDP-galactosamine (UDP-GalNac). The other one can produce GDP-mannose (GDP-Man) and GDP-fucose (GDP-Fuc). Galactose, mannose, fructose as well as other sugars illustrated in the figure with red circle can also be used as substrates for nucleotide sugar synthesis other than glucose. Nucleotide sugars measured in this study were shown in blue box.

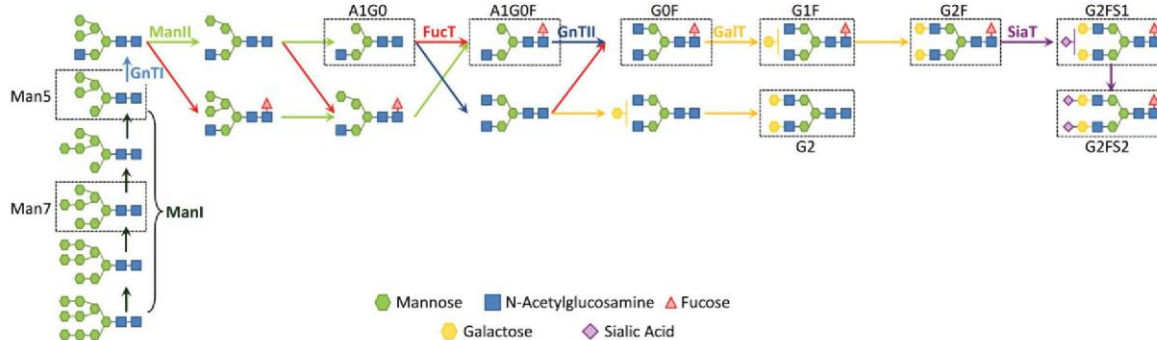


Figure 4. Simplified reaction scheme for IgG Fc *N*-glycosylation. The network begins with a nine mannose oligosaccharide structure, which is sequentially cleaved by α -mannosidase I (ManI) until a five mannose structure is produced (Man5). An *N*-acetylglucosamine residue (GlcNAc) is then added to the Man5 glycan by action of the α -1,3-mannosyl-glycoprotein 2- β -*N*-acetylglucosaminyltransferase (GnTI). After this point, the reaction scheme diverges into two branches, depending on the order in which the reactions occur. Regardless of the order, after the GnTI-catalyzed reaction, additional mannose residues are removed by α -mannosidase II (ManII) to yield the A1G0 glycan. Subsequently, a fucose residue is added by the 6- α -fucosyltransferase enzyme (FucT) to produce A1G0F, followed by addition of a second GlcNAc residue by α -1,6-mannosyl-glycoprotein 2- β -*N*-acetylglucosaminyltransferase (GnTII) to generate the G0F glycan. The reaction sequence concludes with addition of galactose and sialic acid residues to each arm of the biantennary glycan by means of β -1,4 galactosyltransferase (β -GalT) and α -2,6/ α -2,3 sialyltransferase (SiaT), respectively. Addition of these monosaccharides produces the G1F, G2, G2F, and G2FS1 glycans.

Glycosylation of IgG

Intact mass analysis was carried out mainly to provide relative quantification of glycan combinations at the *N*-glycosylation sites of the IgG. Table I shows the glycan combinations on the IgG and their molecular weights that can typically be resolved from the mass spectrum. As shown in Figure 5, the A + FA8 and A + FA4 cultures led to a lower amount of relatively immature glycoform combinations (Man5/Man5, Man5/A1G0F, and A1G0F/G0F) but higher amounts of relatively mature glycoform combinations (G0F/G1F, G1F/G1F or G0F/G2F, and G1F/G2F) than the B + FB4 culture. Particularly, the Man5/Man5 combination from the A + FA8 culture was less than the detectable level of the analytical method used. We also noticed that the 4,384 cell line produced more relatively immature glycoform combinations than the 1,030

cell line in both A + FA8 and B + FB4 cultures. The results were confirmed by glycoprofiling using instant AB labeling, an analysis providing higher resolution (Fig. 6). As shown in Figure 6A and B, the distribution for all cultures ranges from immature glycan structures such as Man7 to highly processed structures such as the G2FS1. The most abundant glycans were found to be G0F, G1F, Man5, and A1G0F. More Man5, G1F, G2F, and G2FS1 were produced by 4,384 cell line than

Table I. Typical glycan combinations on the IgG resolved from intact mass.

Glycan combinations on the IgG	Detected intact mass of IgG (Da)
NG/NG	$MW_{IgG-NG/NG}^a$
G0F/NG	$MW_{IgG-NG/NG} + 1,445^a$
Man5/Man5	$MW_{IgG-NG/NG} + 2,434$
Man5/A1G0F	$MW_{IgG-NG/NG} + 2,458$
A1G0F/A1G0F	$MW_{IgG-NG/NG} + 2,482$
A1G0F/G0F	$MW_{IgG-NG/NG} + 2,687$
G0F/G0F	$MW_{IgG-NG/NG} + 2,891$
G0F/G1F	$MW_{IgG-NG/NG} + 3,053$
G1F/G1F or G0F/G2F	$MW_{IgG-NG/NG} + 3,215$
G1F/G2F	$MW_{IgG-NG/NG} + 3,377$
G2F/G2F	$MW_{IgG-NG/NG} + 3,539$

$MW_{IgG-NG/NG}$ is the molecular weight of the non-glycosylated (NG) IgG in question.

^aDetectable only in high abundance.

Glycan combinations of IgG by intact mass analysis

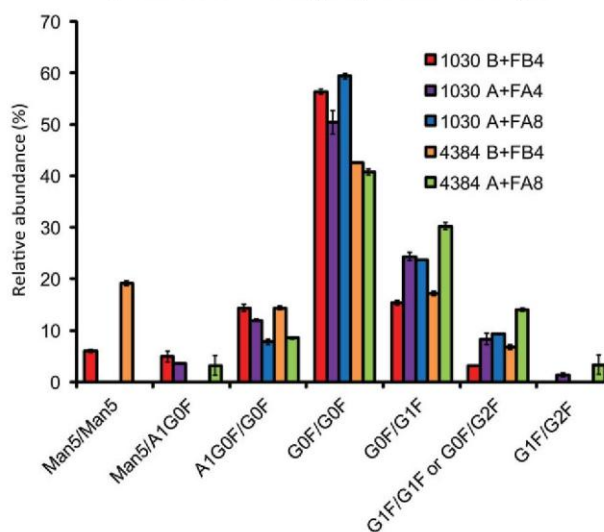


Figure 5. Relative abundance of glycan combinations of IgG detected by intact mass analysis.

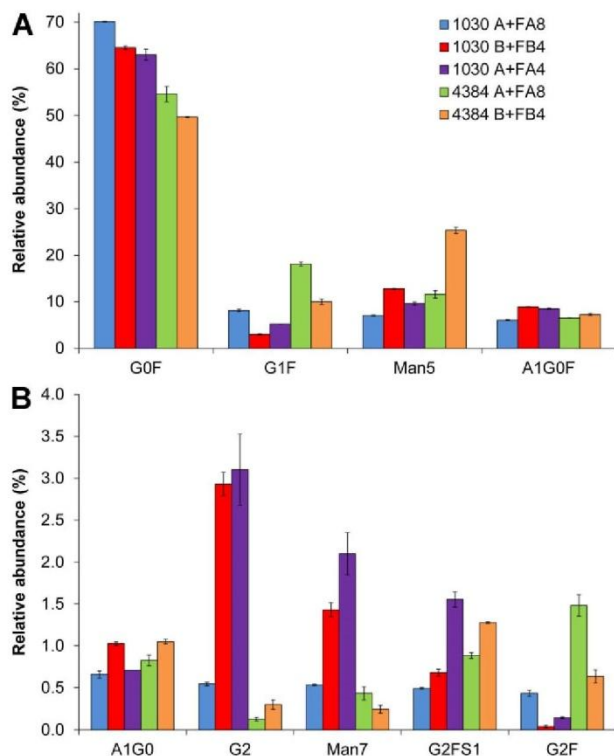


Figure 6. Analysis of IgG glycosylation by Instant-AB labeled glycoprofiling. (A) and (B) Glycan distribution as determined by HPLC.

1,030 cell line in the same cultivation condition. However, cell line 1,030 produces more Man7 than cell line 4,384, regardless of the cultivation condition. Furthermore, the A + FA8 culture gives rise to less Man5 and A1G0F, but more G1F and G2F than the B + FB4 culture.

Western Blot Analysis of GnT1 and UDP-GlcNAc Transporter

Cell pellets (1,030 and 4,384) from day 2 and 11 of the A + FA8 and B + FB4 cultures were collected for Western blot analysis (Fig. S2). The expression levels of GnT1 and UDP-GlcNAc transporter were analyzed with the purpose of understanding the very first steps of the glycan chain elongation reaction in the Golgi, in which UDP-GlcNAc is transported into the organelle and then added onto the Man5 glycan structure. All measurements were first normalized to the internal standard β -Actin and further normalized to the condition of the 1,030 cell line in the A + FA8 culture on day 2. In Figure 7, the expression of GnT1 at both time points seems to be cultivation condition-independent for 1,030 cells. However, a clear difference can be observed for UDP-GlcNAc transporter expression in 1,030 cells. Culture 1,030 A + FA8 shows basal levels of UDP-GlcNAc transporter expression on day 2, which then decrease by $\sim 50\%$ by day 11.

In contrast, culture 1,030 B + FB4 shows slightly low level at day 2, which increases dramatically (~ 2 -fold) by day 11. Expression profiles for both GnT1 and UDP-GlcNAc transporter were similar for the 4,384 cell line, regardless of cultivation conditions. We also noticed that the level of GnT1 was lower in the B + FB4 culture at both time points than in the A + FA8 culture.

Discussion

The understanding of how different nutrients were consumed for different cell activities, specifically cell growth, metabolism and protein production, provides crucial insight for media and process optimization. Our data indicate that faster cell growth, higher IVC and IgG production, and more mature glycopatterns can be obtained as the result of more balanced amino acid concentration in the culture and higher glucose consumption rate when we transition from the B + FB4 to the A + FA8 culture for both 1,030 and 4,384 cell lines. A number of important factors that correlated with the cell growth, specific productivity and glycosylation have been identified in this study.

Oxidative Metabolism and By-Product Formation in Correlation With Cell Growth

In the A + FA8 culture, higher glucose consumption compared to the B + FB4 culture implies that glucose is the major source for energy gain, despite leading to higher lactate levels. It is probably also the main reason why cells in A + FA4 media grow faster and to higher cell density. We have also noticed that more lactate was consumed from day 5 to 11 in the B + FB4 culture. This observation agrees with previous CHO metabolic flux studies that report that exponential growth phase is characterized by lactate production and high glycolysis rate and TCA flux, whereas in stationary phase cells demonstrate lactate consumption, lower glycolysis rate and TCA flux (Ahn and Antoniewicz, 2011; Carinhas et al., 2013). In contrast, we found higher specific glucose consumption rates and higher lactate, Gly and Ala specific production rates in stationary phase (day 9–11) than in late growth phase (day 5–9) of the A + FA8 culture. In fact, leaking from glycolysis is thought to balance the cytosolic NAD/NADH level, so the capacity of the TCA cycle is not exceeded (Mulukutla et al., 2012). When comparing B + FB4 with A + FA8 culture, positive Ala specific production rate, higher Ile and Leu specific consumption rates and higher specific consumption rates of Glu and its possible supplier Pro, His, and Arg indicate higher transamination activities of cells (Chen and Harcum, 2005; Schmelzer and Miller, 2002) and thus more intermediates for entering the TCA cycle in B + FB4 culture. Faster accumulation of NH_4^+ in the growth phase of the B + FB4 culture also provides evidence for oxidative metabolism by means of converting Gly, Ser, and Cys to pyruvate and glutamate to α -ketoglutarate. The high accumulation of NH_4^+ , which is thought to inhibit cell growth (Altamirano et al., 2013), could also be one of the important downsides of

the B + FB4 culture in contrast to the A + FA8 culture. In the A + FA4 culture as an extreme case, very high lactate and NH_4^+ concentrations inhibited cell growth as a consequence of unbalanced nutrient supply to cell activities. Interestingly, Leu has previously been reported to have a detrimental effect on cell growth (Gonzalez-Leal et al., 2011). Therefore, reducing its concentration as in the A + FA8 process appears to be beneficial. It is also worth mentioning that the different behaviors with respect to specific glucose consumption rate from day 5 onwards in the A + FA8 and B + FB4 cultures might not be a direct response to temperature shift and change in growth rate. This would be consistent with previous results showing that the specific glucose consumption is not affected by either temperature reduction or low specific growth rate (Vergara et al., 2014). A possible explanation for such a difference might be that the requirement of glucose and the redistribution of carbon flux for biomass and lactate accumulation in different growth phases depended on the nutrient concentrations in the culture.

Amino Acid Metabolism in Correlation With Specific Productivity

Ser and Leu were the two amino acids with the highest consumption rates in the B + FB4 culture. The fast consumption of Ser and Leu can be attributed to their abundance in the amino acid composition of the produced 4,384 antibody (Table SI). It is also reasonable to find that Arg, which has been reported to have a negative effect on mAb production in CHO DG44 cell culture (Gonzalez-Leal et al., 2011), is present at lower concentrations in A + FA8 culture than B + FB4 culture. More amino acids consumed entered the catabolic process in B + FB4 culture than in A + FA8 culture, in order to complement the energy gain from glucose. Therefore, the building blocks for IgG production may be less and the specific productivity in B + FB4 culture may thus be negatively affected.

Factors that Affect Glycosylation

Here, we also present the mAb Fc *N*-glycosylation distributions resulting from different cell lines cultured in two media with appropriately formulated feeding strategies. In order to identify the cause for the observed differences in glycan profiles, the mechanisms that determine the glycosylation process must be considered.

Product-Associated Mechanisms

The first property that controls *N*-glycosylation is the accessibility of the protein-bound glycan for action by glycosidases and glycosyltransferases. For example, the limited presence of galactose and sialic acid on the Fc glycans of mAbs has, in some cases, been attributed to these effects (Hills et al., 2001; Wormald et al., 1997). This limitation depends solely on the tertiary and quaternary structure of the recombinant protein, and is independent of metabolic and protein expression effects.

Resident Protein-Associated Mechanisms

The second mechanism that influences glycan processing is the abundance and activity of glycosylation-associated Golgi resident proteins relative to the specific productivity of the recombinant protein. The Golgi resident proteins most closely involved in protein glycosylation are nucleotide sugar transport proteins and glycosylation enzymes (glycosidases and glycosyltransferases). Gene expression of these Golgi resident proteins has been reported to vary during cell culture (Pacis et al., 2011; Wong et al., 2010a) and overexpression of glycosyltransferases (Umana et al., 1999; Weikert et al., 1999) and NS transport proteins (Wong et al., 2006) has been used to control or remodel the glycosylation patterns of therapeutic proteins produced in CHO cells. Additional reports have suggested that activity and localization of Golgi resident proteins may be influenced by certain process conditions, such as ammonia accumulation and concomitant changes in culture pH. Specifically, elevated culture pH has been associated with reduced galactosyltransferase and sialyltransferase activities (Gawlitzeck et al., 2000; Muthing et al., 2003; Yoon et al., 2005) and mislocalization of glycosyltransferase enzymes within the Golgi apparatus (Rivinoja et al., 2009). In addition, pH has also been reported to impact UDP-GlcNAc transport into the Golgi apparatus by modifying the ionisation state of UMP, which is the anti-transport substrate used by the UDP-GlcNAc transport protein (Waldman and Rudnick, 1990).

Metabolic Mechanisms

The third mechanism that determines glycan processing is the availability of nucleotide sugars within the Golgi apparatus lumen. Addition of monosaccharides to the protein-bound glycans requires nucleotide sugars as co-substrates. When these species are in low abundance in the Golgi lumen, the extent of glycosylation reactions decreases. Reduced nucleotide sugar concentration within the Golgi apparatus may result from limited transport of these species into the Golgi apparatus (Weikert et al., 1999; Wong et al., 2006) or from nutrient limitations during their biosynthesis (Kochanowski et al., 2008). Specifically, availability of UDP-GlcNAc has been reported to be closely linked with glutamine availability during cell culture (Chee Fung Wong et al., 2005; Nyberg et al., 1999) and strategies to increase the availability of this NS have relied on supplementing culture media with glucosamine and uridine (Baker et al., 2001; Hills et al., 2001). Similarly, availability of UDP-Gal has been linked with glucose metabolism and efforts to control galactosylation of therapeutic proteins have relied on supplementing cell cultures with uridine, manganese, and galactose (Grainger and James, 2013; Gramer et al., 2011).

When analyzing our data for recombinant protein glycosylation within this mechanistic context, we see that the presence of certain glycans results from both resident protein availability and metabolic effects. The relative abundance of Man7 correlates with the specific productivity of each cell line.

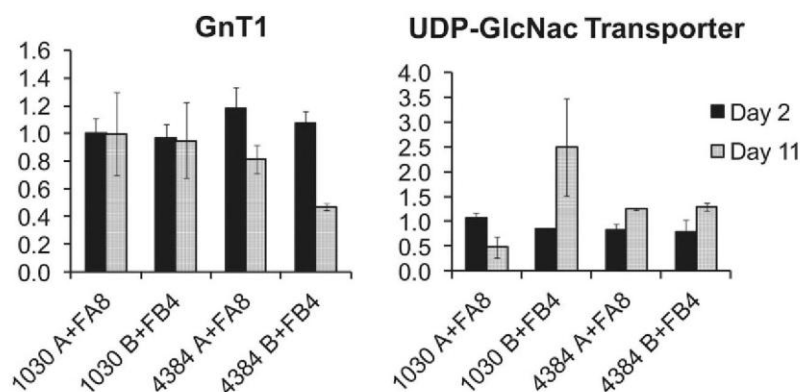


Figure 7. Quantification of intracellular GnT1 and UDP-GlcNac transporter levels by Western blot.

Cell line 1,030, which has the highest average q_p (see Fig. S3), produces more Man7 (up to $2.1\% \pm 0.25\%$) than cell line 4,384 (up to $0.43\% \pm 0.08\%$). It is possible that this occurs because the 1,030 cells have insufficient alpha mannosidase II (ManII) availability to cope with their higher q_p .

In contrast to the Man7 glycan, presence of Man5 can occur because of low abundance or activity of Golgi resident proteins (UDP-GlcNac transporter and GnTI) or low intracellular availability of UDP-GlcNac. Despite similar UDP-GlcNac transporter expression levels, 4,384 cells produce 2.2-fold ± 0.2 ($P = 0.000022$) more Man5 in B + FB4 culture than in A + FA8 culture (Fig. 6). This indicates that, for this cell line, accumulation of the Man5 glycan is likely due to the bottleneck in availability of UDP-GlcNac

and expression of GnTI. This is further confirmed by Figure 3 where the 4,384 cell line was found to have extremely low intracellular UDP-GlcNac concentration and Figure 7 where this cell line exhibited lower expression level of GnTI on both day 2 and 11 in B + FB4 culture. We must emphasize that low intracellular nucleotide sugar concentration may occur due to low levels of biosynthesis or high levels of consumption. Given the low GlcNac occupancy (Fig. 8A) and high amount of Man5 that accumulates for culture 4,384 B + FB4 compared to those of culture 4,384 A + FA8, it is likely that the low intracellular UDP-GlcNac concentration for the former is due to low biosynthesis of this nucleotide sugar, whereas the low UDP-GlcNac concentration observed for 4,384 A + FA8 is likely due to high consumption of this

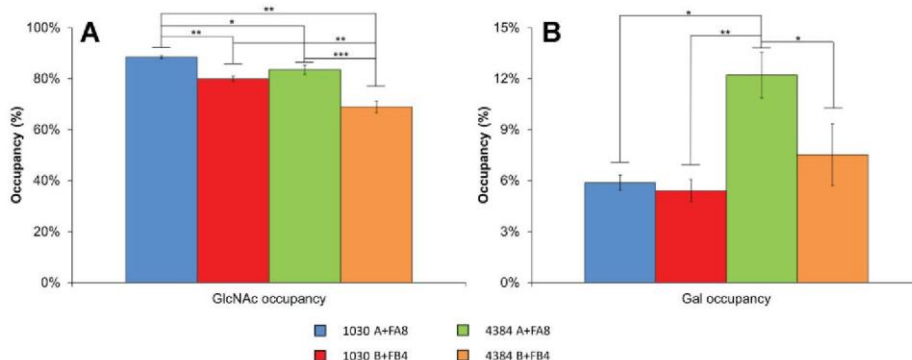


Figure 8. Intracellular NSD concentration and average monosaccharide occupancy on glycans. The percentage of GlcNAc occupancy in all measured glycans is presented in (A) and occupancy of galactose is presented in (B). GlcNAc occupancy was calculated assuming that 100% occupancy involves two moles of GlcNAc being added to all glycans in Golgi: $\text{GlcNAc}_{\text{occ}} = (2^{\circ}\text{G0F} + 2^{\circ}\text{G1F} + 0^{\circ}\text{Man5} + 1^{\circ}\text{A1G0F} + 1^{\circ}\text{A1G0} + 2^{\circ}\text{G2} + 0^{\circ}\text{Man7} + 2^{\circ}\text{G2FS1} + 2^{\circ}\text{G2F})/2$. Similarly, galactose occupancy was calculated assuming that 100% corresponds to two moles of galactose being added to all glycans within the Golgi: $\text{Gal}_{\text{occ}} = (0^{\circ}\text{G0F} + 1^{\circ}\text{G1F} + 0^{\circ}\text{Man5} + 0^{\circ}\text{A1G0F} + 0^{\circ}\text{A1G0} + 2^{\circ}\text{G2} + 0^{\circ}\text{Man7} + 2^{\circ}\text{G2FS1} + 2^{\circ}\text{G2F})/2$.

nucleotide sugar. Limited biosynthesis of UDP-GlcNAc in culture B + FB4 is substantiated by the low extracellular glutamine availability in this culture (Fig. 1D). Limited availability of this nutrient has been widely reported to limit UDP-GlcNAc biosynthesis (Chee Fung Wong et al., 2005; Kochanowski et al., 2008; Nyberg et al., 1999).

Cell line 1,030 exhibits rather different behaviors. In culture B + FB4, 1,030 cells produce $81.1\% \pm 3.5\%$ ($P < 0.0001$) more Man5 and $8.3\% \pm 0.9\%$ ($P = 0.00055$) lower overall GlcNAc occupancy than in the A + FA8 culture. This contrasts heavily with the intracellular UDP-GlcNAc concentration data (Fig. 3), where the culture that generates lowest GlcNAc occupancy and highest Man5 secretion exhibits higher UDP-GlcNAc availability. Therefore, UDP-GlcNAc concentration may not be the limiting factor for the glycosylation processing in this cell line. It is also correlated with previous findings that feeding GlcNAc, although increased intracellular concentration of UDP-GlcNAc (Wong et al., 2010b), could not decrease the level of Man5 or A1G0F of the IgG produced (unpublished data). High UDP-GlcNAc accumulation, high Man5 secretion and a lower overall GlcNAc occupancy can occur if the nucleotide sugar is being consumed at a lower rate than that at which it is being produced. Reduced consumption of UDP-GlcNAc may be attributed to insufficient expression of GnTI or UDP-GlcNAc transporter. However, Figure 7 shows that GnTI is expressed at similar levels in both cultivation conditions for cell line 1,030, suggesting that enzyme expression may not be limiting. We also see that cell line 1,030 in the B + FB4 culture presents a two-fold increase in expression of the UDP-GlcNAc transporter transporter by day 11 of culture despite having slightly lower expression of this transporter on day 2. This suggests that availability of UDP-GlcNAc transporter is also non-limiting. With this analysis, the only remaining causes for reduced UDP-GlcNAc consumption involve the activity of GnTI or UDP-GlcNAc transporter. We also found that high extracellular ammonia accumulation in this cell line correlates with low GlcNAc occupancy and high Man5 secretion. Previous reports have proposed that ammonia accumulation may increase the pH within the Golgi apparatus, thus inhibiting the activity of glycosylation enzymes (Borys et al., 1994; Gawlitzek et al., 2000). It has also been reported that increased Golgi pH causes mislocalization of glycosyltransferases (Rivinoja et al., 2009) and impacts UDP-GlcNAc transport into Golgi by modifying the ionisation state of UMP, which is the anti-transport substrate used by UDP-GlcNAc transporter (Waldman and Rudnick, 1990).

Similarly to GlcNAc occupancy, the addition of galactose to mAb Fc glycans depends both on glycosyltransferase availability and intracellular nucleotide sugar concentration. In addition, however, low abundance of galactose on mAb Fc glycans has also been associated with decreased accessibility of GalT to the oligosaccharides present on this site (Hills et al., 2001; Wormald et al., 1997). Figure 8B shows that cell line 1,030 produces similar levels of galactose occupancy under both tested cultivation conditions. In contrast, culture 4,384 A + FA8 leads to $38.4\% \pm 16.4\%$ ($P = 0.023$) higher

galactose occupancy than culture B + FB4 with the same cell line, indicating that for 4,384 cells, galactosylated glycan production is cultivation condition-dependent. Despite this, the data shows that, on average, 4,384 cells generate higher galactosylation.

This may be attributed to the lower q_p of these cells, which could result in higher relative availability of galactosylation-associated Golgi resident proteins (UDP-Gal transporter and GalT).

Despite having no observable difference in galactosylation, the intracellular profiles of UDP-Gal for 1,030 cells are different. Figure 3 shows that 1,030 A + FA8 culture has higher intracellular UDP-Gal concentration compared to the 1,030 B + FB4 culture. Because both these cultures have similar specific mAb productivities and similar levels of galactosylation, it is likely that the reduced UDP-Gal concentration in culture 1,030 B + FB4 is due to reduced biosynthesis of this nucleotide sugar and not to higher consumption. Indeed, when comparing both cultures, we see that culture 1,030 B + FB4 presents lower extracellular glucose concentration, lower specific glucose consumption rate and considerably lower extracellular Gln availability (Fig. 1C and D). Reduced intracellular UDP-Gal concentration may occur due to all these factors. Broadly, UDP-Gal is produced using two building blocks: the carbohydrate backbone (in this case glucose-derived galactose) and the nucleotide component (UTP), which is the product of pyrimidine metabolism. Low glucose availability and specific consumption would correlate with lower availability of the galactose backbone of UDP-Gal. It has been recently confirmed experimentally that differences of glucose concentration in cell culture and its consumption can affect the level of protein galactosylation (Liu et al., 2014). Similarly, low glutamine availability has been reported to negatively impact intracellular concentration of UTP (Nyberg et al., 1999). It is no coincidence that the most successful strategies in increasing UDP-Gal pools for improved recombinant protein galactosylation have relied on addition of galactose and uridine, a direct precursor of UTP (Grainger and James, 2013; Gramer et al., 2011).

Intracellular UDP-Gal concentrations are also cultivation condition-dependent for 4,384 cells. Similarly to 1,030 cells, the A + FA8 culture yields higher intracellular UDP-Gal than B + FB4 for 4,384 cells. This difference is also likely due to reduced glutamine availability and specific glucose consumption associated with the B + FB4 culture. Given the difference observed in the intracellular UDP-Gal profile, it is possible to attribute the reduction in mAb Fc glycan galactosylation to lack of UDP-Gal availability. Finally, the impact of ammonia accumulation must be discussed to confirm that reduced UDP-Gal biosynthesis is responsible for low galactosylation levels. We see that the culture with lower galactose occupancy (4,384 B + FB4) reaches a peak extracellular ammonium concentration of about 5 mM (Fig. 1G). This value is low when considering that previous publications have observed negative effects on galactosylation at extracellular ammonia concentrations above 10 mM (Borys et al., 1994; Chen and

Harcum, 2005; Gawlitzek et al., 2000), making ammonium effects unlikely and confirming that low galactose occupancy in this culture is likely dominated by low biosynthesis of UDP-Gal.

In conclusion, to the best of our knowledge this is the first study that provides an integrative understanding of cell growth, metabolism, IgG titer, and glycosylation in correlation with the dynamics of glucose and amino acid consumption when optimization of fed-batch culture such as a change in media and feed occurs. Our results demonstrate that the effect of media and process optimization on glycosylation should be understood from case to case and results from the interplay of the protein processing rate, cell metabolism, and expression and activity of Golgi resident proteins. Given the multiplicity of mechanisms involved, systems biology approaches could in the future contribute to the understanding of protein glycosylation and further aid attempts for glycoform control.

References

- Ahn WS, Antoniewicz MR. 2011. Metabolic flux analysis of CHO cells at growth and non-growth phases using isotopic tracers and mass spectrometry. *Metab Eng* 13(5):598–609.
- Ahn WS, Jeon JJ, Jeong YR, Lee SJ, Yoon SK. 2008. Effect of culture temperature on erythropoietin production and glycosylation in a perfusion culture of recombinant CHO cells. *Biotechnol Bioeng* 101(6):1234–1244.
- Altamirano C, Berrios J, Vergara M, Becerra S. 2013. Advances in improving mammalian cells metabolism for recombinant protein production. *Electron J Biotechnol* 16(3): fulltext-2.
- Altamirano C, Cairo JJ, Godia F. 2001. Decoupling cell growth and product formation in Chinese hamster ovary cells through metabolic control. *Biotechnol Bioeng* 76(4):351–360.
- Altamirano C, Illanes A, Becerra S, Cairo JJ, Godia F. 2006. Considerations on the lactate consumption by CHO cells in the presence of galactose. *J Biotechnol* 125(4):547–556.
- Altamirano C, Paredes C, Cairo JJ, Godia F. 2000. Improvement of CHO cell culture medium formulation: Simultaneous substitution of glucose and glutamine. *Biotechnol Prog* 16(1):69–75.
- Altamirano C, Paredes C, Illanes A, Cairo JJ, Godia F. 2004. Strategies for fed-batch cultivation of t-PA producing CHO cells: Substitution of glucose and glutamine and rational design of culture medium. *J Biotechnol* 110(2):171–179.
- Baker KN, Rendall MH, Hills AE, Hoare M, Freedman RB, James DC. 2001. Metabolic control of recombinant protein N-glycan processing in NS0 and CHO cells. *Biotechnol Bioeng* 73(3):188–202.
- Barkholt V, Jensen AL. 1989. Amino acid analysis: Determination of cysteine plus half-cysteine in proteins after hydrochloric acid hydrolysis with a disulfide compound as additive. *Anal Biochem* 177(2):318–322.
- Borys MC, Linzer DI, Papoutsakis ET. 1994. Ammonia affects the glycosylation patterns of recombinant mouse placental lactogen-I by chinese hamster ovary cells in a pH-dependent manner. *Biotechnol Bioeng* 43(6):505–514.
- Burton DR, Dwek RA. 2006. Immunology. Sugar determines antibody activity. *Science* 313(5787):627–628.
- Carinhas N, Duarte TM, Barreiro LC, Carrondo MJ, Alves PM, Teixeira AP. 2013. Metabolic signatures of GS-CHO cell clones associated with butyrate treatment and culture phase transition. *Biotechnol Bioeng* 110(12):3244–3257.
- Chee Fung Wong D, Tin Kam Wong K, Tang Goh L, Kiat Heng C, Gek Sim Yap M. 2005. Impact of dynamic online fed-batch strategies on metabolism, productivity and N-glycosylation quality in CHO cell cultures. *Biotechnol Bioeng* 89(2):164–177.
- Chen P, Harcum SW. 2005. Effects of amino acid additions on ammonium stressed CHO cells. *J Biotechnol* 117(3):277–286.
- Cruz HJ, Moreira JL, Carrondo MJ. 1999. Metabolic shifts by nutrient manipulation in continuous cultures of BHK cells. *Biotechnol Bioeng* 66(2):104–113.
- Dean J, Reddy P. 2013. Metabolic analysis of antibody producing CHO cells in fed-batch production. *Biotechnol Bioeng* 110(6):1735–1747.
- Dorai H, Kyung YS, Ellis D, Kinney C, Lin C, Jan D, Moore G, Betenbaugh MJ. 2009. Expression of anti-apoptosis genes alters lactate metabolism of Chinese hamster ovary cells in culture. *Biotechnol Bioeng* 103(3):592–608.
- Druz A, Son YJ, Betenbaugh M, Shiloach J. 2013. Stable inhibition of mmu-miR-466h-5p improves apoptosis resistance and protein production in CHO cells. *Metab Eng* 16:87–94.
- Ellegaard L, Helenius A. 2003. Quality control in the endoplasmic reticulum. *Nat Rev Mol Cell Biol* 4(3):181–191.
- Fogolin MB, Wagner R, Etcheverrigaray M, Kratje R. 2004. Impact of temperature reduction and expression of yeast pyruvate carboxylase on hGM-CSF-producing CHO cells. *J Biotechnol* 109(1–2):179–191.
- Fox SR, Patel UA, Yap MG, Wang DI. 2004. Maximizing interferon-gamma production by Chinese hamster ovary cells through temperature shift optimization: Experimental and modeling. *Biotechnol Bioeng* 85(2):177–184.
- Gagnon M, Hiller G, Luan YT, Kittredge A, DeFelice J, Drapeau D. 2011. High-end pH-controlled delivery of glucose effectively suppresses lactate accumulation in CHO fed-batch cultures. *Biotechnol Bioeng* 108(6):1328–1337.
- Gambhir A, Europa AF, Hu WS. 1999. Alteration of cellular metabolism by consecutive fed-batch cultures of mammalian cells. *J Biosci Bioeng* 87(6):805–810.
- Gawlitzek M, Ryll T, Lofgren J, Sliwowski MB. 2000. Ammonium alters N-glycan structures of recombinant TNFR-IgG: Degradative versus biosynthetic mechanisms. *Biotechnol Bioeng* 68(6):637–646.
- Gonzalez-Leal JJ, Carrillo-Cocom LM, Ramirez-Medrano A, Lopez-Pacheco F, Bulnes-Abundis D, Webb-Vargas Y, Alvarez MM. 2011. Use of a Plackett-Burman statistical design to determine the effect of selected amino acids on monoclonal antibody production in CHO cells. *Biotechnol Prog* 27(6):1709–1717.
- Gooch CE, Gramer MJ, Andersen DC, Bahr JB, Rasmussen JR. 1991. The oligosaccharides of glycoproteins: Bioprocess factors affecting oligosaccharide structure and their effect on glycoprotein properties. *Biotechnology (N Y)* 9(12):1347–1355.
- Grainger RK, James DC. 2013. CHO cell line specific prediction and control of recombinant monoclonal antibody N-glycosylation. *Biotechnol Bioeng* 110(11):2970–2983.
- Gramer MJ, Eckblad JJ, Donahue R, Brown J, Shultz C, Vickerman K, Priem P, van den Bremer ET, Gerritsen J, van Berkel PH. 2011. Modulation of antibody galactosylation through feeding of uridine, manganese chloride, and galactose. *Biotechnol Bioeng* 108(7):1591–1602.
- Hills AE, Patel A, Boyd P, James DC. 2001. Metabolic control of recombinant monoclonal antibody N-glycosylation in GS-NS0 cells. *Biotechnol Bioeng* 75(2):239–251.
- Holst B, Bruun A, Kielland-Brandt M, Winther J. 1996. Competition between folding and glycosylation in the endoplasmic reticulum. *EMBO J* 15(14):3538–3546.
- Hossler P, Khattak SF, Li ZJ. 2009. Optimal and consistent protein glycosylation in mammalian cell culture. *Glycobiology* 19(9):936–949.
- Huang YM, Hu W, Rustandi E, Chang K, Yusuf-Makagiansar H, Ryll T. 2010. Maximizing productivity of CHO cell-based fed-batch culture using chemically defined media conditions and typical manufacturing equipment. *Biotechnol Prog* 26(5):1400–1410.
- Jassal R, Jenkins N, Charlwood J, Camilleri P, Jefferis R, Lund J. 2001. Sialylation of human IgG-Fc carbohydrate by transfected rat alpha2,6-sialyltransferase. *Biochem Biophys Res Commun* 286(2):243–249.
- Jefferis R. 2007. Antibody therapeutics: Isotype and glycoform selection. *Expert Opin Biol Ther* 7(9):1401–1413.

- Jefferis R. 2009a. Glycosylation as a strategy to improve antibody-based therapeutics. *Nat Rev Drug Discov* 8(3):226–234.
- Jefferis R. 2009b. Recombinant antibody therapeutics: The impact of glycosylation on mechanisms of action. *Trends Pharmacol Sci* 30(7): 356–362.
- Jimenez Del Val I, Kontoravdi C, Nagy JM. 2010. Towards the implementation of quality by design to the production of therapeutic monoclonal antibodies with desired glycosylation patterns. *Biotechnol Prog* 26(6): 1505–1527.
- Jimenez Del Val I, Kyriakopoulos S, Polizzi KM, Kontoravdi C. 2013. An optimized method for extraction and quantification of nucleotides and nucleotide sugars from mammalian cells. *Anal Biochem* 443(2): 172–180.
- Jimenez Del Val I, Nagy JM, Kontoravdi C. 2011. Quantification of intracellular nucleotide sugars and formulation of a mathematical model for prediction of their metabolism. *BMC Proc* 5(Suppl 8):P10.
- Kanda Y, Yamane-Ohnuki N, Sakai N, Yamano K, Nakano R, Inoue M, Misaka H, Iida S, Wakitani M, Konno Y, Yano K, Shitara K, Hosoi S, Satoh M. 2006. Comparison of cell lines for stable production of fucose-negative antibodies with enhanced ADCC. *Biotechnol Bioeng* 94(4): 680–688.
- Kim SH, Lee GM. 2007. Down-regulation of lactate dehydrogenase-A by siRNAs for reduced lactic acid formation of Chinese hamster ovary cells producing thrombopoietin. *Appl Microbiol Biotechnol* 74(1): 152–159.
- Kochanowski N, Blanchard F, Cacan R, Chirat F, Guedon E, Marc A, Goergen JL. 2008. Influence of intracellular nucleotide and nucleotide sugar contents on recombinant interferon-gamma glycosylation during batch and fed-batch cultures of CHO cells. *Biotechnol Bioeng* 100(4): 721–733.
- Kornfeld R, Kornfeld S. 1985. Assembly of asparagine-linked oligosaccharides. *Annu Rev Biochem* 54:631–664.
- Li J, Wong CL, Vijayasankaran N, Hudson T, Amanullah A. 2012. Feeding lactate for CHO cell culture processes: Impact on culture metabolism and performance. *Biotechnol Bioeng* 109(5):1173–1186.
- Liu B, Spearman M, Doering J, Lattova E, Perreault H, Butler M. 2014. The availability of glucose to CHO cells affects the intracellular lipid-linked oligosaccharide distribution, site occupancy and the N-glycosylation profile of a monoclonal antibody. *J Biotechnol* 170:17–27.
- Lu S, Sun X, Zhang Y. 2005. Insight into metabolism of CHO cells at low glucose concentration on the basis of the determination of intracellular metabolites. *Process Biochem* 40(5):1917–1921.
- Mastrangelo AJ, Hardwick JM, Zou S, Betenbaugh MJ. 2000. Part II. Overexpression of bcl-2 family members enhances survival of mammalian cells in response to various culture insults. *Biotechnol Bioeng* 67(5):555–564.
- Mori K, Kuni-Kamochi R, Yamane-Ohnuki N, Wakitani M, Yamano K, Imai H, Kanda Y, Niwa R, Iida S, Uchida K., et al. 2004. Engineering Chinese hamster ovary cells to maximize effector function of produced antibodies using FUT8 siRNA. *Biotechnol Bioeng* 88(7):901–908.
- Mulukutla BC, Gramer M, Hu WS. 2012. On metabolic shift to lactate consumption in fed-batch culture of mammalian cells. *Metab Eng* 14(2):138–149.
- Muthing J, Kemminer SE, Conradt HS, Sagi D, Nimtz M, Karst U, Peter-Katalinic J. 2003. Effects of buffering conditions and culture pH on production rates and glycosylation of clinical phase I anti-melanoma mouse IgG3 monoclonal antibody R24. *Biotechnol Bioeng* 83(3): 321–334.
- Nyberg GB, Balcarcel RR, Follstad BD, Stephanopoulos G, Wang DI. 1999. Metabolic effects on recombinant interferon-gamma glycosylation in continuous culture of Chinese hamster ovary cells. *Biotechnol Bioeng* 62(3):336–347.
- O'Callaghan PM, James DC. 2008. Systems biotechnology of mammalian cell factories. *Brief Funct Genomic Proteomic* 7(2):95–110.
- Pacis E, Yu M, Autsen J, Bayer R, Li F. 2011. Effects of cell culture conditions on antibody N-linked glycosylation—what affects high mannose 5 glycoform. *Biotechnology and Bioengineering* 108(10):2348–2358.
- Paulson JC, Colley KJ. 1989. Glycosyltransferases. Structure, localization, and control of cell type-specific glycosylation. *J Biol Chem* 264(30): 17615–17618.
- Quek LE, Dietmair S, Kromer JO, Nielsen LK. 2010. Metabolic flux analysis in mammalian cell culture. *Metab Eng* 12(2):161–171.
- Raju TS. 2003. Glycosylation variations with expression systems and their impact on biological activity of therapeutic immunoglobulins. *Bio-process Int* 1:44–54.
- Raju TS. 2008. Terminal sugars of Fc glycans influence antibody effector functions of IgGs. *Curr Opin Immunol* 20(4):471–478.
- Rivinoja A, Hassinen A, Kokkonen N, Kauppila A, Kellokumpu S. 2009. Elevated Golgi pH impairs terminal N-glycosylation by inducing mislocalization of Golgi glycosyltransferases. *J Cell Physiol* 220(1): 144–154.
- Schmelzer AE, Miller WM. 2002. Effects of osmoprotectant compounds on NCAM polysialylation under hyperosmotic stress and elevated pCO₂. *Biotechnol Bioeng* 77(4):359–368.
- Sellick CA, Croxford AS, Maqsood AR, Stephens G, Westerhoff HV, Goodacre R, Dickson AJ. 2011. Metabolite profiling of recombinant CHO cells: Designing tailored feeding regimes that enhance recombinant antibody production. *Biotechnol Bioeng* 108(12):3025–3031.
- Senger RS, Karim MN. 2003. Effect of shear stress on intrinsic CHO culture state and glycosylation of recombinant tissue-type plasminogen activator protein. *Biotechnol Prog* 19(4):1199–1209.
- Trummer E, Fauland K, Seidinger S, Schriegl K, Lattenmayer C, Kunert R, Vorauer-Uhl K, Weik R, Borth N, Katinger H., et al. 2006. Process parameter shifting: Part I. Effect of DOT, pH, and temperature on the performance of Epo-Fc expressing CHO cells cultivated in controlled batch bioreactors. *Biotechnol Bioeng* 94(6):1033–1044.
- Umana P, Jean-Mairet J, Moudry R, Amstutz H, Bailey JE. 1999. Engineered glycoforms of an antineuroblastoma IgG1 with optimized antibody-dependent cellular cytotoxic activity. *Nat Biotechnol* 17(2): 176–180.
- Urlaub G, Kas E, Carothers AM, Chasin LA. 1983. Deletion of the diploid dihydrofolate reductase locus from cultured mammalian cells. *Cell* 33(2):405–412.
- Vergara M, Becerra S, Berrios J, Osses N, Reyes J, Rodriguez-Moya M, Gonzalez R, Altamirano C. 2014. Differential effect of culture temperature and specific growth rate on CHO cell behavior in Chemostat culture. *PLoS ONE* 9(4):e93865.
- Waldman BC, Rudnick G. 1990. UDP-GlcNAc transport across the Golgi membrane: Electroneutral exchange for dianionic UMP. *Biochemistry* 29(1):44–52.
- Walsh G. 2003. Biopharmaceutical benchmarks—2003. *Nat Biotechnol* 21(8):865–870.
- Walsh G. 2006. Biopharmaceutical benchmarks 2006. *Nat Biotechnol* 24(7): 769–776.
- Walsh G. 2010. Biopharmaceutical benchmarks 2010. *Nat Biotechnol* 28(9): 917–924.
- Weikert S, Papac D, Briggs J, Cowfer D, Tom S, Gawlitzeck M, Lofgren J, Mehta S, Chisholm V, Modi N., et al. 1999. Engineering Chinese hamster ovary cells to maximize sialic acid content of recombinant glycoproteins. *Nat Biotechnol* 17(11):1116–1121.
- Wong DC, Wong NS, Goh JS, May LM, Yap MG. 2010a. Profiling of N-glycosylation gene expression in CHO cell fed-batch cultures. *Biotechnol Bioeng* 107(3):516–528.
- Wong NS, Wati L, Nissom PM, Feng HT, Lee MM, Yap MG. 2010b. An investigation of intracellular glycosylation activities in CHO cells: Effects of nucleotide sugar precursor feeding. *Biotechnol Bioeng* 107(2): 321–336.
- Wong NSC, Yap MGS, Wang DIC. 2006. Enhancing recombinant glycoprotein sialylation through CMP-sialic acid transporter over expression in chinese hamster ovary cells. *Biotechnol Bioeng* 93(5): 1005–1016.
- Wormald MR, Rudd PM, Harvey DJ, Chang SC, Scragg IG, Dwek RA. 1997. Variations in oligosaccharide-protein interactions in immunoglobulin G determine the site-specific glycosylation profiles and modulate the

- dynamic motion of the Fc oligosaccharides. *Biochemistry* 36(6):1370–1380.
- Yoon SK, Choi SL, Song JY, Lee GM. 2005. Effect of culture pH on erythropoietin production by Chinese hamster ovary cells grown in suspension at 32.5 and 37.0 degrees C. *Biotechnol Bioeng* 89(3):345–356.
- Zhou M, Crawford Y, Ng D, Tung J, Pynn AF, Meier A, Yuk IH, Vijayasankaran N, Leach K, Joly J, et al. 2011. Decreasing lactate level and increasing antibody production in Chinese Hamster Ovary cells (CHO) by reducing the expression of lactate dehydrogenase and pyruvate dehydrogenase kinases. *J Biotechnol* 153(1–2):27–34.

Supporting Information

Additional supporting information may be found in the online version of this article at the publisher's web-site.

Chapter 4 Glycoprofiling the effect of media additives on IgG produced by CHO cells in fed-batch bioreactors

Helene Fastrup Kildegaard^{1,2,#}, Yuzhou Fan^{1,3,#}, Jette Wagtberg Sen³, Bo Larsen^{1,4}, and Mikael Rørdam Andersen^{1,*}

¹*Department of Systems Biology, Technical University of Denmark, 2800 Kgs. Lyngby, Denmark*

²*Current address: The Novo Nordisk Foundation Center for Biosustainability, Technical University of Denmark, 2970 Hørsholm, Denmark*

³*Symphogen A/S, 2750 Ballerup, Denmark*

⁴*Current address: Section for Molecular Plant Physiology, Department of Plant Biology and Biotechnology, Faculty of Life Sciences, University of Copenhagen, 1871 Frederiksberg C, Denmark*

[#]*These authors contributed equally to the work.*

^{*}*Corresponding author. Address correspondence to Mikael Rørdam Andersen, Department of Systems Biology, Technical University of Denmark, Building 223, 2800 Kgs. Lyngby, Denmark; +4545252675; mr@bio.dtu.dk*

Short running title: Glycoprofiling the effect of media additives on IgG

Keywords

Glycosylation, Chinese hamster ovary cells, fed-batch, IgG, medium additives

Abstract

Therapeutic monoclonal antibodies (mAbs) are mainly produced by heterogenous expression in Chinese hamster ovary (CHO) cells. The glycosylation profile of the mAbs has major impact on the efficacy and safety of the drug and is therefore an important parameter to control during production. In this study, the effect on IgG N-glycosylation from feeding CHO cells with eight glycosylation precursors during cultivation was investigated. The study was conducted in fed-batch mode in bioreactors with biological replicates to obtain highly controlled and comparable conditions. We assessed charge heterogeneity and glycosylation patterns of IgG. None of the eight feed additives caused statistically significant changes to cell growth or IgG productivity, compared to controls. However, the addition of 20 mM galactose did result in a reproducible increase of galactosylated IgG from 14 % to 25 %. On the other hand, addition of 20 mM N-acetyl-D-glucosamine (GlcNAc) reduced relative abundance of galactosylated IgG by 4%. Additionally, supplementation with 10mM mannose slightly reduced GlcNAc occupancy of IgG. Overall, comparing the effects of IgG glycosylation, by supplementing the cell culture medium with glycosylation precursors during cultivation, revealed an application of these glycosylation precursors for modulating N-glycosylation of IgG.

4.1. Introduction

The production of monoclonal antibodies (mAbs) of the IgG isotype is a large and rapidly expanding area of biotechnology. In 2009, the market for mAbs constituted 38% of a 99 billion dollar market for biopharmaceuticals (Walsh 2010), and expanded to 45% in 2013. In nearly all cases, the mAb is produced in Chinese hamster ovary (CHO) cells (Walsh 2014). There is thus great commercial interest in production of IgGs in CHO cells, but the production requires considerable know-how to achieve sufficient quality of the produced IgG. IgG glycans play a critical role in a number of IgG effector functions including antibody dependent cellular cytotoxicity (ADCC) (Raju 2008). The length and structure of the glycan furthermore affects stability and clearance (Jones et al. 2007; Sola and Griebenow 2009; Stockert 1995). Important N-glycan features, influencing IgG properties include alpha-1,6-fucosylation of the glycan core (Shields et al. 2002), the presence/absence of a bisecting N-acetylglucosamine (Umana et al. 1999), and the termination of N-glycan antennae with a sialic acid residue (Scallan et al. 2007). For IgG glycans, the largest variation of N-glycans is the number of D-galactose residues (Huhn et al. 2009).

The glycosylation profiles of therapeutic proteins, including IgGs, can be highly affected by the cell line, medium composition and cultivation process conditions (Costa et al. 2013; Hossler 2012). Since glycosylation is an important parameter for IgG function, strategies to modify glycosylation profiles of human IgG or to select the most efficient glycoforms have been explored. While genetic engineering has been employed in many cases, it is often simpler to implement changes to the cell culture medium (For a review, see (Andersen et al. 2009)).

Within this study, we have focused on groups of known and potential precursors for the sugar residues constituting the N-glycan chains. The effect on the N-glycosylation of multiple model proteins by addition of precursors has been performed in human, mouse and CHO cells, e.g. for D-galactose (Andersen 2004; Clark et al. 2005; Hills et al. 2001; Schilling et al. 2008; Tachibana et al. 1994; Wong et al. 2010) and D-mannose (Tachibana et al. 1994). Similar studies on varied cells and proteins have also been made on N-acetylated sugars, namely N-acetyl-D-glucosamine (GlcNAc) (Tachibana et al. 1997), and N-acetyl-D-mannosamine (ManNAc) (Baker et al. 2001; Gu and Wang 1998; Hills et al. 2001; Pels Rijcken et al. 1995; Zanghi et al. 1998). Furthermore, the effect of adding nucleotide precursors for nucleotide-sugar donors, involved in N-glycan biosynthesis, has been examined for uridine and cytidine (Wong et al. 2010; Zanghi et al. 1998). While all of these compounds are reported to affect N-glycosylation in one or more studies, several of these studies report divergent or even contradictory effects on protein N-glycosylation. This variation may be due

to the diversity of the applied cell lines, model proteins and cultivation methods in particular, most of these studies are conducted in non-controlled shake flask cultures.

In this study, we have investigated, under production-like conditions (fed-batch controlled bioreactors), whether supplementing the cell culture medium with a wide range of N-glycan precursors affects the N-glycosylation of IgG produced in CHO cells. This setup allows a close mimicry of the commercially important process of production of recombinant pharmaceutical antibodies. The investigated compounds include D-(+)-Mannose, D-galactose, L-fucose, GlcNAc, ManNAc, N-Acetylneuraminic acid (NeuNAc), uridine, and cytidine. To our knowledge none of these compounds have been investigated in an IgG-producing CHO cell line before, and the results for especially D-galactose and ManNAc have been highly divergent in the conditions studied (Andersen et al. 2009). Analysis of the effect of NeuNAc has not been performed anywhere, to our knowledge. We have performed detailed N-glycosylation profiles to address this.

4.2. Materials and Methods

4.2.1. Cell culture

A CHO DG44-derived suspension cell line secreting recombinant IgG antibody (kindly provided by Symphogen A/S, Denmark) were routinely cultured in shake flasks with serum- and glutamine-free PowerCHO-2 CD (Lonza) medium supplemented with 5 mM L-Glutamine (Lonza), 1/100 Mem-NEAA (Lonza) and 1/40 Anti-clumping agent (Gibco). The cells were maintained in a humidified incubator at 37°C, 5 % CO₂ and 100 rpm. Inoculum for each round of 4 parallel fed-batch bioreactors was prepared from one ampule of 10⁷ cells..

4.2.2. Fed-batch cultures

Fed-batch cultures of cells were performed using four paralleled SR0700 bioreactors with a working volume of 200-1000 mL. Cultivations were controlled by a PH4PO4 sensor module, a MX4/4 gassing system, two MP8 multipump modules, and a TC4SC4 temperature and agitation control unit (Dasgip, Germany). Temperature was maintained at 36.8°C applying a CWD4 cooling water distribution unit (Dasgip, Germany) with a WK500 chiller (LAUDA, Germany). pH was maintained at 6.95 by the sparging of CO₂ or the addition of 0.5 M Na₂CO₃. The dissolved oxygen concentration was maintained at 30 %. Cells were agitated at 80 rpm using a marine impeller. 325 mL medium in each bioreactor were inoculated with a post-inoculum density of 4x10⁶ cells/ml to ensure a high culture density and relatively fresh medium at the time of the feeding of additives. At the time of inoculation, feed was cell culture medium with 8 mM L-glutamine and no anti-clumping

agent. The temperature was shifted to 32°C after 24 hours. After 48 hours, the bioreactors were spiked with the respective additives to achieve final media concentration of 20 mM N-acetyl-D-glucosamine (GlcNAc, A3286, Sigma-Aldrich), 20 mM N-acetyl-D-mannosamine (ManNAc, A8176, Sigma-Aldrich), 10 mM L-fucose (F2252, Sigma-Aldrich), 0.5 mM uridine (U3003, Sigma-Aldrich), 0.5 mM cytidine (C4654, Sigma-Aldrich), 10 mM D-(+)-mannose (M6020, Sigma-Aldrich), 0.5 mM N-acetylneuraminic acid (NeuNAc, A2388, Sigma-Aldrich) or 20 mM D-galactose. The feed was changed to feed with matching concentration of the additive. Glucose was spiked into the bioreactor to obtain 12 mM every time the level decreased below 8 mM. Feed was added to cell culture every 24 hours from 0 h to 216 h with a volume of 57.7, 51.4, 43.1, 34.5, 32, 29.9, 27.8, 26.9, 18.8 and 18.8 ml, respectively. The cultures were discontinued after 336 hours. Additives were dissolved in feed medium and sterile filtered before addition to feed bottles or spiked into the bioreactor. Controls were run in triplicate and additives in duplicate to allow for correct evaluation of biological variance.

4.2.3. Cell, metabolite and product analysis

Daily samples of 2 mL cell suspension were collected and cell viability was measured using a NC-100 nucleocounter (Chemometec, Denmark). Cell-free samples for measurement of metabolite and product concentration were obtained by centrifugation at 20,000 g for 5 min. At the final day, day 14, samples of 50 mL were harvested and cleared for cells by centrifugation at 400 g for 5 min at 4°C. Samples were stored at -20°C until analysis. Glucose, lactate, glutamine and glutamate concentrations in cell-free supernatant samples were measured using Yellow Spring Instrument (YSI) analyzers (model 2300 and 2700). Values were normalized against standards of known concentrations. Recombinant IgG antibody secreted in cell-free supernatant samples were quantified by direct measurement of the binding of IgG to protein A-coated sensors (Fortebio, USA). Samples were calibrated against a standard curve created from measurement of known concentrations of IgG.

4.2.4. Purification of IgG

Clarified supernatants were filtered through a 0.22 µm low protein-binding filter (Millipore) to obtain cell free samples. Purification of IgG was conducted on self-packed MabSelect SuRe Protein A column (GE Healthcare) with 200 µl of protein A resin slurry. The IgG were purified according to manufacturer's recommendations using phosphate-buffered saline (PBS) as wash buffer and 100 mM citrate with pH 3.5 as elution buffer. The eluted IgG were directly applied onto a NAP-5 column (GE Healthcare) and eluted with a buffer containing 10 mM citrate and 150 mM NaCl with

pH 6.0. The concentration of the purified IgG were determined by NanoDrop ND-1000 (Thermo Scientific) and stored at -20°C.

4.2.5. Cation-exchange chromatography of IgG

10 µg of purified IgG per sample were injected in to a Dionex summit system equipped with a p680 pump, UVD170U detector at 280 nm, ASI100 automated sample injector with 1000 µl loop and ProPac WCX-10 column 250x4 mm. The column was equilibrated with 95% Buffer A (25 mM sodium acetate pH 5) and 5% Buffer B (25 mM sodium acetate, 0.5M sodium chloride pH 5), and protein was separated at a flow rate of 1 ml/min with a linear gradient of Buffer B from 5 to 100% over 38 min. The chromatograms were quantified by integration of the heterogeneous peak, which is divided into acidic isoforms, main peak and basic isoforms. The cut-offs at the main peak is set at retention time of the highest peak -0.25 min. and +0.14 min.

4.2.6. Intact mass analysis of IgG

Intact mass analysis was performed the same as described by Fan et al. (2014). The mass of the IgG, without glycosylation, is 145499.8 Da. The assigned peaks were quantitated in the Dionex-Chromeleon Chromatography Data System.

4.2.7. Instant-AB labeled glycoprofiling

50 µg of purified IgG per sample have been processed according to instruction of instant ABTM GlykoPrep[®] kit (Prozyme). Labeled glycans were eluted with Milli-Q water, diluted 1:1 with 100 % acetonitrile and applied to HPLC analysis as reported previously (Fan et al. 2014).

4.2.8. Statistical analysis of glycoform distributions

The integral of cell density (IVC) at harvest, the average cell specific productivity (PCD) from day 3 to day 6, and the distributions of charge variants and glycoforms were evaluated statistically in comparison of experiments to control. Evaluation of statistical significance ($p < 0.05$) was calculated in a one-way ANOVA employing Dunnett 's post hoc pairwise comparison test using GraphPad Prism 5.

4.3. Results

To compare the effect of adding glycosylation precursors to the culture medium during cultivations, fed-batch cultivations of an IgG-producing CHO cell line were conducted in controlled bioreactors in order to investigate the effect on cell growth, product formation, charge heterogeneity, and glycosylation profiles of the produced IgG.

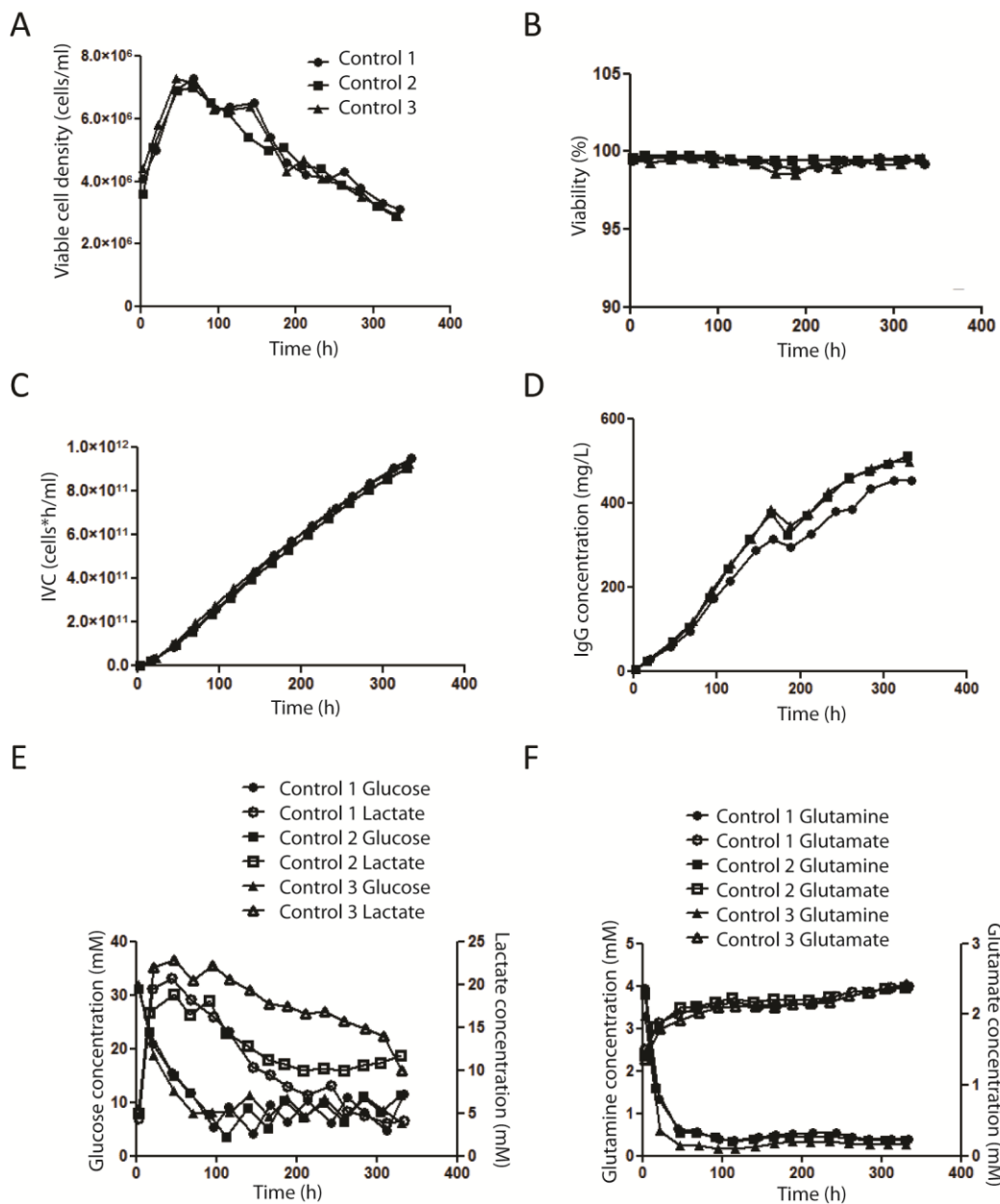


Figure 1. Fed-batch culture performance of three independent controls. (A) viable cell density, (B) viability, (C) integral of viable cell density, (D) IgG titer, (E) glucose/lactate concentration and (F) glutamine/glutamate concentration.

4.3.1. Fed-batch culture

Fed-batch cultures were performed under highly controlled conditions to minimize the effect of cultivation parameters on the glycosylation of IgG. Cell growth was minimized 24 hours after inoculation by a temperature shift; thus also increasing IgG productivity. To analyze the effect of adding glycosylation precursors to the cell culture medium, control cultivations were conducted and compared to cultures supplemented with one of the following eight compounds: D-(+)-Mannose, L-

Fucose, D-galactose, GlcNAc, ManNAc, NeuNAc, uridine, and cytidine. Cell growth and viability were highly reproducible in our controls (Figure 1A-C). IgG titer showed minor variations with a maximum difference of app. 13% on day 14 (Figure 1 D). The lactate concentration of the three different controls was slightly variable with the maximum values at day 2. Glucose concentration also varied slightly among the controls, whereas concentrations of glutamine and glutamate were highly comparable. Overall, our setup gives reproducible results on cell growth, key metabolites, and protein production.

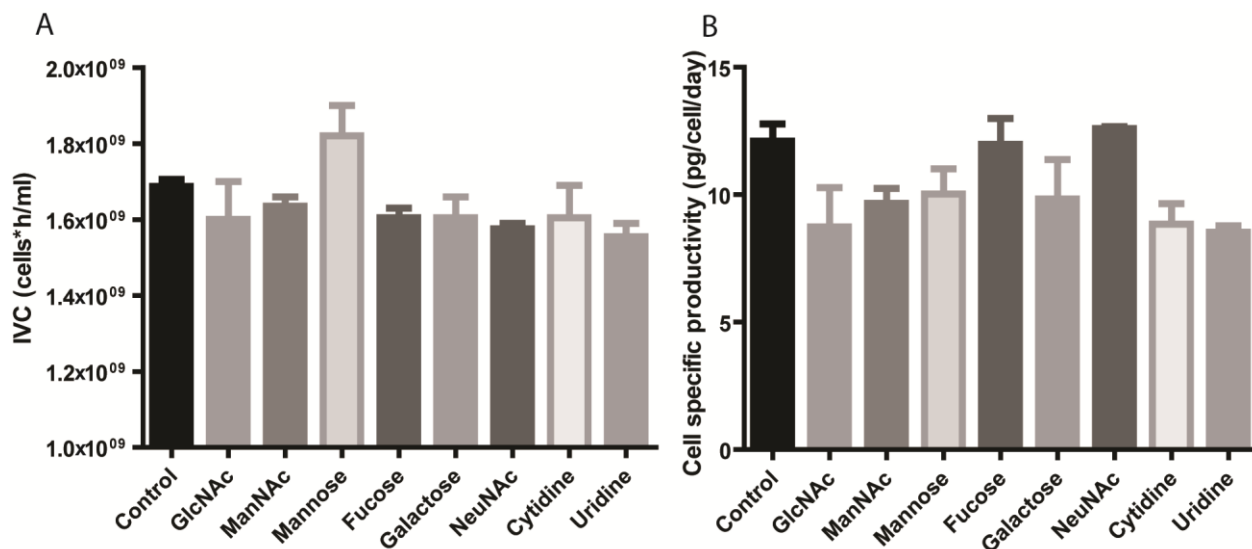


Figure 2. Comparing glycosylation precursor supplemented cultivations to controls. (A) Integral of viable cells, (B) Cell specific productivity. Statistically significant differences are indicated as: * for $p < 0.05$, ** for $p < 0.01$ and *** for $p < 0.001$.

The profiles of cell growth and IgG titer in cultivations supplemented with glycosylation precursors are given in Figure S1 and S2. Data related to the cultures with and without addition of glycosylation precursors are summarized in Table SI. No statistically significant differences were observed between controls and the cultures with additives, although addition of D-mannose seems to slightly increase the IVC (Figure 2A). Cell specific productivities (q_p) of the cultures with additives showed a mild reduction compared to the controls (Figure 2B), except L-fucose and NeuNAc which gives values close to the controls. However, none of these reductions were statistically significant, indicating that the concentrations of the additives used in our setup had no apparent negative effect on IgG specific production rates.

In summary, all of the additives have no statistically significant adverse effects on cell growth and IgG production, making any differences in glycoform frequencies comparable between experiments.

4.3.2. Effect of additives on charge heterogeneity and glycosylation of antibody

To analyze the effect of additives on the glycosylation of the IgG produced by the cells, IgG were purified from the supernatant on the last day of cultivation (day 14). The intact mass analysis was performed to provide quantification of the N-glycans on the IgG molecules.

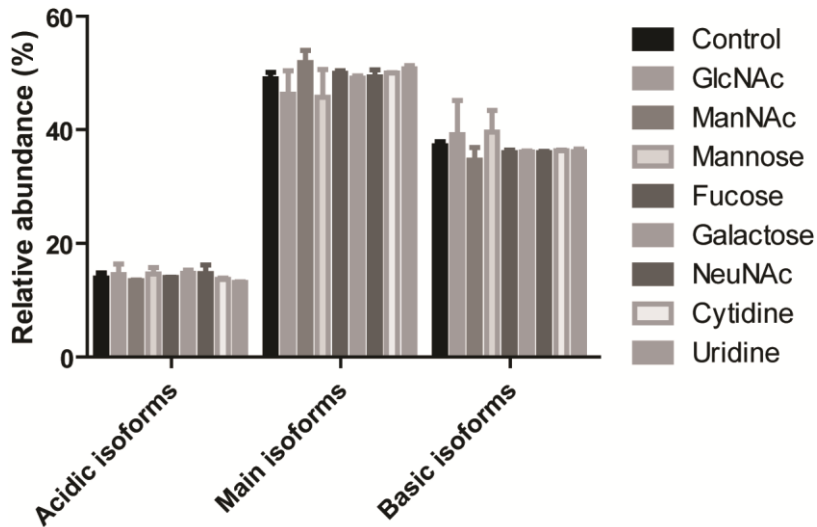


Figure 3. Distribution of charge isoforms of IgG produced from controls and the cultures with feed additives. Statistical significance: * for $p < 0.05$, ** for $p < 0.01$ and *** for $p < 0.001$.

The purified antibodies were analyzed for IgG charge heterogeneity (Figure 3). We see no significant changes in IgG charge between the controls and different additives occur. This suggests that post-translational modifications, for example C-terminal lysine processing, deamidation and oxidation, which can affect the net surface charges and conformational structure of IgG, are relatively constant among the different groups.

Furthermore, we examined glycan combinations detected on the purified IgG (Figure 4). In the groups with galactose added, we saw highly significant ($p < 0.001$) decrease of less processed glycan combinations (A1G0F/G0 and G0F/G0F) and increase ($p < 0.001$) of glycan combinations with more galactose residues (G0F/G1F, G1F/G1F or G0F/G2F and G1F/G2F). In contrast to galactose addition, GlcNAc induces an opposite effect, namely a small increase in A1G0F/G0 and G0F/G0F glycans at the expense of the higher glycosylated forms. Notably, and contrary to several of the previous reported studies, the other additives tested did not cause significant changes to the glycan combinations.

To achieve more detailed information of N-glycan distribution, glycoprofiling using instant-AB labeling was conducted to complement the intact mass analysis (Figure 5). In brief, we identified no

statistical significant changes in GlcNAc occupancy between the controls and the groups with additives, except for mannose addition experiments, which exhibit a lower GlcNAc occupancy (Figure 5A). This is likely due to elevated levels of high mannose forms (Figure S3). Comparison of the relative abundance of galactosylation confirmed a highly significant ($p < 0.001$) increase in the amount of galactose residues attached to the glycans resulting from D-galactose addition (Figure 5B). This was evident in a lower level of G0F glycosylation, a large increase in G1(1,6)F and to a lesser extent G1(1,3)F and G2F glycosylation (Figure S3). Additionally, GlcNAc addition was shown to inhibit galactosylation. Interesting, a slight increase in fucosylation ($p < 0.05$) was observed from ManNAc supplementation. None of the other additives had any significant effects.

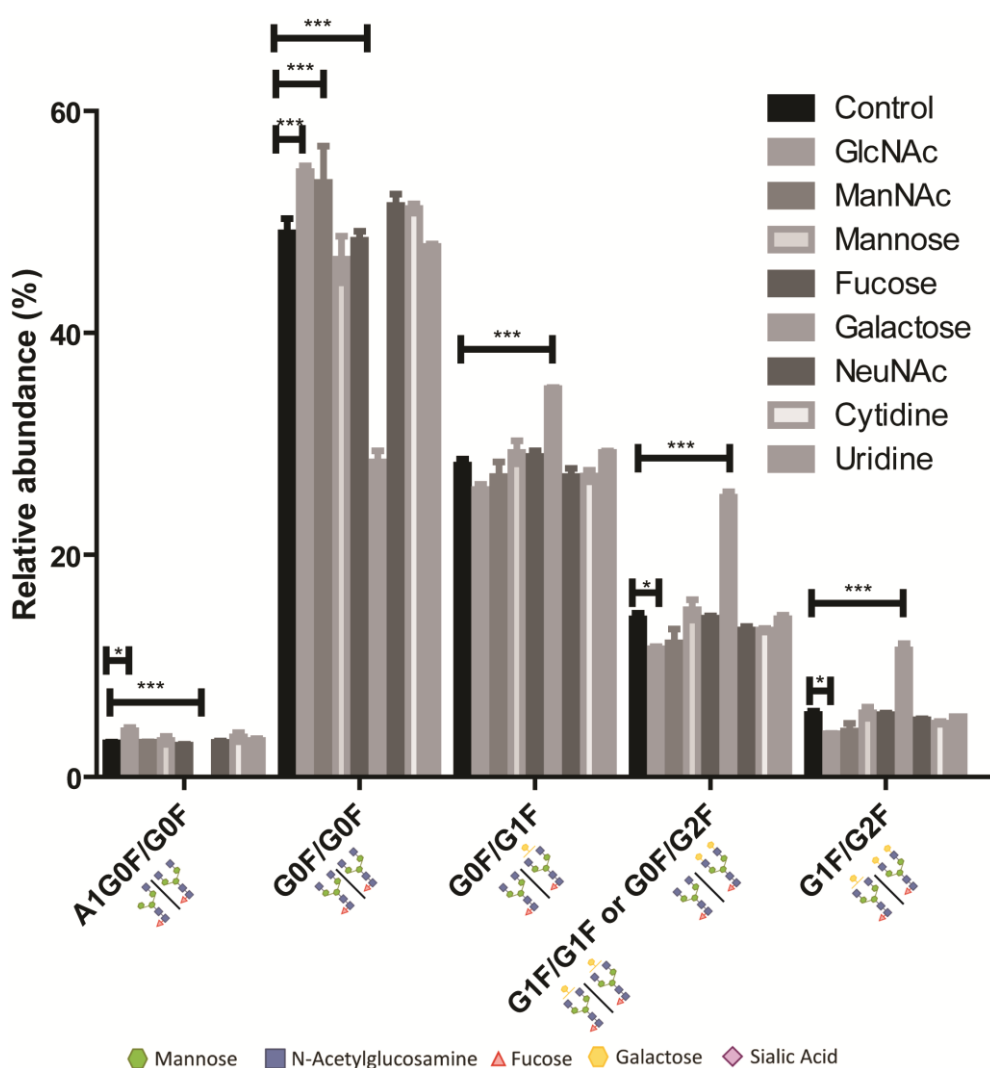


Figure 4. Intact mass analysis of IgG produced from controls and the cultures with feed additives. Statistical significance: * for $p < 0.05$, ** for $p < 0.01$ and *** for $p < 0.001$.

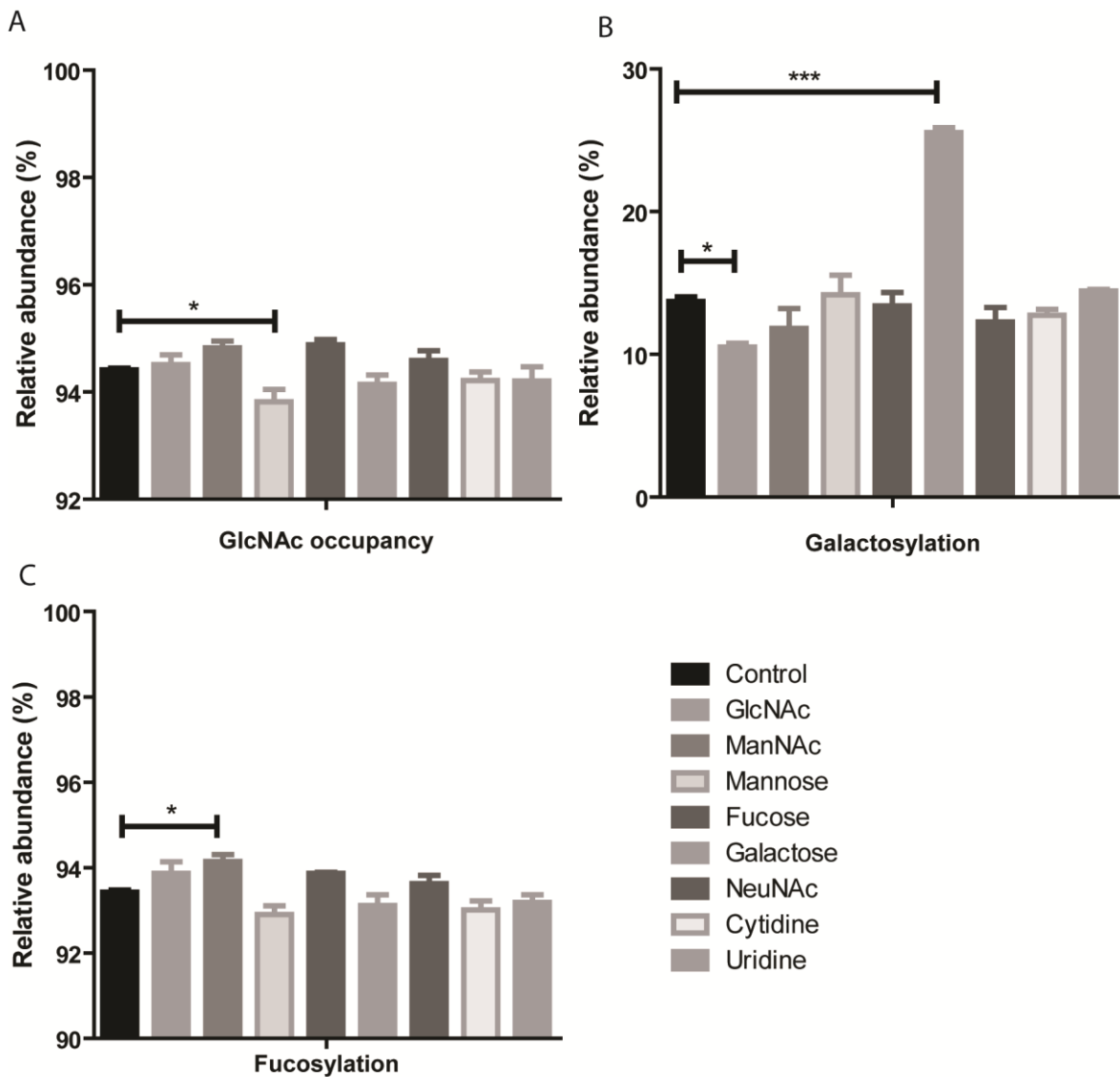


Figure 5. Glycoprofiling of IgG produced from controls and the cultures with feed additives. (A) Relative abundance of GlcNAc occupancy, (B) Relative abundance of galactosylation, (C) Relative abundance of fucosylation. The GlcNAc occupancy and galactosylation was calculated as described in (Fan et al. 2014) Statistical significance: * for $p < 0.05$, ** for $p < 0.01$ and *** for $p < 0.001$.

4.4. Discussion

The availability of intracellular nucleotide sugars (NSs) is key to controlling N-glycosylation (Fan et al. 2014). The feed additives were expected to increase intracellular NS pool by increasing their biosynthesis. In Figure 6, all feed additives used in this study were mapped into the biosynthesis pathway of NSs in order to help understand their effects on cell metabolism.

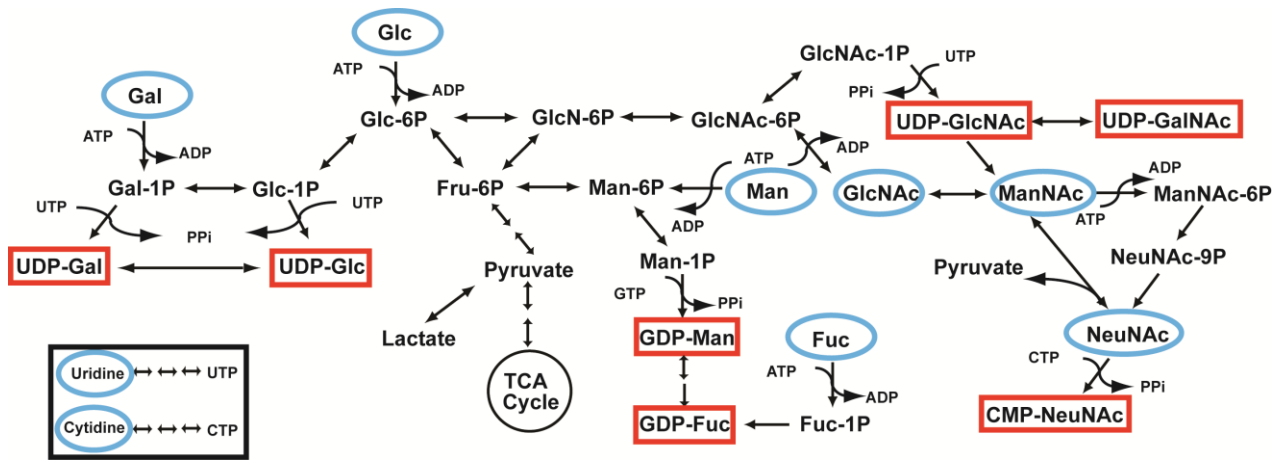


Figure 6. Integrated map of nucleotide sugar synthesis pathway and feed additives. Red rectangle: nucleotide sugars; Blue circle: feed additives studied. Galactose (Gal); Glucose (Glc); Mannose (Man); Fucose (Fuc); N-acetyl-D-glucosamine (GlcNac); N-acetyl-D-mannosamine (ManNac); N-Acetylneuraminic acid (NeuNac)

It has previously been demonstrated that supplementing galactose can increase galactosylation of recombinant proteins (Andersen 2004; Schilling et al. 2008). This was in line with our finding of increased galactosylation of IgG without affecting cell growth and q_p . It has also been reported that addition of 10 mM galactose increases the UDP-Gal pool nearly five-fold in GS-NS0-cells (Hills et al. 2001). This may be attributed to the relatively short biosynthesis pathway from galactose to UDP-Gal (Figure 6). Considering these results, we propose that the biosynthesis of UDP-Gal is a limiting factor for galactosylation of the IgG in our cell line. Addition of galactose to the culture media may elevate the intracellular concentration of UDP-Gal and subsequently increase the presence of terminal galactose residues in the glycans.

Unexpectedly, addition of 20 mM GlcNac decreased galactosylation. This may be explained by the fact that UDP-GlcNac has to be transported into Golgi apparatus to partake in glycosylation processes. Supplementing GlcNac may enhance the biosynthesis of UDP-GlcNac and increase its intracellular concentration. Since no increase in GlcNac occupancy was observed, we suggest that the cellular level of UDP-GlcNac was sufficient for delivery of GlcNac residues for N-glycosylation. On the other hand, we have shown that the UDP-Gal pool is a limiting factor for galactosylation in this cell line. It has also been reported that UDP-GlcNac transporter can partially restore galactosylation in a CHO cell line, which is defective in UDP-Gal transport (Maszczak-Senczko et al. 2011). This indicates that UDP-Gal is transported into the Golgi apparatus via, UDP-Gal transporters but also UDP-GlcNac transporters. Increases in intracellular UDP-GlcNac concentrations, caused by GlcNac feeding, may compete with UDP-Gal for Golgi

loading/uptake/import, reduced availability of UDP-Gal inside Golgi apparatus and consequently decrease galactosylation.

Supplementation with 10mM mannose slightly increased high mannose glycoforms levels and consequently decreased GlcNAc occupancy of the produced IgG. This indicates that an excess of intracellular mannose may increase the intracellular GDP-Man pool.

No increase in fucosylation of the IgG was detected in this study, even though addition of fucose was reported previously to enhance GDP-Fuc biosynthesis and subsequent incorporation into glycans (Pels Rijcken et al. 1995). This implies that the abundance of intracellular GDP-Fuc is not a limiting factor of fucosylation in our process. Therefore, the bottleneck of fucosylation in this case may be the activity of the fucosyltransferase and not metabolic effect of the additives. For these reasons, we suggest that the minor increase in fucosylation, when adding ManNAc to the cell culture, was unrelated to NS metabolism.

As shown in Figure 6, ManNAc and NeuNAc addition may increase the flux towards CMP-NeuNAc and enhance sialylation of IgGs in our cell line. This effect has been confirmed for the production of interferon gamma (IFN- γ) (Gu and Wang 1998; Wong et al. 2010). However, different results were reported elsewhere (Baker et al. 2001; Hills et al. 2001), where feeding with 20 mM ManNAc had no effect on sialylation of recombinant proteins (IgG and TIMP-1), even though an increase in intracellular concentration of CMP-NeuNAc was confirmed. In our case, the sialylation of IgG is extremely low in the controls (<0.2%, Figure S3), and no change was observed when feeding ManNAc or NeuNAc. This is possibly due to the main limitation of IgG-sialylation being steric hindrance of the sialyl transferase. Additionally, it has been demonstrated that increased intracellular level of CMP-NeuNAc can lead to strong feed-back inhibition of UDP-GlcNAc 2-epimerase activity. This in turn prevented ManNAc biosynthesis from UDP-GlcNAc in rat hepatocytes (Pels Rijcken et al. 1995). Therefore when supplementing ManNAc and NeuNAc to cell cultures, we would further expect a slightly increased accumulation of UDP-GlcNAc. This should lead to a decrease in galactosylation. This effect has actually been observed in Figure 5B, although the decrease is minor and not statistically significant.

Uridine or cytidine addition did not change the glycosylation patterns in our study, which indicates that these two additives are not limiting factors for the NSs biosynthesis and glycosylation in our cell line. However, many studies show that combining uridine or cytidine with other NS precursors (for example uridine + galactose, uridine + GlcNAc, and cytidine + ManNAc) can lead to a

synergistic effect on glycosylation (Baker et al. 2001; Grainger and James 2013; Gramer et al. 2011; Wong et al. 2010).

In conclusion, supplementing cell cultures with glycosylation precursors can be a fast and effective way of modulating some features of N-glycosylation of recombinant proteins. For example, addition of galactose consistently increased galactosylation of IgG in this process. Additionally, most of other additives tested didn't show a significant effect on glycosylation patterns. However, several metabolic bottlenecks in NS biosynthesis and glycosylation could be expected across cell lines, and we can therefore not rule out the effectiveness of these additives on glycosylation (showed no effect in our cell line) in other cell lines. Future investigation, testing more cell lines with different concentrations and combinations of glycosylation precursors, could help to advance our understanding of the metabolic limits of different cell lines. This will aid us to improve current strategies for controlling and optimizing glycosylation patterns of heterologously expressed biopharmaceuticals.

4.5. Acknowledgements

This work was supported by the Lundbeck foundation, Symphogen A/S, and the Novo Nordisk Foundation. The authors would like to thank Novo Nordisk A/S for IgG quantification and Symphogen A/S for glycosylation analysis and providing the cell line.

4.6. References

- Andersen D. 2004. Cell culture effects on the glycosylation of therapeutic proteins. Bioprocess International IBC LifeSciences.
- Andersen MR, Hyun Nam J, Sharfstein ST, Flickinger MC. 2009. Protein Glycosylation: Analysis, Characterization, and Engineering. Encyclopedia of Industrial Biotechnology: John Wiley & Sons, Inc.
- Baker KN, Rendall MH, Hills AE, Hoare M, Freedman RB, James DC. 2001. Metabolic control of recombinant protein N-glycan processing in NS0 and CHO cells. *Biotechnol Bioeng* 73(3):188-202.
- Clark KJ, Griffiths J, Bailey KM, Harcum SW. 2005. Gene-expression profiles for five key glycosylation genes for galactose-fed CHO cells expressing recombinant IL-4/13 cytokine trap. *Biotechnol Bioeng* 90(5):568-77.
- Costa AR, Rodrigues ME, Henriques M, Oliveira R, Azeredo J. 2013. Glycosylation: impact, control and improvement during therapeutic protein production. *Crit Rev Biotechnol*.

- Fan Y, Jimenez Del Val I, Müller C, Wagtberg Sen J, Rasmussen SK, Kontoravdi C, Weilguny D, Andersen MR. 2014. Amino acid and glucose metabolism in fed-batch CHO cell culture affects antibody production and glycosylation. *Biotechnology and Bioengineering*:n/a-n/a.
- Grainger RK, James DC. 2013. CHO cell line specific prediction and control of recombinant monoclonal antibody N-glycosylation. *Biotechnol Bioeng* 110(11):2970-83.
- Gramer MJ, Eckblad JJ, Donahue R, Brown J, Shultz C, Vickerman K, Priem P, van den Bremer ET, Gerritsen J, van Berkel PH. 2011. Modulation of antibody galactosylation through feeding of uridine, manganese chloride, and galactose. *Biotechnol Bioeng* 108(7):1591-602.
- Gu X, Wang DI. 1998. Improvement of interferon-gamma sialylation in Chinese hamster ovary cell culture by feeding of N-acetylmannosamine. *Biotechnol Bioeng* 58(6):642-8.
- Hills AE, Patel A, Boyd P, James DC. 2001. Metabolic control of recombinant monoclonal antibody N-glycosylation in GS-NS0 cells. *Biotechnol Bioeng* 75(2):239-51.
- Hossler P. 2012. Protein glycosylation control in Mammalian cell culture: past precedents and contemporary prospects. *Adv Biochem Eng Biotechnol* 127:187-219.
- Huhn C, Selman MH, Ruhaak LR, Deelder AM, Wuhrer M. 2009. IgG glycosylation analysis. *Proteomics* 9(4):882-913.
- Jones AJ, Papac DI, Chin EH, Keck R, Baughman SA, Lin YS, Kneer J, Battersby JE. 2007. Selective clearance of glycoforms of a complex glycoprotein pharmaceutical caused by terminal N-acetylglucosamine is similar in humans and cynomolgus monkeys. *Glycobiology* 17(5):529-40.
- Maszczyk-Seneczko D, Olczak T, Jakimowicz P, Olczak M. 2011. Overexpression of UDP-GlcNAc transporter partially corrects galactosylation defect caused by UDP-Gal transporter mutation. *FEBS Lett* 585(19):3090-4.
- Pels Rijcken WR, Overdijk B, Van den Eijnden DH, Ferwerda W. 1995. The effect of increasing nucleotide-sugar concentrations on the incorporation of sugars into glycoconjugates in rat hepatocytes. *Biochem J* 305 (Pt 3):865-70.
- Raju TS. 2008. Terminal sugars of Fc glycans influence antibody effector functions of IgGs. *Curr Opin Immunol* 20(4):471-8.
- Scallon BJ, Tam SH, McCarthy SG, Cai AN, Raju TS. 2007. Higher levels of sialylated Fc glycans in immunoglobulin G molecules can adversely impact functionality. *Mol Immunol* 44(7):1524-34.
- Schilling BM, Gangloff S, Kothari D, Leister K, Matlock L, Zegarelli SG, Joosten CE, Basch JD, Sakhamuri S, Lee SS. 2008. Production quality enhancements in mammalian cell culture process for protein production. US Patent 7,332,303.

- Shields RL, Lai J, Keck R, O'Connell LY, Hong K, Meng YG, Weikert SHA, Presta LG. 2002. Lack of Fucose on Human IgG1 N-Linked Oligosaccharide Improves Binding to Human FcγRIII and Antibody-dependent Cellular Toxicity. *Journal of Biological Chemistry* 277(30):26733-26740.
- Sola RJ, Griebenow K. 2009. Effects of glycosylation on the stability of protein pharmaceuticals. *J Pharm Sci* 98(4):1223-45.
- Stockert RJ. 1995. The asialoglycoprotein receptor: relationships between structure, function, and expression. *Physiol Rev* 75(3):591-609.
- Tachibana H, Kim JY, Shirahata S. 1997. Building high affinity human antibodies by altering the glycosylation on the light chain variable region in N-acetylglucosamine-supplemented hybridoma cultures. *Cytotechnology* 23(1-3):151-9.
- Tachibana H, Taniguchi K, Ushio Y, Teruya K, Osada K, Murakami H. 1994. Changes of monosaccharide availability of human hybridoma lead to alteration of biological properties of human monoclonal antibody. *Cytotechnology* 16(3):151-7.
- Umana P, Jean-Mairet J, Moudry R, Amstutz H, Bailey JE. 1999. Engineered glycoforms of an antineuroblastoma IgG1 with optimized antibody-dependent cellular cytotoxic activity. *Nat Biotechnol* 17(2):176-80.
- Walsh G. 2010. Biopharmaceutical benchmarks 2010. *Nat Biotechnol* 28(9):917-24.
- Walsh G. 2014. Biopharmaceutical benchmarks 2014. *Nat Biotechnol* 32(10):992-1000.
- Wong NS, Wati L, Nissom PM, Feng HT, Lee MM, Yap MG. 2010. An investigation of intracellular glycosylation activities in CHO cells: effects of nucleotide sugar precursor feeding. *Biotechnol Bioeng* 107(2):321-36.
- Zanghi JA, Mendoza TP, Schmelzer AE, Knop RH, Miller WM. 1998. Role of nucleotide sugar pools in the inhibition of NCAM polysialylation by ammonia. *Biotechnol Prog* 14(6):834-44.

Chapter 5 CHO 'Omics-based bioprocessing

Very recently, CHO cell-based bioprocessing entered omics era. How to apply this type of data to facility cell line and process development for producing recombinant proteins with higher titer and better quality became a challenge. In this chapter, we will present our review paper published in *Pharmaceutical Bioprocessing*, 2014, Vol. 2, No. 5, Pages 437-448, which highlight the status and recent update in the field of CHO 'omics studies and the potential application in genome scale modeling of CHO cells.

Towards Genome-Scale-models of the Chinese Hamster Ovary cells: Incentives, Status, and Perspectives

Christian S. Kaas^{1,2}, Yuzhou Fan^{1,3}, Dietmar Weilguny³, Claus Kristensen², Helene Fastrup Kildegaard⁴, Mikael R. Andersen^{1,*}

¹Department of Systems Biology, Technical University of Denmark, Denmark

²Mammalian Cell Technology, Biopharmaceutical Research Unit, Novo Nordisk A/S, Maaloev, Denmark

³Symphogen A/S, Ballerup, Denmark

⁴The Novo Nordisk Foundation Center for Biosustainability, Hørsholm, Denmark

*Corresponding author. E-mail: mr@bio.dtu.dk

Keywords

Chinese hamster ovary cells; genome-scale metabolic models; genomics; transcriptomics; metabolomics; proteomics; cell factories; genetic engineering.

Abstract

Bioprocessing of the important Chinese hamster ovary (CHO) cell lines for used production of biopharmaceuticals stands at the brink of several redefining events. In 2011, the field entered the genomics era, which has accelerated omics-based phenotyping of the cell lines. In this review we describe one possible application of this data: The generation of computational models for predictive and descriptive analysis of CHO cellular metabolism. We describe relevant advances in other organisms and how they can be applied to CHO cells. The immediate implications of the implementation of these methods will be accelerated development of the next generation of CHO cell lines and derived biopharmaceuticals.

5.1. Introduction

It is generally appreciated that cell culture based on Chinese hamster ovary (CHO) cells holds substantial economical and medical importance. The global market for biologics was 99 billion USD in 2009, where 60-70% of the products were produced in CHO cells [1]. Over 40 biopharmaceuticals have been produced in CHO cells so far, including monoclonal antibodies, hormones, cytokines and blood-coagulation factors. It is furthermore evident that the impact of

CHO cell culture will only increase in the immediate future: The US market for biologics alone has been climbing from 51.3 billion USD in 2010 to 63.6 billion USD in 2012, and expected to increase at higher rates with the US Affordable Care Act [2]. The global market for biologics is expected to rise to 190 billion USD in 2015 [3], and the percentage of CHO-derived products in approved new biologics are climbing. In 2010 and 2011 combined, 14 out of 19 approved biopharmaceuticals were derived from cell culture, the majority of these using CHO cells as hosts [4].

Despite this impact, the development of CHO cell processes - although highly successful - has been mainly driven by medium development and process engineering and to a lesser extent genomic technologies such as enhanced expression technologies for heterologous proteins [5]. Metabolic engineering, such as seen in microbial cell factories [6,7], has been very limited, although with some notable exceptions (see e.g. [8,9]). We will argue that this has been due to the relatively late arrival of genome sequences for CHO cell lines; even though the first CHO EST sequences were published in 2005 [10], the first CHO genome sequences were published in 2011 [11,12], an entire decade after the first draft publication of the human genome [13], and two decades after the genome of the first eukaryote, *S. cerevisiae* [14]. As a result, most early genome-based studies of CHO cells were performed by using the genome sequences from other mammals e.g. human, mouse, or rat [15,16], which generally limits the possible experiments and interpretation of the results.

However, there is now ample genomic information available for the CHO cell lines. The CHO-K1 genome sequence [11], has been supplemented by the 2013 release of two draft genomes for the Chinese Hamster (*Cricetulus griseus*) [17,18] from which the CHO cell line was originally isolated in 1957 [19]. Additionally, draft sequences for a number of CHO cell lines including the industrially relevant CHO-S and CHO DG44 have been published [18]. While this still leaves a few widely used cell lines, e.g. the CHO DXB11 cell line [20,21], unsequenced, and a general need for improved genome quality, it is clear that CHO cell research has reached the genomic era.

One highly promising application of genomics-based research is the generation of genome-scale models of CHO cells (Figure 1).

5.2. Potential Applications of Metabolic Models to CHO Cell Cultures

A genome-scale metabolic model (GSM) is a systematic correlation of the genomic information of an organism to a metabolic network, effectively reconstructing the metabolic network of the cell type in question. Such a network is most often built from available generic pathway databases (e.g. KEGG [22]) and specific literature for the organism being modeled, combined with an annotated

genome [23]. This underlying network is often called a genome-scale reconstruction or GENRE. Integration of the GENRE with a linear programming-based mathematical framework allows modelling of the metabolic fluxes of the cell, which is often predictive and nearly always helpful in data interpretation. The actual model and computational framework applies the laws of mass conservation and balances of metabolic fluxes around single metabolites to compute enzymatic rates for every single enzyme present in the model. These rates are seen as averages for the culture and are most often given as specific rates relative to a certain number of cells. Additional algorithms may be applied to predict the effect of e.g. gene deletions/insertions, perturbations of feeding rates/nutrient uptake or increased production rates (e.g. [24]). Pioneering work and additional application such as integration of the protein secretion network and regulatory information has been driven forward in *E. coli* [25–27]. As CHO cells are arguably more complex in terms of gene numbers and cellular compartments than *E. coli*, the work associated with building a CHO GSM is more laborious and complicated, in particular in terms of assigning correct genes to enzymatic functions, and assigning enzymatic reactions to the correct compartments. However, the algorithms and uses of these models are general, and examples of potential applications from *E. coli* are equally relevant for CHO cells. In addition to this, implementation has been performed in a wide span of eukaryotic organisms as well, several of which with a complexity and quality of annotation resembling CHO cells. Examples of eukaryotic models include eukaryotic microbes, e.g. industrially relevant yeasts such as *S. cerevisiae*, *Kluyveromyces lactis*, and *Pichia pastoris* [28–31], filamentous fungi applied for enzyme production, e.g. *Aspergillus niger* [32–34], and also higher eukaryotes such as *Arabidopsis* [35], mouse hybridoma cells [36], and human cells [37,38]. In these examples, cells, arguably as complex as CHO cells, have had their metabolism reconstructed. Cells from mouse, *Arabidopsis*, and human are evidently of similar or higher complexity than the CHO cell. Even eukaryotic microbes such as filamentous fungi have a more complex growth physiology, with multicellular growth compared to the relatively homogeneous CHO cells with a more uniform growth. While the current annotation of the CHO genome is far from the quality of annotation and gene characterization found for human cells or even mouse cells [39], models can to a large part be generated by inferring function by homology to organisms with better annotation, e.g. mouse or human in the case of CHO.

The primary applications of these models can be divided into at least five major categories: 1) metabolic engineering, 2) model-directed discovery, 3) interpretations of phenotypes, 4) analysis of network properties, and 5) studies of evolutionary processes [40,41]. All of these applications are

highly relevant and interesting for CHO cell culture in their omics-driven approach to cellular physiology (Figure 1E).

Metabolic engineering holds considerable promise for CHO cell culture, as GSMs have the possibility of predicting the effect of gene deletions, additions and over-/under-expression. Several phenotypic traits of the CHO cells are sub-optimal for prolonged culture and protein productivity. Some examples of this are the conversion of high glycolytic flux to lactate, or the formation of ammonium by conversion of amino acids in the medium. Both are detrimental to cell growth and product quality [42,43]. Accordingly, these processes have been subjected to metabolic engineering with varying success [8,9], but definitive solutions have not been found at the cell engineering level, and have to a large extent been addressed and alleviated with process and medium design (See e.g. [44] for an example for lactate production). Model-driven engineering presents an interesting angle on these problems, by generating platform cell lines incapable of producing such by-products or producing them in highly reduced amounts. Other possibilities are found in areas addressed in microbial cell factories, e.g. increasing the number of sugars available for carbon catabolism to decrease the problems with high glycolytic flux [45]. GSMs also provide attractive possibilities to model decreased by-product formation [46], generally applicable to any biotechnological production process. Another tantalizing possibility is the extension of the significant advances in CHO culture medium development [5]. One could imagine that it would be interesting to perform model-guided systemic cell line engineering to tailor the cell lines to a specific medium, or a certain feeding profile. The capabilities of GSMs to model cellular metabolism on a systemic scale, allows the combination of e.g. consumption rates of medium components with model predictions. The result of this would be further improvement of platform media and processes with a tailored cell line.

Model-directed discovery has been useful in many microbial systems, in particular for improving gene annotation and functional assignment [32,33,41]. With the current state of CHO genomics being in its infancy, the annotation of the identified genes is very preliminary. The state of the CHO genome annotation on one hand complicates accurate model reconstructions, due to the challenges of linking genes with function, but also presents opportunities. In particular the reconstruction of CHO metabolism (GENRE) will suggest tentative assignment for a high percentage of the metabolic genes, as is seen in other eukaryotic microbes organisms [28,32,34], where the genes involved in metabolism have not been studied as extensively as in leading model organisms e.g. yeast or *E. coli* [25,29]. However, even in *E. coli* has the metabolic network been applied to find and characterize candidate genes for a specific function [47]. This type of application of the

metabolic network is particularly powerful when combined with other omics-data types such as metabolomics and proteomics (see below). Here one can e.g. integrate orphan metabolites into the metabolic network and thus improve our understanding of CHO metabolism, or identify active isoenzymes for specific pathways from protein expression data coupled with tentative metabolic enzyme networks. As this application of the model is fairly independent of the computational predictive power, it is relevant to CHO cells no matter how accurate the models might become. The same holds true for the next application:

Interpretation of phenotypes is perhaps the most universally applicable use of the GSMs and GENREs. The network – irrespective of predictive power – provides a framework for interpretation of experimental data. For CHO cells, the calculation of metabolite consumption/production rates, growth rates and specific product formation rates has long been standard for cell culture medium and process design. However, a theoretical and computational framework for holistic interpretation of the data has not previously been available. These reconstructed networks can aid the interpretation of experimental data related to growth, as well as multiple types of omics data [41]. Models have proven important in interpretation of metabolic/flux data [48], transcriptomics [49], and proteomics [50]. The approaches are listed in an excellent recent review [51], which also covers mammalian cell types. A related example from medical research is the interpretation of proteomic and DNA microarray data from human macrophages through a reconstructed metabolic network of the cell type [38]. In this study, a holistic view of the process of activation of macrophages was achieved, and systemic activation and inactivation of parts of metabolism was identified.

In many cases, models are also capable of quite persuasive prediction of phenotypes. Especially interesting, considering the costs and time required to produce stable genetic changes in CHO cells, is prediction of phenotypes of genetic mutants [52,53].

Analysis of network properties is generally speaking a computational exercise, in which one analyzes the network structure of the GENRE to discover inherent features or emergent properties of the metabolic network. In some cases, this analysis has become mainly an arithmetic exercise, applying standard network topology algorithms, and has generated limited biological insight. However, in some cases, deep insights are found. The most easily applicable example in the context of CHO cell and process engineering, is the application of elementary flux modes [54] to identify the smallest possible set of essential metabolic genes in CHO cells, such as achieved for individual pathways in *E. coli* [55] or *S. cerevisiae* [56]. Such identification could be applied for generating cell lines with a trimmed metabolism, thus decreasing the variability of the system. This would be

feasible for CHO, despite the presence of extra isoenzymes or alternate pathways in many enzymatic steps. For several enzymatic functions, only one of the isoenzymes are detected at the protein level [57]. Alternatively, one can delete steps in the enzymatic pathways/elementary flux modes, where only one enzyme exists.

Studies of evolutionary processes have been a re-occurring theme in several applications of bacterial network, in particular the *E. coli* GENRE [40,41]. In such studies, specialized models have e.g. been developed to describe specific strains of *E. coli*, and compared these to identify the genetic origin of specific phenotypes [58]. Given the availability of the genomic sequence for multiple CHO cell lines with varying properties [18] and surely more to come, such an exercise would hold exciting perspectives for interpreting these genomes. One possible application would be the genetic basis for certain metabolic features in cell lines generated by mutagenesis, and the possibility of *de novo* engineering the features into a "clean" background. This would reduce possible complications from decreased genetic stability in mutants subjected to mutagenesis [59].

With the above-mentioned being only a small percentage of the possible applications of such models for CHO cell lines, the potential is clearly large for the generation and application of GENREs and GSMs for CHO cells.

5.3. Additional Available Data Sources for Increased Applicability of CHO Models

The availability of an annotated genome for CHO cells is the bare minimum of information required to generate a draft model for CHO cells. Models of microbial systems have been published based mainly on literature on characterized genes (e.g. for *Corynebacterium glutamicum* [60] or *Aspergillus niger* [32,61]), but this requires detailed legacy data for a wide selection of metabolic pathways. In general, most recent generation of GSMs is based on variations of a standardized protocol for metabolic network reconstruction and model validation published in 2010 [23], using basic genome annotation as a starting point for the organism of choice.

However, other types of omics data have proven highly valuable for model generation, validation and application. Here, the CHO field is maturing at an impressive pace, considering the quite recent publication of the first public CHO genome [11], followed by a wealth of other omics types being published in these years [62]. Here we will briefly emphasize selected studies which provide data highly applicable to CHO modelling, either due to the experimental setup of the study, the type of the data, or the perspectives these offer for CHO modeling. Several of these data types are discussed

in detail in other reviews in this issue, to which we direct the reader interested in further depth on specific data types [Add reference(s) in Proof].

5.3.1. Genomics

A well-annotated genome with a high coverage is a crucial component in building a GSM with predictive power or a GENRE with a potential for informative data integration and interpretation. It is essential to be able to identify the genes of all major metabolic pathways in order to generate an accurate GENRE and following that a GSM. This requires a genome coverage of ideally >99% of the genes. Early EST sequencing efforts [10] identified only less than 20% of the genes, shown to be present in the CHO-K1 cell line draft genome [11]. Convenient for model construction, the genome sequence has been made accessible at the online database www.CHOgenome.org [63] as well as at the NCBI genbank. The coverage appears to be at least 99%, at least it was demonstrated that homologs existed for 99% of the genes in the human genome associated with glycosylation.

Due to the variability of the cell lines, it can be argued that it would be most appropriate to use the progenitor Chinese hamster (*C. griseus*) both as the source of a reference genome, and as a scaffold for a master CHO GSM, from which specialized models can be generated for individual cell lines. This is now possible due to the publication of draft genomes for *C. griseus* [17,18]. This publication showed that there are more than 3.7 million point mutations between the progenitor hamster and the CHO cell lines [18] and extensive chromosomal rearrangements that has occurred between CHO-K1 and CHO-DG44 [64] emphasizing the effects of the mutagenesis that occurred in the process of creating the various cell lines. Currently, in order to fully exploit these sequences, these genomes must be mapped against reference genomes with gene annotation. Improving the gene annotation for the *C. griseus* genome and CHO-K1, which has become the de-facto reference genome for cell lines, would be beneficial to model building. Current and new genomes could thus be aligned to these references for detection of mutations.

Furthermore, the state of genome assembly should be improved. Currently the genomes for both hamster and cell lines are divided into at least 4000 contigs per genome, which means that genes for important metabolic functions may be lost in the sequencing gaps. Such gaps can to some extent be detected and fixed in the network reconstruction process [23,32]. Even so, an appropriate solution would be to apply 3rd generation sequencing to yield longer sequenced reads that can assemble the contigs to improve the coverage of the genomes. Such efforts are in progress in the community (Prof. Nicole Borth, personal communications), and should have a substantial positive impact on the models, which can be constructed for CHO cells.

5.3.2. *Transcriptomics*

In general, it is only a low percentage of the CHO genes which are actually expressed under normal condition, e.g. only ~50% of the genes involved in protein glycosylation are transcriptionally active [11]. Consequently, integration of dynamic omics-data such as transcriptomics and proteomics are important for accurate prediction of gene deletion/silencing effects. Several studies and tools are now available for this, including both sequencing and DNA microarray based methods. Naturally, some of the first transcriptome data was generated prior to the genome sequence based on EST sequences from CHO and mouse used for design of microarrays [65,66].

Worth particular mention is a large-scale comparison of microarray data from more than 120 individual CHO cultures [67]. The data can be accessed through the web-based CHO gene co-expression database (CGCDB) allowing easy access to the list of genes found to co-express with e.g. cell specific productivity and growth rate. Such data could be used for model improvement and validation. For easy and relatively inexpensive assessment of the CHO transcriptome in future experiments, a new generation of the Affymetrix CHO DNA microarray has been launched with up to 26 unique sequences of each transcript with a total of more than 644,000 probes [68].

RNA-sequencing is expanding for CHO culture as in many other fields [69]. Recently, a transcriptome database for CHO RNA sequencing data has been developed and is available at <https://gendbe.cebitec.uni-bielefeld.de/cho.html> [70].

In summary, transcriptomics data is abundantly available, and will only increase in the coming years.

5.3.3. *Proteomics*

The CHO proteome is interesting in the context of CHO metabolic modelling as it can provide additional functional information, in some cases expanding on transcriptomic evidence. The proteome of CHO-K1 was thoroughly characterized by Baycin-Hizal in 2012 [57]. Here, 6164 proteins were detected. Of these, only 60% were also detected at the mRNA level by Xu in 2011 [11]. The functional application of the data and the need for having models specialized to individual cell lines becomes apparent from this study. Statistical analysis indicated that some pathways such as fatty acid metabolism, amino sugar and nucleotide sugar metabolism, which provide important precursors for recombinant protein synthesis, as well as protein processing and apoptosis, were enriched in CHO-K1 [57].

Given the principal application of CHO cells for production of secreted proteins, in this content, secretome data, such as characterized from the CHO DG44 and CHO-S cell lines by Slade [71], is interesting to incorporate. Such data can help identify secretory bottlenecks or extracellular proteases as seen for microbial cell factories [72,73].

CHO specific protein databases have been constructed based on data from the CHO-K1 genome [11] and the CHO transcriptome [74], and have been shown to increase the number of identified proteins by 40-50% from proteomics studies compared to only using protein databases based on e.g. the murine proteome [75].

It is generally accepted that the generation of proteomics data is more technically challenging than transcriptome data, but the pilot studies within CHO cells, such as those mentioned above, show that there is clearly additional value to be gained from interrogating this data set.

5.3.4. *Metabolomics*

As mentioned in the text above, metabolomics has considerable value to add in the model building process, as this type of data can help identify metabolic pathways, which are experimentally shown to be occurring in the cells due to the presence of metabolic intermediates or products, but the genetic basis is not necessarily clear. Being able to identify and include these pathways can increase the predictive power of the model.

For such inclusion, several studies of high quality [76,77] and standardized protocols [77–80] have been available for several years, as metabolomics are not as such dependent on the availability of a genome.

Two studies are of particular interest in terms of getting data of a sufficient quality for model integration. The first was published by Dietmair et al [81] correlating intracellular and extracellular metabolite concentrations with growth. The second is the work of Chong et al [82] where intracellular metabolite profiles were obtained for eight single cell clones with high and low q_{mAb} at the mid-exponential phase during shake flask batch cultures. Such studies can give insight in metabolic responses, and help validate CHO metabolic models, in that one can examine and adapt the ability of the model to predict these responses.

The application of the metabolic networks to interpret metabolomics data, can also be exemplified in a 2012 study by Selvarasu et al [83], where a generalized metabolic network of mammalian cells was adapted to CHO cells to aid in metabolomics data interpretation (see further details below). The

coupling of the network, genome-scale-modeling, and metabolomics data allowed the identification of growth-limiting factors.

Overall, the CHO field is at this point uniquely poised to utilize the substantial amounts of available omics data in building high quality models for CHO cells. An overview is presented in Figure 1. During any future model building efforts, one should draw upon the current availability of computational models for CHO and similar systems, and incorporate this where appropriate.

5.4. Overview of Cellular Modelling Efforts in CHO cells and Beyond

So far, no dedicated effort to building a CHO GSM *de novo* has been published. The closest example is the adaptation of a model of mouse hybridoma cells [36] to CHO cells by the addition of 35 CHO-specific metabolic reactions and subsequent model curation resulting in a model comprising 1,540 reactions and 1,302 metabolites [83]. This model has been further developed by other groups, although not published through a journal at this time, but is available for download from <http://cho.sourceforge.net/>. A similar approach of adapting a mouse GSM was employed by Martínez et al [84] for examining the energy consumption and metabolism surrounding lactate formation and consumption in CHO cells.

Dedicated models have been developed for related cell lines in other systems, as mentioned a generic model for mouse cells, applied to mouse hybridoma cell lines [36], and a model for the HEK-293 cell line has been developed as well [85]. This study is particularly promising for CHO cell modelling, as the HEK-293 model was developed by reducing the generic model for human cellular metabolism [37] to a model specific for HEK-293 metabolism. Furthermore, this model was employed to interpret both transcriptomic, metabolomic, and flux data to gain functional understanding of glucose and glutamine metabolism; both key features for CHO metabolism [85]. A similar study has been seen for BHK cells for interpretation of metabolomics data [86].

These models listed above represent the full list of available metabolic genome-scale models with relevance to CHO cells. However, to the best of our knowledge, a model specific for CHO cells, or any specific cell line has still have not been generated.

One area, where modelling in CHO cells is more developed, is the kinetic modelling of protein N-glycosylation, in particular integrated with mass spectrometry on glycans. Here, very accurate predictions and substantial networks have been generated and improved over the last two decades. The first mathematical model for protein N-glycosylation process was built in 1997 by the complementary studies of a single-compartmental model [87] and a multi-compartmental model

[88]. Later work expanded upon the previous work to involve glycosylation processes as galactosylation, fucosylation, sialylation, and addition of N-acetylglucosamine residues [89]. This model had up to 7,565 N-glycans and 22,871 reactions included. Furthermore, two glycosylation models based on different views of protein transport across the Golgi, namely Golgi maturation mechanism and vesicular transport mechanism, were studied and compared. This model was highly expanded and sophisticated by the same group to include interpretative power of N-glycan MS data [90]. More recently, an optimized model considering 77 N-glycans, 8 enzymes, 4 nucleotide transporters and 95 reactions with individual rate expressions were built on the basis of Golgi maturation mechanism with an improvement of taking Golgi protein recycling into account [91]. On top of that, a more comprehensive glycosylation model that link a model that described the metabolism of nucleotides and nucleotide sugars to the previous N-glycosylation model was developed by the same group [92]. These networks have been shown to have both high predictive and interpretative power, and would be unique key features to have integrated in CHO GSMs, to the extent that it is possible. Such additions could predict effects of glycosylation engineering and/or the effect of different substrate uptake rates.

5.5. Future Perspectives

With the potential of GSMs tailored to CHO cells as demonstrated above, it is not surprising that several groups in the CHO community are working on building whole and partial reconstructions of CHO metabolism, including some of the authors of this review. These groups have this year formed a consortium compiling their work, and are working towards generating a community consensus model for CHO cells (Nathan E. Lewis, personal communications). Such models and network reconstructions are known from several other research communities, including *Salmonella Typhimurium* [93], yeast [29,94], and human [37] metabolism.

The future arrival of the CHO GSM will probably raise the same discussion that followed the release of the first CHO genome: How well does this model describe each of the different CHO cell lines? Each of the cell lines have undergone rearrangements and have diverse transcriptomes and for this reason several parameters will need to be investigated. Future and current sequencing projects for individual cell lines should be combined with bioreactor characterization of the cell lines and their corresponding models to gain a functional understanding of the differences (Figure 1C-D). The next years will tell whether these models will be able to model the complex behaviour of the CHO cell and open up new design targets such as it has been the case in microbes. Making such specialized models will be a substantial amount of work, but this task will be made easier, if a

generic CHO model of high quality based on an assembled and annotated reference genome is generated first. From that, specialized models can be made in semi-automated fashion through comparative genomics. This would have the additional advantage, that annotation of the genomes of the individual cell lines would not be required (as this is currently not available [18]), but could be achieved by alignment to the reference genome.

Should the models be able to deliver on the promise and potential seen in other cells, it is bound to trigger a second wave of CHO cell line engineering. Notably CRISPR Cas9-based genome editing systems being made available at non-cost prohibitive prices [95] and efficient high-through-put mammalian vector design systems [96], support the development of faster and cheaper genome engineering tools to accelerate future cell line engineering efforts in CHO.

In summary, the potential of genome-scale models stands to be unleashed in CHO cells within a very short time span. Combined with the genomes ushering in the genomics era for CHO, substantial amounts of omics-data is being generated, and the development of efficient genetic engineering tools, CHO cell culture will soon move into the next generation of cell line development. Such advances promise better and cheaper development of biopharmaceuticals for this important group of cell factories.

5.6. Executive Summary

- Genome-scale metabolic models have been applied with success in many other prokaryotic and eukaryotic cell factories.
- The CHO field now has all of the relevant information and methods needed to construct and apply such models.
- A CHO metabolic model will have applications both in design and engineering of cells, but equally important also in interpretation of omics-data. The potential is large.
- Initial CHO models have adapted from models of mouse metabolism, but no de novo CHO models have been published at this time.
- The community is currently constructing a consensus model for CHO metabolism.
- Added value will come from generating specialized models for individual cell lines.

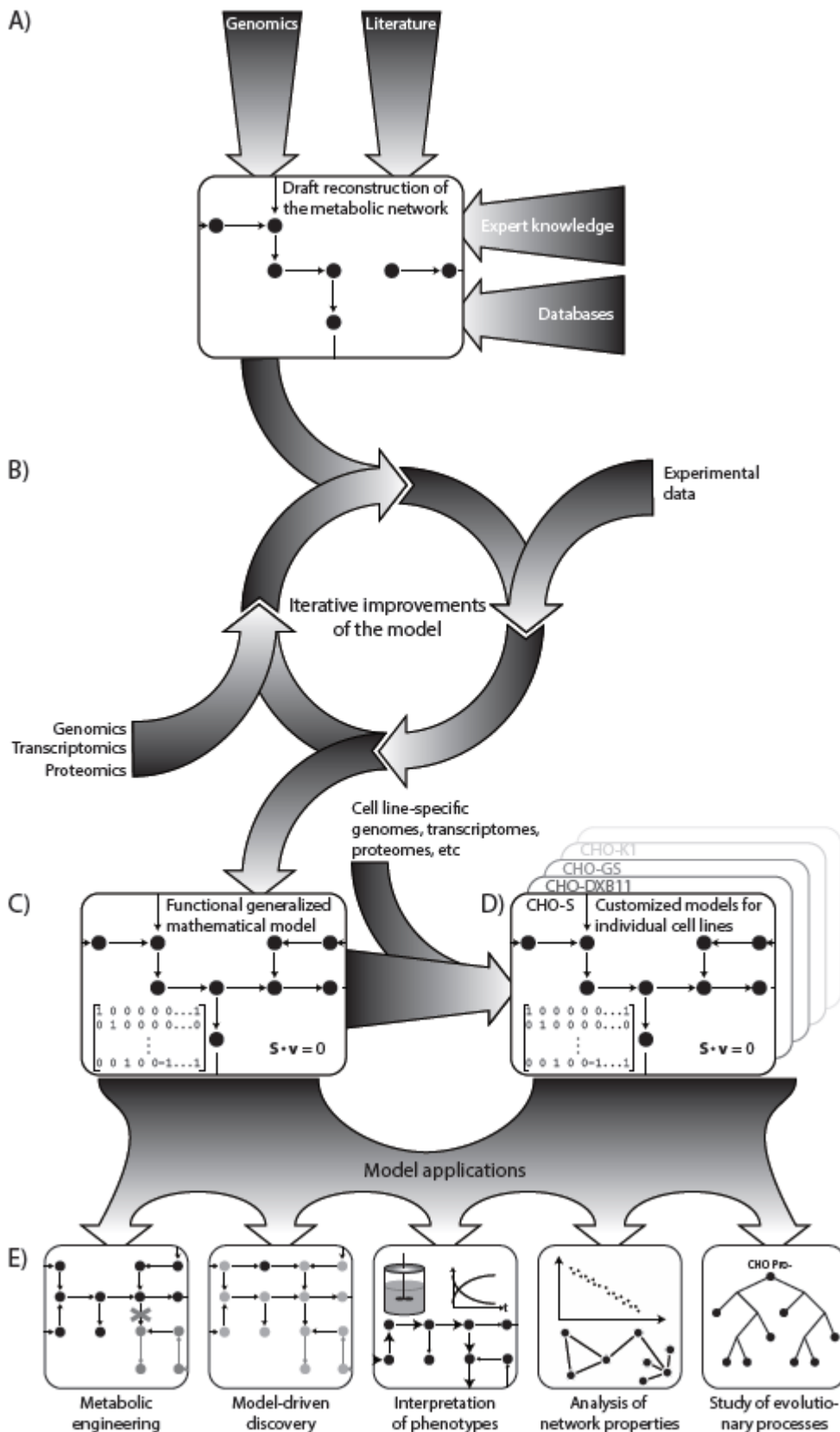


Figure 1 - Model building and application in CHO cells. A) Initial drafting of a genome-scale metabolic model (GSM) requires genomic annotation supplemented with available literature and knowledge on the metabolism of choice. This generates a draft genome-scale metabolic network reconstruction (GENRE). B)

Multiple iterations of model improvement and testing, supplemented with available omics and phenotypic data generates a GSM capable of computation. C) A generalized GSM for CHO cells can be tailored to specific cell lines (D) by the inclusion of additional omics data specific for the individual cell lines. E) Both generalized and specialized CHO GSMs may be applied to engineer cell lines, interpret data and increase functional understanding of these important cell lines.

5.7. References

1. Walsh G. Biopharmaceutical benchmarks 2010. *Nat. Biotechnol.* **28(9)**, 917–924 (2010).
2. Aggarwal RS. What’s fueling the biotech engine-2012 to 2013. *Nat. Biotechnol.* **32(1)**, 32–9 (2014).
3. IMS Institute for Healthcare Informatics. The Global Use of Medicines: Outlook Through 2015. .
4. Walsh G. New Biopharmaceuticals. *BIOPHARM Int.* **25(6)**, 34 – 36 (2012).
5. Wurm FM. Production of recombinant protein therapeutics in cultivated mammalian cells. *Nat. Biotechnol.* **22(11)**, 1393–1398 (2004).
6. Bailey JE. Toward a science of metabolic engineering. *Science.* **252(5013)**, 1668–75 (1991).
7. Nielsen J. Metabolic engineering: techniques for analysis of targets for genetic manipulations. *Biotechnol. Bioeng.* **58(2-3)**, 125–32 (1998).
8. Kim SH, Lee GM. Down-regulation of lactate dehydrogenase-A by siRNAs for reduced lactic acid formation of Chinese hamster ovary cells producing thrombopoietin. *Appl Microbiol Biotechnol.* **74(1)**, 152–159 (2007).
9. Zhang F, Sun X, Yi X, Zhang Y. Metabolic characteristics of recombinant Chinese hamster ovary cells expressing glutamine synthetase in presence and absence of glutamine. *Cytotechnology.* **51(1)**, 21–28 (2006).
10. Wlaschin KF, Nissom PM, de Leon Gatti M, *et al.* EST sequencing for gene discovery in Chinese hamster ovary cells. *Biotechnol Bioeng.* **91(5)**, 592–606 (2005).

11. Xu X, Nagarajan H, Lewis NE, *et al.* The genomic sequence of the Chinese hamster ovary (CHO)-K1 cell line. *Nat Biotechnol.* **29(8)**, 735–741 (2011).
12. Hammond S, Swanberg JC, Kaplarevic M, Lee KH. Genomic sequencing and analysis of a Chinese hamster ovary cell line using Illumina sequencing technology. *BMC Genomics.* **12(1)**, 67 (2011).
13. Lander ES, Linton LM, Birren B, *et al.* Initial sequencing and analysis of the human genome. *Nature.* **409(6822)**, 860–921 (2001).
14. Goffeau A, Barrell BG, Bussey H, *et al.* Life with 6000 genes. *Science.* **274(5287)**, 546, 563–7 (1996).
15. Gibbs RA, Weinstock GM, Metzker ML, *et al.* Genome sequence of the Brown Norway rat yields insights into mammalian evolution. *Nature.* **428(6982)**, 493–521 (2004).
16. Waterston RH, Lindblad-Toh K, Birney E, *et al.* Initial sequencing and comparative analysis of the mouse genome. *Nature.* **420(6915)**, 520–62 (2002).
17. Brinkrolf K, Rupp O, Laux H, *et al.* Chinese hamster genome sequenced from sorted chromosomes. *Nat. Biotechnol.* **31(8)**, 694–5 (2013).
18. Lewis NE, Liu X, Li Y, *et al.* Genomic landscapes of Chinese hamster ovary cell lines as revealed by the *Cricetulus griseus* draft genome. *Nat. Biotechnol.* **31(8)**, 759–65 (2013).
19. Puck TT, Cieciura SJ, Robinson A. Genetics of somatic mammalian cells. III. Long-term cultivation of euploid cells from human and animal subjects. *J Exp Med.* **108(6)**, 945–956 (1958).
20. Graf LH, Chasin LA. Direct demonstration of genetic alterations at the dihydrofolate reductase locus after gamma irradiation. *Mol. Cell. Biol.* **2(1)**, 93–96 (1982).
21. Urlaub G, Chasin LA. Isolation of Chinese hamster cell mutants deficient in dihydrofolate reductase activity. *Proc. Natl. Acad. Sci. U. S. A.* **77(7)**, 4216–20 (1980).

22. Kanehisa M, Goto S, Sato Y, Kawashima M, Furumichi M, Tanabe M. Data, information, knowledge and principle: back to metabolism in KEGG. *Nucleic Acids Res.* **42(Database issue)**, D199–205 (2014).
23. Thiele I, Palsson BØ. A protocol for generating a high-quality genome-scale metabolic reconstruction. *Nat. Protoc.* **5(1)**, 93–121 (2010).
24. Burgard AP, Pharkya P, Maranas CD. Optknock: a bilevel programming framework for identifying gene knockout strategies for microbial strain optimization. *Biotechnol. Bioeng.* **84(6)**, 647–57 (2003).
25. Orth JD, Conrad TM, Na J, *et al.* A comprehensive genome-scale reconstruction of *Escherichia coli* metabolism. *Mol. Syst. Biol.* **7(535)**, 535 (2011).
26. Monk JM, Charusanti P, Aziz RK, *et al.* Genome-scale metabolic reconstructions of multiple *Escherichia coli* strains highlight strain-specific adaptations to nutritional environments. *Proc. Natl. Acad. Sci. U. S. A.* **110(50)**, 20338–43 (2013).
27. Edwards JS, Palsson BO. The *Escherichia coli* MG1655 in silico metabolic genotype: Its definition, characteristics, and capabilities. *Proc. Natl. Acad. Sci.* **97(10)**, 5528–5533 (2000).
28. Chung BKS. Genome-scale metabolic reconstruction and in silico analysis of methylotrophic yeast *Pichia pastoris* for strain improvement. *Microb. Cell Fact.* **9** (2010).
29. Herrgård MJ, Swainston N, Dobson P, *et al.* A consensus yeast metabolic network reconstruction obtained from a community approach to systems biology. *Nat. Biotechnol.* **26(10)**, 1155–60 (2008).
30. Zomorodi AR, Maranas CD. Improving the iMM904 *S. cerevisiae* metabolic model using essentiality and synthetic lethality data. *BMC Syst. Biol.* **4**, 178 (2010).
31. Dias O, Pereira R, Gombert AK, Ferreira EC, Rocha I. iOD907, the first genome-scale metabolic model for the milk yeast *Kluyveromyces lactis*. *Biotechnol. J.* (2014).
32. Andersen MR, Nielsen ML, Nielsen J. Metabolic model integration of the bibliome, genome, metabolome and reactome of *Aspergillus niger*. *Mol. Syst. Biol.* **4**, 178 (2008).

33. Vongsangnak W, Olsen P, Hansen K, Krogsgaard S, Nielsen J. Improved annotation through genome-scale metabolic modeling of *Aspergillus oryzae*. *BMC Genomics*. **9**, 245 (2008).
34. Dreyfuss JM, Zucker JD, Hood HM, Ocasio LR, Sachs MS, Galagan JE. Reconstruction and validation of a genome-scale metabolic model for the filamentous fungus *Neurospora crassa* using FARM. *PLoS Comput. Biol.* **9(7)**, e1003126 (2013).
35. De Oliveira Dal'Molin CG, Quek L-E, Palfreyman RW, Brumbley SM, Nielsen LK. AraGEM, a genome-scale reconstruction of the primary metabolic network in *Arabidopsis*. *Plant Physiol.* **152(2)**, 579–89 (2010).
36. Selvarasu S, Karimi IA, Ghim G-H, Lee D-Y. Genome-scale modeling and in silico analysis of mouse cell metabolic network. *Mol. Biosyst.* **6(1)**, 152–61 (2010).
37. Thiele I, Swainston N, Fleming RMT, *et al.* A community-driven global reconstruction of human metabolism. *Nat. Biotechnol.* **31(5)**, 419–25 (2013).
38. Bordbar A, Mo ML, Nakayasu ES, *et al.* Model-driven multi-omic data analysis elucidates metabolic immunomodulators of macrophage activation. *Mol. Syst. Biol.* **8**, 558 (2012).
39. Karp PD, Keseler IM, Shearer A, *et al.* Multidimensional annotation of the *Escherichia coli* K-12 genome. *Nucleic Acids Res.* **35(22)**, 7577–90 (2007).
40. Feist AM, Palsson BØ. The growing scope of applications of genome-scale metabolic reconstructions using *Escherichia coli*. *Nat. Biotechnol.* **26(6)**, 659–67 (2008).
41. McCloskey D, Palsson BØ, Feist AM. Basic and applied uses of genome-scale metabolic network reconstructions of *Escherichia coli*. *Mol. Syst. Biol.* **9**, 661 (2013).
42. Yang M, Butler M. Effects of ammonia and glucosamine on the heterogeneity of erythropoietin glycoforms. *Biotechnol Prog.* **18(1)**, 129–138 (2002).
43. Lao MS, Toth D. Effects of ammonium and lactate on growth and metabolism of a recombinant Chinese hamster ovary cell culture. *Biotechnol. Prog.* **13(5)**, 688–91 (1997).

44. Gagnon M, Hiller G, Luan Y-T, Kittredge A, DeFelice J, Drapeau D. High-end pH-controlled delivery of glucose effectively suppresses lactate accumulation in CHO fed-batch cultures. *Biotechnol. Bioeng.* **108(6)**, 1328–37 (2011).
45. Richard P, Verho R, Putkonen M, Londesborough J, Penttila M. Production of ethanol from L-arabinose by containing a fungal L-arabinose pathway. *FEMS Yeast Res.* **3(2)**, 185–189 (2003).
46. Vemuri GN, Eiteman MA, McEwen JE, Olsson L, Nielsen J. Increasing NADH oxidation reduces overflow metabolism in *Saccharomyces cerevisiae*. *Proc. Natl. Acad. Sci. U. S. A.* **104(7)**, 2402–7 (2007).
47. Fuhrer T, Chen L, Sauer U, Vitkup D. Computational prediction and experimental verification of the gene encoding the NAD⁺/NADP⁺-dependent succinate semialdehyde dehydrogenase in *Escherichia coli*. *J. Bacteriol.* **189(22)**, 8073–8 (2007).
48. Choi HS, Kim TY, Lee D-Y, Lee SY. Incorporating metabolic flux ratios into constraint-based flux analysis by using artificial metabolites and converging ratio determinants. *J. Biotechnol.* **129(4)**, 696–705 (2007).
49. Lee KH, Park JH, Kim TY, Kim HU, Lee SY. Systems metabolic engineering of *Escherichia coli* for L-threonine production. *Mol Syst Biol.* **3**, 149 (2007).
50. Lewis NE, Hixson KK, Conrad TM, *et al.* Omic data from evolved *E. coli* are consistent with computed optimal growth from genome-scale models. *Mol. Syst. Biol.* **6**, 390 (2010).
51. Hyduke DR, Lewis NE, Palsson BØ. Analysis of omics data with genome-scale models of metabolism. *Mol. Biosyst.* **9(2)**, 167–74 (2013).
52. Famili I, Forster J, Nielsen J, Palsson BO. *Saccharomyces cerevisiae* phenotypes can be predicted by using constraint-based analysis of a genome-scale reconstructed metabolic network. *Proc. Natl. Acad. Sci. U. S. A.* **100(23)**, 13134–9 (2003).
53. Fong SS, Palsson BØ. Metabolic gene-deletion strains of *Escherichia coli* evolve to computationally predicted growth phenotypes. *Nat. Genet.* **36(10)**, 1056–8 (2004).

54. Schuster S. Detection of elementary flux modes in biochemical networks: a promising tool for pathway analysis and metabolic engineering. *Trends Biotechnol.* **17(2)**, 53–60 (1999).
55. De Figueiredo LF, Podhorski A, Rubio A, *et al.* Computing the shortest elementary flux modes in genome-scale metabolic networks. *Bioinformatics.* **25(23)**, 3158–65 (2009).
56. Jonnalagadda S, Srinivasan R. An efficient graph theory based method to identify every minimal reaction set in a metabolic network. *BMC Syst. Biol.* **8**, 28 (2014).
57. Baycin-Hizal D, Tabb DL, Chaerkady R, *et al.* Proteomic analysis of Chinese hamster ovary cells. *J Proteome Res.* **11(11)**, 5265–5276 (2012).
58. Baumler DJ, Peplinski RG, Reed JL, Glasner JD, Perna NT. The evolution of metabolic networks of *E. coli*. *BMC Syst. Biol.* **5**, 182 (2011).
59. Morgan WF, Hartmann A, Limoli CL, Nagar S, Ponnaiya B. Bystander effects in radiation-induced genomic instability. *Mutat. Res.* **504(1-2)**, 91–100 (2002).
60. Kjeldsen KR, Nielsen J. In silico genome-scale reconstruction and validation of the *Corynebacterium glutamicum* metabolic network. *Biotechnol. Bioeng.* **102(2)**, 583–97 (2009).
61. David H, Akesson M, Nielsen J. Reconstruction of the central carbon metabolism of *Aspergillus niger*. *Eur. J. Biochem.* **270(21)**, 4243–53 (2003).
62. Kildegaard HF, Baycin-Hizal D, Lewis NE, Betenbaugh MJ. The emerging CHO systems biology era: Harnessing the 'omics revolution for biotechnology. *Curr. Opin. Biotechnol.* **24(6)**, 1102–1107 (2013).
63. Hammond S, Kaplarevic M, Borth N, Betenbaugh MJ, Lee KH. Chinese hamster genome database: an online resource for the CHO community at www.CHOgenome.org. *Biotechnol. Bioeng.* **109(6)**, 1353–6 (2012).
64. Cao Y, Kimura S, Itoi T, Honda K, Ohtake H, Omasa T. Construction of BAC-based physical map and analysis of chromosome rearrangement in Chinese hamster ovary cell lines. *Biotechnol. Bioeng.* **109(6)**, 1357–67 (2012).

65. Kantardjieff A, Nissom PM, Chuah SH, *et al.* Developing genomic platforms for Chinese hamster ovary cells. *Biotechnol Adv.* (2009).
66. Yee JC, de Leon Gatti M, Philp RJ, Yap M, Hu W-S. {G}enomic and proteomic exploration of {CHO} and hybridoma cells under sodium butyrate treatment. *Biotechnol Bioeng.* **99(5)**, 1186–1204 (2008).
67. Clarke C, Henry M, Doolan P, *et al.* Integrated miRNA, mRNA and protein expression analysis reveals the role of post-transcriptional regulation in controlling CHO cell growth rate. *BMC Genomics.* **13(1)**, 656 (2012).
68. Affymetrix. Data Sheet GeneChip® CHO Gene 2.0 ST Array. .
69. McGettigan PA. Transcriptomics in the RNA-seq era. *Curr. Opin. Chem. Biol.* **17(1)**, 4–11 (2013).
70. Rupp O, Becker J, Brinkrolf K, *et al.* Construction of a public CHO cell line transcript database using versatile bioinformatics analysis pipelines. *PLoS One.* **9(1)**, e85568 (2014).
71. Slade PG, Hajivandi M, Bartel CM, Gorfien SF. Identifying the CHO secretome using mucin-type O-linked glycosylation and click-chemistry. *J. Proteome Res.* **11(12)**, 6175–86 (2012).
72. Meerman HJ, Georgiou G. Construction and characterization of a set of E. coli strains deficient in all known loci affecting the proteolytic stability of secreted recombinant proteins. *Biotechnology. (N. Y).* **12(11)**, 1107–10 (1994).
73. Jin FJ, Watanabe T, Juvvadi PR, Maruyama J, Arioka M, Kitamoto K. Double disruption of the proteinase genes, tppA and pepE, increases the production level of human lysozyme by *Aspergillus oryzae*. *Appl. Microbiol. Biotechnol.* **76(5)**, 1059–68 (2007).
74. Becker J, Hackl M, Rupp O, *et al.* Unraveling the Chinese hamster ovary cell line transcriptome by next-generation sequencing. *J. Biotechnol.* **156(3)**, 227–35 (2011).
75. Meleady P, Hoffrogge R, Henry M, *et al.* Utilization and evaluation of CHO-specific sequence databases for mass spectrometry based proteomics. *Biotechnol. Bioeng.* **109(6)**, 1386–94 (2012).

76. Sellick CA, Croxford AS, Maqsood AR, *et al.* Metabolite profiling of recombinant CHO cells: designing tailored feeding regimes that enhance recombinant antibody production. *Biotechnol. Bioeng.* **108(12)**, 3025–31 (2011).
77. Sellick CA, Hansen R, Maqsood AR, *et al.* Effective quenching processes for physiologically valid metabolite profiling of suspension cultured Mammalian cells. *Anal. Chem.* **81(1)**, 174–83 (2009).
78. Sellick CA, Hansen R, Stephens GM, Goodacre R, Dickson AJ. Metabolite extraction from suspension-cultured mammalian cells for global metabolite profiling. *Nat. Protoc.* **6(8)**, 1241–9 (2011).
79. Kronthaler J, Gstraunthaler G, Heel C. Optimizing high-throughput metabolomic biomarker screening: a study of quenching solutions to freeze intracellular metabolism in CHO cells. *OMICS.* **16(3)**, 90–7 (2012).
80. Dietmair S, Timmins NE, Gray PP, Nielsen LK, Krömer JO. Towards quantitative metabolomics of mammalian cells: development of a metabolite extraction protocol. *Anal Biochem.* **404(2)**, 155–164 (2010).
81. Dietmair S, Hodson MP, Quek L-E, *et al.* Metabolite profiling of CHO cells with different growth characteristics. *Biotechnol. Bioeng.* **109(6)**, 1404–14 (2012).
82. Chong WPK, Goh LT, Reddy SG, *et al.* Metabolomics profiling of extracellular metabolites in recombinant Chinese Hamster Ovary fed-batch culture. *Rapid Commun Mass Spectrom.* **23(23)**, 3763–3771 (2009).
83. Selvarasu S, Ho YS, Chong WPK, *et al.* Combined in silico modeling and metabolomics analysis to characterize fed-batch CHO cell culture. *Biotechnol. Bioeng.* **109(6)**, 1415–29 (2012).
84. Martínez VS, Dietmair S, Quek L-E, Hodson MP, Gray P, Nielsen LK. Flux balance analysis of CHO cells before and after a metabolic switch from lactate production to consumption. *Biotechnol. Bioeng.* **110(2)**, 660–6 (2013).
85. Dietmair S, Hodson MP, Quek L-E, Timmins NE, Gray P, Nielsen LK. A multi-omics analysis of recombinant protein production in Hek293 cells. *PLoS One.* **7(8)**, e43394 (2012).

86. Vernardis SI, Goudar CT, Klapa MI. Metabolic profiling reveals that time related physiological changes in mammalian cell perfusion cultures are bioreactor scale independent. *Metab. Eng.* **19**, 1–9 (2013).
87. Monica TJ, Andersen DC, Goochee CF. A mathematical model of sialylation of N-linked oligosaccharides in the trans-Golgi network. *Glycobiology.* **7(4)**, 515–521 (1997).
88. Umaña P, Bailey JE. A mathematical model of N-linked glycoform biosynthesis. *Biotechnol Bioeng.* **55(6)**, 890–908 (1997).
89. Krambeck FJ, Betenbaugh MJ. A mathematical model of N-linked glycosylation. *Biotechnol Bioeng.* **92(6)**, 711–728 (2005).
90. Krambeck FJ, Bennun S V, Narang S, Choi S, Yarema KJ, Betenbaugh MJ. A mathematical model to derive N-glycan structures and cellular enzyme activities from mass spectrometric data. *Glycobiology.* (2009).
91. Jimenez Del Val I, Nagy JM, Kontoravdi C. A dynamic mathematical model for monoclonal antibody N-linked glycosylation and nucleotide sugar donor transport within a maturing Golgi apparatus. *Biotechnol. Prog.* **44(0)**, 1–44 (2011).
92. Jedrzejewski PM, Del Val IJ, Constantinou A, *et al.* Towards controlling the glycoform: a model framework linking extracellular metabolites to antibody glycosylation. *Int. J. Mol. Sci.* **15(3)**, 4492–522 (2014).
93. Thiele I, Hyduke DR, Steeb B, *et al.* A community effort towards a knowledge-base and mathematical model of the human pathogen Salmonella Typhimurium LT2. *BMC Syst. Biol.* **5**, 8 (2011).
94. Heavner BD, Smallbone K, Price ND, Walker LP. Version 6 of the consensus yeast metabolic network refines biochemical coverage and improves model performance. *Database (Oxford).* **2013**, bat059 (2013).
95. Ronda C, Pedersen LE, Hansen HG, *et al.* Accelerating genome editing in CHO cells using CRISPR Cas9 and CRISPy, a web-based target finding tool. *Biotechnol. Bioeng.* **111(8)**, 1604–16 (2014).

96. Lund AM, Kildegaard HF, Petersen MBK, *et al.* A Versatile System for USER Cloning-Based Assembly of Expression Vectors for Mammalian Cell Engineering. *PLoS One.* **9(5)**, e96693 (2014).

Chapter 6 Systems biology-based investigation into the effect of glucose starvation and culture duration on fed-batch CHO cell culture

Yuzhou Fan^{1,2}, Ioscani Jimenez Del Val³, Christian Müller², Anne Mathilde Lund¹, Jette Wagtberg Sen², Søren Kofoed Rasmussen², Cleo Kontoravdi³, Michael J. Betenbaugh⁴, Dietmar Weilguny^{2*} and Mikael Rørdam Andersen^{1*}

¹Network Engineering of Eukaryotic Cell Factories, Department of Systems Biology, Technical University of Denmark, Building 223, 2800 Kgs. Lyngby, Denmark

²Symphogen A/S, Pederstrupvej 93, 2750 Ballerup, Denmark

³Center for Process Systems Engineering, Department of Chemical Engineering, Imperial College London, South Kensington Campus, London SW7 2AZ, UK

⁴Department of Chemical and Biomolecular Engineering, Johns Hopkins University, Baltimore, MD 21218, USA

*Corresponding author.

Address correspondence to Mikael Rørdam Andersen, Department of Systems Biology, Technical University of Denmark, Building 223, 2800 Kgs. Lyngby, Denmark; +4545252675; mr@bio.dtu.dk

Address correspondence to Dietmar Weilguny, Cell line and Upstream, Symphogen A/S, Pederstrupvej 93, 2750 Ballerup, Denmark; +4588382683; dw@symphogen.com

Short running title: Systems biology-based investigation of fed-batch CHO cell culture

Keywords

Chinese hamster ovary cells; fed-batch; monoclonal antibody; glycosylation; charge heterogeneity; proteomics; glucose starvation; culture duration.

Abstract

In this study, systems biology tools were used to explore the effect of glucose starvation and culture duration on monoclonal antibody (mAb) production in fed-batch CHO cell culture to gain better insight into how these parameters can be controlled to ensure optimal mAb productivity and quality. Titer, N-glycosylation and charge heterogeneity of mAbs, as well as proteomic signature and metabolic status of the production cells in the culture were assessed.

We found that the impact of glucose starvation on the titer, N-glycosylation and charge heterogeneity of mAbs was dependent on the degree of starvation during the stationary phase of the fed-batch culture. Higher degree of glucose starvation reduced intracellular concentrations of UDP-GlcNAc and UDP-GalNAc, but increased the levels of UDP-Glc and UDP-Gal. Increased GlcNAc and Gal occupancy correlated well with increased degree of glucose starvation, which can be attributed to the interplay between the dilution effect associated with change in specific productivity of mAbs and the changed nucleotide sugar metabolism.

Herein, we also show and discuss that increased cell culture duration negatively affect the maturation of glycans. In addition, comparative proteomics analysis of cells was conducted to observe differences in protein abundance between growth and stationary phases. Generally higher expression of proteins involved in regulating cellular metabolism, extracellular matrix, apoptosis, protein secretion and glycosylation was found in stationary phase. These analyses offered a systematic view of the intrinsic properties of these cells and allowed us to explore the root causes correlating culture duration with variations in the productivity and glycosylation quality of monoclonal antibodies produced with CHO cells.

6.1. Introduction

Over the last decade Chinese hamster ovary (CHO) cells have been the predominant expression system used in the pharmaceutical bioprocessing of recombinant monoclonal antibodies (mAbs) due to their adaptability to industrial manufacturing environment and post-translational modification compatibility with human patients (Lim et al. 2010). Fed-batch culture has become a widely used approach for mAb production because of its value in extending the viable and productive phase of the culture (Rouiller et al. 2013).

The manufacturing process is typically optimized for increasing the productivity of mAbs, but this often increases the risk of compromising the critical quality attributes of the recombinant product. A number of strategies aiming at improving final titer have been proposed. For example, limiting the feed of glucose to minimize lactate accumulation (Dean and Reddy 2013; Gagnon et al. 2011) and extending culture duration to prolong the production window (Druz et al. 2013; Robinson et al. 1994), have been successfully implemented. However, all these strategies require precise control of the production process. The level of glucose limitation is crucial for the process, since it may cause undesired glucose starvation and lead to reduced cell growth and productivity (Hu et al. 1987) and altered N-glycosylation quality (Liu et al. 2014). Extended culture duration may also affect the mAb quality in terms of N-glycosylation patterns (Pacis et al. 2011) and charge heterogeneity (Kaneko et al. 2010).

N-glycosylation of mAbs affects their pharmacokinetic characteristics and efficacy as a drug, including clearance rate, stability, immunogenicity, antibody-dependent cellular cytotoxicity (ADCC) and complement-dependent cytotoxicity (CDC) (Goetze et al. 2011; Hossler et al. 2009; Jefferis 2012; Raju 2008; Zheng et al. 2011). A further quality criterion is the charge heterogeneity of the mAb, which provides information concerning net surface charges and conformational structure of the mAbs. Charge heterogeneity may be affected by different types of post-translational modification, such as N-glycosylation (mAbs with more processed glycans appear as more acidic forms), C-terminal lysine processing (processed mAbs appear as more acidic forms), deamidation (deamidated mAbs appear as more acidic forms), and oxidation (oxidated mAbs appear as more basic forms) (Chumsae et al. 2007; Hong et al. 2014; Liu et al. 2006; Perkins et al. 2000).

Recently, CHO cell bioprocessing entered the omics era (Kildegaard et al. 2013), thanks to the availability of the CHO-K1 and Chinese hamster genome sequences, along with draft genomes of multiple cell lines (Cao et al. 2012; Lewis et al. 2013; Xu et al. 2011). This has made other omics-based technologies more readily available for CHO cell culture, including RNA-sequencing transcriptomics analysis (McGettigan 2013) and tandem mass spectrometry-based proteomics analysis (Baycin-Hizal et al. 2012). In order to increase the understanding of CHO cell physiology to better control the quality attributes of mAbs, systems-biology based approaches that integrate data from cell culture behavior, metabolism, mAb quality and omics-based phenotyping will become a trend for CHO cell culture process development in the future.

This study is, to our best knowledge, the first time a multi-pronged approach has been used to investigate the effect of glucose starvation and culture duration on mAb production in fed-batch CHO cell culture. Here, we aim to understand how the titer, N-glycosylation and charge heterogeneity of the mAb product, as well as the proteomic signature and the intrinsic properties of the cells, are affected by changing these process parameters. The results presented herein provide mechanistic insight into how these process parameters influence mAb productivity and quality, and thus should aid in the identification of an appropriate operating windows for glucose limitation without running into glucose starvation and of the optimal harvest time.

6.2. Materials and methods

6.2.1. Cell culture and fed-batch process

Cell line A, an in-house CHO DG44 cell line producing mAb A was used as model cell line in this study. Cells were maintained in proprietary serum-free basal medium in shake flask at 37°C, 5% CO₂, 200 rpm prior to the fed-batch process.

Fed-batch culture was carried out in 500 ml shake flasks (working volume 50 – 100 ml) at 37°C, 5% CO₂, 200 rpm with an initial seeding density of 4×10⁵ viable cells/mL and temperature shift from 37°C to 33.5°C on day 5. Proprietary feed was added to the culture on days 2, 5, 7, 9 and 12 (10% of the initial culture volume). Glucose concentration was adjusted to 33mM on day 5 and to 50mM on day 12. Cell culture was sampled before feeding on days 2, 5, 7, 9, 12 and 14 for monitoring cell growth (Vi-CELL XR, Beckman Coulter, Brea, CA), cell metabolism (Bioprofile 100plus, Nova BioMedical, Waltham, WA) and mAb production (Octet QK384 equipped with Protein A biosensors, ForteBio, Menlo Park, CA). Sampling for intracellular nucleotide sugar quantification and mAb glycoprofiling was performed on days 2, 5, 9 and 12. Harvesting criteria for the culture was considered to be either when cell viability fell below 70% or on day 14, whichever occurred first. Four different fed-batch processes were performed in duplicate: severe glucose starvation (SGS), high glucose starvation (HGS), low glucose starvation (LGS) and no glucose starvation (NGS). In each of these processes, glucose concentration was set to 11mM (SGS), 22mM (HGS), 33mM (LGS) and 50mM (NGS) on day 9 of the fed-batch culture. Additional sampling for comparative proteomics analysis was performed on days 2 and 9 of the NGS process.

6.2.2. *Nucleotide sugar analysis*

Nucleotide sugar analysis was performed on harvested cell pellets using acetonitrile extraction followed by high-performance anion-exchange (HPAEC) HPLC as described previously (Fan et al. 2014; Jimenez Del Val et al. 2013).

6.2.3. *Semi-high throughput mAb purification*

The supernatant harvested from cell culture was filtered through a 0.22µm filter (Millipore, Billerica, MA) and applied onto a Protein A HP MultiTrap™ 96-well filter plate (GE Healthcare, Fairfield, CA) which had been previously equilibrated with PBS following the manufacturer's instructions. Elution was performed using 0.1M citrate buffer (pH=3.5, Sigma-Aldrich). The eluate was immediately transferred to a Zeba™ spin desalting plate (Thermo Scientific, Waltham, MA) previously equilibrated with a 10mM citrate, 150mM NaCl (pH=6.0) buffer (Sigma-Aldrich, St. Louis, MO). Purified mAb concentration was measured using a NanoDrop ND-1000 system (Thermo Scientific) prior to sample storage at -20°C.

6.2.4. *Cation-Exchange chromatography*

10µg purified mAbs were subjected to Cation-Exchange chromatography (CEX) on a ProPac WCX-10 column (250 x 4 mm, Dionex, Sunnyvale, CA) fitted to a Dionex HPLC system equipped

with UV detection set at 280nm. The flow rate was set to 1mL/min with a linear gradient ($T_{0 \text{ min}}=5\% \text{ B}$, $T_{6 \text{ min}}=5\% \text{ B}$, $T_{22 \text{ min}}=100\% \text{ B}$, $T_{38 \text{ min}}=100\% \text{ B}$, $T_{38,1 \text{ min}}=5\% \text{ B}$, $T_{47 \text{ min}}=5\% \text{ B}$) between solvent A (25mM sodium acetate, pH =5, Sigma-Aldrich) and solvent B (25mM sodium acetate, 0.5M NaCl, pH=5, Sigma-Aldrich). The shoulders of the heterogeneous peak obtained with CEX chromatography are identified as acidic, main, basic 1 and basic 2 mAb isoforms depending on the order in which they appear (Figure 1S, from left to the right) and can be quantified individually.

6.2.5. *mAb Glycoprofiling*

mAb Glycoprofiling was performed with an in-house HPLC analysis method using InstantAB labeled (Prozyme, Hayward, CA) glycans (Fan et al. 2014).

6.2.6. *Statistical analysis of glycoform distributions*

Differences among the glycoform distributions were evaluated by comparing the mean obtained from two independent experiments. Depending on equality of variances, different post-hoc tests were performed to assess the statistical significance of the differences among the means. First, the variances of each treatment were compared using Levene's test. If the variances were observed to be equal, a one-way ANOVA was performed to evaluate the differences between the means of the treatments. Where the ANOVA yielded statistically significant differences ($p_{\text{ANOVA}} < 0.05$), Tukey's honestly significant difference test was performed post-hoc for pairwise comparisons. For data where the variances were found to be unequal, a one-way Welch's ANOVA was performed, and if this analysis yielded statistical significance ($p_{\text{WELCH}} < 0.05$), the Games-Howell post hoc test was performed for pairwise comparisons. All statistical analysis was performed using the IBM SPSS Statistics software, v.20 (SPSS Inc. 2011).

6.2.7. *Sample preparation for proteomics analysis*

Two biological replicates from days 2 and 9 of the NGS fed batch process were subjected to proteomics analysis using iTRAQ (isobaric Tags for Relative and Absolute Quantification) labeling mass spectrometry (Aggarwal et al. 2006; Pottiez et al. 2012). The harvested cells were washed with ice-cold PBS (Invitrogen, Life Technologies, Carlsbad, CA), flash-frozen in liquid nitrogen and stored at -80°C prior to cell lysis. For lysis, the cells were thawed and immediately resuspended in SDS-lysis buffer (2% SDS (w/v), 1mM EDTA and 0.1mM phenylmethylsulfonyl fluoride [PMFS], pH = 8 adjusted with triethylammonium bicarbonate [TEABC], Sigma-Aldrich) and sonicated on ice three times for 30 seconds with a probe sonicator. The total protein concentration of the lysate was measured with the BCA assay (Thermo scientific).

The lysates were then reduced by incubation in a final concentration of 4.5mM Tris-(2-carboxyethyl) phosphine (TCEP, Sigma-Aldrich) at 60°C for 1 hour and subsequently alkylated by incubation in a final concentration of 8.3mM methyl methanethiosulfonate (MMTS, Sigma-Aldrich) at room temperature in the dark for 30 min using a modified filter-aided sample preparation (FASP) protocol based on Wisniewski et al. (2009). 90µg of the obtained protein from each sample were diluted with 9M Sequanal grade urea (Thermo scientific) to obtain a final SDS concentration of 0.09% (w/v). This mixture was incubated at room temperature in the dark for 1 hour after which the low-molecular-weight substances were removed by ultracentrifugation using a 10KDa cutoff 0.5ml Amicon filter (Millipore). The retained proteins were digested by incubation with 50µL of LysC digestion buffer (50 mM TEABC, pH=8) containing 4.5 µg of LysC enzyme (Wako Pure Chemical Industries, Japan) at 37°C for 4 hours and additional incubation with 350µL trypsin LysC digestion buffer (50 mM TEABC, pH=8) containing 10 µg trypsin enzyme (Promega Corporation, Madison, WI) at 37°C overnight. The digested peptides were dried using SpeedVac (Savant, Thermo Scientific) prior to iTRAQ labelling. The iTRAQ 8-plex reagent was dissolved in 50µL of isopropanol following the manufacturer's instructions (AB Sciex, Framingham, MA). Each dried peptide sample was dissolved in a mixture of 17µL H₂O, 20µL 0.5M TEABC and 50µL of iTRAQ 8-plex reagent solution and incubated for 2 hours at room temperature in the dark. Peptides from different samples with their unique iTRAQ labeling were mixed, dried and resuspended into 1mL of 10mM TEABC prior to peptide fractionation using basic pH reversed-phase liquid chromatography (bRPLC).

6.2.8. Fractionation of peptides

The bRPLC method was performed to improve identification of unique peptides in the sample as was described by Baycin-Hizal et al. (2012). Peptides were fractionated on an XBridge C18 Column (5 µm, 2.1 x 100 mm, Waters, Milford, MA) with an XBridge C18 Guard Column (5 µm, 2.1 x 10 mm, Waters), using an Agilent HPLC system consisting of a 1100 series binary pump, a 1200 series UV detector and a 1200 series micro-fraction collector. Fractionation of peptides was carried out by a linear gradient (T0 min =10% B, T10 min=10% B, T50 min=35% B, T50.1 min=70% B, T60 min =70% B, T60,1min = 100% B, T70 min = 100% B, T70.1 min = 10% B, T95 min = 10% B) between solvent A (10 mM TEABC, Sigma-Aldrich) and solvent B (10 mM TEABC in 90% v/v Acetonitrile, Sigma-Aldrich) with a flow rate of 250µL/min. 84 bRP fractions were collected and re-combined into 24 fractions and then dried in a SpeedVac (Savant, Thermo Scientific) prior to liquid chromatography/tandem mass spectrometry (LC-MS/MS) analysis.

6.2.9. LC-MS/MS analysis

The LC-MS/MS analysis of the different fractions of the peptides was performed using an LTQ Orbitrap Velos MS/MS in FTFT (Thermo Scientific) interfaced with a 2D nanoLC system (Eksigent, AB Sciex), as described previously (Baycin-Hizal et al. 2012), but with the following modified parameters. Precursor and fragment ions were explored in tandem MS analysis at a resolution of 30000 and 15000, respectively. Survey scans (full ms) were acquired on the Orbitrap within an m/z range between 350-1700Da. Precursor ions were individually isolated with a 1.2Da window and fragmented (MS/MS) using 40% collision energy in order to achieve higher collision dissociation (HCD) activation. The MS/MS spectra were analyzed using the Mascot software (v2.2.2, Matrix Science, London, UK) in the framework of ProteomeDiscoverer v1.4 (PD1.3; Thermo Scientific) with fixed modifications of N-terminal 8-plex-iTRAQ labeling and cysteine methylthiolation and variable modifications of methionine oxidation and 8-plex-iTRAQ labeling of tyrosine and lysine.

6.2.10. MS data analysis

The obtained MS data was compared against the *cricketulus_g_v2* custom database, which was constructed using the RefSeq annotation of the CHO genomic sequence downloaded in October, 2013. Protein identification was performed using Mascot v2.2.2 (Matrix Science) where the searches were processed with a confidence threshold of 1% False Discovery Rate (FDR). Protein ratios were calculated based on the median value of the unique peptide ratios.

6.2.11. Comparative proteomics analysis

A BLASTp search of all identified proteins was performed against the mouse, human and rat RefSeq databases (accessed on November, 2013) in order to find the closest homologous proteins (lowest E-value) in these species. Identifiers, including RefSeq Protein Accession, ENSEMBL gene ID, UNIPROT accession and Agilent ID for each protein were subsequently obtained using the Gene ID conversion Tool from the DAVID database (Huang da et al. 2009a; Huang da et al. 2009b) (from November, 2013). Gene set enrichment analysis (GSEA) (Subramanian et al. 2005) was performed on the proteins that exhibited differential expression between days 2 and 9. The resulting data were used to identify the up and down-regulated gene sets (between 15 and 500 genes per set) between days 2 and 9 of the NGS fed-batch process. This analysis was performed using both the functional database (a combination of Biocarta, KEGG and Reactome databases) and the gene ontology database (downloaded from Molecular Signatures Database v4.0, <http://www.broadinstitute.org/gsea/msigdb/index.jsp>). Leading edge genes (genes that are core

representatives of their gene set with FDR q-value cutoff of 0.25) were identified using Leading-edge analysis. An enrichment map (Merico et al. 2010) of the gene clusters were obtained in Cytoscape v3.1.1 using the GSEA results as input, a p-value cutoff of 0.05 and an FDR q-value cutoff of 0.25. A direct search using all identified proteins from MS analysis against an in-house reconstruction of the CHO secretory pathway network (Table S8) was performed with a log2 expression cut off of ± 0.8 and a p-value cutoff of 0.05 in order to analyze the secretion machinery of the cells. Moreover, all identified proteins that are involved in nucleotide sugar biosynthesis pathway and glycan biosynthesis pathway were sorted out and evaluated.

6.3. Results and Discussion

During fed-batch manufacturing of mAbs, glucose concentration and culture duration are considered to be critical parameters for both productivity and quality (Pacis et al. 2011; Xie et al. 1997). Therefore, lack of control in these parameters is always risky for mAb manufacture. Here, we investigate the effect of glucose starvation during the stationary phase of fed-batch culture and the effect of culture duration on mAb productivity, glycosylation and charge heterogeneity. Our results contribute to further understand how glucose starvation and culture duration impact CHO cell physiology in fed-batch culture processes and yields insight into potential metabolic and/or proteomic causes for these effects.

6.3.1. Effect of glucose starvation

Culture performance and mAb productivity of four culture processes with different degrees of glucose starvation (SGS, HGS, LGS and NGS) are shown in Figure 1 and are summarized in Table I. As would be expected, glucose starvation during the stationary phase resulted in earlier onset of cell death (Figures 1 A and B), reduced integral viable cell concentration (IVC) (Figure 1 C), lactate depletion (Figure 1 E), and increased accumulation of NH_4^+ (Figure 1 F). Additionally, the level of glucose starvation negatively correlated with mAb titer (Figure 1 C) and specific productivity (q_p) (Figure 1 C slope of the curves).

Table I. Culture performance and mAb production under glucose starvations. * Control.

Process name	Description	Glutamine	Glutamate	Lactate	NH4+	Culture process	mAb production
NGS*	No glucose starvation	Not consumed	Highly consumed	Almost not consumed	Consumed	Uninterrupted	Uninterrupted
LGS	Low glucose starvation	Consumed	Highly consumed	Consumed and depleted	Produced	Uninterrupted	Reduced
HGS	High glucose starvation	Highly consumed	Consumed	Highly consumed and depleted	Highly produced	Early-ended	Highly reduced
SGS	Severe glucose starvation	Highly consumed	Consumed	Highly consumed and depleted	Extremely produced	Early-ended	Extremely reduced

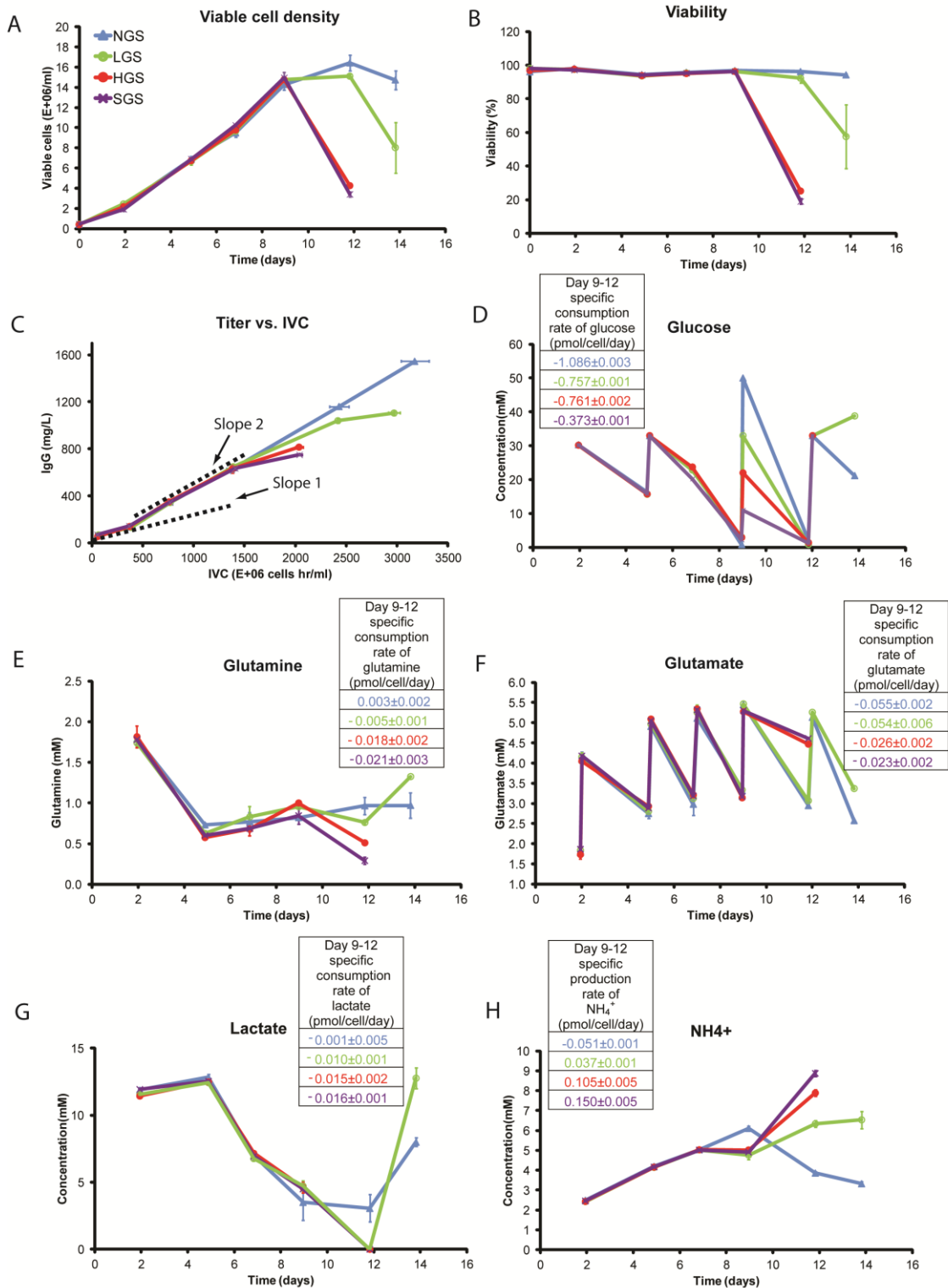


Figure 1. Comparison of four fed-batch cultures with different levels of glucose starvation. Viable cell density, viability and integral of viable cells (IVC) vs. titer are presented in A, B and C, respectively. Glucose, lactate and ammonia concentrations in the course of cell culture are shown in D, E and F, respectively. The error bars represent the standard deviation calculated from duplicate experiments. The average specific production (+) or consumption (–) rate of glucose, lactate, glutamine, glutamate and

ammonia from day 9 to day 12 were calculated as: $q_x = \frac{C_x^{\text{day12}} - C_x^{\text{day9}}}{\text{IVC}^{\text{day12}} - \text{IVC}^{\text{day9}}} \cdot C_x^{\text{day9}}$ and C_x^{day12} and C_x^{day9} are the concentration of nutrients or metabolites in the cell culture on day 9 after feeding and on day 12 before feeding, respectively. IVC^{day9} and $\text{IVC}^{\text{day12}}$ are IVC on day 9 and day 12, respectively. Slope 1: from day 2 to day 5; slope 2: from day 5 to day 9.

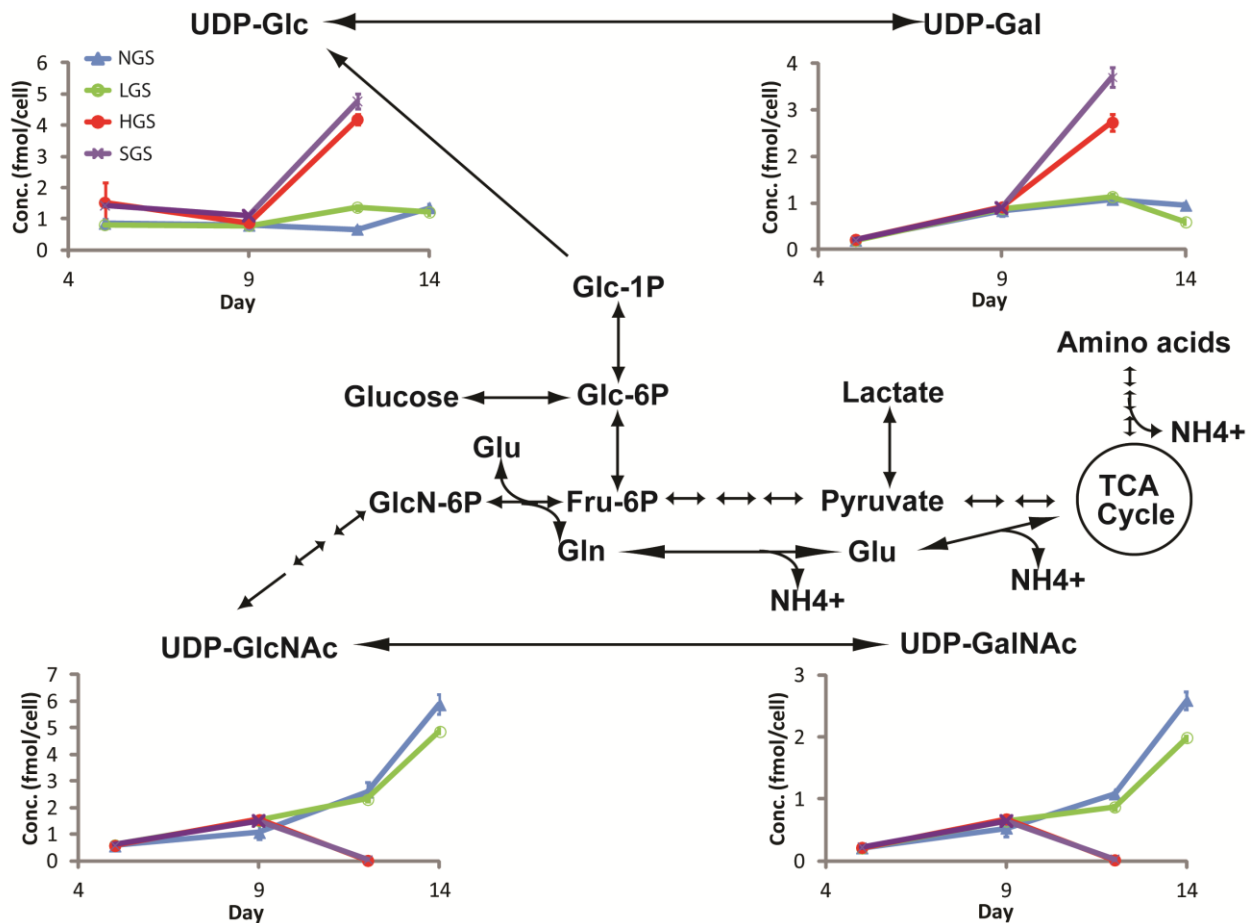


Figure 2. Intracellular nucleotide sugar analysis. Time course of concentration of intracellular nucleotide sugars (UDP-Glc, UDP-Gal, UDP-GlcNAc and UDP-GalNAc) from the cell cultures with different levels of glucose starvation were shown. Nucleotide sugar synthesis typically starts from degradation of glucose through glycolysis, in which glucose converts into glucose-6-phosphate and fructose-6 phosphate. Degradation of intracellular glucose generates Glucose-6-phosphate (Glc-6P), which is a critical substrate involved in glycolysis. Glc-6P can further become Fructose-6-phosphate (Fru-6P), which can enter into the TCA cycle for energy production, or together with glutamine supply biosynthesis of UDP-glucosamine (UDP-GlcNAc) and UDP-galactosamine (UDP-GalNAc). Alternatively, Glc-6P can turn into Glucose-1-phosphate (Glc-1P), which is responsible for generating UDP-glucose (UDP-Glc), UDP-galactose (UDP-Gal). In case of glucose starvation, lactate can be used as alternative carbon source to drive the TCA cycle. Once lactate is depleted, cells will mainly depend on using glutamine and other amino acids to support energy production and thus generate NH_4^+ .

Nucleotide sugars (NSs) are metabolites that are required as substrates for the elongation of oligosaccharide chains during the process of glycosylation. Their concentrations in the cell have been demonstrated to be one of the major causes of alterations in mAb glycopatterns (Chee Fung Wong et al. 2005; Fan et al. 2014; Wong et al. 2010b). It has been previously suggested that glucose depletion can reduce the biosynthesis of nucleotide sugars (Kochanowski et al. 2008). In accordance with this hypothesis, we observed reduced (LGS) or even fully depleted (HGS and SGS) intracellular concentrations of uridine diphosphate N-acetylglucosamine (UDP-GlcNAc) and uridine diphosphate N-acetylgalactosamine (UDP-GalNAc) when glucose availability was limited during the stationary phase of the fed-batch culture (Figure 2 – bottom). Counterintuitively though, considerable accumulation of uridine diphosphate glucose (UDP-Glc) and uridine diphosphate galactose (UDP-Gal) was observed after glucose starvation was induced at day 9 of culture (Figure 2 – top). Although this finding may be seen as conflicting, a clear explanation can be found when considering the steps involved in NS biosynthesis and glutamine metabolism in CHO cells. Figure 2 shows a simplified metabolic diagram for NS biosynthesis from glucose and glutamine (Gln) as primary substrates. There, we see that Fru-6P and Gln are combined to yield glucosamine 6-P (GlcN-6P), which eventually is converted to UDP-GlcNAc. Glutamine, in turn, has been widely reported to be consumed as an important carbon and energy source by CHO cells (Ahn and Antoniewicz 2013; Dean and Reddy 2013; Templeton et al. 2013; Young 2013). These authors have reported that considerable amounts of the Gln consumed during CHO cell culture is deamidated to yield ammonia and glutamate (Glu), the latter of which is then converted to TCA cycle intermediates such as oxaloacetate and α -ketoglutarate (α -KG). It is likely that under glucose starvation, glutamine and other amino acids uptake towards TCA cycle intermediates is increased in an attempt to sustain cellular energetic requirements, and that this increased glutaminolysis towards TCA cycle intermediates translates into a decreased flux of Gln towards GlcN-6P and eventual UDP-GlcNAc formation. Simultaneously, the flux of glucose that is not being converted to UDP-GlcNAc due to lack of Gln availability can be funneled towards UDP-Glc and UDP-Gal formation, possibly generating the observed accumulation in the HGS and SGS cultures. This mechanism is further substantiated by the observed increase in both Glu and NH_4^+ concentration seen in Figures 1 E and H, respectively, and a considerably higher Gln uptake rate in processes SGS and HGS. Alongside the possible metabolic effects described above, the consumption rate of the NSs for the glycosylation reactions must be considered. It is possible that UDP-Gal accumulates in the HGS and SGS cases because they present lower specific mAb productivity (Figure 1 C). If the drop in q_p for these cases is higher than the drop in UDP-Gal biosynthesis, this NS would accumulate. Similarly, the NGS and LGS cases present accumulation of UDP-GlcNAc (Figure 2), higher Man 5

(Figure 3 A) and lower GlcNAc occupancy (Figure 4 A) after glucose starvation is induced. It is possible that UDP-GlcNAc accumulates in these cases because consumption of this NS towards glycosylation is lower. These results highlight the interplay between nucleotide sugar metabolism and recombinant protein productivity.

To further elucidate whether changes in intracellular NS profiles are due to reduced biosynthesis associated with glucose starvation, changes in the mAb glycosylation distributions must be considered. The considerable changes in glycoform distribution observed between days 5 and 9 of culture reduce visibility of changes in glycosylation after glucose starvation is induced in Figures 3 and 4. However, a positive correlation between the degree of glucose starvation and the maturation of glycans was observed in repeated experiments.

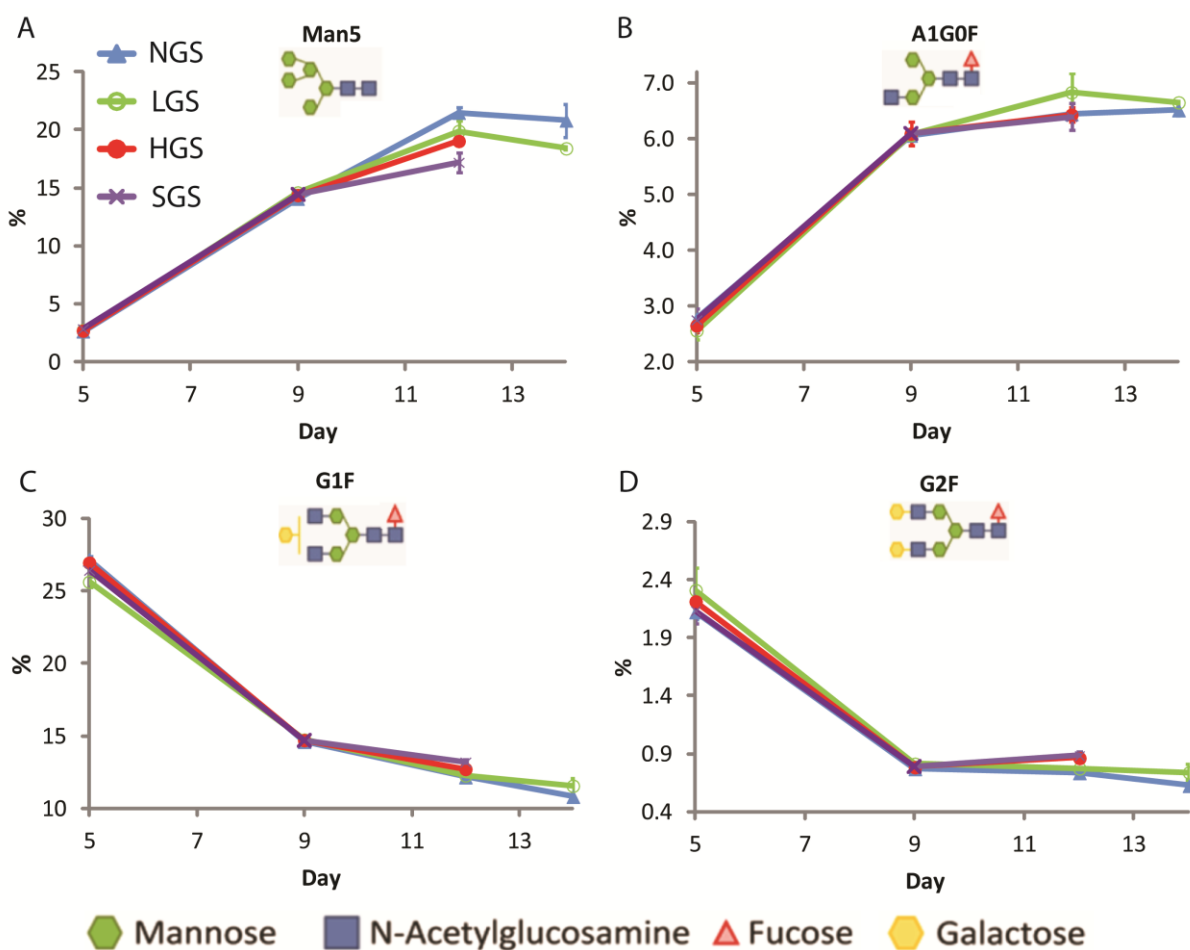


Figure 3. Glycoprofiles of mAbs produced from the cell cultures with different levels of glucose starvation. (A) Mannose 5, (B) A1G0F, (C) G1F and (D) G2F

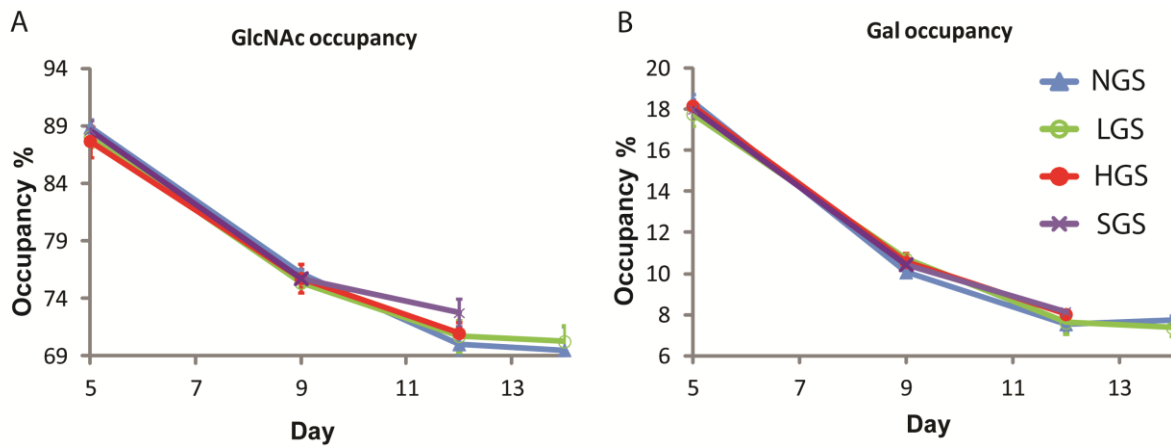


Figure 4. Average monosaccharide occupancy on glycans. (A) The percentage of GlcNAc occupancy (B) The percentage of galactose occupancy. The GlcNAc and Gal occupancy was calculated as reported in (Fan et al. 2014).

Table II. Fraction of total mAb secreted during each time interval and for all glucose limitation cases

Time interval	NGS	LGS	HGS	SGS
0 to 5d	8.7% ± 0.6%	11.9% ± 0.7%	17.1% ± 1.4%	19.2% ± 0.3%
5 to 9d	31.9% ± 2.4%	46.7% ± 0.5%	60.3% ± 4.7%	65.6% ± 0.2%
9 to 12d	34.5% ± 2.1%	35.5% ± 1.6%	22.6% ± 3.2%	15.2% ± 0.5%
12 to 14d	24.9% ± 0.3%	5.9% ± 1.8%	-----	-----

Table II shows the relative amount of mAb secreted during each time interval relative to the final mAb titer. There, we see that the fractions of secreted mAb change during the intervals depending on variations in specific productivity (q_p), which are most likely a consequence of glucose availability for each case. Specifically, we see that a smaller fraction of the total mAb produced is being secreted by the HGS and SGS cases in the interval where glucose limitation was introduced (9 to 12d). When considering these changes in q_p with respect to glucose availability, the reason why SGS yields a distribution with more highly processed glycoforms at day 12 is that during the starvation period, only 15.2% ± 0.5% of the total amount of mAb is produced. This lower fraction is diluted with the product that has been secreted up to that point in culture (84.8% ± 0.5%), and it is the dilution effect which leads to lower apparent decreases in mature glycoforms between days 9 and 12 (Figure 4). In contrast, a larger fraction of the total mAb is produced for the cases of less glucose starvation during the starvation period and thus, the dilution effect associated with changes in q_p may mask the impact of cellular metabolism (via nucleotide sugar biosynthesis) on glycosylation.

limitation during the day 9 to 12 period: NGS (■), LGS (■), HGS (■) and SGS (■). The values shown correspond to means for duplicate (n=2) cultures and statistical analysis was performed as described in the materials and methods. The criteria for significant differences are: * for $p<0.05$, ** for $p<0.01$ and *** for $p<0.001$.

In order to account for the effect of q_p on the glycan distributions after glucose limitation, the relative amount of each mAb glycoform produced (f_i) during the interval was calculated based on a material balance for glycoform i (mAb_i) over the starvation period:

$$f_i = \frac{[mAb_i](t_2) - [mAb_i](t_1)}{q_p X_v (t_2 - t_1)} \dots \text{Eq. 1}$$

Where q_p is the mAb specific productivity and X_v is the average cell density over the time interval (from $t_1=9d$ to $t_2=12d$ for the starvation period). And considering that $q_p X_v (t_2 - t_1) = [mAb_{Tot}](t_2) - [mAb_{Tot}](t_1)$, we find a simpler expression for f_i :

$$f_i = \frac{[mAb_i](t_2) - [mAb_i](t_1)}{[mAb_{Tot}](t_2) - [mAb_{Tot}](t_1)} \dots \text{Eq. 2}$$

In equation 2, f_i represents the mass fraction of mAb glycoform i produced relative to the total amount of mAb secreted during the time interval. Because Fc glycan variation accounts for very small changes in mAb molecular weight (<0.05%), f_i was assumed to be a close approximation to the mole fraction of mAb glycoform i per total moles of mAb produced over the starvation interval. Figure 5 shows the fractions calculated with equation 2 for the interval before (day 5 to 9) and after (day 9 to 12) glucose starvation is induced for all degrees of glucose limitation (NGS, LGS, HGS and SGS). As expected, there are no statistical differences between the cases prior to glucose starvation (day 5 to 9) given that up to this point, all cultures were performed under similar conditions. However, statistically significant differences can be observed for Man5, G1F and G2F between the time intervals and among certain glucose starvation conditions during the 9 to 12d interval.

Figure 5A shows that more Man5 is secreted during the 9 to 12d interval for all but the SGS culture. Within this interval, and depending on the different glucose starvation conditions, there is a decreasing trend where less Man5 is produced at higher glucose starvation. Specifically, the observed increases in Man5 secretion between both culture intervals are: NGS, $11.7\% \pm 0.8\%$; LGS, $7.8\% \pm 2.2\%$; HGS, $6.3\% \pm 0.5\%$; SGS, no statistical difference ($p<0.01$ for all comparisons). These results are reflected in GlcNAc occupancy (Figure 5, bottom row), where this value was reduced by $10.5\% \pm 1.1\%$ (NGS), $7.1\% \pm 1.3\%$ (LGS) and $5.7\% \pm 0.7\%$ (HGS) ($p<0.01$), and no statistically significant decrease was observed for the SGS culture.

When considering the intracellular UDP-GlcNAc concentrations presented in Figure 2, it is evident that lack of availability of this NS is not causing the increase in Man5 secretion for the NGS and LGS cultures. This is further substantiated by the small ($4.4\% \pm 0.9\%$, $p < 0.05$) decrease in G0F glycoform secretion after glucose starvation for NGS, and no statistically significant changes in A1G0F secretion (Figures 5 B and C). If UDP-GlcNAc availability were limiting, secretion of both these glycoforms would also be negatively impacted. Furthermore, the intracellular accumulation of UDP-GlcNAc, the increase in Man5 secretion, and the relative stability of G0F secretion imply that the rate limiting step is the reaction catalysed by the GnTI enzyme. The measured ranges for extracellular pH and ammonia concentration are below those that have been previously reported to impact the activity or Golgi localisation of GnTI (Borys et al. 1993; Gawlitzek et al. 2000; Rivinoja et al. 2009). The remaining possible cause for increased Man5 secretion in the least glucose-deprived cultures is the abundance of GnTI relative to specific mAb productivity. When considering this is the limitation, intracellular accumulation of UDP-GlcNAc is explained: a low GnTI to q_p ratio in NGS and LGS reduces the rate of GlcNAc transfer onto Man5, and because less UDP-GlcNAc is being consumed for this reaction, this NS accumulates within the cells.

In contrast to GlcNAc occupancy, production of galactosylated glycoforms (G1F and G2F, Figures 5 D and E, respectively) increases with higher glucose starvation. No statistical differences were observed for G1F secretion before and after starvation for the HGS and SGS cultures, but a decrease of $1.5\% \pm 0.3\%$ was observed for NGS and LGS ($p < 0.05$). In general, more G2F glycoform was produced during the starvation interval. However, a more pronounced increase in G2F secretion before and after starvation was observed for the HGS and SGS cultures ($P < 0.001$). The above results are also clearly reflected in Gal occupancy (Figure 5, bottom row). Specifically, galactose occupancy was not affected for the HGS and SGS cases, but was observed to decrease for NGS and LGS ($1.0\% \pm 0.2\%$ for both cases, $p < 0.05$).

When comparing galactose occupancy with intracellular UDP-Gal availability (Figure 2), we see a positive correlation. Higher intracellular UDP-Gal availability occurs for the most glucose starved cultures (HGS and SGS). In turn, these cultures present higher galactose occupancy during the starvation interval. The mechanisms underlying the interplay between intracellular UDP-Gal concentration, galactose occupancy and specific mAb productivity are consistent with the arguments put forth for GlcNAc. UDP-Gal accumulation in HGS and SGS is unlikely due to excess biosynthesis because these cultures were performed under considerable glucose limitation. Considering this, the most likely cause for intracellular UDP-Gal accumulation is that it is being consumed at a lower rate due to the low specific mAb productivity observed under these glucose starvation conditions (HGS and SGS). In turn, a lower q_p also implies higher residence time within

the Golgi apparatus which would allow for further processing of the mAb-bound glycans, leading to higher galactose occupancy. In summary, higher galactosylation occurs in the HGS and SGS cultures because the amount of galactosylation machinery (GalT and UDP-Gal transporter) is in excess relative to the specific mAb productivity.

Regarding charge heterogeneity of the mAbs by CIE analysis, slightly higher amount of basic variants (basic 1 and 2 isoforms) as well as slightly lower amount of acidic variants was associated with increasing degree of glucose starvation (Figure 6). This confirmed our findings in the glycoprofile in view of the fact that the mAbs with Man5 may contribute to basic variant (Yan et al. 2009). It is also likely that the amount of deamidated (contributing to the acidic variants) and methionine-oxidated or succinimide-contained mAb (contributing to the basic variants), which could be altered under different degree of glucose starvation (Chumsae et al. 2007; Harris et al. 2001; Perkins et al. 2000; Zhang et al. 2011).

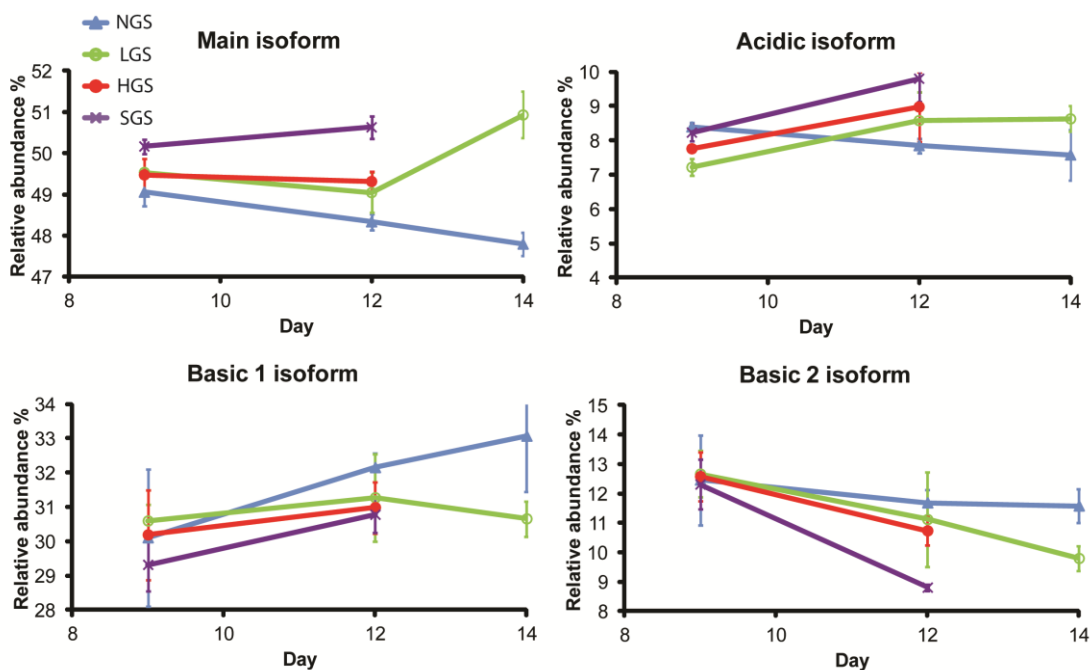


Figure 6. Charge heterogeneity of mAbs produced from the cell cultures with different levels of glucose starvation.

It is also worth mentioning that no peak representing non-glycosylated mAbs (typically appeared as a very basic distinct peak (Gaza-Bulsecu et al. 2008) separated from the main peak with heterogenic shoulders) was detected in samples from any of the four processes using CIE analysis. The result was also confirmed by intact mass analysis of the mAbs using LC-MS (data not shown). This indicated that no change in glycosylation site occupancy due to glucose starvation was observed in this study.

Previous results showed that glucose starvation can cause an increasing amount of non-glycosylated mAbs and less matured glycoforms (Liu et al. 2014). However, our findings concerning the effect of glucose starvation on both microheterogeneity and macroheterogeneity of the mAb glycosylation are contradictory to that. A possible reason could be that glucose starvation in this study occurred in the stationary phase of fed-batch culture compared to the previous study, in which glucose starvation occurred in the beginning of the batch culture. Hence, the physiological status of the cells and the interplay between nucleotide sugar availability and q_p are not comparable in these two cases, which in turn lead to different impact on mAb glycosylation. Furthermore, we have found that intracellular availability of nucleotide sugars may be dictated by the rate of consumption for glycosylation and not being themselves the limiting substrates for glycosylation. Although this may be a cell line or process-specific observation, we have shown that integrating nucleotide sugar availability with additional cell culture data is crucial for elucidating the metabolic mechanisms underlying mAb glycosylation during cell culture.

6.3.2. *Effect of culture duration*

Appropriate harvest criteria need to be selected for mAb manufacture. Here, we analyzed the fed-batch culture at different time points and try to understand the balance between titer and quality of the mAbs in relation to the culture duration.

As shown in Figure 1 C, the specific productivity of mAbs was lower in early growth phase (slope 1, day 2 to 5) comparing to that in late growth phase and early stationary phase (slope 2, day 5 to 9), which indicates there is an increase in q_p after temperature shift.

In the process with no glucose starvation (NGS), we found that all measured NSs accumulated as cultivation duration increased, which implies the biosynthesis rates were generally higher than the consumption rates of these nucleotide sugars along the culture process. Interestingly, UDP-GlcNAc and UDP-GalNAc accumulation was considerably increased at the end of the fed-batch process (from day 12 to 14). This can be attributed to increased UDP-GlcNAc biosynthesis, given a decrease in NH_4^+ accumulation in the culture after day 9 (Figure 1 H).

The variations in charge heterogeneity along the cell culture (Figure 6) can be attributed to combinations of many different factors, including increased deamidation, oxidation and less-processed glycosylation of the mAbs. Therefore, the trend of such changes may be quite different from case to case. On the other hand, charge heterogeneity of mAbs can therefore be used as a general indicator to access the quality of mAbs.

With regards to glycosylation (Figure 3 and Figure 4), it has been demonstrated by a trend of overall increases in Man5 and A1G0F, and decreases in G1F, G2F, and GlcNAc and galactose occupancy along cultivation. This finding is in accordance with the apparent accumulation of UDP-GlcNAc and UDP-Gal during the cell culture as well (Figure 2).

More specifically, the most dramatic changes in glycoform distribution observed in this study occur between days 5 and 9 (Figure 3), where Man5 glycoform abundance increases by $11.6\% \pm 0.3\%$ (from $2.7\% \pm 0.2\%$ to $14.4\% \pm 0.2\%$) and the G1F glycoform decreases by $11.9\% \pm 0.7\%$ (from $26.6\% \pm 0.7\%$ to $14.7\% \pm 0.1\%$). The similarity between the changes in Man5 and G1F abundance is striking and is likely related: higher Man5 production leaves less glycoprotein substrate available for galactosylation during later stages of the glycosylation process within the Golgi apparatus. It is therefore possible that the drop in galactosylation is a direct consequence of high Man5 secretion.

A similar correlation (glycans become less processed with extended culture duration) has also been reported in other studies (Bibila and Robinson 1995; Hooker et al. 1995; Pacis et al. 2011; Robinson et al. 1994; Shi and Goudar 2014), which indicate that this could be a general phenomenon. Three major hypotheses have been proposed explaining such a phenomenon: 1) A bottleneck in the availability of nucleotide sugar substrates with respect to culture duration may exist (Hooker et al. 1995). However, this possibility can be ruled out in the NGS process, as the nucleotide sugar substrates such as UDP-GlcNAc and UDP-Gal were accumulated in the cells over time (Figure 2). In addition, no considerable drop in G0F glycoform was observed along the cell culture (data not shown), indicating that UDP-GlcNAc availability is not limiting. 2) Cell death and lysis, may elevate the activity of extracellular glycosidase, especially sialidase in the culture, and thus increase the glycan degradation (Chee Fung Wong et al. 2005). However, it has also been demonstrated that CHO-derived glycosidases including β -galactosidase, β -hexosaminidase may be less likely to contribute to the lower GlcNAc and Gal occupancy, since they exhibit very low activity at typical culture pH (Gramer and Goochee 1993). 3) Reduced expression or activity of Golgi-associated mannosidase and glycosyltransferases during the course of culture (Robinson et al. 1994) can lead to high mannose and low galactosylation. However, as reported previously, the changes in expression of GlcNAc transferase I (GnT1) during the course of a cell culture is cell line-dependent and do not show any general trend of decline (Fan et al. 2014; Pacis et al. 2011). Additionally, no apparent down-regulation was observed in the expressions of GlcNAc transferase II (GnTII) and various galactose transferases (GalT) along with increased culture duration (Wong et al. 2010a). Although the activities of these enzymes may be inhibited by temperature shift or by changed pH inside Golgi apparatus, especially when ammonia accumulation increased in the culture,

the reported effective concentration of ammonia on glyco-alterations was above 10mM (Borys et al. 1994; Chen and Harcum 2005; Gawlitzek et al. 2000). In our case, ammonia accumulation in the cell culture without glucose starvation is less than 6mM, which is well below the effective concentration. Therefore, reduced activities of glycosylation-associated Golgi resident proteins in the course of cell culture due to ammonia accumulation may not be the right explanation for the culture duration-dependent glyco-alterations. Temperature shift may contribute to the decreases before and after day 5 in glycan maturation as a result of reduced activities of these enzymes. Additionally, Figure 1 C also shows that the q_p increases after the temperature shift on day 5 (slope 1 vs. slope 2). Therefore, it is possible that this increase in q_p causes the decrease in glycoform complexity between 5 and 9 days of culture. If the abundance of GnTI relative to the q_p goes below a certain level, lower GlcNAc occupancy will be achieved. These results point to the importance of considering the capability of glycosylation machinery available with respect to specific productivity. However, it cannot fully explain the continuous decrease in glycan maturation during the period after the temperature shift. As all three major hypotheses do not completely fit the reported system-level data, further investigations are needed in understanding the root cause of this type of glycosylation change.

6.3.3. Comparative proteomics analysis between growth phase and stationary phase in fed-batch

In order to gain insight into the fundamental differences in the cell culture from growth phase to stationary phase, in-depth analysis of proteome changes in cells from the two phases in the NGS process was performed.

In total across all samples, 5113 proteins were identified with FDR<1% in the proteomics data (Table S1), in which 4647 proteins were processed using gene set enrichment analysis (GSEA, Table S3). 3294 proteins were enriched into 228 and 334 gene sets using functional database and gene ontology database, respectively (Table S4 and S6). Enrichment maps illustrating GSEA results were built. The enriched gene sets containing genes with statistically significant changes in protein level between the growth phase and stationary phase were shown in Figure 7. In growth phase, the genes in the gene sets with transcription, cell cycle and nucleotide metabolism related activity were generally expressed at higher level, which is consistent with the rapid cell growth during this phase. On the other hand, the genes in the gene sets regarding glucose, lipid, and nucleotide sugar metabolism, environmental sensing and signal transduction, protein trafficking and secretion, glycosylation and apoptosis related activity were up-regulated in the stationary phase. Specifically, increasing environmental sensing and signal transduction related activity in stationary phase involved a number of gene sets found in both databases. This implies that cells may be more

sensitive to and tightly regulated upon environmental changes, for example media and process conditions in the stationary phase than in growth phase. Another interesting point we found is that protein trafficking and secretion were more active in the stationary phase with regard to in the growth phase, as a large set of genes involved in this activity were up-regulated. Therefore, we suggest that the cellular machinery in relation to protein secretion was more active for cells in stationary phase than in growth phase. In contrast to that, genes in the gene sets regarding glycosylation related activity are very few, although they were shown to be up-regulated (Figure 7). Taking one step more, we further specifically analyzed the proteome involved in the secretion machinery (Table S9), nucleotide sugar synthesis pathway (Table S10) and biosynthesis pathway of N-glycans (Table S11).

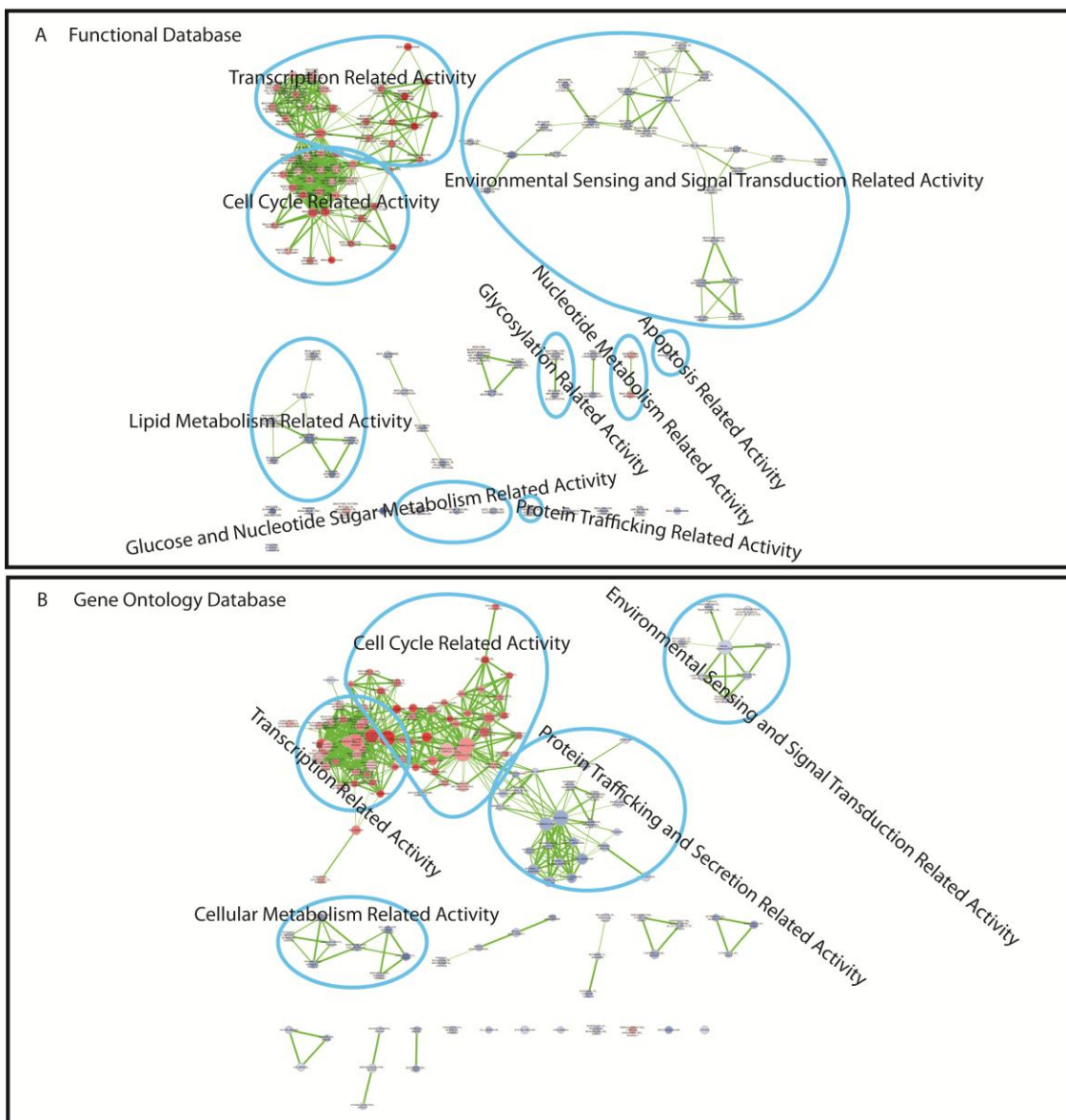


Figure 7. Enrichment map based on gene set enrichment analysis of comparative proteomics. The analysis has been done using (A) functional database and (B) gene ontology database, respectively. All enriched

gene sets are represented as dots. The size of the dot indicates the size of the gene set. Red dot signifies the genes in that gene set is generally up-regulated in the growth phase (on day 2) of the fed-batch culture, whereas blue dot stands for general up-regulation of the genes in the stationary phase (on day 9). Overlapped genes between the two gene sets were shown as green line. The thickness of the green line represents the size of the overlapped genes. Further clustering of the enriched gene sets based on their descriptions was indicated using light blue circles.

The relative activation of secretion machinery during the stationary phase has been demonstrated in (Table S9). We found that 12 proteins were up-regulated in stationary phase within our cut-off criteria. Out of the 12 proteins three (XP_003514816, XP_003499981 and XP_003512468) are directly related to protein transport in the cell and three (XP_003504664, XP_003501071 and XP_003507839) are responsible for protein folding. In contrast, only seven proteins were up-regulated in growth phase within the cut-off criteria. Interestingly, three of them were heat-shock proteins (HSP), which may reflect the effect of temperature shift during the culture. It is also worth to mention that many of the HSPs are glycosylated (Baycin-Hizal et al. 2012), and the glycosylation of them might compete with recombinant protein glycosylation.

In the nucleotide sugar synthesis pathway, Proteins XP_003497644, NP_001233687 and XP_003515993 that are responsible for UDP-Glc and UDP-Gal biosynthesis were slightly up-regulated in stationary phase (Table S10). The expressions of NP_001233638 and XP_003514714 that can direct UDP-GlcNAc to UDP-GalNAc and N-Acetyl-D-mannosamine (ManNAc), respectively, were higher in stationary phase. These results are in agreement with the findings above (Figure 7) that genes involved in nucleotide sugar metabolism were generally up-regulated in stationary phase.

Regarding the biosynthesis pathway of N-glycans (Table S11), three proteins (XP_003500143, XP_003500900, XP_003508783) that are responsible for initiation of N-glycosylation in the ER were slightly up-regulated during the stationary phase. Very interestingly, the expression of only two protein α -mannosidase II (XP_003499415) and GnT1 (NP_001230909) involved in glycan maturation in Golgi apparatus were slightly higher during the stationary phase.

Taken together, the essential causal link between producing the less processed glycans with increasing culture duration could be narrowed down to the following two possibilities: First and most likely, it can be attributed to the overall capabilities of protein secretion machinery from growth phase to stationary phase in the cells gradually exceeding the capability of protein glycosylation machinery that is specifically responsible for glycan maturation. Secondly, it is also possible that the activities of enzymes that raise GlcNAc and Gal occupancy may be reduced due to certain environmental change and/or physiological response (e.g. temperature shift and/or pH

gradient across the network of ER and Golgi apparatus) of the cells with the cultivation duration increased.

Further leading-edge analysis (LEA) was performed using the output from GSEA. Based on the functional database and the gene ontology database, we identified 655 leading edge genes in 172 gene sets and 568 leading edge genes in 144 gene sets, respectively (Table S4-S7). The top 10 up and down-regulated genes and enriched gene sets from LEA were shown from Table III to Table VI. The majority of the top up-regulated genes on day 2 are related to cell growth and cell cycle progression and are located in nucleus (Table IV and VI), including TOP2A, KPNA2, KIF22, UBE2C, DNMT1, LIG1, KIF4A, and MCM2, 3 and 5 (Table III and V).

Table III. Up and down regulated proteins on day 2 comparing to day 9 gene ontology database using leading-edge analysis. H: Human; M: Mouse; E: Eukaryote; C: CHO; R: Rat. #overlapped genes in Table V.

CHO RefSeq	Gene Symbol	Log2ratio	Cells studied	Function	Reference
Up-regulated					
NP_001233667	TOP2A	1.82	H	Transcription, DNA replication	(Belluti et al. 2013)
XP_003501907	KPNA2 #	1.63	H	Cell proliferation, cell cycle	(Huang et al. 2013)
XP_003510169	KIF22 #	1.61	H	Cell mitosis, cell cycle	(Yu et al. 2014)
XP_003504632	UBE2C #	1.55	H	Ubiquitylation, cell cycle	(Mocciaro and Rape 2012)
XP_003499794	DNMT1	1.53	H	DNA replication	(Shimamura and Ishikawa 2008)
XP_003500203	LIG1 #	1.39	H	DNA repair, DNA replication	(Ferrari et al. 2003)
XP_003504365	HMGB2	1.36	H	DNA repair	(Nagaki et al. 1998)
XP_003499302	KIF1A	1.33	M	Axonal transport	(Okada et al. 1995)
XP_003509164	KIF4A #	1.32	H	Cell mitosis	(Mazumdar et al. 2004)
XP_003500277	MCM2 #	1.25	E	DNA replication	(Bell and Dutta 2002)
Down-regulated					
XP_003510318	LGALS1	-1.22	H, M	Apoptosis	(Scott and Weinberg 2002)
XP_003510519	ANXA1 #	-1.27	H, C	Apoptosis; protein productivity	(Meleady et al. 2011; Wu et al. 2000)
XP_003500109	LGALS3	-1.30	H	Apoptosis	(Nakahara et al. 2005)
XP_003515030	COL5A2 #	-1.44	R	Extracellular matrix regulation	(Liu et al. 2010)
XP_003500579	PLTP #	-1.51	H, C	Lipid transfer	(Vuletic et al. 2009)
XP_003504285	COL7A1 #	-1.63	R	Extracellular matrix regulation	(Liu et al. 2010)
XP_003496178	MMP12	-1.69	C	Extracellular matrix regulation	(Sandberg et al. 2006)
XP_003515352	FCGRT	-1.71	H	IgG binding and protection	(Story et al. 1994)
XP_003514816	VAMP3 #	-1.74	H	Protein secretion	(Kean et al. 2009)
XP_003503110	PLG #	-1.75	C	Extracellular matrix regulation	(Rossignol et al. 2004)

Table IV. Up and down regulated gene sets on day 2 comparing to day 9 using gene ontology databases.

Size: numbers of genes consist in enriched gene set; NES: normalized enrichment score of enriched gene set; NoM p: normalized p value of enriched gene set; FDR q: false positive rate of enriched gene set.

GENE SET	SIZE	NES	NoM p	FDR q
DNA Binding	76	2.661	0	0
Nucleus	283	2.586	0	0
Nuclear Part	122	2.557	0	0
RNA Processing	47	2.494	0	0
Cell Cycle	59	2.391	0	0
Chromosome	29	2.388	0	0
Nuclear Lumen	71	2.383	0	0
Nucleobase/nucleoside/nucleotide and Nucleic Acid	227	2.376	0	0

Metabolic Process				
Nucleoplasm	48	2.299	0	0
RNA Metabolic Process	148	2.29	0	0
Endopeptidase Activity	24	-1.959	0	0.006
Tissue Development	15	-1.961	0	0.006
Membrane	262	-1.963	0	0.008
Extracellular Region Part	29	-1.963	0	0.007
Plasma Membrane Part	100	-2.005	0	0.006
Plasma Membrane	139	-2.066	0	0.003
Cellular Lipid Metabolic Process	44	-2.078	0	0.003
Extracellular Region	45	-2.111	0	0.002
Receptor Binding	42	-2.126	0	0.002
Lipid Metabolic Process	57	-2.277	0	0

Table V. Up and down regulated proteins on day 2 comparing to day 9 found in functional database using leading-edge analysis. H: Human; M: Mouse; E: Eukaryote; C: CHO; # overlapped genes in Table III.

CHO RefSeq	Gene Symbol	Log2ratio	Cells studied	Function	Reference
Up-regulated					
XP_003501907	KPNA2 #				
XP_003510169	KIF22 #				
XP_003504632	UBE2C #				
XP_003500203	LIG1 #			Same as in table III	
XP_003509164	KIF4A #				
XP_003500277	MCM2 #				
XP_003509175	MCM3	1.25	E	DNA replication	(Bell and Dutta 2002)
XP_003506293	DUT	1.25	H	DNA replication	(McIntosh et al. 1992)
XP_003498829	EIF5	1.15	R	Translation initiation	(Si et al. 1996)
XP_003512004	MCM5	1.14	E	DNA replication	(Bell and Dutta 2002)
Down-regulated					
XP_003498026	CTSB	-1.22	H	Apoptosis,	(Bruneel et al. 2005)
XP_003502412	IDUA	-1.22	H	Glycosaminoglycan metabolism	(Bie et al. 2013)
XP_003515581	ABCA4	-1.22	M	Phospholipid translocation	(Weng et al. 1999)
NP_001233729	NEU1	-1.26	C	Glycosylation	(Chee Fung Wong et al. 2005)
XP_003510519	ANXA1 #				
XP_003515030	COL5A2 #				
XP_003500579	PLTP #				
XP_003504285	COL7A1 #			Same as in table III	
XP_003514816	VAMP3 #				
XP_003503110	PLG #				

Table VI. Up and down regulated gene sets on day 2 comparing to day 9 found in functional database. Size: numbers of genes consist in enriched gene set; NES: normalized enrichment score of enriched gene set; NoM p: normalized p value of enriched gene set; FDR q: false positive rate of enriched gene set.

GENE SET	SIZE	NES	NoM p	FDR q
Reactome mRNA processing	50	2.704	0	0
Reactome processing of capped intron containing pre-mRNA	44	2.643	0	0
Reactome RNA splicing	32	2.55	0	0
KEGG spliceosome	43	2.539	0	0
KEGG cell cycle	30	2.459	0	0
Reactome transcription	41	2.399	0	0
Reactome cell cycle mitotic	81	2.312	0	0
Reactome RNA Polymerase II Transcription	31	2.295	0	0
Reactome DNA repair	25	2.272	0	0
Reactome Transcription-coupled NER (TC-NER)	15	2.255	0	0
Reactome platelet activation signaling and aggregation	49	-1.965	0	0.007
Reactome phospholipid metabolism	38	-1.989	0	0.006

KEGG fatty acid metabolism	17	-1.999	0	0.006
KEGG PPAR signaling pathway	17	-2.005	0	0.006
KEGG ECM receptor interaction	15	-2.109	0	0.003
Reactome metabolism of lipids and lipoproteins	104	-2.126	0	0.003
Reactome sphingolipid metabolism	16	-2.137	0	0.003
KEGG focal adhesion	50	-2.237	0	0
Reactome extracellular matrix organization	17	-2.238	0	0.001
KEGG lysosome	38	-2.603	0	0

Taking a few examples, TOP2A encoding a nuclear DNA topoisomerase, which regulates topologic states of DNA during transcription and replication (Belluti et al. 2013). KPNA2 nuclear transport of proteins have recently been confirm to promote cell proliferation via c-Myc and cyclin-dependent kinase CDK regulation (Huang et al. 2013). KIF22 (a molecular motor) and UBE2C (a cell cycle regulators) have been reported to be involved in cell division (Mocciaro and Rape 2012; Yu et al. 2014). Additionally, MCM2, 3 and 5 are implicated in the formation of replication forks during DNA replication (Bell and Dutta 2002). These findings are in agreement with the results from the enrichment maps in figure 7 and the nature of the cells in growth phase.

On the other hand, the top up-regulated genes on day 9 are located at membrane and extracellular region and are mainly involved in extracellular matrix regulation, cell proliferation and apoptosis, protein secretions, lipid transport and glycosylation (Table IV and VI).

COL5A2 and COL7A1 regulate the expression of collagens may cause alterations in extracellular matrix (Liu et al. 2010). Previous studies also show that change in the expression of COL5A2 was observed in sodium butyrate treated CHO cells based on the mRNA-seq data (Birzele et al. 2010). Additionally, PLG were also shown to participant in degradation of extracellular matrix (Rossignol et al. 2004). MMP12 functioning in extracellular matrix degradation, were found to be released from CHO cells producing recombinant factor VIII during the production phase (Sandberg et al. 2006). VAMP3 has been postulated to be a component of early/recycling endosomal v-SNARE responsible for protein trafficking and secretion and may contribute to extracellular matrix degradation (Kean et al. 2009). Taking all these into consideration, the change in extracellular matrix may be a physiological characteristic of cells in stationary phase.

Highly regulated apoptosis seems to be another molecular feature during the stationary phase. ANXA1 belongs to annexin protein family, can bind phospholipid in a calcium-dependent manner, which was demonstrated to be essential for cell proliferation and apoptosis (McKanna 1995; Wu et al. 2000). It was also suggested to be in association with sustaining high productivity of recombinant protein over the duration of a CHO fed-batch culture (Meleady et al. 2011). LGALS1 and LGALS3 code for Galectin-1 and Galectin-3, respectively. Galectins are types of lectins that bind β -galactosides. Galectin-1 has been demonstrated to play different roles in cell survival and proliferation as a mitogen, a cell proliferation inhibitor, or a cell apoptosis promoter (Scott and

Weinberg 2002). Similarly, Galectin-3 was also found to have a biological function in regulating cell proliferation and apoptosis (Nakahara et al. 2005).

Also notably, the expression of sialidase-1 (encoded by NEU1) that cleaves terminal sialic acid residues from glycans is up-regulated in the stationary phase. This is the likely basis of the report that decreased sialylation of recombinant proteins correlates with the increased culture duration (Chee Fung Wong et al. 2005).

6.4. Conclusion

Using systems biology-based approaches, we have shown here the effects of glucose starvation and culture duration on fed-batch CHO cell culture producing monoclonal antibody and the underlying reasons that cause such effects. Glucose starvation at the stationary phase of the fed-batch culture exhibited a negative impact on growth, viability, and specific productivity of the cells. It was also shown that the changes of glycoforms (increased GlcNAc and Gal occupancy) in regard to increased degree of glucose starvation are as a result of interplay between the dilution effect associated with change in q_p and the changed nucleotide sugar metabolism. On the other hand, the effect of culture duration on the glycopatterns is dramatic. In general, longer culture duration leads to a higher abundance of less processed glycan structures. Especially between samples from growth phase and stationary phase, the extent of such effect is immense, which was thought to be correlated with the fundamental physiological difference between cells in the two phases. For that reason, we took one step further to examine the differences between proteome levels in these two phases. We found that the expression of proteins regarding cell cycle progression and cell divisions are generally up-regulated in growth phase. On the other hand, expression of proteins that is responsible for regulating cellular metabolism, extracellular matrix, apoptosis, protein secretion and glycosylation is generally higher in stationary phase. Very importantly, a large repertoire of proteins concerning secretion machinery was generally up-regulated in the stationary phase, whereas only two proteins (α -mannosidase II and GnT1) regarding glycan maturation in Golgi apparatus were found to be slightly up-regulated. In this way, we gained deeper insight into the culture behavior and recombinant protein production on the basis of the molecular features of the cells. From the process control perspective, this proteome information could help discover and apply knowledge of cellular functions in response to changes in process conditions, in order to explore possibilities of producing recombinant product with optimal productivity and quality.

We have not excluded the possibility of cell line specific effects on our data, and ideally different cell lines should be further investigated. However, the systems biology-based analysis constitutes a

powerful tool for studying the physiological profiles of cells under different culture conditions and linking that with the quantity and quality of the recombinant product.

6.5. References

- Aggarwal K, Choe LH, Lee KH. 2006. Shotgun proteomics using the iTRAQ isobaric tags. *Brief Funct Genomic Proteomic* 5(2):112-20.
- Ahn WS, Antoniewicz MR. 2013. Parallel labeling experiments with [1,2-(13)C]glucose and [U-(13)C]glutamine provide new insights into CHO cell metabolism. *Metab Eng* 15:34-47.
- Baycin-Hizal D, Tabb DL, Chaerkady R, Chen L, Lewis NE, Nagarajan H, Sarkaria V, Kumar A, Wolozny D, Colao J and others. 2012. Proteomic analysis of Chinese hamster ovary cells. *J Proteome Res* 11(11):5265-76.
- Bell SP, Dutta A. 2002. DNA REPLICATION IN EUKARYOTIC CELLS. *Annual Review of Biochemistry* 71(1):333-374.
- Belluti S, Basile V, Benatti P, Ferrari E, Marverti G, Imbriano C. 2013. Concurrent inhibition of enzymatic activity and NF-Y-mediated transcription of Topoisomerase-II[alpha] by bis-DemethoxyCurcumin in cancer cells. *Cell Death Dis* 4:e756.
- Bibila TA, Robinson DK. 1995. In pursuit of the optimal fed-batch process for monoclonal antibody production. *Biotechnology Progress* 11(1):1-13.
- Bie H, Yin J, He X, Kermode AR, Goddard-Borger ED, Withers SG, James MN. 2013. Insights into mucopolysaccharidosis I from the structure and action of alpha-L-iduronidase. *Nat Chem Biol* 9(11):739-45.
- Birzele F, Schaub J, Rust W, Clemens C, Baum P, Kaufmann H, Weith A, Schulz TW, Hildebrandt T. 2010. Into the unknown: expression profiling without genome sequence information in CHO by next generation sequencing. *Nucleic Acids Research* 38(12):3999-4010.
- Borys MC, Linzer DI, Papoutsakis ET. 1993. Culture pH affects expression rates and glycosylation of recombinant mouse placental lactogen proteins by Chinese hamster ovary (CHO) cells. *Bio/Technology* 11(6):720-724.
- Borys MC, Linzer DI, Papoutsakis ET. 1994. Ammonia affects the glycosylation patterns of recombinant mouse placental lactogen-I by chinese hamster ovary cells in a pH-dependent manner. *Biotechnol Bioeng* 43(6):505-14.
- Bruneel A, Labas V, Mailloux A, Sharma S, Royer N, Vinh J, Pernet P, Vaubourdolle M, Baudin B. 2005. Proteomics of human umbilical vein endothelial cells applied to etoposide-induced apoptosis. *Proteomics* 5(15):3876-84.

- Cao Y, Kimura S, Itoi T, Honda K, Ohtake H, Omasa T. 2012. Construction of BAC-based physical map and analysis of chromosome rearrangement in Chinese hamster ovary cell lines. *Biotechnol Bioeng* 109(6):1357-67.
- Chee Fung Wong D, Tin Kam Wong K, Tang Goh L, Kiat Heng C, Gek Sim Yap M. 2005. Impact of dynamic online fed-batch strategies on metabolism, productivity and N-glycosylation quality in CHO cell cultures. *Biotechnol Bioeng* 89(2):164-77.
- Chen P, Harcum SW. 2005. Effects of amino acid additions on ammonium stressed CHO cells. *J Biotechnol* 117(3):277-86.
- Chumsae C, Gaza-Bulseco G, Sun J, Liu H. 2007. Comparison of methionine oxidation in thermal stability and chemically stressed samples of a fully human monoclonal antibody. *J Chromatogr B Analyt Technol Biomed Life Sci* 850(1-2):285-94.
- Dean J, Reddy P. 2013. Metabolic analysis of antibody producing CHO cells in fed-batch production. *Biotechnol Bioeng* 110(6):1735-47.
- Druz A, Son YJ, Betenbaugh M, Shiloach J. 2013. Stable inhibition of mmu-miR-466h-5p improves apoptosis resistance and protein production in CHO cells. *Metab Eng* 16:87-94.
- Fan Y, Jimenez Del Val I, Müller C, Wagtberg Sen J, Rasmussen SK, Kontoravdi C, Weilguny D, Andersen MR. 2014. Amino acid and glucose metabolism in fed-batch CHO cell culture affects antibody production and glycosylation. *Biotechnology and Bioengineering*:n/a-n/a.
- Ferrari G, Rossi R, Arosio D, Vindigni A, Biamonti G, Montecucco A. 2003. Cell Cycle-dependent Phosphorylation of Human DNA Ligase I at the Cyclin-dependent Kinase Sites. *Journal of Biological Chemistry* 278(39):37761-37767.
- Gagnon M, Hiller G, Luan YT, Kittredge A, DeFelice J, Drapeau D. 2011. High-end pH-controlled delivery of glucose effectively suppresses lactate accumulation in CHO fed-batch cultures. *Biotechnol Bioeng* 108(6):1328-37.
- Gawlitzeck M, Ryll T, Lofgren J, Sliwkowski MB. 2000. Ammonium alters N-glycan structures of recombinant TNFR-IgG: degradative versus biosynthetic mechanisms. *Biotechnol Bioeng* 68(6):637-46.
- Gaza-Bulseco G, Bulseco A, Chumsae C, Liu H. 2008. Characterization of the glycosylation state of a recombinant monoclonal antibody using weak cation exchange chromatography and mass spectrometry. *J Chromatogr B Analyt Technol Biomed Life Sci* 862(1-2):155-60.
- Goetze AM, Liu YD, Zhang Z, Shah B, Lee E, Bondarenko PV, Flynn GC. 2011. High-mannose glycans on the Fc region of therapeutic IgG antibodies increase serum clearance in humans. *Glycobiology* 21(7):949-59.

- Gramer MJ, Goochee CF. 1993. Glycosidase Activities in Chinese Hamster Ovary Cell Lysate and Cell Culture Supernatant. *Biotechnology Progress* 9(4):366-373.
- Harris RJ, Kabakoff B, Macchi FD, Shen FJ, Kwong M, Andya JD, Shire SJ, Bjork N, Totpal K, Chen AB. 2001. Identification of multiple sources of charge heterogeneity in a recombinant antibody. *J Chromatogr B Biomed Sci Appl* 752(2):233-45.
- Hong JK, Lee SM, Kim KY, Lee GM. 2014. Effect of sodium butyrate on the assembly, charge variants, and galactosylation of antibody produced in recombinant Chinese hamster ovary cells. *Appl Microbiol Biotechnol* 98(12):5417-25.
- Hooker AD, Goldman MH, Markham NH, James DC, Ison AP, Bull AT, Strange PG, Salmon I, Baines AJ, Jenkins N. 1995. N-glycans of recombinant human interferon- γ change during batch culture of chinese hamster ovary cells. *Biotechnology and Bioengineering* 48(6):639-648.
- Hossler P, Khattak SF, Li ZJ. 2009. Optimal and consistent protein glycosylation in mammalian cell culture. *Glycobiology* 19(9):936-49.
- Hu WS, Dodge TC, Frame KK, Himes VB. 1987. Effect of glucose on the cultivation of mammalian cells. *Dev Biol Stand* 66:279-90.
- Huang da W, Sherman BT, Lempicki RA. 2009a. Bioinformatics enrichment tools: paths toward the comprehensive functional analysis of large gene lists. *Nucleic Acids Res* 37(1):1-13.
- Huang da W, Sherman BT, Lempicki RA. 2009b. Systematic and integrative analysis of large gene lists using DAVID bioinformatics resources. *Nat Protoc* 4(1):44-57.
- Huang L, Wang HY, Li JD, Wang JH, Zhou Y, Luo RZ, Yun JP, Zhang Y, Jia WH, Zheng M. 2013. KPNA2 promotes cell proliferation and tumorigenicity in epithelial ovarian carcinoma through upregulation of c-Myc and downregulation of FOXO3a. *Cell Death Dis* 4:e745.
- Jefferis R. 2012. Isotype and glycoform selection for antibody therapeutics. *Arch Biochem Biophys* 526(2):159-66.
- Jimenez Del Val I, Kyriakopoulos S, Polizzi KM, Kontoravdi C. 2013. An optimized method for extraction and quantification of nucleotides and nucleotide sugars from mammalian cells. *Anal Biochem* 443(2):172-80.
- Kaneko Y, Sato R, Aoyagi H. 2010. Changes in the quality of antibodies produced by Chinese hamster ovary cells during the death phase of cell culture. *J Biosci Bioeng* 109(3):281-7.
- Kean MJ, Williams KC, Skalski M, Myers D, Burtnik A, Foster D, Coppolino MG. 2009. VAMP3, syntaxin-13 and SNAP23 are involved in secretion of matrix metalloproteinases, degradation of the extracellular matrix and cell invasion. *Journal of Cell Science* 122(22):4089-4098.

- Kildegaard HF, Baycin-Hizal D, Lewis NE, Betenbaugh MJ. 2013. The emerging CHO systems biology era: harnessing the 'omics revolution for biotechnology. *Curr Opin Biotechnol* 24(6):1102-7.
- Kochanowski N, Blanchard F, Cacan R, Chirat F, Guedon E, Marc A, Goergen JL. 2008. Influence of intracellular nucleotide and nucleotide sugar contents on recombinant interferon-gamma glycosylation during batch and fed-batch cultures of CHO cells. *Biotechnol Bioeng* 100(4):721-33.
- Lewis NE, Liu X, Li Y, Nagarajan H, Yerganian G, O'Brien E, Bordbar A, Roth AM, Rosenbloom J, Bian C and others. 2013. Genomic landscapes of Chinese hamster ovary cell lines as revealed by the *Cricetulus griseus* draft genome. *Nat Biotechnol* 31(8):759-65.
- Lim Y, Wong NS, Lee YY, Ku SC, Wong DC, Yap MG. 2010. Engineering mammalian cells in bioprocessing - current achievements and future perspectives. *Biotechnol Appl Biochem* 55(4):175-89.
- Liu B, Spearman M, Doering J, Lattova E, Perreault H, Butler M. 2014. The availability of glucose to CHO cells affects the intracellular lipid-linked oligosaccharide distribution, site occupancy and the N-glycosylation profile of a monoclonal antibody. *J Biotechnol* 170:17-27.
- Liu H, Gaza-Bulseco G, Sun J. 2006. Characterization of the stability of a fully human monoclonal IgG after prolonged incubation at elevated temperature. *Journal of Chromatography B* 837(1-2):35-43.
- Liu Y, Taylor NE, Lu L, Usa K, Cowley AW, Jr., Ferreri NR, Yeo NC, Liang M. 2010. Renal medullary microRNAs in Dahl salt-sensitive rats: miR-29b regulates several collagens and related genes. *Hypertension* 55(4):974-82.
- Mazumdar M, Sundareshan S, Misteli T. 2004. Human chromokinesin KIF4A functions in chromosome condensation and segregation. *J Cell Biol* 166(5):613-20.
- McGettigan PA. 2013. Transcriptomics in the RNA-seq era. *Curr Opin Chem Biol* 17(1):4-11.
- McIntosh EM, Ager DD, Gadsden MH, Haynes RH. 1992. Human dUTP pyrophosphatase: cDNA sequence and potential biological importance of the enzyme. *Proc Natl Acad Sci U S A* 89(17):8020-4.
- McKanna JA. 1995. Lipocortin 1 in apoptosis: Mammary regression. *The Anatomical Record* 242(1):1-10.
- Meleady P, Doolan P, Henry M, Barron N, Keenan J, O'Sullivan F, Clarke C, Gammell P, Melville M, Leonard M and others. 2011. Sustained productivity in recombinant Chinese Hamster

- Ovary (CHO) cell lines: proteome analysis of the molecular basis for a process-related phenotype. *BMC Biotechnology* 11(1):78.
- Merico D, Isserlin R, Stueker O, Emili A, Bader GD. 2010. Enrichment Map: A Network-Based Method for Gene-Set Enrichment Visualization and Interpretation. *PLoS ONE* 5(11):e13984.
- Mocciaro A, Rape M. 2012. Emerging regulatory mechanisms in ubiquitin-dependent cell cycle control. *Journal of Cell Science* 125(2):255-263.
- Nagaki S, Yamamoto M, Yumoto Y, Shirakawa H, Yoshida M, Teraoka H. 1998. Non-histone chromosomal proteins HMG1 and 2 enhance ligation reaction of DNA double-strand breaks. *Biochem Biophys Res Commun* 246(1):137-41.
- Nakahara S, Oka N, Raz A. 2005. On the role of galectin-3 in cancer apoptosis. *Apoptosis* 10(2):267-275.
- Okada Y, Yamazaki H, Sekine-Aizawa Y, Hirokawa N. 1995. The neuron-specific kinesin superfamily protein KIF1A is a unique monomeric motor for anterograde axonal transport of synaptic vesicle precursors. *Cell* 81(5):769-80.
- Pacis E, Yu M, Autsen J, Bayer R, Li F. 2011. Effects of cell culture conditions on antibody N-linked glycosylation—what affects high mannose 5 glycoform. *Biotechnology and Bioengineering* 108(10):2348-2358.
- Perkins M, Theiler R, Lunte S, Jeschke M. 2000. Determination of the origin of charge heterogeneity in a murine monoclonal antibody. *Pharm Res* 17(9):1110-7.
- Pottiez G, Wiederin J, Fox HS, Ciborowski P. 2012. Comparison of 4-plex to 8-plex iTRAQ quantitative measurements of proteins in human plasma samples. *J Proteome Res* 11(7):3774-81.
- Raju TS. 2008. Terminal sugars of Fc glycans influence antibody effector functions of IgGs. *Curr Opin Immunol* 20(4):471-8.
- Rivinoja A, Hassinen A, Kokkonen N, Kauppila A, Kellokumpu S. 2009. Elevated Golgi pH impairs terminal N-glycosylation by inducing mislocalization of Golgi glycosyltransferases. *J Cell Physiol* 220(1):144-154.
- Robinson DK, Chan CP, Yu Lp C, Tsai PK, Tung J, Seamans TC, Lenny AB, Lee DK, Irwin J, Silberklang M. 1994. Characterization of a recombinant antibody produced in the course of a high yield fed-batch process. *Biotechnology and Bioengineering* 44(6):727-735.
- Rossignol P, Ho-Tin-Noe B, Vranckx R, Bouton MC, Meilhac O, Lijnen HR, Guillin MC, Michel JB, Angles-Cano E. 2004. Protease nexin-1 inhibits plasminogen activation-induced apoptosis of adherent cells. *J Biol Chem* 279(11):10346-56.

- Rouiller Y, Perilleux A, Collet N, Jordan M, Stettler M, Broly H. 2013. A high-throughput media design approach for high performance mammalian fed-batch cultures. *MAbs* 5(3):501-11.
- Sandberg H, Lutkemeyer D, Kuprin S, Wrangel M, Almstedt A, Persson P, Ek V, Mikaelsson M. 2006. Mapping and partial characterization of proteases expressed by a CHO production cell line. *Biotechnol Bioeng* 95(5):961-71.
- Scott K, Weinberg C. 2002. Galectin-1: A bifunctional regulator of cellular proliferation. *Glycoconjugate Journal* 19(7-9):467-477.
- Shi HH, Goudar CT. 2014. Recent advances in the understanding of biological implications and modulation methodologies of monoclonal antibody N-linked high mannose glycans. *Biotechnology and Bioengineering* 111(10):1907-1919.
- Shimamura S, Ishikawa F. 2008. Interaction between DNMT1 and DNA replication reactions in the SV40 in vitro replication system. *Cancer Science* 99(10):1960-1966.
- Si K, Das K, Maitra U. 1996. Characterization of multiple mRNAs that encode mammalian translation initiation factor 5 (eIF-5). *J Biol Chem* 271(28):16934-8.
- SPSS Inc. 2011. *IBM SPSS Statistics for Windows*. Armonk, NY: IBM Corp.
- Story CM, Mikulska JE, Simister NE. 1994. A major histocompatibility complex class I-like Fc receptor cloned from human placenta: possible role in transfer of immunoglobulin G from mother to fetus. *J Exp Med* 180(6):2377-81.
- Subramanian A, Tamayo P, Mootha VK, Mukherjee S, Ebert BL, Gillette MA, Paulovich A, Pomeroy SL, Golub TR, Lander ES and others. 2005. Gene set enrichment analysis: A knowledge-based approach for interpreting genome-wide expression profiles. *Proceedings of the National Academy of Sciences of the United States of America* 102(43):15545-15550.
- Templeton N, Dean J, Reddy P, Young JD. 2013. Peak antibody production is associated with increased oxidative metabolism in an industrially relevant fed-batch CHO cell culture. *Biotechnology and Bioengineering* 110(7):2013-+.
- Vuletic S, Dong W, Wolfbauer G, Day JR, Albers JJ. 2009. PLTP is present in the nucleus, and its nuclear export is CRM1-dependent. *Biochimica et Biophysica Acta (BBA) - Molecular Cell Research* 1793(3):584-591.
- Weng J, Mata NL, Azarian SM, Tzekov RT, Birch DG, Travis GH. 1999. Insights into the function of Rim protein in photoreceptors and etiology of Stargardt's disease from the phenotype in abcr knockout mice. *Cell* 98(1):13-23.
- Wisniewski JR, Zougman A, Nagaraj N, Mann M. 2009. Universal sample preparation method for proteome analysis. *Nat Methods* 6(5):359-62.

- Wong DC, Wong NS, Goh JS, May LM, Yap MG. 2010a. Profiling of N-glycosylation gene expression in CHO cell fed-batch cultures. *Biotechnol Bioeng* 107(3):516-28.
- Wong NS, Wati L, Nissom PM, Feng HT, Lee MM, Yap MG. 2010b. An investigation of intracellular glycosylation activities in CHO cells: effects of nucleotide sugar precursor feeding. *Biotechnol Bioeng* 107(2):321-36.
- Wu Y-L, Jiang X-R, Lillington DM, Newland AC, Kelsey SM. 2000. Upregulation of lipocortin 1 inhibits tumour necrosis factor-induced apoptosis in human leukaemic cells: a possible mechanism of resistance to immune surveillance. *British Journal of Haematology* 111(3):807-816.
- Xie L, Nyberg G, Gu X, Li H, Mollborn F, Wang DI. 1997. Gamma-interferon production and quality in stoichiometric fed-batch cultures of Chinese hamster ovary (CHO) cells under serum-free conditions. *Biotechnol Bioeng* 56(5):577-82.
- Xu X, Nagarajan H, Lewis NE, Pan S, Cai Z, Liu X, Chen W, Xie M, Wang W, Hammond S and others. 2011. The genomic sequence of the Chinese hamster ovary (CHO)-K1 cell line. *Nat Biotechnol* 29(8):735-41.
- Yan B, Steen S, Hambly D, Valliere-Douglass J, Vanden Bos T, Smallwood S, Yates Z, Arroll T, Han Y, Gadgil H and others. 2009. Succinimide formation at Asn 55 in the complementarity determining region of a recombinant monoclonal antibody IgG1 heavy chain. *J Pharm Sci* 98(10):3509-21.
- Young JD. 2013. Metabolic flux rewiring in mammalian cell cultures. *Curr Opin Biotechnol* 24(6):1108-15.
- Yu Y, Wang X-Y, Sun L, Wang Y-L, Wan Y-F, Li X-Q, Feng Y-M. 2014. Inhibition of KIF22 suppresses cancer cell proliferation by delaying mitotic exit through upregulating CDC25C expression. *Carcinogenesis*.
- Zhang T, Bourret J, Cano T. 2011. Isolation and characterization of therapeutic antibody charge variants using cation exchange displacement chromatography. *J Chromatogr A* 1218(31):5079-86.
- Zheng K, Bantog C, Bayer R. 2011. The impact of glycosylation on monoclonal antibody conformation and stability. *MAbs* 3(6):568-76.

Chapter 7 Chinese hamster ovary cell engineering to improve the maturation of recombinant monoclonal antibody N-glycosylation

Yuzhou Fan^{1, 2}, Ioscani Jimenez Del Val³, Christian Müller², Jette Wagtberg Sen², Søren Kofoed Rasmussen², Cleo Kontoravdi³, Michael J. Betenbaugh⁴, Dietmar Weilguny^{2*} and Mikael Rørdam Andersen^{1*}

¹Network Engineering of Eukaryotic Cell Factories, Department of Systems Biology, Technical University of Denmark, Building 223, 2800 Kgs. Lyngby, Denmark

²Symphogen A/S, Pederstrupvej 93, 2750 Ballerup, Denmark

³Center for Process Systems Engineering, Department of Chemical Engineering, Imperial College London, South Kensington Campus, London SW7 2AZ, UK

⁴Department of Chemical and Biomolecular Engineering, Johns Hopkins University, Baltimore, MD 21218, USA

*Corresponding author.

Address correspondence to Mikael Rørdam Andersen, Department of Systems Biology, Technical University of Denmark, Building 223, 2800 Kgs. Lyngby, Denmark; +4545252675; mr@bio.dtu.dk; Dietmar Weilguny, Cell line and Upstream, Symphogen A/S, Pederstrupvej 93, 2750 Ballerup, Denmark; +4588382683; dw@symphogen.com

Keywords

Chinese hamster ovary cells; metabolic engineering; N-glycosylation; fed-batch; monoclonal antibody

Abstract

In this study, metabolic engineering have been carried out in order to develop cell lines that have better capacity of producing monoclonal antibodies (mAbs) with more matured glycans. IgG-producing cell lines with stable overexpression of α -1,3-mannosyl-glycoprotein 2- β -N-acetylglucosaminyltransferase (GnTI) or UDP-GlcNAc transporter was generated. To gain better insight of the interplays among GnTI or UDP-GlcNAc expression, mAb productivity, nucleotide sugar metabolism, N-glycosylation quality during fed-batch culture, selected cell lines are assessed and compared.

We found that overexpression of GnTI can be use as a strategy to generate cell lines that produce less Man5 and higher GlcNAc occupancy of mAb N-glycans. On the other hand, overexpression of

UDP-GlcNAc transporter seems to have no apparent effect on increasing GlcNAc occupancy in the cell lines tested. Moreover, clone specific effect in association with specific productivity of mAb can also influence the maturation of glycans. In general, cell lines with lower specific productivity may have the tendency to produce mAb with higher level of GlcNAc and Gal occupancy.

7.1. Introduction

Recombinant therapeutic protein glycosylation plays a critical role in changing several product-associated attributes, including bioactivity, stability, immunogenicity and etc. (Arnold et al. 2007; Costa et al. 2013). In the biopharmaceutical industry, an absolute glycosylation requirement is one of the main reasons that mammalian cell culture systems, in particular, Chinese hamster ovary (CHO) cells were used for the manufacturing process. Despite the human-like glycosylation patterns of CHO-derived recombinant proteins, controlling and modulating recombinant protein glycosylation in CHO cells towards more desired patterns remains one of the major challenges during cell line and process development.

CHO cell engineering has been demonstrated to be able to, for example shift metabolic pathways for more efficient energy utilization (Jeon et al. 2011; Kim and Lee 2007a; Kim and Lee 2007b; Park et al. 2000), enhance productivity of the cells (Dreesen and Fussenegger 2011; Meleady et al. 2012; Tigges and Fussenegger 2006), and improve longevity of the culture (Banmeyer et al. 2004; Druz et al. 2013; Figueroa et al. 2007; Mastrangelo et al. 2000). More importantly, CHO cell engineering has been extensively used in optimizing quality attributes of the product, particularly glycosylation (Chapter 2) (Le Fourn et al. 2014). For example, many studies have been focused on improving ADCC activity of IgG by engineering CHO cells using two different strategies, namely producing bisecting GlcNAc (Davies et al. 2001; Umana et al. 1999) or afucosylated glycan structure (Imai-Nishiya et al. 2007; Kanda et al. 2007; Mori et al. 2004; Yamane-Ohnuki et al. 2004). In the light of recent advance in CHO genomics (Xu et al. 2011), new exploration and innovation in CHO cell engineering, especially in glycosylation engineering become more feasible (Maszczak-Seneczko et al. 2011; North et al. 2010; Sealover et al. 2013).

One of the key objectives of recent cell line and process development is to increase productivity of a cell line, so that higher yield of product can be achieved. However, as a cost of that, reduced maturation of glycans, for example increased Man5, decreased GlcNAc and Gal occupancy of glycans are always associated (Chapter 6). That is always due to bottlenecks in glycosylation-associated Golgi resident protein availability relative to recombinant protein productivity of the cells (Fan et al. 2014). It has been reported that elevated high mannose glycans and reduced

GlcNAc and Gal occupancy of glycans may increase immunogenicity and influence the serum half-life of mAbs (Shi and Goudar 2014). Therefore, during the cell line and process development, strategies of improving the maturation of glycans need to be addressed as well.

In this study, we use metabolic engineering approaches to develop cell lines that may have better capacity of producing mAbs with more matured glycans. α -1,3-mannosyl-glycoprotein 2- β -N-acetylglucosaminyltransferase (GnTI, which is the enzyme in Golgi that is responsible of transferring a GlcNAc residue onto Man5 glycan) or UDP-GlcNAc transporter (the enzyme that can transport UDP-GlcNAc from cytosol into Golgi apparatus) was overexpressed in two parental mAb-producing cell lines. Fed-batch culture performance, mAb production, intracellular nucleotide sugar availability and glycoprofiles of parental and engineered cell lines are evaluated and compared. Our results demonstrate potential strategies of generating cell lines that can produce less Man5 and higher GlcNAc occupancy of glycans and provide a holistic understanding of interrelations of cell growth, mAb production, glycosylation-associated enzymes, nucleotide sugar metabolism and glycosylation in fed-batch CHO cell culture.

7.2. Materials and Methods

7.2.1. High throughput USER Cloning

Plasmids used in this study were modified from Selexis mammalian expression SLXplasmid_0191 (containing puromycin-resistance gene) and SLXplasmid_0192 (containing hygromycin-resistance gene). The GFP sequence of both original plasmids was replaced by a USER cassette to create USER cloning-compatible plasmids (Figure S1). A USER cloning-based mammalian expression vector assembly method (Lund et al. 2014) was used for constructing the plasmids used in this study (Figure 1). DNA building blocks were amplified by PCR using proofreading polymerase *PfuX7* (Norholm 2010). Primers used in this study were listed in Table S1. PCR templates in this study are all commercially available (Table S2). The cDNA sequences of Chinese hamster GnTI (NM_001243980) and UDP-GlcNAc transporter (NM_001246818) were obtained from gene bank. DNA fragment of C-terminal HA-tagged GnTI and N-terminal FLAG-tagged UDP-GlcNAc transporter were synthesis and cloned in to pUC57 by GenScript. Four plasmids (p1, p2, p3 and p4) have been generated by USER assembly. The sequences of PCR amplified regions in all plasmids have been confirmed by sequencing.

7.2.2. *Transfection and stable cell line generation*

Cell lines A and B, which were used in this study, are two Symphogen in-house IgG1-producing CHO DG44 suspension cell lines. Cells were thawed and maintained in proprietary serum-free basal medium at 37°C, 5% CO₂, 200 rpm. Two hours prior to transfection, cells were transferred to transfection medium, which consists of freestyle CHO expression medium (Gibco) supplemented with 8 mM L-glutamine (Gibco). Transfection mix for each transfection was prepared, which contains 10 µg of plasmid, 500 µl Opti-MeM[®] reduced serum media (Invitrogen, Life Technologies) and 40 µl of FuGENE HD reagent (Roche). Upon transfection, the transfection mix was incubated with 5x10⁶ cells resuspended in 10 ml transfection medium in 50 ml TPP[®] TubeSpin bioreactor tube (Sigma-Aldrich) for two hours. After transfection, cells were cultivated in proprietary cloning medium. Two days after transfection, 5 µg/ml puromycin (Invitrogen, Life Technologies) or 250 µg/ml hygromycin (Invitrogen, Life Technologies) selection was applied to the cells accordingly. Cells were continued to cultivate under the selection pressure for three weeks. Stable single cell clones were generated using FACS Aria[™] II flow cytometry (BD biosciences) and were expanded in the proprietary cloning medium. Further clone selection was carried out based on the intensity of corresponding fluorescence signals (eGFP or mCherry) of the cells using Cellavista imaging system (SynGene). Cells that are expected to have stable and relative higher overexpression of GnTI (strong mCherry signal) or UDP-GlcNAc transporter (strong eGFP signal) were selected and maintained in the proprietary basal medium for further analysis.

7.2.3. *Confirmation of the overexpression*

The expression level of GnTI or UDP-GlcNAc transporter in the parental (A and B) and engineered (A-M18, A-E15, B-M4, B-M7 and B-E15) cell lines was determined by Western blot analysis as described in (Fan et al. 2014). Intracellular immunostaining was carried out to confirm the subcellular localization of the overexpressed enzymes. Cells expressed HA-tagged GnTI and FLAG-tagged UDP-GlcNAc transporter were washed with PBS (Invitrogen, Life Technologies) and fixed with 4 % paraformaldehyde (PFA; Thermo Scientific) for 20 min. The cells were subsequently permeabilized with 0.2 % Triton X-100 for 3 min and blocked with 1% BAS in PBS for 15 min. The cells were then incubated with rabbit anti-GM130 Golgi protein antibody (1:135, Abcam) and mouse anti-HA (1:160, Sigma-Aldrich) or anti-FLAG (1:160, Sigma-Aldrich) antibody for 1h and washed three times with 1% BAS in PBS. After 1 h incubation with goat anti-rabbit Alexa Fluor 647-conjugated antibody (for the detection of Golgi marker antibody; 1:100; Invitrogen, Life Technologies) and goat anti-mouse Alexa Fluor 488 (for the detection of HA tag; 1:100; Invitrogen, Life Technologies) or 546-conjugated antibody (for the detection of FLAG tag; 1:100;

Invitrogen, Life Technologies), the cells were stained with 1:10000 Hoechst 33342 dye (Invitrogen, Eugene) for 15 min and then subjected to Opera fluorescence confocal microscope System (Perkin Elmer) using 40x magnification for localization analysis of GnTI and UDP-GlcNAc transporter. Constant imaging parameters were used for acquiring images within the same set of experiments. ImageJ 1.47 (NIH) was used to crop representative areas and to produce the final figures.

7.2.4. Cell culture and fed-batch process

Fed-batch culture was carried out using the cell lines A, A-M18, A-E15, B, B-M4, B-M7 and B-E15 under the cultivation conditions as described in Chapter 6. Proprietary feed (10% of the initial culture volume) was added to the culture on days 2, 5, 7, 9 and 11. Glucose concentration was adjusted to 33mM on day 5 and to 50mM on days 9 and 11. Similar as described in Chapter 6, cell growth, metabolism and mAb production was monitored during the fed-batch process on days 2, 5, 7, 9, 11 and 14, and intracellular nucleotide sugar quantification was carried out on days 2, 5, 9 and 11. Cell culture was harvested and mAb glycoprofiling was performed on day 14.

7.2.5. mAb purification and glycoprofiling

mAb purification was carried out as described previously (Chapter 6). Glycoprofiling of the purified mAb was performed using the same method as reported in (Fan et al. 2014).

7.2.6. Statistical analysis of glycoform distributions

Differences in the expression level of GnTI or UDP-GlcNAc transporter and in glycoforms of mAb produced among original and engineered cell lines were evaluated statistically. Statistical significant difference ($p_{ANOVA} < 0.05$) was evaluated by One-way ANOVA with Dunnett post hoc pairwise comparison test using GraphPad Prism 5.

7.2.7. Nucleotide sugar analysis

Nucleotide sugar analysis was carried out as previously described using acetonitrile extraction and high-performance anion-exchange (HPAEC) HPLC (Fan et al. 2014; Jimenez Del Val et al. 2013).

7.3. Results

Improving mAb productivity without reducing the maturation of N-glycosylation is one of the major concerns during cell line and process development. Therefore, it is extremely valuable to explore efficient ways of improving the maturation of glycans, in particular, reducing high mannose forms and increasing GlcNAc and Gal occupancy of the glycans. Here, we overexpress either GnTI

or UDP-GlcNAc transporter in two mAb producing cell lines and investigate the impact on the fed-batch culture performance, mAb productivity and glycosylation.

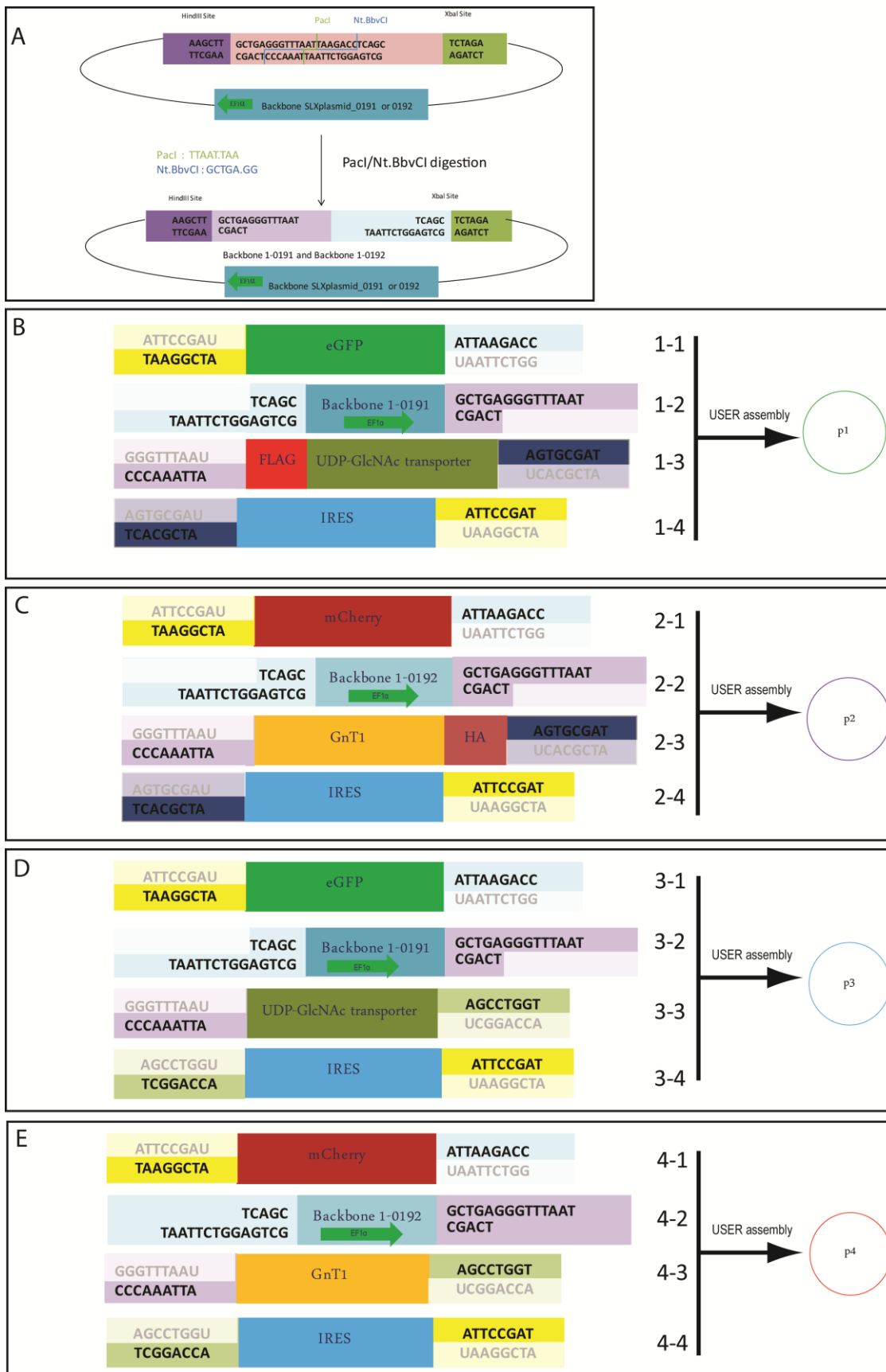


Figure 1. Construction of Plasmids. PacI/Nt.BbCI digestion of USER cloning-compatible version of SLXplasmid_0191 or 0192 is presented in A. USER assembly of DNA fragments containing functional elements for p1 (SLX0191_PuroR_EF1 α _FLAG-tag::UDP-GlcNAcTransporter_IRES_eGFP) , p2 (SLX0192_HygR_EF1 α _GnTI::HA-tag_IRES_mCherry), p3 (SLX0191_PuroR_EF1 α _UDP-GlcNAcTransporter_IRES_eGFP) and p4 (SLX0192_HygR_EF1 α _GnTI_IRES_mCherry) are illustrated in B, C, D and E.

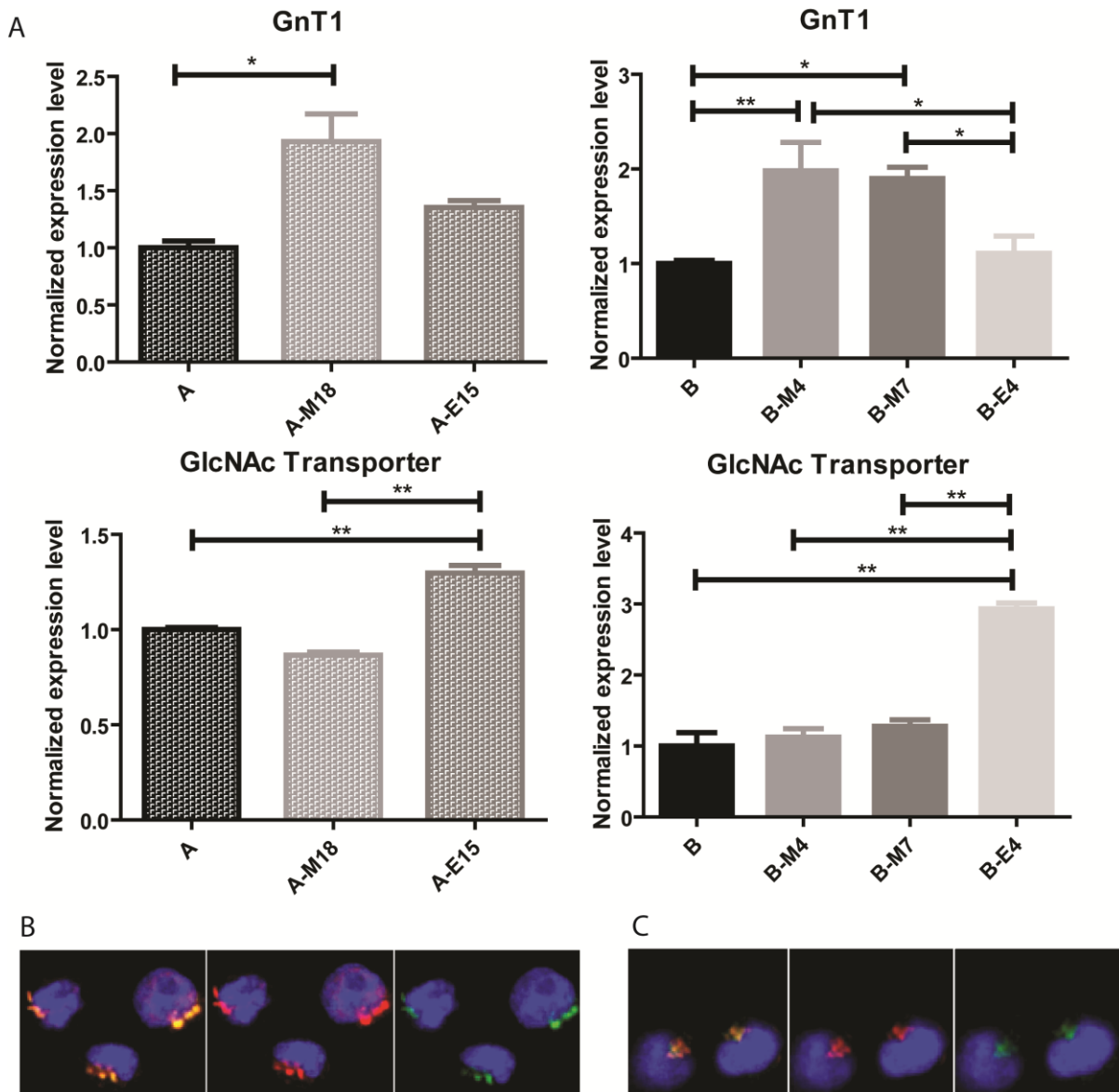


Figure 2. Analysis of intracellular GnTI and UDP-GlcNAc overexpression. (A) Quantification of intracellular GnTI and UDP-GlcNAc transporter levels in the parental (A and B) and engineered (A-M18, A-E15, B-M4, B-M7 and B-E15) cell lines by western bolt. The criteria for significant differences are: * for $p < 0.05$, ** for $p < 0.01$ and *** for $p < 0.001$. (B) Subcellular localization of the overexpressed GnTI in cell line B-Mt. HA-tagged GnTI (Red); GM130 Golgi marker (Green); Co-localization (Yellow). (C)

Subcellular localization of the overexpressed UDP-GlcNAc transporter in cell line B-Et. FLAG-tagged UDP-GlcNAc transporter (Red); GM130 Golgi marker (Green); Yellow: Co-localization.

7.3.1. Plasmids and cell line engineering

Cell lines A and B were transfected using the plasmids constructed by USER cloning (Figure 1). Various engineered cell lines that overexpressed GnTI or UDP-GlcNAc transporter were generated and isolated by single cell sorting. According to the strength of fluorescent signals, 8 cell lines were selected for further investigation (Table I).

Table I. Engineered cell lines used in the study.

Cell line	Plasmid used	Overexpression	Florescent signal
A-M18	p4	GnTI	mCherry
A-E15	p3	UDP-GlcNAc transporter	eGFP
B-M4	p4	GnTI	mCherry
B-M7	p4	GnTI	mCherry
B-E4	p3	UDP-GlcNAc transporter	eGFP
B-Mt	p2	GnTI:HA	mCherry
B-Et	p1	FLAG: UDP-GlcNAc transporter	eGFP

In order to quantify the overexpression levels, western blot analysis of GnTI and UDP-GlcNAc transporter on the selected cell lines were carried out. As shown in Figure 2A, cell lines A-M18, B-M4 and B-M7 have 2-fold overexpression of GnTI in comparison to their parental cell line. Additionally, overexpression of UDP-GlcNAc transporter with statistical significance in cell lines A-E15 and B-E4 can also be confirmed. Figures 2B and 2C indicate that the overexpressed GnTI and UDP-GlcNAc transporter are correctly localized in Golgi, and thus they are considered to properly function in the cells. It is also necessary to mention that no change in UDP-GlcNAc transporter expression can be observed when overexpressing GnTI in both A and B cell lines and *vice versa*. This implies that there are no regulatory interactions between GnTI and UDP-GlcNAc transporter in our cells.

7.3.2. Fed-batch performance and mAb production

Culture performance and mAb productivity of culture processes with eight different cell lines (A, A-M18, A-E15, B, B-M4, B-M7 and B-E4) are shown in Figure 3. Minor clone specific effect can be observed in A-M18 and A-E15 cell lines. They have faster cell growth, increased integral of viable cells (IVC), similar specific productivity (q_p) of mAb and comparable metabolic profile of lactate and NH_4^+ in comparison with their parental cell line. On the other hand, cell lines that

engineered from cell line B shows larger variations of clone specific effect. Cell line B-M4 has comparable q_p as cell line B, but dramatically higher IVC. In contrast to that, cell line B-M7 has comparable cell growth as cell line B, but lower q_p . Additionally, when comparing to cell line B, B-E4 cell line shows earlier onset of cell death and reduced IVC and q_p . This may be attributed to higher lactate accumulation during the cell culture that inhibits the cell growth and threatens the culture longevity.

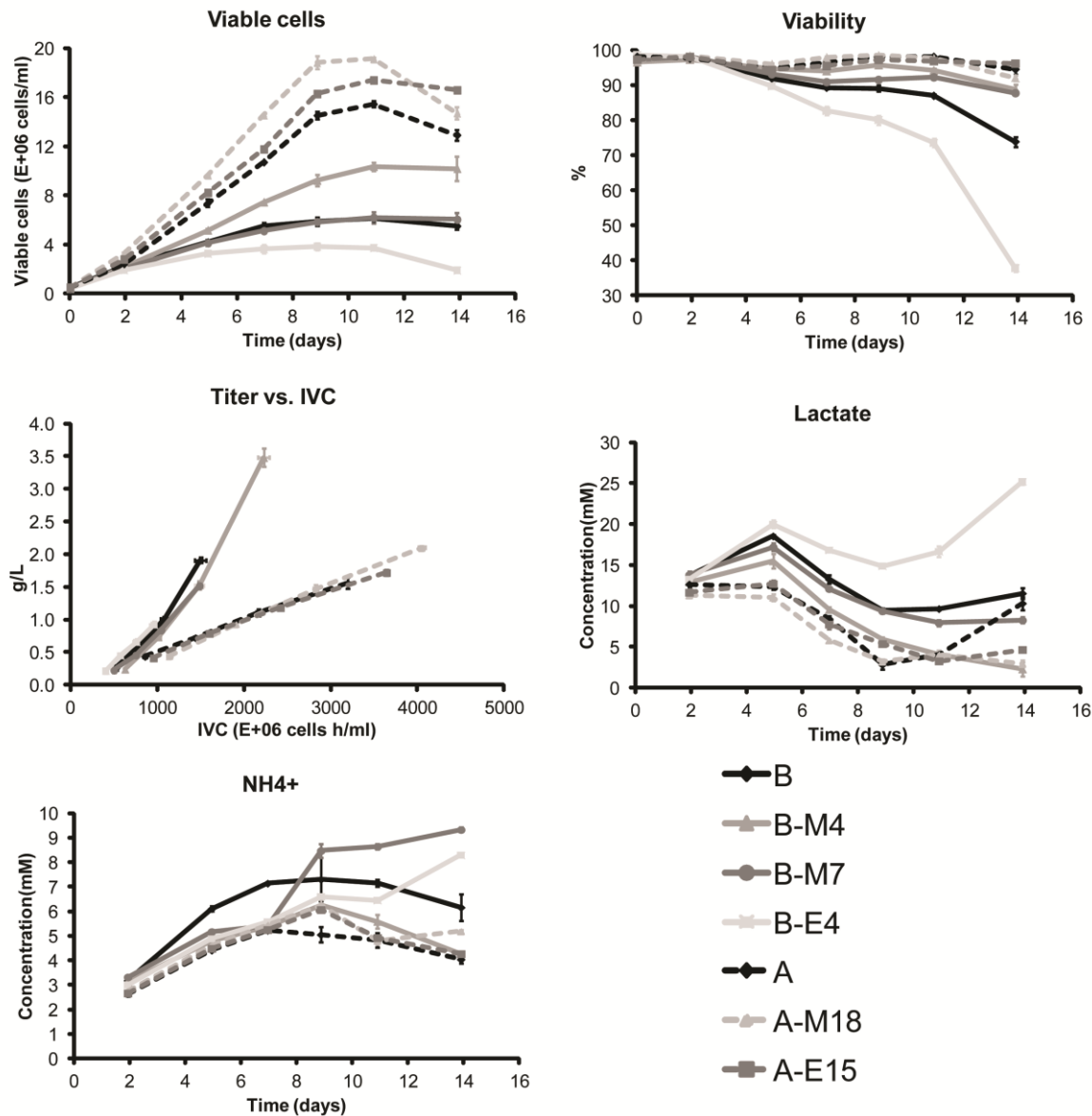


Figure 3. Comparison of fed-batch cultures of the parental (A and B) and engineered (A-M18, A-E15, B-M4, B-M7 and B-E15) cell lines. Viable cell density, viability and IgG titer vs. integral of viable cells (IVC) are presented in A, B and C, respectively. Variations of lactate and ammonia concentrations during the cell culture are shown in D and E. The error bars indicates the standard deviation of duplicate experiments.

7.3.3. Glycosylation profiles of mAbs produced from engineered and parental cell lines

The glycosylation profiles are shown in Figure 4. Cell line A-M18 presented lower high mannose forms (Man9, Man7, Man6, Man5 and Mannose core) and higher A1G0, G0 and G0F forms than cell line A. Especially, the reduction of Man5 and the elevation of A1G0 is in accordance with the expected function of GnTI overexpression. On the other hand, cell line A-E15, which has an overexpression in UDP-GlcNAc transporter, showed no apparent decreasing in Man5 and increasing in A1G0. This implies that overexpression in UDP-GlcNAc transporter may not facilitate the GlcNAc addition reactions in the glycan maturation process in cell line A.

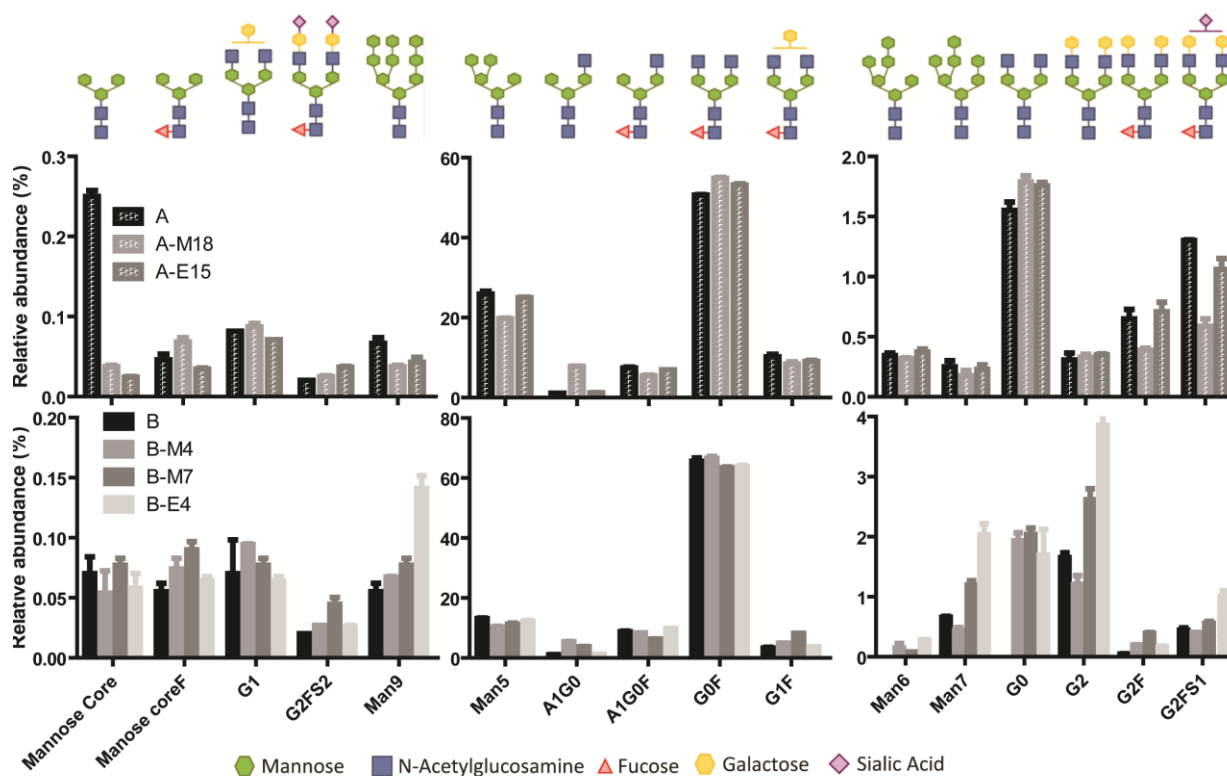


Figure 4. Intracellular nucleotide sugar analysis. The intracellular levels of UDP-GlcNAc and UDP-Gal in the parental (A and B) and engineered (A-M18, A-E15, B-M4, B-M7 and B-E15) cell lines are shown.

Similar as cell line A, increased A1G0 and decreased Man5 glycoforms can be observed when overexpressing GnTI in cell line B (B-M4 and B-M7 cell lines). This once again indicated that increase GnTI availability can slightly relieve the limitation of glycan maturation at the stage from Man5 to A1G0 glycoforms. However, no apparent changes in the major glycoforms observed (Man5, A1G0, A1G0F, G0F and G1F) when overexpressing UDP-GlcNAc transporter in cell line B (B-E4 cell line).

7.3.4. Intracellular nucleotide sugar metabolism

Nucleotide sugars are synthesized in the cytosol and transported into Golgi to be able to act as donors for glycan elongation reaction. The levels of the intracellular nucleotide sugars are therefore strongly associated with glycosylation. As shown in Figure 5, increasing accumulation of UDP-GlcNAc during the cell culture can be observed in both cell lines A and B. In general, all engineered cell lines displayed lower levels of intracellular UDP-GlcNAc than that in their parental cell lines from day 5 to day 11. In addition, A-M18 and A-E15 cell lines showed higher accumulation of UDP-Gal, whereas B-M4, B-M7 and B-E4 presented lower intracellular concentration of UDP-Gal, in comparison with the corresponding parental cell line from day 5 to day 11.

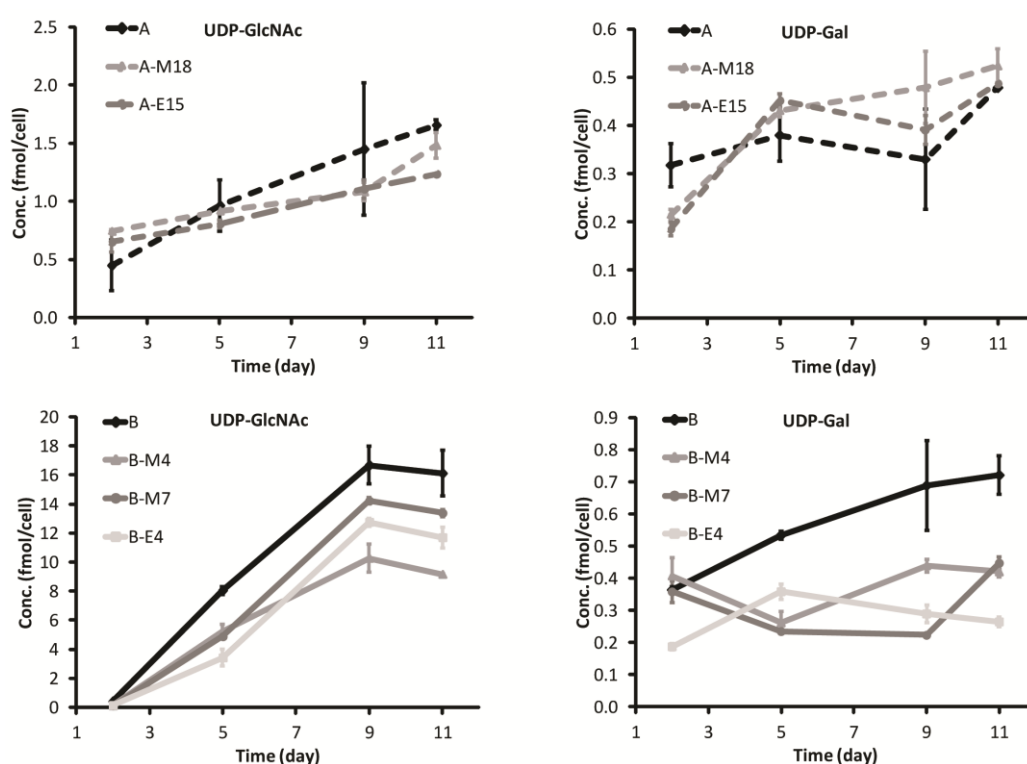


Figure 5. Glycoprofiles of mAbs produced from the cell cultures of the parental (A and B) and engineered (A-M18, A-E15, B-M4, B-M7 and B-E15) cell lines.

7.4. Discussion

In this study, we have established a number of mAb production cell lines with GnTI or UDP-GlcNAc transporter overexpressed stably, using random integration approaches. The resulting engineered cell lines have been tested in fed-batch culture in order to evaluate the impact on glycosylation patterns.

Golgi GnTI activity is essential for adding a GlcNAc residue to Man5 glycan in N-glycosylation process. A number of studies demonstrated that knock-out GnTI inhibits glycan maturation process and generates high mannose structure, mainly Man5 glycan (Sealover et al. 2013; Zhong et al. 2012). In contrast to that, a reduction of Man5 should therefore be expected, when GnTI is overexpressed. This is due to the fact that the abundance of glycosyltransferase relative to the specific productivity of the recombinant protein can be one of the bottlenecks that prevent glycan maturation.

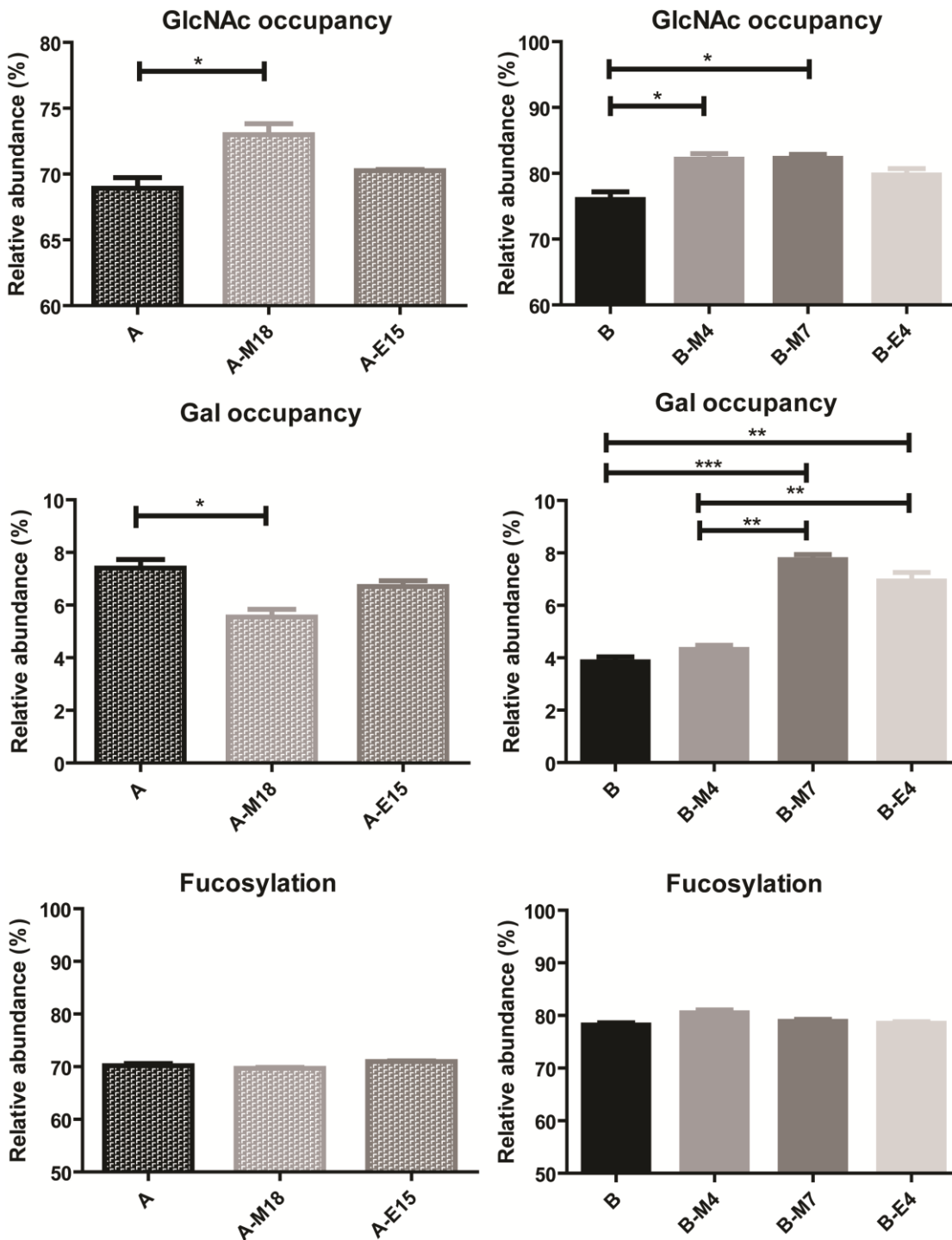


Figure 6. Average GlcNAc and galactose occupancy on glycans. The GlcNAc and Gal occupancy was calculated as described in (Fan et al. 2014). Statistical significance criteria: * for $p < 0.05$, ** for $p < 0.01$ and *** for $p < 0.001$.

Another possible bottleneck that can limit the glycan maturation is the availability of nucleotide sugars within the Golgi apparatus. This may be affected by the efficiency of nucleotide sugars synthesis in cytosol (Kochanowski et al. 2008) and the capability of transfer these species into the Golgi apparatus (Weikert et al. 1999; Wong et al. 2006). It has been reported previously that UDP-GlcNAc transporter can not only transport UDP-GlcNAc but also UDP-Gal into Golgi apparatus (Maszczak-Seneczko et al. 2011). In order to reduce Man5, increase GlcNAc and probably also Gal occupancy, overexpression of UDP-GlcNAc transporter was anticipated to be a feasible approach.

In consistency with our hypothesis of the effect of GnTI overexpression on mAb glycosylation, we found that overexpression of GnTI in both A and B cell lines statistically significant increase GlcNAc occupancy (Figure 6). Especially cell lines A-M18 and B-M4, comparing to their parental cell lines, presented an about 4% increase in GlcNAc occupancy despite their relatively higher average q_p (Figure 7). This indicates that the increase in GlcNAc occupancy is purely attributed to the increased expression of GnTI in Golgi that transfer GlcNAc residues to Man5 glycans more efficiently. Additionally, the increasing in average q_p in A-M18 cell line may overload the capacity of galactosylation and thus decreasing Gal occupancy in comparison with cell line A.

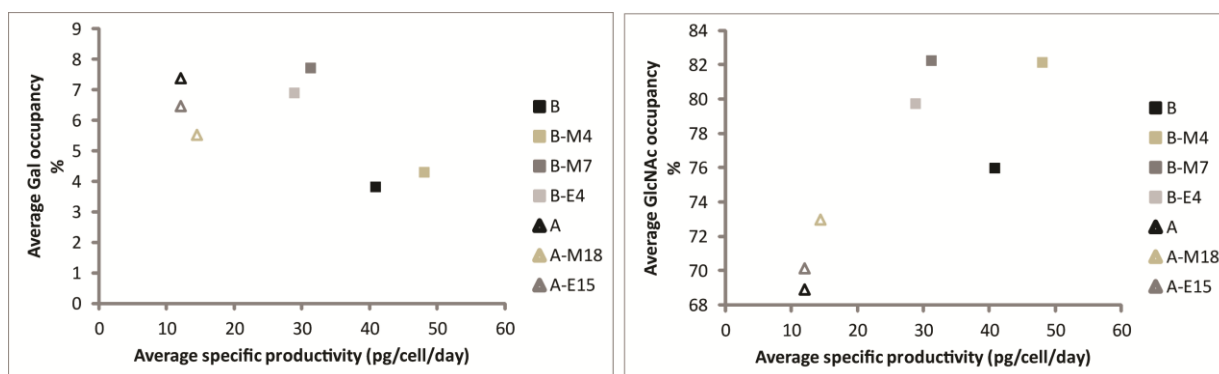


Figure 7. Relationship between average specific productivity of cell lines during the fed-batch culture and average GlcNAc and galactose occupancy.

On the other hand, the higher GlcNAc and GalNAc occupancy in cell line B-M7 may be a combinatory effect of increased GnTI expression and decreased q_p . It is also worth to mention that the increase in GlcNAc occupancy in A-M18, B-M4 and B-M7 cell lines although was mainly as a result of decrease Man5, did not change the fucosylation level of the produced mAb. The reduced Man5 was mainly turn into non-fucosylated A1G0 glycoforms in consequence of a limitation in fucosylation capacity.

Overexpression of UDP-GlcNAc transporter did not show the expected effect on glycosylation as described above. Both A-E15 and B-E4 cell lines present no statistically significant increase in GlcNAc occupancy. The increase in Gal occupancy in B-E4 cell line is as a result of clone specific effect that reduced the average qp of the cells (Figure 7). Our data suggest that the capacity of UDP-GlcNAc transport is not a limitation factor that prevents glycan maturation in both cell lines A and B. The availability of UDP-GlcNAc is well-matched with GnTI activity in both cell lines.

Additionally, the concentrations of intracellular nucleotide sugars UDP-GlcNAc and UDP-Gal were in consistency with the levels of them consumed by glycosylation processing. In general, the engineered cell lines with increased GlcNAc and Gal occupancy displayed lower accumulation of UDP-GlcNAc and UDP-Gal concentration. This suggests that the biosynthesis of UDP-GlcNAc and UDP-Gal are independent processes and overexpression of GnTI or UDP-GlcNAc transporter have no regulation effect on their biosynthesis.

In conclusion, overexpression of GnTI in mAb producing cell lines generate less Man5 and higher GlcNAc occupancy. However, overexpression of UDP-GlcNAc transporter cannot increase GlcNAc occupancy in our cell lines. The clone specific effect that affects the average specific productivity of mAb is a critical issue that can influence the maturation of glycans.

One of the perspectives in cell line engineering is to minimize clone specific effect, for example using site-specific integration instead of random integration. With recent development of genome editing tools, including CRISPR/Cas9, TALEN, ZFN system, to generate gain/enhance-of-function phenotype without inducing clone specific effect became possible. Future cell line development in modulating glycosylation towards more matured glycans can be done by further exploring the effect of combinatory overexpression of GnT1 and GlcNAc and overexpression of other glycotransferases, for example galactosyltransferase.

7.5. Reference

- Arnold JN, Wormald MR, Sim RB, Rudd PM, Dwek RA. 2007. The impact of glycosylation on the biological function and structure of human immunoglobulins. *Annu Rev Immunol* 25:21-50.
- Banmeyer I, Marchand C, Verhaeghe C, Vucic B, Rees JF, Knoops B. 2004. Overexpression of human peroxiredoxin 5 in subcellular compartments of Chinese hamster ovary cells: effects on cytotoxicity and DNA damage caused by peroxides. *Free Radic Biol Med* 36(1):65-77.
- Costa AR, Rodrigues ME, Henriques M, Oliveira R, Azeredo J. 2013. Glycosylation: impact, control and improvement during therapeutic protein production. *Crit Rev Biotechnol*.

- Davies J, Jiang L, Pan LZ, LaBarre MJ, Anderson D, Reff M. 2001. Expression of GnTIII in a recombinant anti-CD20 CHO production cell line: Expression of antibodies with altered glycoforms leads to an increase in ADCC through higher affinity for FC gamma RIII. *Biotechnol Bioeng* 74(4):288-94.
- Dreesen IA, Fussenegger M. 2011. Ectopic expression of human mTOR increases viability, robustness, cell size, proliferation, and antibody production of chinese hamster ovary cells. *Biotechnol Bioeng* 108(4):853-66.
- Druz A, Son YJ, Betenbaugh M, Shiloach J. 2013. Stable inhibition of mmu-miR-466h-5p improves apoptosis resistance and protein production in CHO cells. *Metab Eng* 16:87-94.
- Fan Y, Jimenez Del Val I, Müller C, Wagtberg Sen J, Rasmussen SK, Kontoravdi C, Weilguny D, Andersen MR. 2014. Amino acid and glucose metabolism in fed-batch CHO cell culture affects antibody production and glycosylation. *Biotechnology and Bioengineering*:n/a-n/a.
- Figueroa B, Jr., Ailor E, Osborne D, Hardwick JM, Reff M, Betenbaugh MJ. 2007. Enhanced cell culture performance using inducible anti-apoptotic genes E1B-19K and Aven in the production of a monoclonal antibody with Chinese hamster ovary cells. *Biotechnol Bioeng* 97(4):877-92.
- Imai-Nishiya H, Mori K, Inoue M, Wakitani M, Iida S, Shitara K, Satoh M. 2007. Double knockdown of alpha1,6-fucosyltransferase (FUT8) and GDP-mannose 4,6-dehydratase (GMD) in antibody-producing cells: a new strategy for generating fully non-fucosylated therapeutic antibodies with enhanced ADCC. *BMC Biotechnol* 7:84.
- Jeon MK, Yu DY, Lee GM. 2011. Combinatorial engineering of *ldh-a* and *bcl-2* for reducing lactate production and improving cell growth in dihydrofolate reductase-deficient Chinese hamster ovary cells. *Appl Microbiol Biotechnol* 92(4):779-90.
- Jimenez Del Val I, Kyriakopoulos S, Polizzi KM, Kontoravdi C. 2013. An optimized method for extraction and quantification of nucleotides and nucleotide sugars from mammalian cells. *Anal Biochem* 443(2):172-80.
- Kanda Y, Imai-Nishiya H, Kuni-Kamochi R, Mori K, Inoue M, Kitajima-Miyama K, Okazaki A, Iida S, Shitara K, Satoh M. 2007. Establishment of a GDP-mannose 4,6-dehydratase (GMD) knockout host cell line: a new strategy for generating completely non-fucosylated recombinant therapeutics. *J Biotechnol* 130(3):300-10.
- Kim SH, Lee GM. 2007a. Down-regulation of lactate dehydrogenase-A by siRNAs for reduced lactic acid formation of Chinese hamster ovary cells producing thrombopoietin. *Appl Microbiol Biotechnol* 74(1):152-9.

- Kim SH, Lee GM. 2007b. Functional expression of human pyruvate carboxylase for reduced lactic acid formation of Chinese hamster ovary cells (DG44). *Appl Microbiol Biotechnol* 76(3):659-65.
- Kochanowski N, Blanchard F, Cacan R, Chirat F, Guedon E, Marc A, Goergen JL. 2008. Influence of intracellular nucleotide and nucleotide sugar contents on recombinant interferon-gamma glycosylation during batch and fed-batch cultures of CHO cells. *Biotechnol Bioeng* 100(4):721-33.
- Le Fourn V, Girod PA, Buceta M, Regamey A, Mermod N. 2014. CHO cell engineering to prevent polypeptide aggregation and improve therapeutic protein secretion. *Metab Eng* 21:91-102.
- Lund AM, Kildegaard HF, Petersen MB, Rank J, Hansen BG, Andersen MR, Mortensen UH. 2014. A versatile system for USER cloning-based assembly of expression vectors for mammalian cell engineering. *PLoS One* 9(5):e96693.
- Mastrangelo AJ, Hardwick JM, Zou S, Betenbaugh MJ. 2000. Part II. Overexpression of bcl-2 family members enhances survival of mammalian cells in response to various culture insults. *Biotechnol Bioeng* 67(5):555-64.
- Maszczyk-Seneczko D, Olczak T, Jakimowicz P, Olczak M. 2011. Overexpression of UDP-GlcNAc transporter partially corrects galactosylation defect caused by UDP-Gal transporter mutation. *FEBS Lett* 585(19):3090-4.
- Meleady P, Gallagher M, Clarke C, Henry M, Sanchez N, Barron N, Clynes M. 2012. Impact of miR-7 over-expression on the proteome of Chinese hamster ovary cells. *J Biotechnol* 160(3-4):251-62.
- Mori K, Kuni-Kamochi R, Yamane-Ohnuki N, Wakitani M, Yamano K, Imai H, Kanda Y, Niwa R, Iida S, Uchida K and others. 2004. Engineering Chinese hamster ovary cells to maximize effector function of produced antibodies using FUT8 siRNA. *Biotechnol Bioeng* 88(7):901-8.
- Norholm MH. 2010. A mutant Pfu DNA polymerase designed for advanced uracil-excision DNA engineering. *BMC Biotechnol* 10:21.
- North SJ, Huang HH, Sundaram S, Jang-Lee J, Etienne AT, Trollope A, Chalabi S, Dell A, Stanley P, Haslam SM. 2010. Glycomics profiling of Chinese hamster ovary cell glycosylation mutants reveals N-glycans of a novel size and complexity. *J Biol Chem* 285(8):5759-75.
- Park H, Kim IH, Kim IY, Kim KH, Kim HJ. 2000. Expression of carbamoyl phosphate synthetase I and ornithine transcarbamoylase genes in Chinese hamster ovary dhfr-cells decreases accumulation of ammonium ion in culture media. *J Biotechnol* 81(2-3):129-40.

- Sealover NR, Davis AM, Brooks JK, George HJ, Kayser KJ, Lin N. 2013. Engineering Chinese hamster ovary (CHO) cells for producing recombinant proteins with simple glycoforms by zinc-finger nuclease (ZFN)-mediated gene knockout of mannosyl (alpha-1,3-)-glycoprotein beta-1,2-N-acetylglucosaminyltransferase (Mgat1). *J Biotechnol* 167(1):24-32.
- Shi HH, Goudar CT. 2014. Recent advances in the understanding of biological implications and modulation methodologies of monoclonal antibody N-linked high mannose glycans. *Biotechnology and Bioengineering* 111(10):1907-1919.
- Tigges M, Fussenegger M. 2006. Xbp1-based engineering of secretory capacity enhances the productivity of Chinese hamster ovary cells. *Metab Eng* 8(3):264-72.
- Umana P, Jean-Mairet J, Moudry R, Amstutz H, Bailey JE. 1999. Engineered glycoforms of an antineuroblastoma IgG1 with optimized antibody-dependent cellular cytotoxic activity. *Nat Biotechnol* 17(2):176-80.
- Weikert S, Papac D, Briggs J, Cowfer D, Tom S, Gawlitzek M, Lofgren J, Mehta S, Chisholm V, Modi N and others. 1999. Engineering Chinese hamster ovary cells to maximize sialic acid content of recombinant glycoproteins. *Nat Biotechnol* 17(11):1116-21.
- Wong NSC, Yap MGS, Wang DIC. 2006. Enhancing recombinant glycoprotein sialylation through CMP-sialic acid transporter over expression in chinese hamster ovary cells. *Biotechnology and Bioengineering* 93(5):1005-1016.
- Xu X, Nagarajan H, Lewis NE, Pan S, Cai Z, Liu X, Chen W, Xie M, Wang W, Hammond S and others. 2011. The genomic sequence of the Chinese hamster ovary (CHO)-K1 cell line. *Nat Biotechnol* 29(8):735-41.
- Yamane-Ohnuki N, Kinoshita S, Inoue-Urakubo M, Kusunoki M, Iida S, Nakano R, Wakitani M, Niwa R, Sakurada M, Uchida K and others. 2004. Establishment of FUT8 knockout Chinese hamster ovary cells: an ideal host cell line for producing completely defucosylated antibodies with enhanced antibody-dependent cellular cytotoxicity. *Biotechnol Bioeng* 87(5):614-22.
- Zhong X, Cooley C, Seth N, Juo ZS, Presman E, Resendes N, Kumar R, Allen M, Mosyak L, Stahl M and others. 2012. Engineering novel Lec1 glycosylation mutants in CHO-DUKX cells: molecular insights and effector modulation of N-acetylglucosaminyltransferase I. *Biotechnol Bioeng* 109(7):1723-34.

Chapter 8 Conclusion and future perspectives

In order to explore potentials and develop novel strategies to control and optimize N-glycosylation of CHO-derived recombinant monoclonal antibody (mAb), we conducted the research of CHO cell bioprocessing using systems biology approaches, where better understanding of interrelations among physiological, metabolic and proteomic status of CHO cells during manufacturing processes and the quantity and quality of produced mAbs was achieved.

Two major strategies were tested to modulate N-glycosylation of mAb. First strategy was to optimize culture media and improve upstream process. Second strategy was to genetically modified glycosylation genes in CHO cells. Although the effect and efficiency were cell line dependent, both strategies were shown to work in different study cases.

A number of important findings were demonstrated using the first strategy: (1) Balance of glucose and amino acid concentration in the culture can affect specific consumption rate of amino acid and glucose in CHO cells. Elevated Man5 glycan structure was in association with high specific amino acid consumption, whereas more matured glycans can be produced when high specific glucose consumption rate was achieved. (2) Reduced specific productivity of mAb (q_p), as a result of glucose starvation at stationary phase of fed-batch culture, can improve the level of glycan maturation. (3) Feeding galactose as feed additives can increase the level of galactosylation. (4) Increased cultivation duration can cause elevated Man5 glycan.

The second strategy was also shown valuable results in controlling N-glycosylation: (1) Overexpression of N-acetylglucosaminyltransferase I (GnTI) could also increase GlcNAc and/or Gal occupancy of mAb for certain cell line. (2) Overexpression of N-acetylglucosamine (GlcNAc) transporter in CHO cells, which was expected to increase UDP-GlcNAc and UDP-Gal transportation from cytosol to Golgi apparatus do not seem to improve maturation of glycans for the cell lines tested.

Integrating systems biology with CHO cell bioprocessing (i.e. linking various omics data, cultivation process data and protein quality data together from more cell lines) in the future will be an important approach of exploring possible bottlenecks in the glycosylation process in different cell lines. By doing that, both the established and new approaches that could modulate N-glycosylation toward more desired patterns can be developed to targeting different cell lines with better specificity and higher efficiency.

Appendix I: Supporting information of Chapter 3

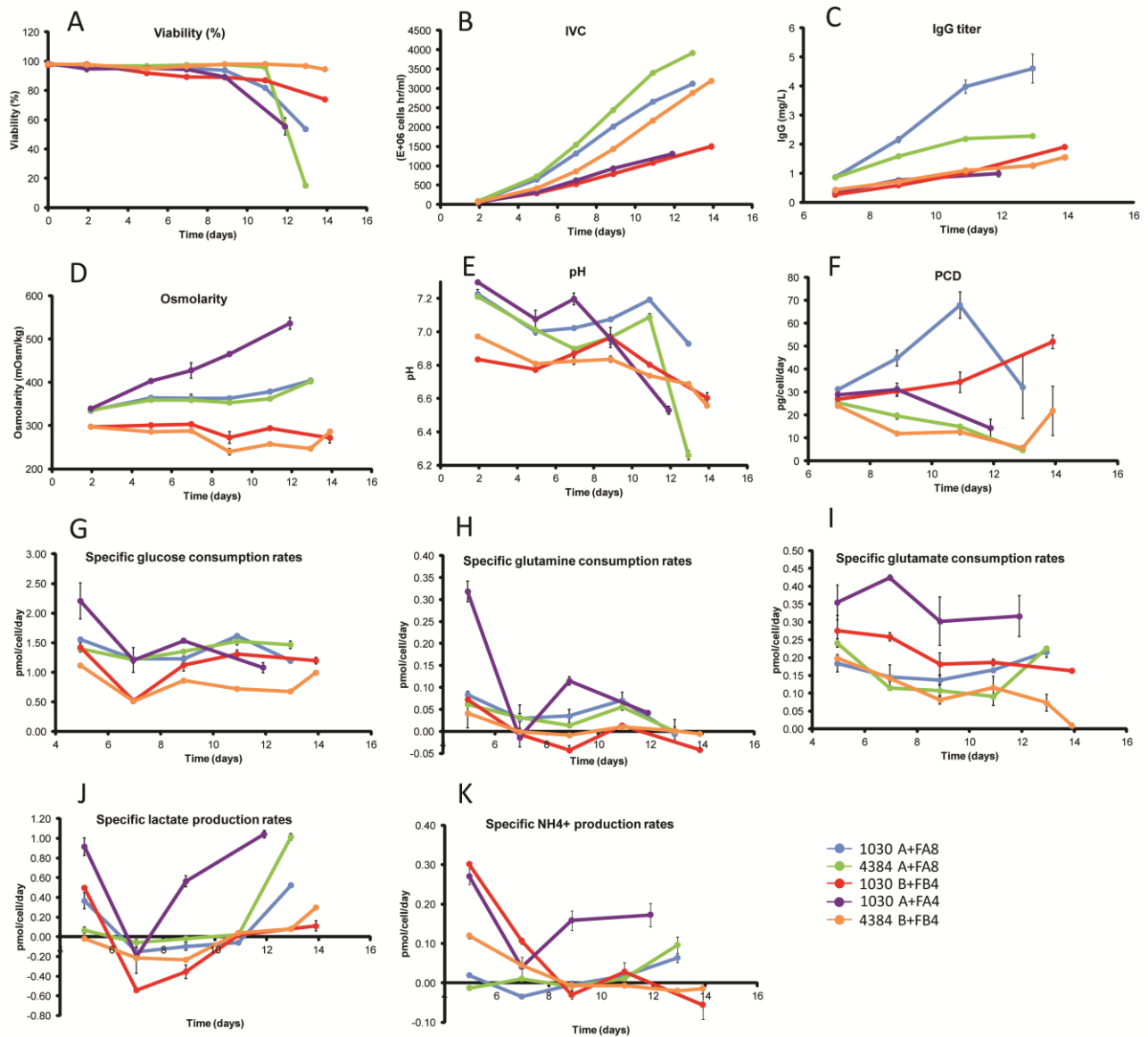
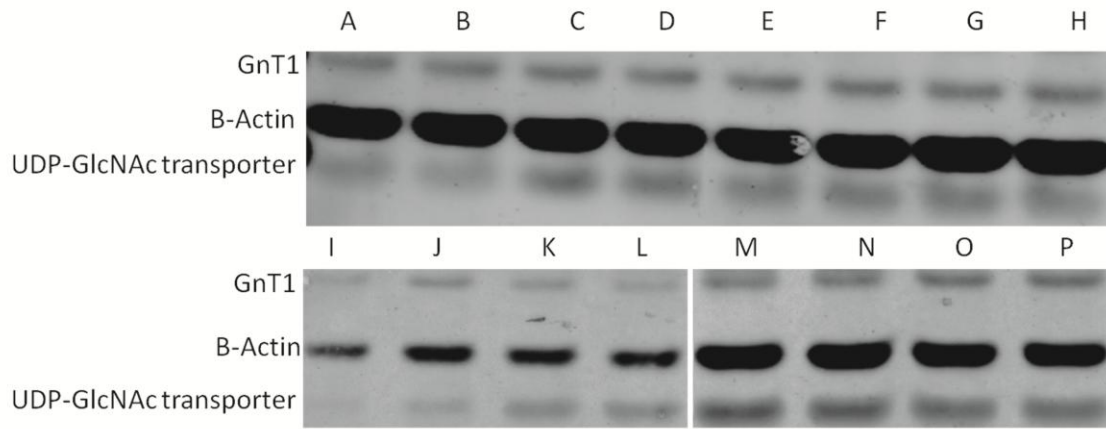


Figure S1. Additional data for comparison of five fed-batch cultures with different cell lines and cultivation conditions. (A) Viability, (B) Integral of viable cells (IVC), (C) IgG titer, (D) Osmolarity, (E) pH, (F) Specific IgG production rate (PCD) are shown. Specific consumption rates of glucose (G), glutamine (H) and glutamate (I) are also shown. Specific lactate (J) and ammonia (K) production rates are presented.



A	4384 B+FB4-1 on day2
B	4384 B+FB4-2 on day2
C	1030 A+FA8-1 on day2
D	1030 A+FA8-2 on day2
E	4384 A+FA8-1 on day2
F	4384 A+FA8-2 on day2
G	1030 B+FB4-1 on day2
H	1030 B+FB4-2 on day2
I	1030 A+FA8-2 on day 11
J	1030 A+FA8-2 on day 11
K	1030 B+FB4-1 on day 11
L	1030 B+FB4-1 on day 11
M	4384 B+FB4-1 on day 11
N	4384 B+FB4-2 on day 11
O	4384 A+FA8-1 on day 11
P	4384 A+FA8-2 on day 11

Figure S2. Western blot analysis of GnT1 and UDP-GlcNAc transporter in this study.

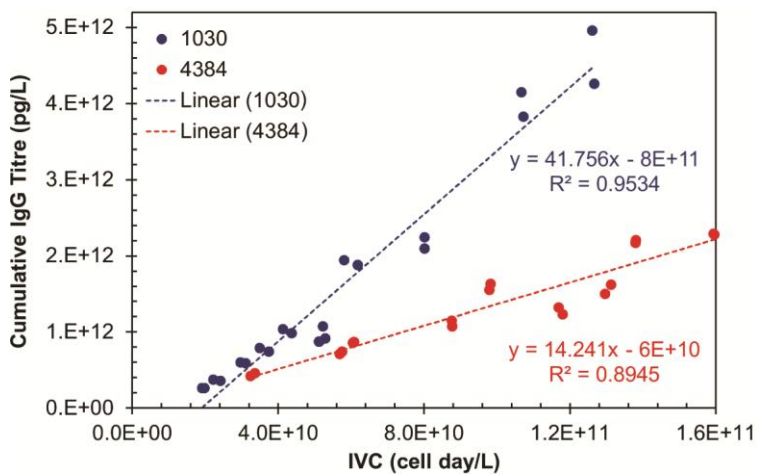


Figure S3. Average specific IgG productivity. Linear regressions were performed on raw data grouped by cell line.

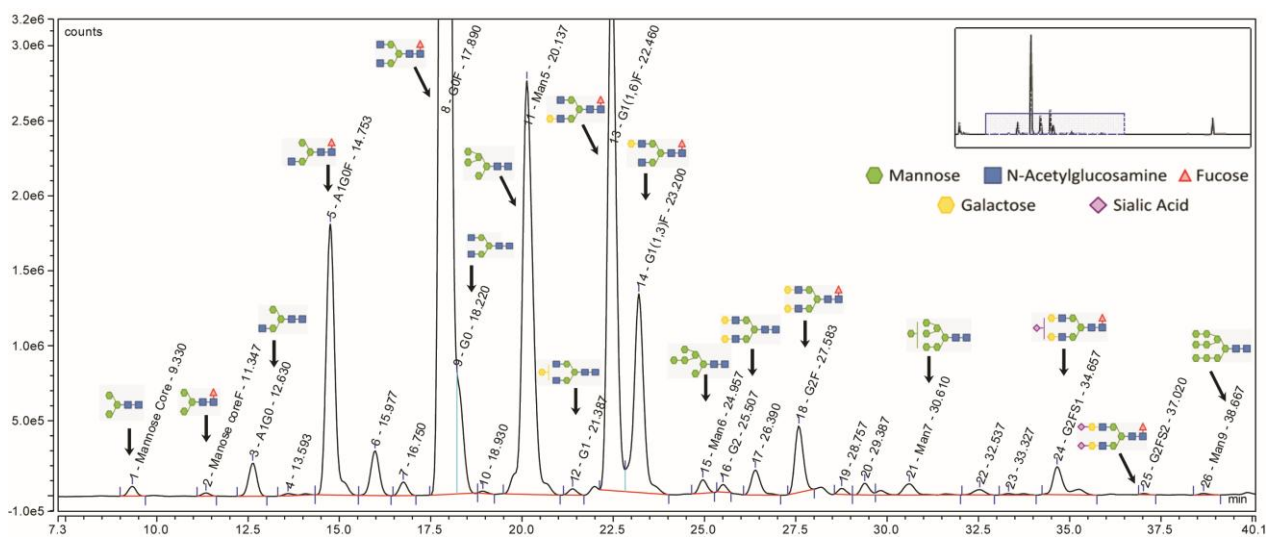


Figure S4. HPLC Chromatogram of instant-AB labeled glycoprofiling.

Table SI. Amino acid composition of 4384 IgG.

4384 IgG	%
Ser	13.16
Val	8.62
Thr	8.17
Leu	8.02
Lys	6.81
Pro	6.51
Gly	6.20
Glu	4.99
Gln	4.99
Ala	4.69
Asn	4.39
Tyr	4.39
Asp	3.78
Phe	3.18
Arg	2.57
Cys	2.42
Ile	2.12
His	2.12
Trp	1.82
Met	1.06

Appendix II: Supporting information of Chapter 4

Table SI. Detailed cultivation parameters.

Average	Control	GlcNAc	ManNAc	Mannose	Fucose	Galactose	NeuNAc	Cytidine	Uridine
Final volume of bioreactor (mL)	667.4	673.2	680.1	669.5	653.8	657.9	664.1	661.3	656.2
Maximum VCC (cells mL⁻¹)	7.2E+06	7.8E+06	8.0E+06	7.9E+06	6.6E+06	6.9E+06	6.8E+06	7.3E+06	6.6E+06
IVC (cells h/ml)	1.69E+09	1.60E+09	1.63E+09	1.82E+09	1.60E+09	1.60E+09	1.58E+09	1.60E+09	1.55E+09
qp (day 3-6) (pg cell⁻¹ day⁻¹)	12.10	8.74	9.66	10.02	11.98	9.83	12.59	8.84	8.52
Final VCC (cells mL⁻¹)	2.97E+06	2.81E+06	2.37E+06	3.44E+06	3.08E+06	2.96E+06	2.93E+06	2.59E+06	2.88E+06
Final antibody concentration (mg L⁻¹)	488.67	383.50	365.50	424.00	470.50	425.00	448.50	339.50	329.00
Stdev									
Final volume of bioreactor (mL)	4.4	3.0	16.9	6.8	4.2	6.7	7.1	4.9	1.3
Maximum VCC (cells mL⁻¹)	1.6E+05	7.0E+05	7.3E+05	1.2E+06	4.3E+05	4.2E+04	1.5E+05	8.7E+05	1.2E+05
IVC (cells h/ml)	3.32E+07	1.42E+08	3.14E+07	1.09E+08	3.84E+07	7.66E+07	1.76E+07	1.20E+08	5.02E+07
qp (day 3-6) (pg cell⁻¹ day⁻¹)	1.16	2.17	0.83	1.41	1.43	2.19	0.12	1.14	0.37
Final VCC (cells mL⁻¹)	9.39E+04	2.62E+04	2.38E+05	1.27E+05	1.13E+05	2.10E+05	1.32E+05	3.13E+05	1.17E+05
Final antibody concentration (mg L⁻¹)	30.11	89.80	61.52	25.46	27.58	32.53	6.36	13.44	7.07

x

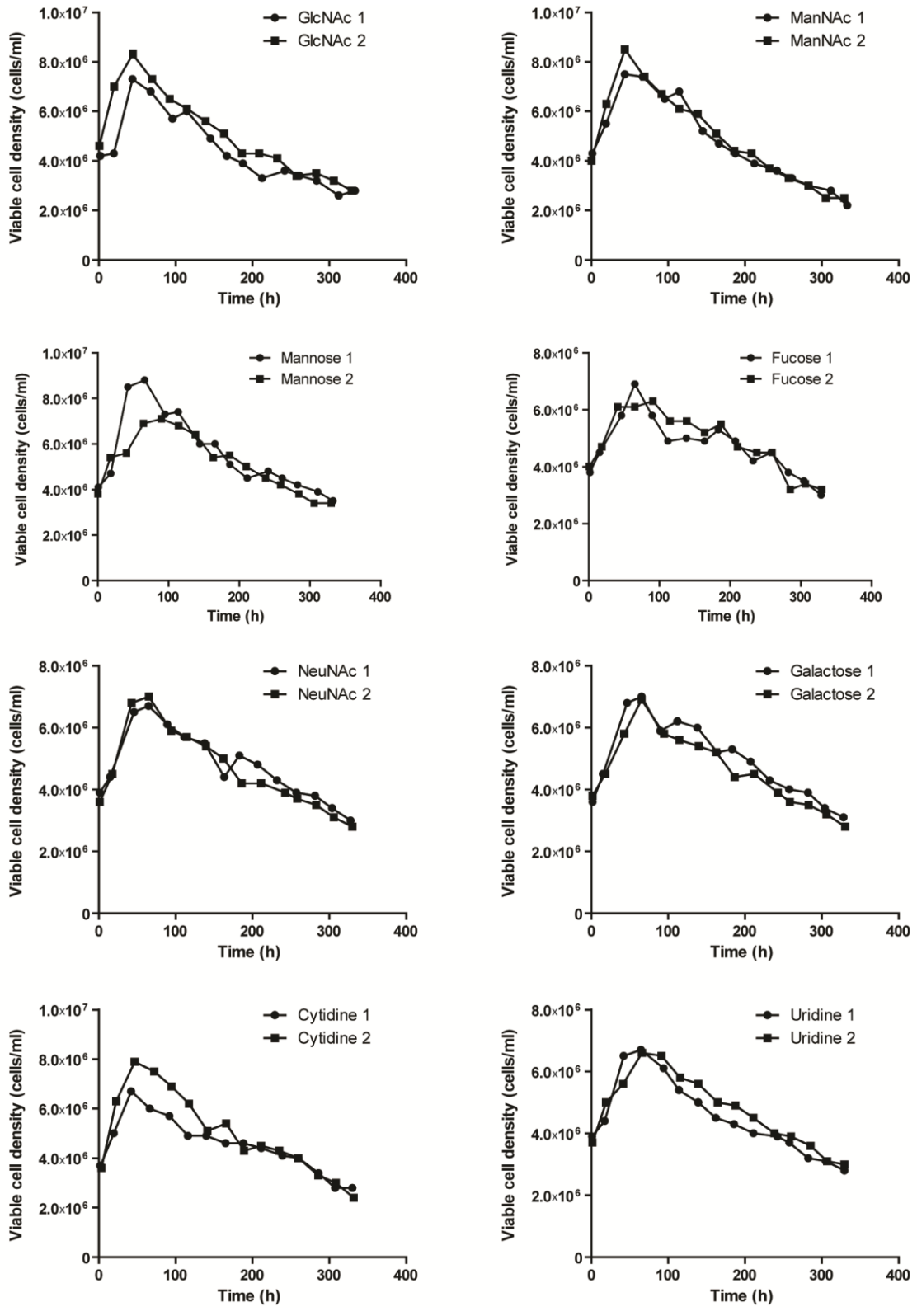


Figure S1 Viable cell density of all cell cultures with feed additives.

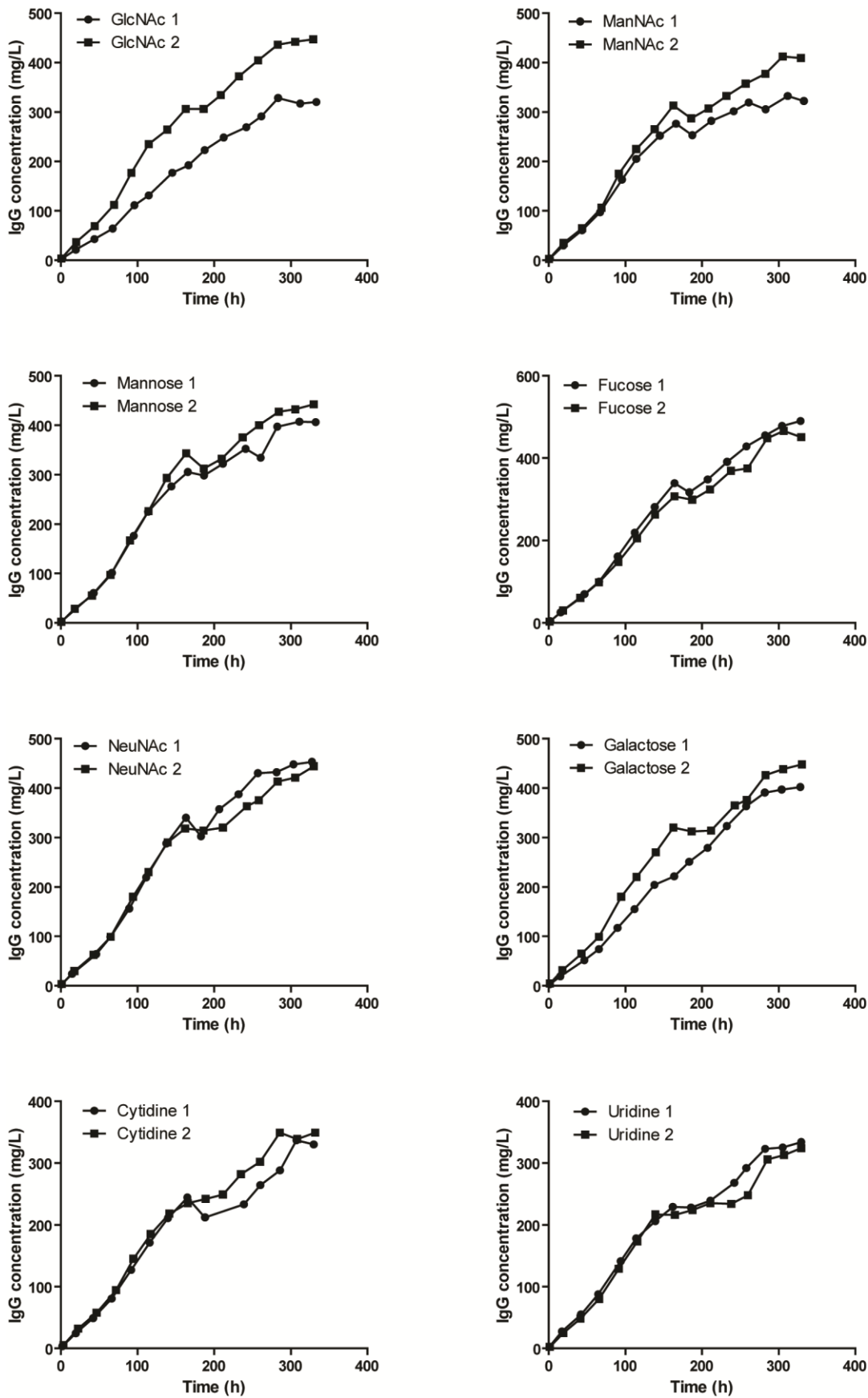


Figure S2 IgG titer of all cell cultures with feed additives.

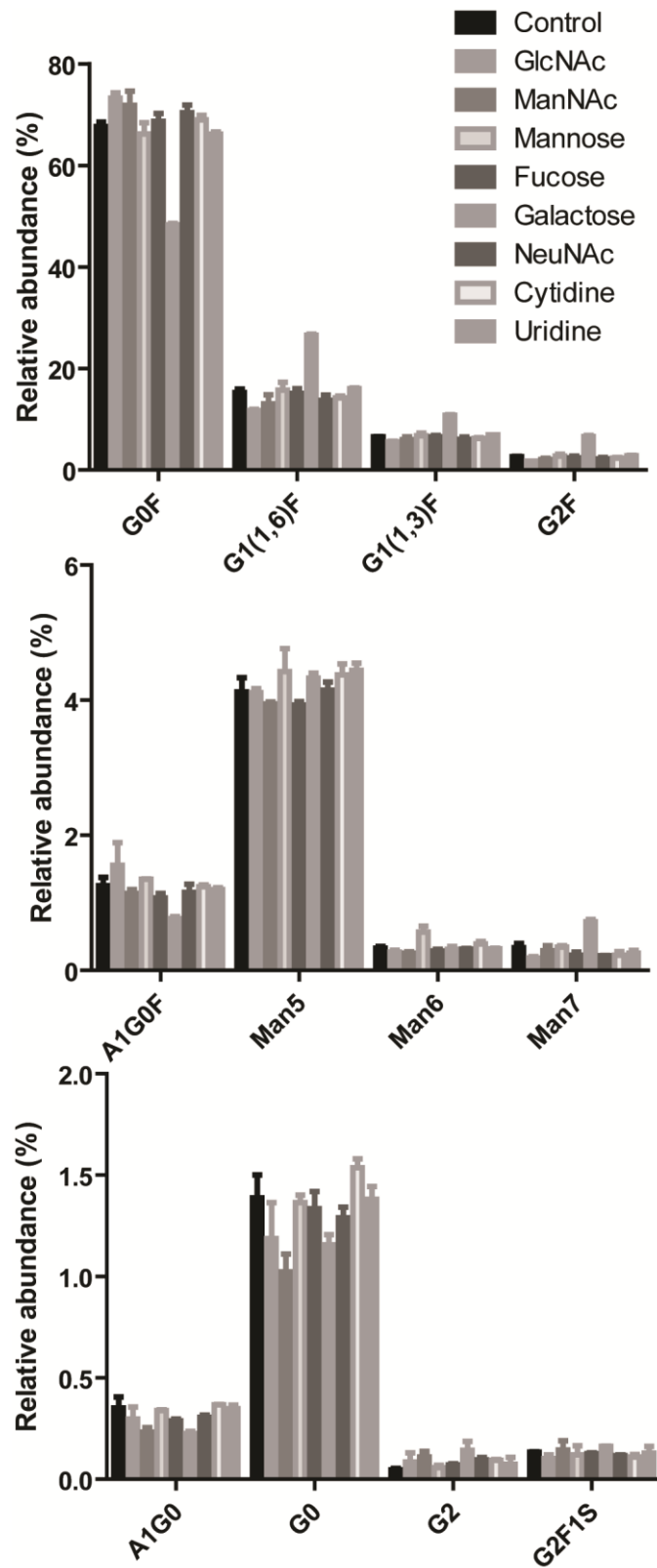


Figure S3 Detailed glycoprofiles of all cell cultures.

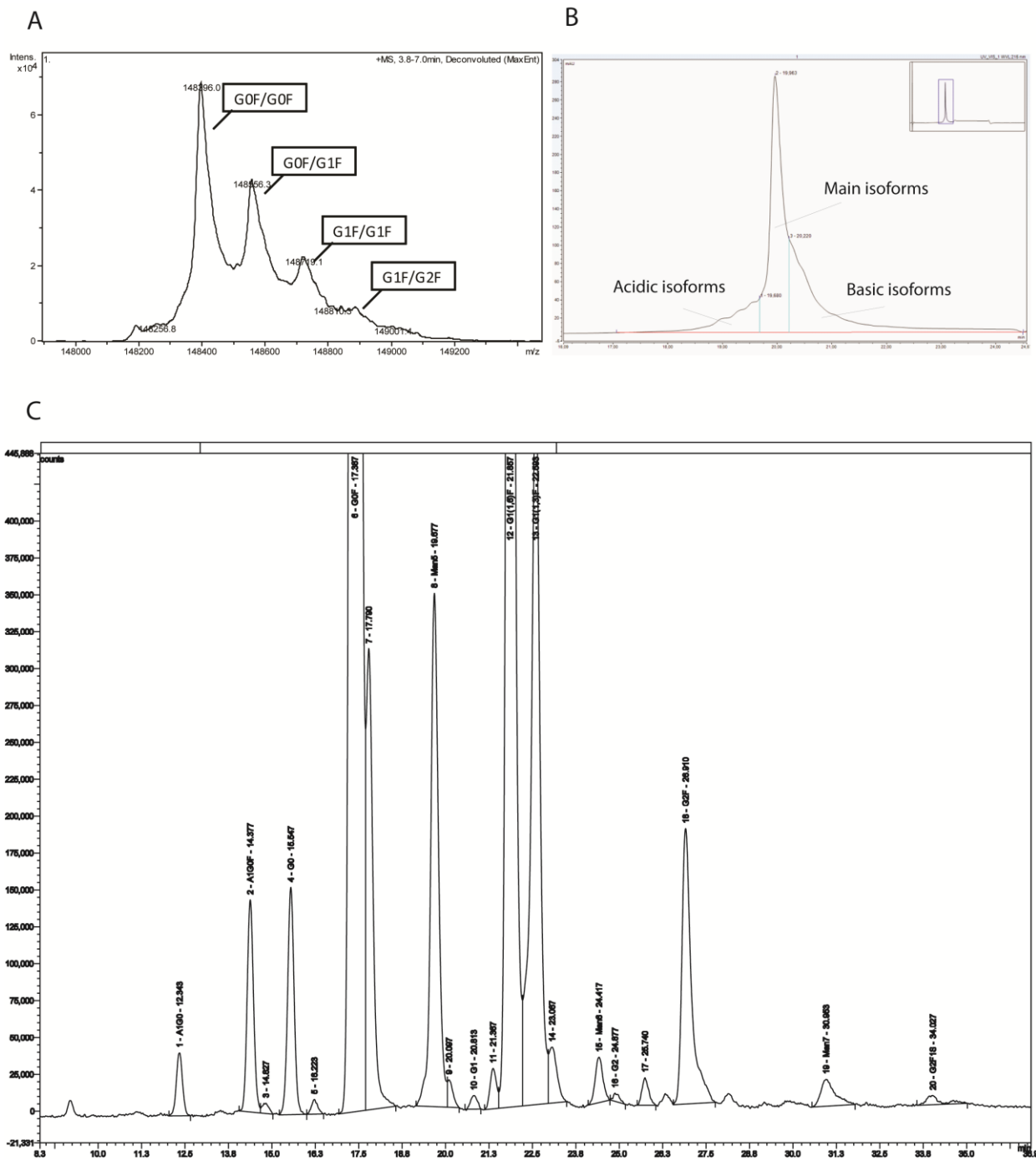


Figure S4 Spectrum and chromatogram peak assignment. (A) Peak assignment of intact mass analysis spectrum; (B) Peak assignment of cation exchange chromatogram; (C) Peak assignment of glycoprofiling chromatogram.

Appendix III: Supporting information of Chapter 6

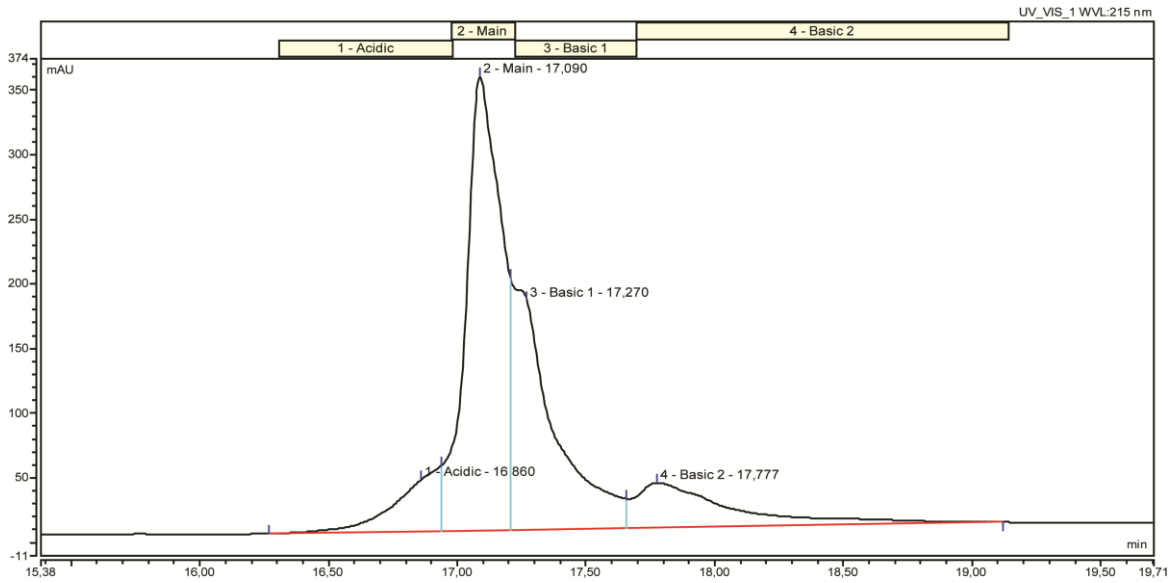


Figure S1. Chromatogram of CEX and assignment of charge variants

Table S1-11 can be found in an excel file on a webpage:

<https://www.dropbox.com/sh/d56e21intwzq3pf/AACJQtgM81fu5aUMWnLXpSjza?dl=0>

Appendix IV: Supporting information of Chapter 7

Table S1 Primers used in this study

Primer name	Description	Sequences	Tm	Template	p 1	p 2	p 3	p 4
EYF-1	eGFP_USER_FW	ATTCCGAUCGC CACCATGGTGA GCAAG	62,78	peGFP-1	739bp		739bp	
EYF-2	eGFP_USER_RW	AGCTTAAUCTT GTACAGCTCGT CCATGCC	60,58	peGFP-1	739bp		739bp	
EYF-3	FLAG-tag_UDPGlcNAcTrans_USER_FW	ACGTCGCUATG GACTACAAAGA CCATGACGG	60,65	pUC57_FLAG::UDPGI cNAcTransporter	1063bp			
EYF-4	FLAG-tag_UDPGlcNAcTrans_USER_RW	ATCGCACUCTA TGCTTTAATGGG ATTCCTGC	59,64	pUC57_FLAG::UDPGI cNAcTransporter	1063bp			
EYF-5	IRES_USER_FW	AGTGCGAUAAT TCCGCCCTCTC CCC	63,21	pIRES-DHFR	612bp	612bp		
EYF-6	IRES_USER_RW	ATCGGAUUTTA TCATCGTGTTT TCAAAGGAA	58,99	pIRES-DHFR	612bp	612bp	612bp	612bp
EYF-7	GnTI_HA-tag_USER_FW	ACGTCGCUATG CTGAAGAAGCA GTCTGCA	58,48	pUC57_GnTI::HA		1387bp		
EYF-8	GnTI_HA-tag_USER_RW	ATCGCACUCTA AGCGTAATCTG GAACATCG	57,37	pUC57_GnTI::HA		1387bp		
EYF-9	mCherry_USER_FW	ATTCCGAUCGC CACCATGGTGA GCAAG	62,78	pmCherry-N1		734bp		734bp
EYF-10	mCherry_USER_RW	AGCTTAAUCTA CTTGACAGCTC GTCCATGCC	63,06	pmCherry-N1		734bp		734bp
EYF-11	UDPGlcNAcTrans_USER_FW_2	ACTTGCGUATG TCCGCCAACCT AAAATATC	58,08	pUC57_FLAG::UDPGI cNAcTransporter			997bp	
EYF-12	UDPGlcNAcTrans_USER_RW_2	ACCAGGCUCTA TGCTTTAATGGG ATTCCTGC	59,64	pUC57_FLAG::UDPGI cNAcTransporter			997bp	
EYF-13	IRES_USER_FW_2	ACCAGGCUAAT TCCGCCCTCTC CCC	63,21	pIRES-DHFR			612bp	612bp
EYF-14	GnTI_USER_FW_2	ACTTGCGUATG CTGAAGAAGCA GTCTGCA	58,48	pUC57_GnTI::HA				1360bp
EYF-15	GnTI_USER_RW_2	ACCAGGCUCTA ATTCAGCTAG GATCATAGCC	59,06	pUC57_GnTI::HA				1360bp

Table S2 Plasmid and PCR template used in this study

Template	Functional elements	Source
peGFP-1	eGFP	Clontech
pIRES-DHFR	IRES	(Lund et al. 2014)
pmCherry-N1	mCherry	Clontech
pUC57_FLAG::UDPGlcNAcTransporter	UDPGlcNAcTransporter ± FLAG-tag	GenScript
pUC57_GnTI::HA	GnTI ± HA-tag	GenScript
SLXplasmid_0191	SLXplasmid_0191 backbone	Selexis
SLXplasmid_0192	SLXplasmid_0192 backbone	Selexis

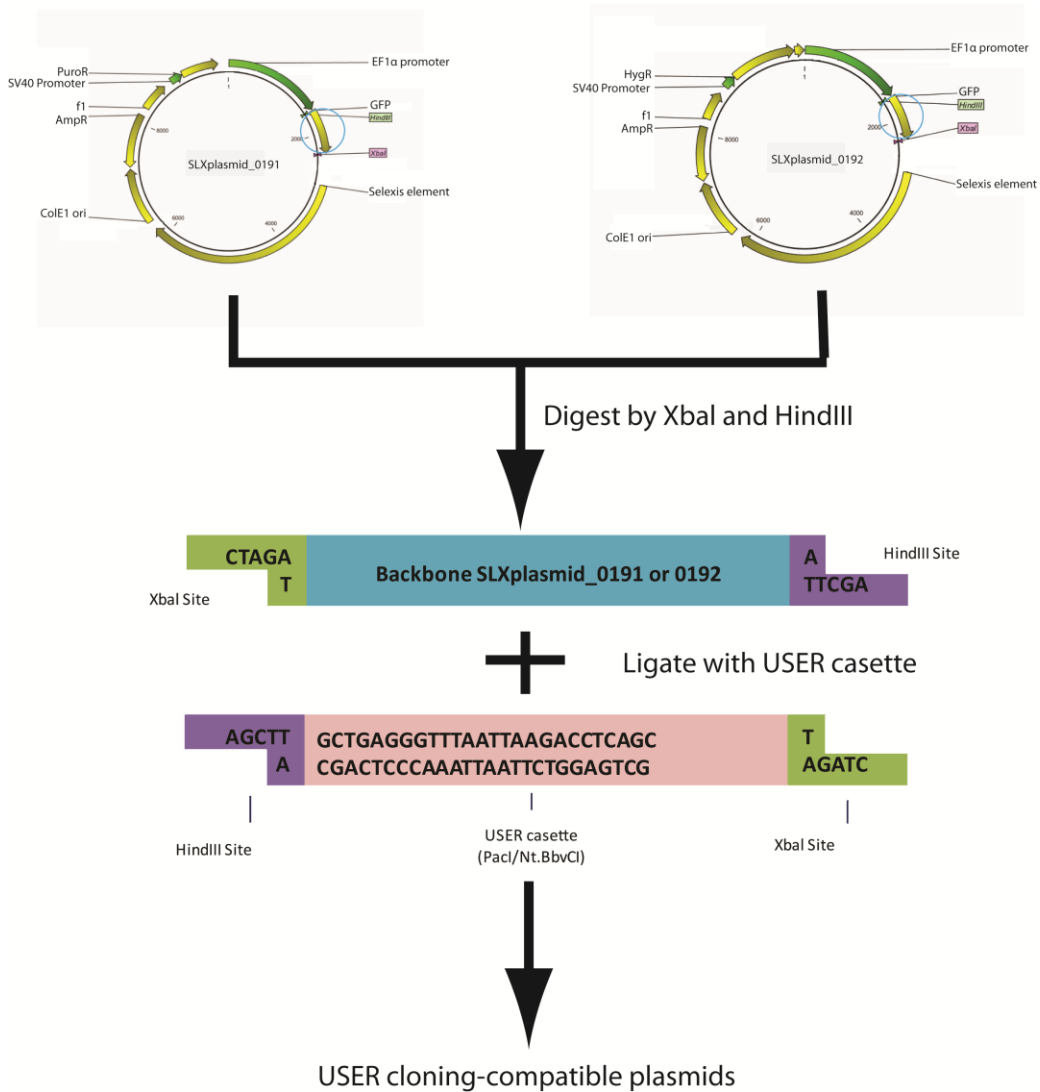


Figure S1. Construction of USER compatible plasmids

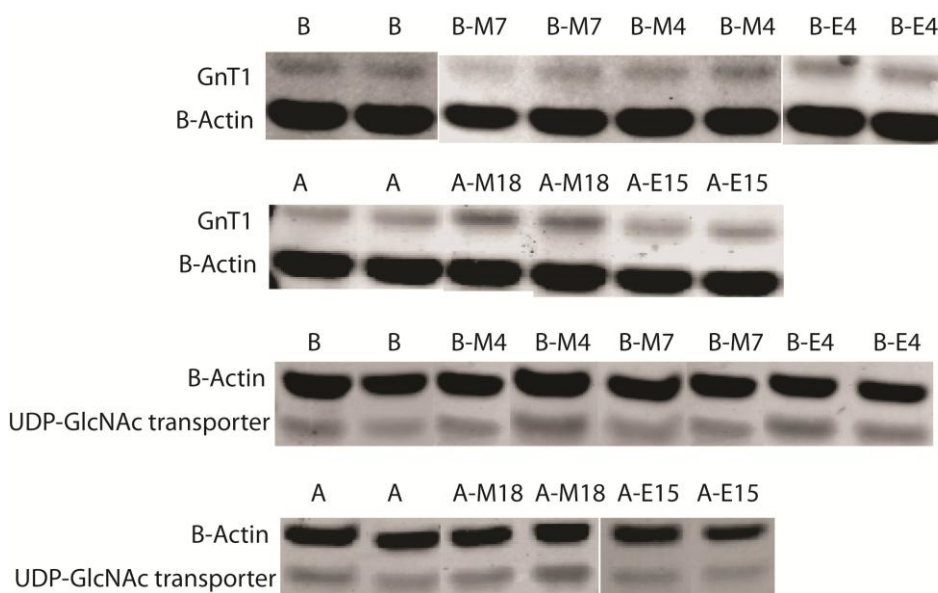


Figure S2. Western blot analysis of GnTI and UDP-GlcNAc transporter of cell lines selected in this study